

Functionalization of sp^2 -carbon atoms via visible-light photoredox catalysis

Dissertation

Zur Erlangung des Doktorgrades der Naturwissenschaften

(Dr. rer. nat.)

an der Fakultät für Chemie und Pharmazie

der Universität Regensburg



vorgelegt von

Simon Josef Siegfried Düsel

aus Bayreuth

2019

The experimental work was carried out between November 2015 and March 2019 under the supervision of Prof. Dr. Burkhard König at the University of Regensburg, Institute of Organic Chemistry.

Date of submission: 25.03.2019

Date of colloquium: 26.04.2019

Board of examiners:

Prof. Dr. Arno Pfitzner	(Chair)
Prof. Dr. Burkhard König	(1 st Referee)
Prof. Dr. Julia Rehbein	(2 nd Referee)
Prof. Dr. Frank-Michael Matysik	(Examiner)

This thesis is dedicated to

My parents Christian & Christine

My brother Andreas

And my wife Anna-Lena

Table of Contents

1. Impact of visible-light photoredox catalysis on traditional synthetic protocols	1
1.1 Introduction	2
1.2. Photoredox catalyzed versions of classic radical reactions	3
1.3. Replacement of transition metal catalysts by organic dyes	8
1.4. Combination of photoredox catalysis with other catalytic systems.....	12
1.6. Concluding remarks	18
1.7 References	19
2. Visible-light mediated nitration of protected anilines	22
2.1 Introduction	23
2.2 Results and discussion	24
2.2.1 Synthesis.....	24
2.2.2 Mechanistic investigations	27
2.3 Conclusion	30
2.4 Experimental part.....	31
2.4.1 General information	31
2.4.2 General experimental procedures.....	34
2.4.3 Product characterization	36
2.4.4 Spectroscopic characterization	41
2.5 References	43
3. Oxidative photochlorination of electron rich arenes via <i>in situ</i> bromination	45
3.1 Introduction	46
3.2 Results and discussion	47
3.2.1 Synthesis.....	47
3.2.2 Mechanistic investigations	51
3.3 Conclusion	55
3.4 Experimental part.....	56
3.4.1 General information	56
3.4.2 Mechanistic investigations	56

3.4.2.1 Bromination of arenes by elementary bromine	56
3.4.2.2 Emission quenching experiments	57
3.4.2.3 Cyclic voltammetry measurements	58
3.4.3 General experimental procedure	60
3.4.4 Product characterization	62
3.5 References	69
4. Alkenylation of unactivated alkyl bromides through visible-light photocatalysis	72
4.1 Introduction	73
4.2 Results and discussion	74
4.2.1 Synthesis	74
4.2.2 Mechanistic investigations	79
4.3 Conclusion	80
4.4 Experimental part	81
4.4.1 General information	81
4.4.2 Mechanistic investigations	82
4.4.2.1 Steady-state and time-resolved emission quenching experiments	82
4.4.2.2 Quantum yield measurements	84
4.4.2.3 Cyclic voltammetry measurements	85
4.4.3 General experimental procedures	88
4.4.4 Product characterization	90
4.5 References	103
5. Visible-light photo-Arbuzov reaction of aryl bromides and trialkyl phosphites yielding aryl phosphonates	106
5.1 Introduction	107
5.2 Results and discussion	108
5.2.1 Synthesis	108
5.2.2 Mechanistic investigations	114
5.3 Conclusion	115
5.4 Experimental part	116
5.4.1 General Information	116

5.4.2 Cyclic voltammetry measurements	116
5.4.3 General experimental procedure	117
5.4.4 Product characterization	117
5.5 References	138
6. Summary	141
7. Zusammenfassung	142
8. Abbreviations	143
9. Curriculum Vitae	147
10. Danksagung	150

1. Impact of visible-light photoredox catalysis on traditional synthetic protocols

In this chapter, several selected examples of classic organic reactions and their photoredox-catalyzed versions are discussed in direct comparison. The reaction conditions and mechanistic pathways are briefly discussed and potential benefits of photoredox-catalyzed versions are highlighted. Every scheme displays the reaction conditions of the photoredox-catalyzed version (top part) and the classic version (bottom part).

This Chapter has been submitted as a book chapter for "Photochemistry: Volume 47 - Specialist Periodical Reports". Editors: Stefano Protti and Angelo Albini. Publisher: The Royal Society of Chemistry.

S. J. S. Düsel and B. König, **2019**.

Author contributions:

SJSD selected the examples and wrote the manuscript. BK refined the manuscript, supervised the project and is the corresponding author.

1.1 Introduction

The scientific investigation and design of synthetic reactions in organic chemistry started in the middle of the 19th century. In this context, the synthesis of alizarin was patented 150 years ago.^[1] It was the first commercially important natural dye that was produced synthetically. Through the following decades, more and more sophisticated methods for the formation of organic compounds were developed and diverse fields of catalysis gained importance. Among these great methodological tools, one of the youngest is visible-light photoredox catalysis. The timely topic experienced a renaissance and popularized radical reactions in synthetic applications. As a result, new reaction pathways became possible and traditional synthetic routes are reconsidered in a new light.

The catalyst dye molecules absorb light in the visible spectral range, avoiding direct UV-irradiation and therefore possible side reactions, and the requirement of special quartz equipment. A general mechanistic pathway of photoredox-catalyzed reactions is displayed in Figure 1-1. Upon light excitation, the dye molecule becomes a better oxidant and reductant at the same time. Consequently, a single electron transfer (SET) between the excited catalyst and a substrate molecule or a sacrificial electron donor or acceptor (Figure 1-1, Substrate A or B) can occur. Reactive radical species are generated and can undergo bond-forming reactions or serve as hydrogen atom donors or acceptors. A quencher molecule, the substrate or the open-shell product of a radical reaction then regenerates the catalyst's initial state (Figure 1-1, Substrate C or D). Light energy can overcome activation barriers at low temperatures or even allow endothermic reaction steps.

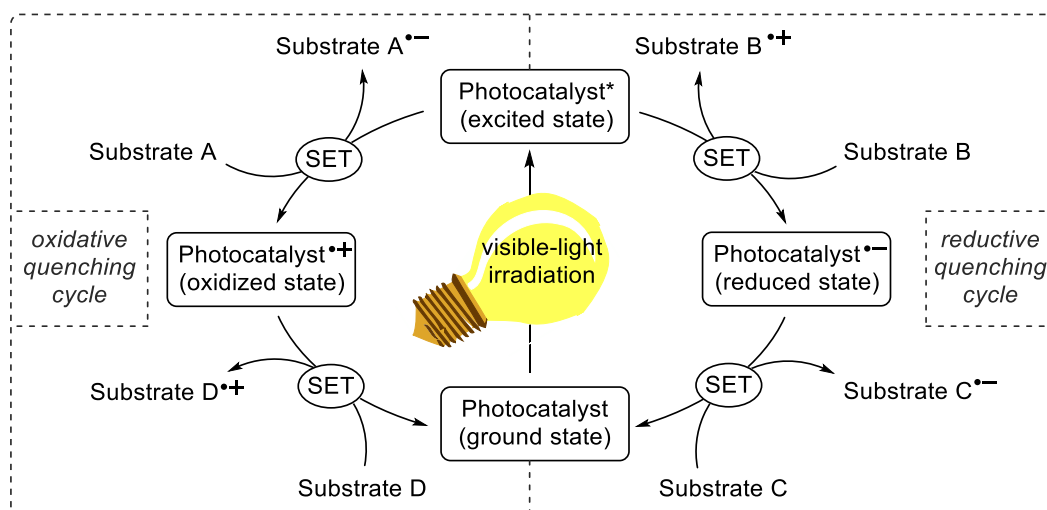
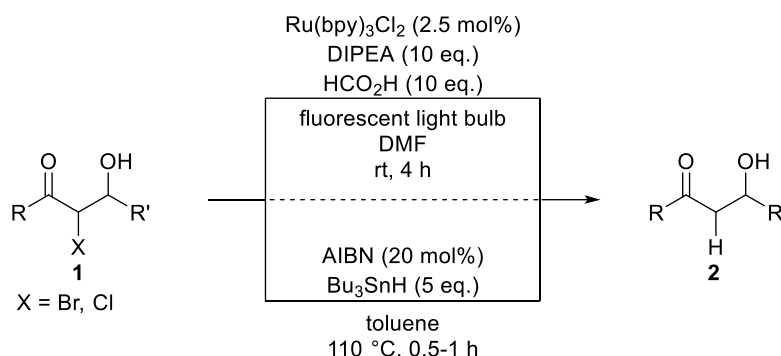


Figure 1-1

This concept applies for both, coloured stable metal-containing complexes (mainly ruthenium or iridium based) and organic dye molecules (e.g. acridinium or xanthene dyes). The avoidance of high temperatures, radical starters, and, in some cases, strong oxidants or reductants are some of the intrinsic benefits of visible-light photoredox catalysis. In the following, we compare several selected examples of “classic” organic reactions and their photoredox-catalyzed versions.^[2] The photocatalytic reactions use similar or identical starting materials and yield the same product structure, as their thermal counterparts. This allows us to discuss and highlight the benefits, but also some limitations, of photoredox reactions in direct comparison.

1.2. Photoredox catalyzed versions of classic radical reactions

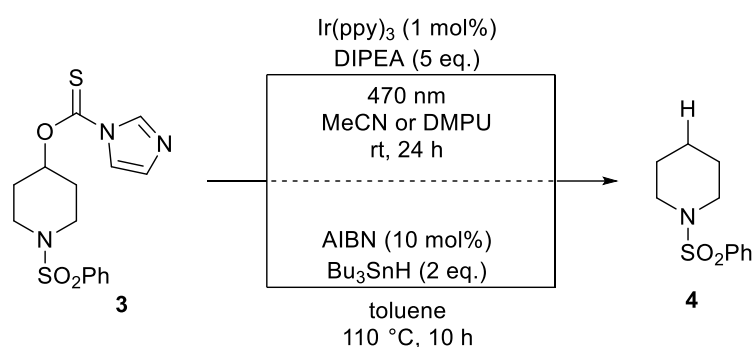
Radical species or radical ions are typical intermediates in photoredox-catalyzed reactions. In difference to electrochemical processes and conventional radical reactions, electrodes and radical initiators (e.g. azobisisobutyronitrile (AIBN) and di-*tert*-butylperoxid (DTPB)) are not required, but replaced by the photoredox catalyst.



Scheme 1-1

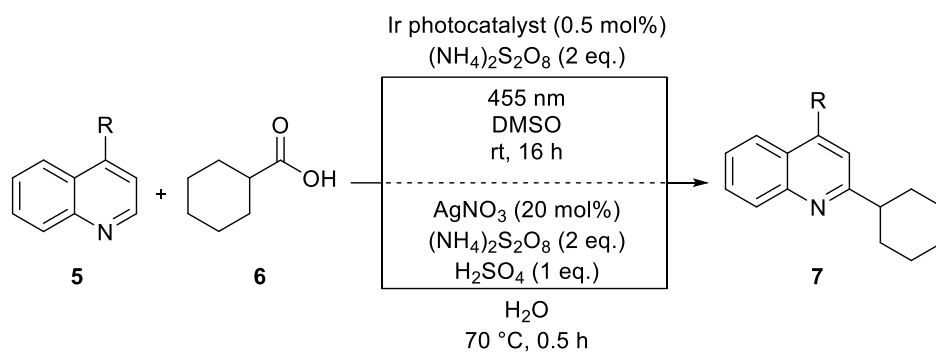
Organotin hydrides are potent hydrogen donating reagents to reduce radical species. However, stannanes are toxic, environmentally harmful and usually avoided in modern synthesis. Stephenson and coworkers developed a tin- and AIBN-free photoredox catalyzed system for the reductive dehalogenation of organic compounds (Scheme 1-1).^[3] *N,N*-diisopropylethylamine (DIPEA) serves as sacrificial electron donor, reducing the photocatalyst after its excitation. Carbon centered radicals and halides are formed after a SET from ruthenium(II). The *in situ* generated amine radical cation is postulated to serve as the hydrogen atom donor that reduces the C-centered radical by a hydrogen atom transfer (HAT). The authors do not report the quantum yield (i.e. formed product molecules per absorbed photon) of this reaction and their postulated pathway does not include a radical chain mechanism. The

classic pathway is different, as the reaction is started by the thermal decomposition of AIBN. The obtained radicals will react with the stannane yielding stannyl radicals that will subsequently abstract a halide atom from the substrate molecule. After HAT from Bu_3SnH a new stannyl radical is generated in this self-sustaining radical chain reaction. The high efficiency of this process will result in short reaction times.^[4] It should be noted that both, classic and photoredox catalyzed systems were developed, in which the toxic stannane was replaced by organosilanes that inherit only slightly higher M-H bond dissociation energies than Sn-H compounds.^[5]



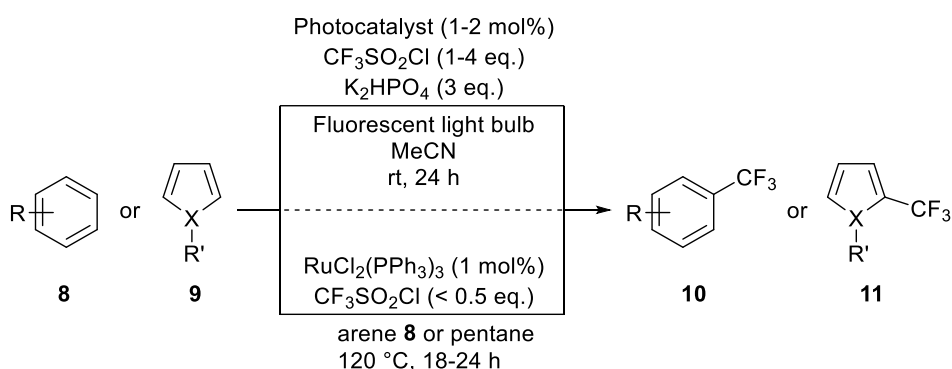
Scheme 1-2

Stannanes also play an essential role in other defunctionalization reactions. They are the key reactant of the Barton decarboxylation and the Barton-McCombie deoxygenation.^[6] The removal of hydroxyl and carboxylic acid groups is an important reaction, since many natural bulk products (e.g. carbohydrates or fatty and amino acids) possess those groups. A comparable photoredox catalyzed example for a reductive deoxygenation was reported by Fensterbank and coworkers.^[7] They prepared the respective O-thiocarbamates from the corresponding alcohols and reduced them via SET from excited Ir(ppy)_3 (Scheme 1-2). The cycle is closed by DIPEA, serving as electron and hydrogen donor. Moderate to good yields of the reduced product are obtained by both, Fensterbank's and Barton's conditions, when imidazolyl O-thiocarbamates are applied. The use of thiocarbonates or dithiocarbonates with organotin hydrides generally provides better yields.^[8] However, the thermal cleavage of AIBN and efficient chain propagation requires a high reaction temperature.



Scheme 1-3

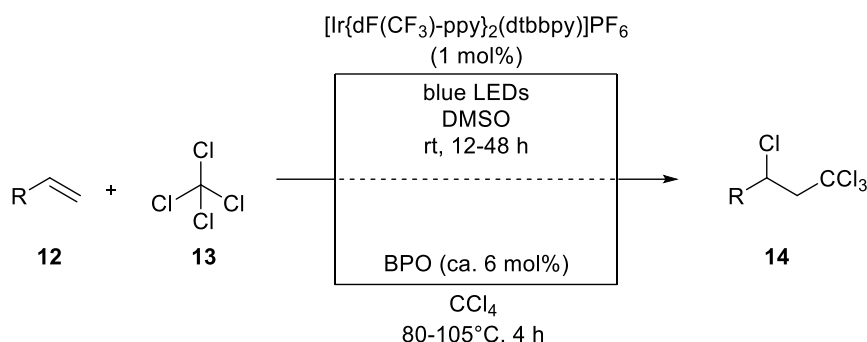
Decarboxylation of aliphatic organic acids can also be achieved without prefunctionalization. Deprotonated carboxylates are oxidized by SET, yielding the respective carboxyl radicals. These species are unstable and release CO_2 , generating the respective C-centered radicals. The obtained radicals can be applied in numerous coupling reactions.^[9] A classic example of such a decarboxylative coupling with nitrogen heterocycles is the Minisci reaction that is originally promoted by a combination of a silver(I) salt and persulfate.^[10] The reaction time is short and for simple acids and heterocycles the yields are high. However, functional group tolerance of this reaction is sometimes limited (e.g. vs fluorine atoms). Glorious and coworkers published a photoredox catalyzed version of the Minisci reaction that proceeds at room temperature without the addition of AgNO_3 and sulfuric acid (Scheme 1-3).^[11] The yields of this reaction are generally moderate to good and the functional group tolerance was improved. However, over-stoichiometric amounts of peroxides are required for both reaction types. Other photoredox catalyzed oxidative decarboxylation-addition reactions have been reported that do only require oxygen as electron acceptor or proceed in a redox neutral fashion.^[9, 12]



Scheme 1-4

Besides defunctionalization, radical functionalization reactions are commonly applied in chemical synthesis. Trifluoromethylation is a strategy that is widely used in medicinal chemistry for the synthesis of pharmacophores, possessing designed stability and binding properties.^[13] The formal coupling with a CF_3 group can be achieved by several procedures, including radical

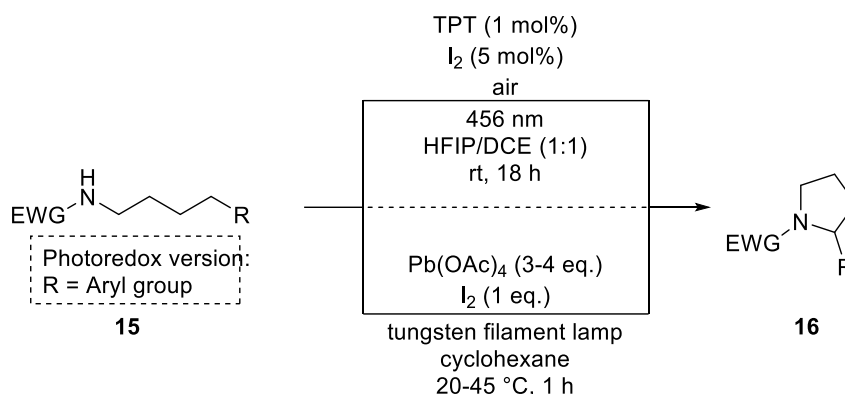
trifluoromethylation reactions.^[14] Trifluoromethanesulfonyl chloride has a reduction potential of ca. -0.2 V (vs standard calomel electrode) and therefore is easily reduced to the corresponding radical anion, which is unstable and will usually decompose to SO₂, a chloride anion and a trifluoro methyl radical. The [•]CF₃ radical readily reacts with benzene or more electron rich arenes and heteroarenes. Kamigata *et al.* showed that trifluoromethylated products can be obtained at elevated temperature with RuCl₂(PPh₃)₃ as catalyst.^[15] A SET from the Ru(II) complex is postulated to trigger the described reduction reaction of the [•]CF₃-precursor. However, good yields (based on triflyl chloride) were only obtained when the aromatic compound was applied as solvent or in excess concentration. The scope of this reaction was more deeply investigated with another type of perfluoroalkanesulfonyl chloride. MacMillan demonstrated a much milder photocatalyzed version of this reaction that was also proven to be suitable for late-stage functionalization of pharmacophores (Scheme 1-4).^[16] Ruthenium and iridium complexes can catalyse this visible-light mediated reaction, yielding up to 94% of the corresponding product based on the arene.



Scheme 1-5

A different method for the introduction of CF₃-groups into organic molecules are so called atom transfer radical addition (ATRA) reactions.^[17] This Kharasch reaction type is not limited to trifluoromethylation.^[18] Various addition reactions were reported that are promoted by radical initiators, metal catalysts, UV-light irradiation or visible-light photoredox catalysis. Usually a halogen atom is added to an olefin, together with an organic moiety. Probably the first photoredox catalyzed ATRA reaction was reported by Barton in 1994.^[19] However, Stephenson's photocatalyzed addition reactions gained more attention, as the product scope was broader, compared to the addition of PhSeTos to olefins by Barton. Furthermore, Stephenson presented examples that were also comparable to the compounds obtained by Kharasch and successors (Scheme 1-5).^[20] The classic reaction proceeds via a radical chain mechanism that is initiated by the homolytic cleavage of a peroxide, whereas the photoredox catalyzed reaction proceeds via the following pathway: The photocatalyst reduces the activated organohalide to form a halide anion and a radical species that will add to the olefin, creating a secondary radical. This species then promotes a radical chain reaction, or is

oxidized to the carbocation by the photocatalyst. The previously generated halide anion then adds to the carbocation yielding the final product (**14**).

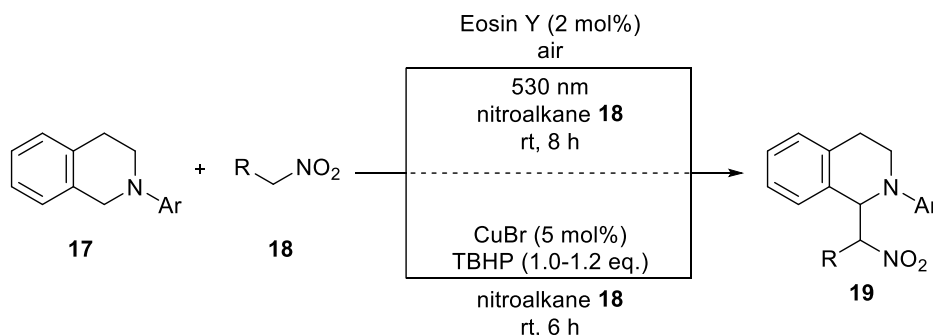


Scheme 1-6

A further classic radical reaction is the Hofmann-Löffler-Freytag reaction.^[21] This reaction is used for the synthesis of cyclic secondary or tertiary amines. Usually, *N*-halogenated acyclic amines are employed as starting materials at low pH values. After the initiation of a homolytic cleavage of the *N*-halide bond, the *N*-centered amidyl radical will abstract intramolecularly a hydrogen atom in the δ -position, resulting in the formation of a C-centered radical. The desired products (**16**) are formed upon halogen radical addition and a subsequent substitution reaction with the original amide moiety. Suárez *et al.* improved this reaction by the addition of iodine and Pb(OAc)₄ to electron deficient amines.^[22] Under these conditions, an unstable *N*-iodo intermediate is formed *in situ*. Cleavage of the labile N-I bond initiates then the described reaction. The Suárez modification greatly simplifies the synthesis, but over-stoichiometric amounts of Pb(OAc)₄ and one equivalent of iodine were required. Later, hypervalent iodine species were applied instead of lead(IV),^[23] and finally, Muñiz *et al.* managed to use molecular oxygen as oxidation agent in combination with 5% of iodine (Scheme 1-6). His group used triphenylpyrylium tetrafluoroborate (TPT) as photoredox catalyst to regenerate the I₂ species in the described reaction, which does anyhow require light irradiation to proceed. Aerial oxygen serves as sacrificial electron acceptor for the regeneration of the photocatalyst.

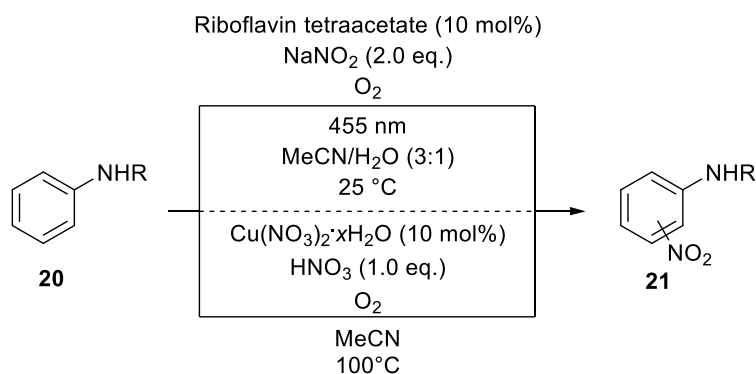
1.3. Replacement of transition metal catalysts by organic dyes

In some syntheses, e.g. the last steps of drugs, the use of transition metals should be avoided, as they are usually toxic and traces are laborious to remove. Organic photoredox catalysts can be a practical alternative to replace certain heavy metals in one electron oxidation or reduction reactions.^[24]



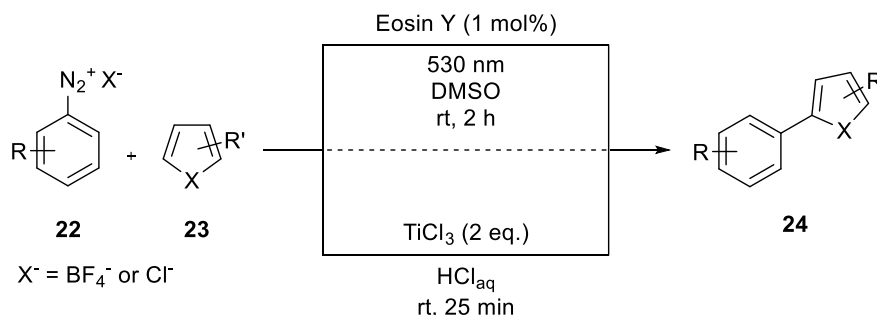
Scheme 1-7

Amino functionalities are easily oxidized to the respective radical cations that may rearrange under loss of a proton to α -amino radicals. However, if a suitable oxidant is present, a second oxidation step (e.g. HAT) yields the corresponding iminium cations. These cationic species readily react with various C-nucleophiles, resulting in the formation of new C-C bonds. With nitromethane as nucleophile the products of aza-Henry type reactions are obtained. A first photocatalytic example for the reaction with nitromethane was reported by Stephenson with an Ir(III)-photocatalyst.^[25] Our group developed a metal-free version, with Eosin Y as catalyst dye (Scheme 1-7).^[26] An advantage of this reaction is that aerial oxygen sufficiently promotes the regeneration of the catalyst's ground state and the subsequent oxidation of the amino radical cation to its iminium form. Li et al reported a classic copper catalyzed counterpart that is promoted by the addition of *tert*-butyl hydroperoxide (TBHP), as stoichiometric oxidant.^[27] This reaction, as the photocatalyzed version, proceeds at room temperature, whereas the replacement of the peroxide by oxygen in a metal catalyzed version requires higher temperatures.^[28] In both, the metal and the organo photocatalyzed reaction, the nitroalkane was used as the solvent. Nevertheless, also other nucleophiles (e.g. malonates or dialkyl phosphonates) are suitable coupling partners for the photocatalyzed reaction in DMF.^[26]



Scheme 1-8

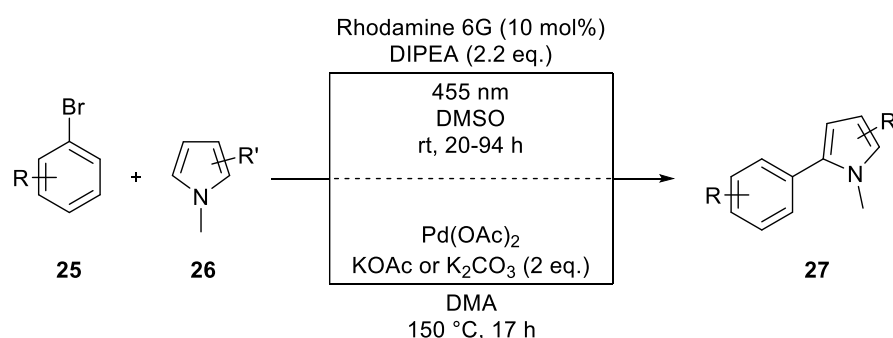
A further example is the nitration of protected anilines, promoted by a copper (I/II) redox pair in the presence of HNO₃ or riboflavin tetraacetate (RFTA) under blue light irradiation (Scheme 1-8).^[29] The RFTA photocatalyst has a dual purpose, as it can oxidize the aniline as well as the nitrite salt to the respective radical species. Thereby generated radicals can combine, as NO₂[•] is a persistent open-shell species. The visible-light mediated reaction is performed under acid-free conditions and proceeds well at 25 °C. In contrast, the metal catalyzed reaction benefits from elevated temperatures and the NO₂-source must be present in a higher oxidation state. Nevertheless, the copper catalyzed version affords higher yields for most substrates and the ligand-free metal species is more robust than the organic dye.



Scheme 1-9

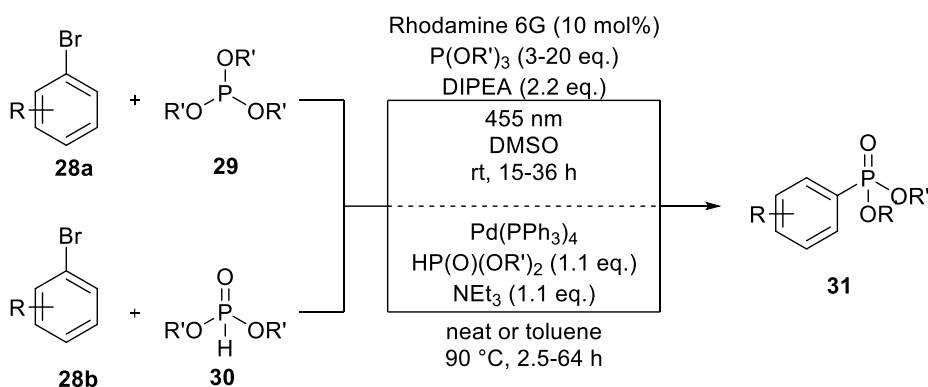
Another type of classic radical reactions are Meerwein-type arylation reactions, with aryl diazonium salts as starting material.^[30] Even weakly reducing metal species (usually copper or iron salts) can trigger the release of dinitrogen to promote the aryl radical formation. However, yields of the reaction products are often low. Cano-Yelo and Deronzier described the first photocatalytic intramolecular Pschorr-type version already in 1984.^[31] An intermolecular metal-free reaction was described by our group in 2012 (Scheme 1-9).^[32] This Eosin Y catalyzed metal-free aryl-heteroaryl coupling provides better yields than the classic Meerwein-conditions. The excited photocatalyst reduces the diazonium salt via SET. The reduced photocatalyst is later regenerated by re-oxidation of the radical coupling product. Eosin Y was

also applied in aryl-alkene couplings, although the yields are lower than those obtained with $\text{Ru}(\text{bpy})_3\text{Cl}_2$ as photocatalysts, or direct metal catalyzed aryl-alkene coupling.^[33] Heinrich et al. reported that TiCl_3 in hydrochloric acid can also be employed as reducing agent to promote classic aryl-aryl coupling reactions.^[34] Amino groups are stable under these conditions and good yields are obtained. However, an acid aqueous reaction media is required and the use of an over-stoichiometric amount of reducing agent is recommended by the authors.



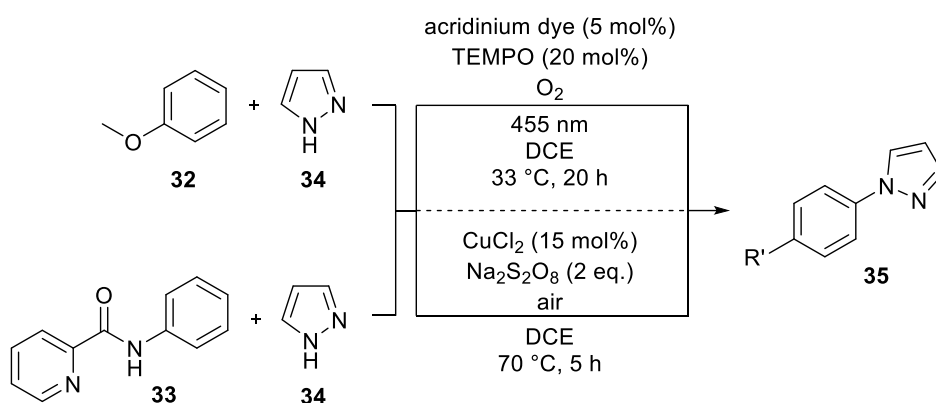
Scheme 1-10

A further method for the generation of aryl radicals is the reduction of aryl halides via SET. Whereas electron deficient iodo arenes can be reduced by common photocatalysts in presence of a sacrificial electron donor (e.g. trimethylamine or Hünig's base (DIPEA)), a consecutive photo induced electron transfer (conPET) system is required for the more challenging reduction of aryl bromides or chlorides.^[35] Perylenediimides or rhodamine 6G are organic dyes that can be reduced to coloured radical anions in a photocatalytic process.^[36] The radical anion absorbs a second photon and the highly reducing state of the excited radical anion is then promoting the reduction of an aryl halide to generate a C-centered radical upon release of a halogen anion. Thereby formed radicals are trapped with a sufficient trapping agent, such as electron rich (hetero)arenes (Scheme 1-10). Comparable products are obtained via C-H arylation palladium catalysis under alkaline conditions at high temperature.^[37] Nevertheless, the latter classic method bears some benefits, as no sacrificial amine is necessary, the catalyst loading is low, and most notably, only a slight excess of the trapping reagent is needed. In contrast, 5-25 equivalents of coupling partner are required for the photocatalyzed version, to prevent the formation of reduced compounds via hydrogen abstraction. It should be noted that despite aryl radical formation via conPET is postulated, a general Meerwein-type reactivity (e.g. for aryl-alkene coupling) was not observed.



Scheme 1-11

The conPET system was also applied for the formation of aryl phosphonates from trialkyl phosphites (Scheme 1-11).^[38] This class of compounds is traditionally obtained by a palladium catalyzed Hirao coupling of dialkyl phosphites with phenyl halides.^[39] Both types of reactions are variations of the Michaelis-Arbuzov reaction that can only deliver alkyl phosphonates.^[40] Like for the previously described systems, the amount of trapping reagent (i.e. phosphite) is higher for the photoredox catalyzed room temperature reaction (3-20 eq.), whereas high temperatures are required for the metal catalyzed reaction system.



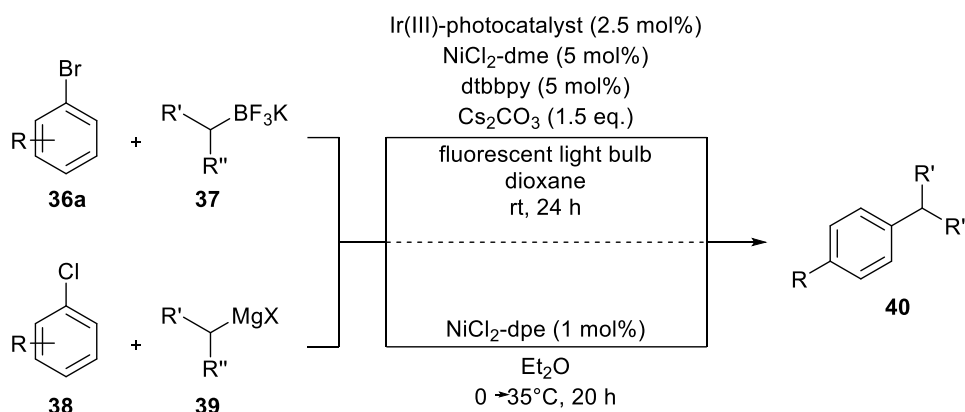
Scheme 1-12

Another classic reaction type for formation of C-C or C-heteroatom bonds by the conversion of aryl halides are copper catalyzed Ullmann type coupling reactions. Taillefer et al reported a method for the coupling of aryl bromides with pyrazole in 2004.^[41] Copper(I) oxide in combination with an oxime ligand was employed at elevated temperature to obtain the product in high yield and, due to the directing leaving group, in perfect regioselectivity. Direct C-H functionalization with pyrazole was reported for arenes containing directing groups in the presence of CuCl_2 and persulfate (Scheme 1-12).^[42] Copper(II) is coordinated by a picolinamide moiety and addition of pyrazole occurs in para position after a SET from the arene to the copper(II) species. The product is obtained after re-oxidation of copper(I) and

deprotonation of the arene. The directing group can be cleaved off afterwards by the reaction with NaOH at elevated temperature. The previously depicted photocatalyzed arylation reactions (Schemes 1-9 to 1-11) proceed via the formation of aryl radical species with localized single occupied sp^2 orbitals. However, Fukuzumi and others described the formation of delocalized aryl radical cations by visible-light mediated oxidation of arenes with organic acridinium dyes.^[43] Nicewicz and coworkers synthesized a library of these organic photoredox catalysts and presented an oxidative aryl amination reaction with (2,2,6,6-tetramethylpiperidin-1-yl)oxyl (TEMPO) as co-catalyst (Scheme 1-12).^[44] Electron rich arenes (e.g. anisole) are oxidized under oxygen atmosphere to the respective aryl radical cations that will react with pyrazole derivatives as nucleophiles. The oxidation potential of the arene is lower than the oxidation potential of the nucleophilic pyrazole, whereas the excited catalyst's potential is in-between. A great benefit of this reaction is that no leaving groups are required. Still, good side-selectivity is obtained for most substrates in this C-H functionalization reaction. In contrast to the Ullmann reaction, electron deficient arenes are not suitable. Our group reported a general protocol for the direct C-H amination of arenes with 2,3-dichloro-5,6-dicyano-p-benzoquinone (DDQ) under aerobic conditions.^[45] Due to the high oxidation potential of the triplet state of DDQ ($E_{ox} \approx 3.18$ V vs SCE), electron deficient arenes are successfully coupled.

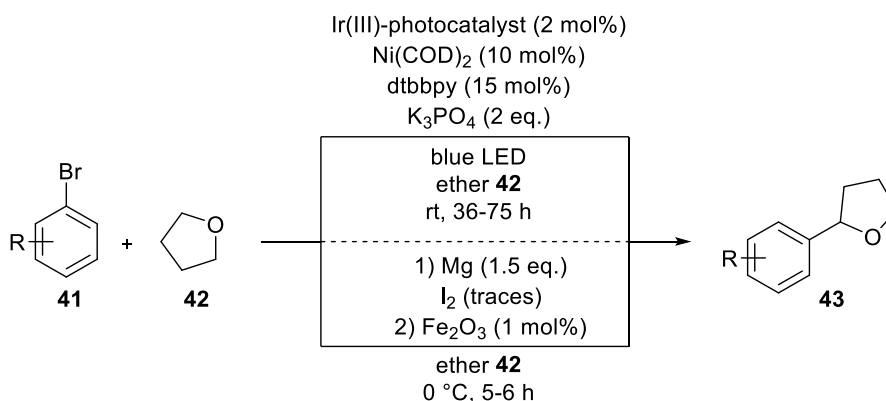
1.4. Combination of photoredox catalysis with other catalytic systems

Photoredox catalysis should not just be seen as an alternative catalytic approach to replace common strategies. It is also a tool that can be combined with other catalytic approaches, to achieve synthetic goals. The classic Nobel Prize awarded transition metal catalyzed cross coupling reactions offer great reactivity and are therefore widely applied in organic synthesis. However, slow reaction kinetics of the two-electron transmetalation step can hamper the effectivity of the sp^2 - sp^3 coupling in Suzuki-Miyaura type reactions. The integration of photocatalytically generated radicals into the catalytic cycle of a transition metal addresses this problem, as the open shell transmetalation is very efficient.^[46] Photoredox catalysis was merged with the catalytic benefits of numerous d-block elements. Especially the combination with nickel catalysis gained the attraction of many work groups during the last years.^[47] Apart from that, photoredox catalysis was combined with covalent and non-covalent organo catalysis.^[48] An example for this type of reactivity is presented at the end of this Chapter.



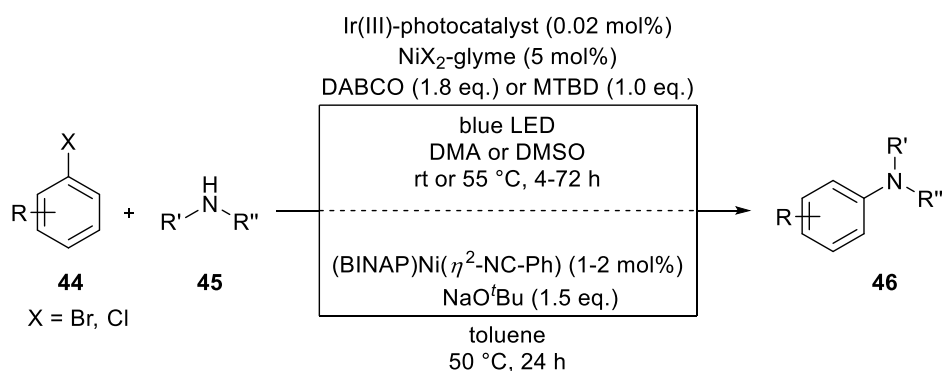
Scheme 1-13

The Kumada coupling is a well-known nickel (or palladium) catalyzed C-C bond forming reaction.^[49] Usually, sp² hybridized halides are coupled with aryl, vinyl or alkyl Grignard reagents, even though, coupling of alkyl halides is also possible with some limitations. The generally accepted mechanism proceeds via the common steps of an “oxidative addition – transmetalation – isomerization – elimination” pathway, including nickel(0) and nickel(II) species. The reaction is applied also in industrial synthesis, however, the use of magnesium organyls somewhat limits this reaction, concerning the functional group tolerance and reagent stability. Molander and coworkers replaced the metal organyl moiety by trifluoroborate salts that are bench stable and barely unreactive without an external trigger, but can easily be oxidized by a photoredox catalyst (Scheme 1-13).^[50] Upon an oxidative SET, BF₃ is released and the respective carbon-centered radical is formed. Like in the traditional reaction pathway of the Kumada or Suzuki coupling, an oxidative insertion of nickel(0) into the aryl bromide bond will take place. After radical addition to the nickel(II) complex a new instable nickel(III) species is formed that will eliminate the coupling product. The initial nickel(0) species can be regenerated by SET to nickel(I) from the reduced photocatalyst. This reaction was also investigated in an enantioselective fashion using chiral ligands.^[51] A radical addition to the nickel(0) species before the oxidative metal insertion into the carbon-halide bond is an alternative mechanism proposed for this reaction type.



Scheme 1-14

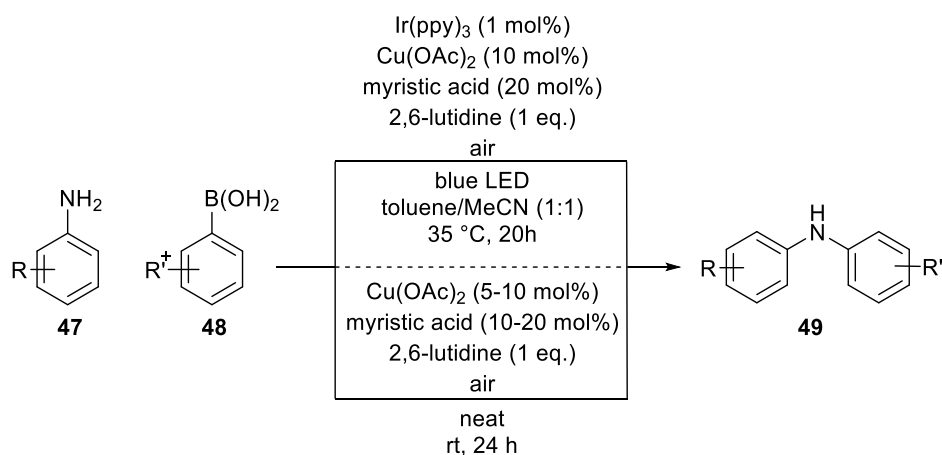
Multiple other types of leaving groups are suitable for radical-involving dual-catalytic reactions.^[48] Furthermore, also direct visible-light mediated photoredox C-H activation can afford radicals entering the catalytic cycle of a nickel complex. Doyle and Molander reported the α -arylation of ethers, such as tetrahydrofuran, by dual catalysis (Scheme 1-14).^[52] Hydrogen atoms are abstracted in α -position to the oxygen atom by in situ generated halide atoms. This kind of reactivity is hard to achieve under mild reaction conditions without the use of a photoredox catalyst. Nevertheless, the product can also be formed by the reaction of arylmagnesium halides with THF in the presence of 1 mol% of Fe₂O₃.^[53] This iron oxide catalyzed version proceeds well at 0 °C and generally delivers yields higher than 90%. However, metal organyls impose functional group limitations and the ether reactant is used as solvent for both reactions.



Scheme 1-15

Photoredox-nickel dual catalysis is also applicable for the formation of carbon-heteroatom bonds (e.g. C-N or C-O). The Buchwald-Hartwig amination is a highly elaborated palladium catalyzed reaction that was constantly improved since it was first described in 1994.^[54] The careful ligand design is essential for adapting the catalyst to the desired reaction. The replacement of palladium by less expensive nickel is challenging, as the reductive elimination of C-N compounds is thermodynamically disfavoured for nickel(II) complexes. Nevertheless,

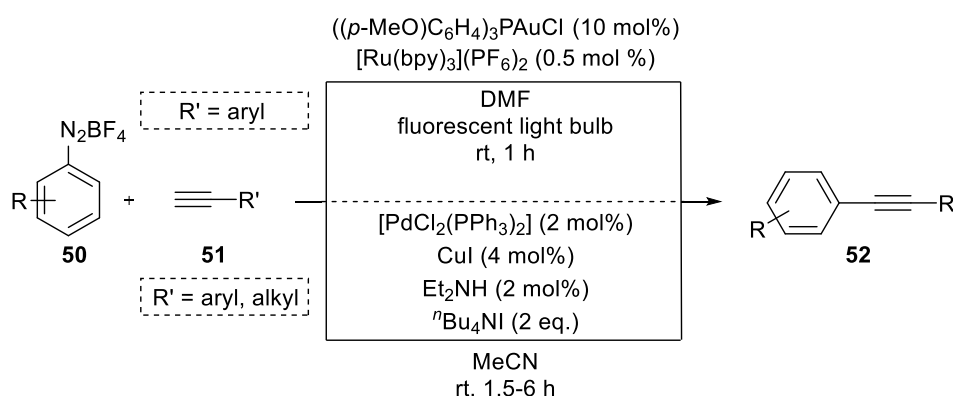
Hartwig and coworkers realized the effective amination of aryl halides, also with primary amines, by the use of a potent but air sensible ligated nickel(0) species in the presence of a strong base.^[55] Another approach was presented by Buchwald together with the MacMillan group.^[56] The authors reported a nickel based “ligand-free” system that is enabled by the combination of an iridium(III) photoredox catalyst with a nickel(II) salt (Scheme 1-15). The required nickel(0) species is formed *in situ*. Many compounds were synthesized at room temperature in the presence of an organic base, but slightly elevated temperatures are beneficial for some reactions. In contrast to the previously discussed dual-catalytic systems, no free radicals are involved in this reaction as the photocatalyst alters the oxidation states of the nickel co-catalyst in the catalytic cycle of the transition metal. After the formation of a C-Ni(II)-N adduct, this species is proposed to be oxidized by SET to the photoredox catalyst. The elimination of the coupling product from the resulting nickel(III) species is then thermodynamically favoured. Aryl bromides and electron deficient aryl chlorides can be converted, whereas the procedure of Hartwig gives high yields even for electron rich aryl chlorides.



Scheme 1-16

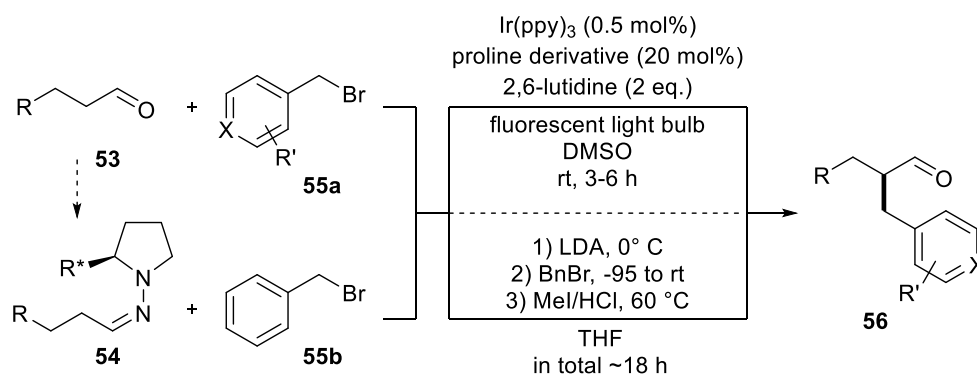
The combination of photoredox catalysis with metal catalysis was extended to other transition metal systems. The Chan-Lam reaction is another textbook name reaction that is used for C-N coupling of aryl boronic acids with amines under mild conditions and copper acetate as catalyst.^[57] The oxidative formation of a Cu(III) species is considered as key step. The reaction is generally conducted under air. Buchwald and Antilla presented a general procedure for the coupling of amines with boronic acids.^[58] Whereas the yields for aniline derivatives are generally moderate to high, the coupling with electron deficient halogenated boronic acids is not satisfying. Kobayashi and coworkers improved the reaction by the use of a photoredox catalyst (Scheme 1-16).^[59] They postulated that the excited state of the Ir(ppy)₃ catalyst will be quenched by air to form an Ir(IV) species that can promote the oxidation of Cu(II) to Cu(III).

Kobayashi states that the dual-catalytic conditions are not always better, also concerning a practical point of view, than Buchwald's classic reaction conditions. Still, for many examples good to excellent yields were obtained. A drawback is that only arylamines are reported to be suitable for this photoredox enhanced Chan-Lam reaction. Buchwald showed that also *N*-alkyl aniline products are obtained in moderate yield by the coupling of *N*-alkyl amines under his reaction conditions.



Scheme 1-17

Photoredox catalyzed variations of the Sonogashira cross coupling were presented by our group^[33] and the group of Glorius.^[60] Whereas the traditional Sonogashira coupling describes a palladium catalyzed sp-sp² coupling of terminal alkynes with halides or triflates,^[61] Glorius used a gold(I) complex for the coupling of aryl diazonium salts with alkynes (Scheme 1-17). A palladium catalyzed version, without photocatalyst, but with a copper iodide co-catalysts, was published by Cacchi in 2010.^[62] A benefit of the photoredox dual-catalysis system is that no additional base is required. However, the gold-catalyst loading is relatively high. The postulated mechanism proceeds via the reductive photocatalyzed formation of aryl radicals. Upon radical addition to the Au(I) complex, the formed Au(II) species is oxidized by the photocatalyst and the alkyne can coordinate to the generated Au(III) species. Release of the product will regenerate the initial Au(I) catalyst. The quantum yield of this reaction is larger than one. Therefore, an efficient radical chain process must take place and short reaction times of 1 h are possible. A further benefit is the stability of additional aryl bromide moieties under these conditions. The palladium catalyzed version is postulated to proceed via a classic reaction mechanism after *in situ* "iododediazotiation" of the diazonium salt (i.e. replacement of $-\text{N}_2^+$ by the halide).^[63] Palladium(0) inserts into the generated aryl iodine bond and the aryl palladium iodide reacts with *in situ* formed copper acetylides, before the release of the coupling product. The latter reaction also proceeds, in contrast to photoredox catalyst version, with aliphatic alkynes within short reaction times at room temperature. It should be noted that also other gold catalyzed systems were reported that do not require a photoredox co-catalyst.^[64]



Scheme 1-18

As a last example, we discuss the combination of photoredox catalysis and covalent organocatalysis. The enantioselective α -alkylation of carbonyl groups is an important task, wherefore diverse systems have been developed for this type of functionalization. The stoichiometric transformation of the carbonyl group into a stable enolate-type derivative in combination with chiral Lewis acids or the use of chiral auxiliaries are typical procedures.^[65] Nevertheless, the α -alkylation of aldehydes is demanding, as side reactions can easily occur. Enders and coworkers reported the formation of stable chiral hydrazones by the reaction of aldehydes with chiral hydrazine auxiliaries (e.g. (S)-1-amino-2-(methoxymethyl)pyrrolidine = SAMP).^[66] These hydrazones can be deprotonated in α -position with LDA. The formed anion species will then react via substitution with an alkyl halide. Finally, the auxiliary has to be cleaved off by the use of ozone or a combination of methyl iodide and hydrochloric acid. The discovery of proline organocatalysis facilitated the direct chiral α -functionalization of aldehydes, especially for aldol and Michael addition reactions. Nevertheless, alkylation by halide substitution was reported by List to occur only in an intramolecular fashion.^[67] By photoredox catalysis a different reaction pathway becomes possible. The respective halide is reduced via SET, in order to form an alkyl radical together with a halide anion. Electrophilic radicals will readily react in α -position with *in situ* formed chiral enamines.^[68] The resulting alpha amino radical is then re-oxidized by the catalyst, and the product subsequently liberated by hydrolysis of the iminium ion (Scheme 1-18). This method is easy applicable and gives good results. However, radical formation must be feasible, wherefore radical stability and the reduction potentials of catalyst and substrate must match. Non-activated alkyl bromides and chlorides are not converted under the currently available conditions.

1.6. Concluding remarks

We compared exemplary photoredox-catalyzed reactions with non-photochemical methods and some well-known textbook reactions. It is not intended nor possible to provide a comprehensive overview, but more highlighting some unique features and differences of the two approaches. Photoredox catalysis can be a valuable alternative replacing classic reaction conditions. Furthermore, combining photoredox catalysis with existing catalytic methods can provide unprecedented reactivity. However, the practical implementation of photoredox catalysis in synthesis requires attention and skills. The extinction coefficient of the photocatalyst and its concentration limit the light penetration depth into reactions mixtures. Capillary flow photoreactors provide a solution and allow for continuous larger-scale synthesis. Although organic photoredox catalysts can in many cases replace redox active transition metal complexes, such as $\text{Ru}(\text{bpy})_3^{2+}$ or $\text{Ir}(\text{ppy})_3$, their stability under the reaction conditions can be insufficient. Heterogenous photocatalysts may become the material of choice for continuous or larger-scale synthetic photocatalysis, but their development is still at an early stage.^[69]

Oxidation and reduction reactions, with or without light, require either terminal oxidants or reductants, respectively, in stoichiometric amounts. Photocatalysis can enhance their reduction or oxidation power and aerial oxygen or simple amines can be used as electron acceptors or donors. However, the resulting products may cause side reactions and diminish the overall atom economy. Regeneration of oxidizing and reducing reagents by electrochemical methods may improve this for photocatalytic and non-photocatalytic reactions.

Photocatalytic reaction conditions have evolved over the last 15 years into valuable alternatives, extensions and in some cases even unique transformations. The development is still ongoing and many more reactions and catalyst systems will be reported in the next years. However, like every methodology in chemistry, photochemistry also comes with limitations and challenges. It is therefore important to evaluate for each synthetic step the available method options, and chose the best one depending on the given constrains and demands.

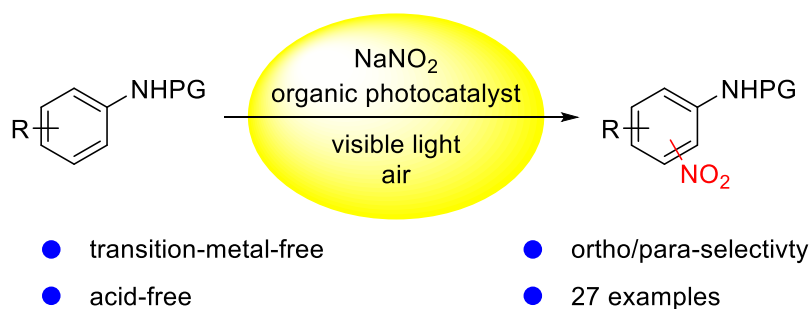
1.7 References

- [1] W. M. Jarman, K. Ballschmiter, *Endeavour* **2012**, 36, 131-142.
- [2] L. Marzo, S. K. Pagire, O. Reiser, B. König, *Angew. Chem., Int. Ed.* **2018**, 57, 10034-10072.
- [3] J. M. R. Narayanam, J. W. Tucker, C. R. J. Stephenson, *J. Am. Chem. Soc.* **2009**, 131, 8756-8757.
- [4] a) E. J. Corey, S. Choi, *Tetrahedron Lett.* **1991**, 32, 2857-2860; b) F. Alonso, I. P. Beletskaya, M. Yus, *Chem. Rev.* **2002**, 102, 4009-4092.
- [5] C. Chatgililoglu, C. Ferreri, Y. Landais, V. I. Timokhin, *Chem. Rev.* **2018**, 118, 6516-6572.
- [6] D. Crich, L. Quintero, *Chem. Rev.* **1989**, 89, 1413-1432.
- [7] L. Chenneberg, A. Baralle, M. Daniel, L. Fensterbank, J.-P. Goddard, C. Ollivier, *Adv. Synth. Cat.* **2014**, 356, 2756-2762.
- [8] D. H. R. Barton, S. W. McCombie, *J. Chem. Soc., Perkin Trans. 1* **1975**, 1574-1585.
- [9] J. Schwarz, B. König, *Green Chem.* **2018**, 20, 323-361.
- [10] F. Minisci, R. Bernardi, F. Bertini, R. Galli, M. Perchinnunmo, *Tetrahedron* **1971**, 27, 3575-3579.
- [11] R. A. Garza-Sanchez, A. Tlahuext-Aca, G. Tavakoli, F. Glorius, *ACS Catalysis* **2017**, 7, 4057-4061.
- [12] L. Chu, C. Ohta, Z. Zuo, D. W. C. MacMillan, *J. Am. Chem. Soc.* **2014**, 136, 10886-10889.
- [13] S. Purser, P. R. Moore, S. Swallow, V. Gouverneur, *Chem. Soc. Rev.* **2008**, 37, 320-330.
- [14] A. Studer, *Angew. Chem., Int. Ed.* **2012**, 51, 8950-8958.
- [15] N. Kamigata, T. Ohtsuka, T. Fukushima, M. Yoshida, T. Shimizu, *J. Chem. Soc., Perkin Trans. 1* **1994**, 1339-1346.
- [16] D. A. Nagib, D. W. C. MacMillan, *Nature* **2011**, 480, 224-228.
- [17] D. B. Bagal, G. Kachkovskiy, M. Knorn, T. Rawnier, B. M. Bhanage, O. Reiser, *Angew. Chem., Int. Ed.* **2015**, 127, 7105-7108.
- [18] F. Minisci, *Acc. Chem. Res.* **1975**, 8, 165-171.
- [19] D. H. R. Barton, M. A. Csiba, J. C. Jaszberenyi, *Tetrahedron Lett.* **1994**, 35, 2869-2872.
- [20] M. S. Kharasch, E. V. Jensen, W. H. Urry, *Science* **1945**, 102, 128-128.
- [21] G. Majetich, K. Wheless, *Tetrahedron* **1995**, 51, 7095-7129.
- [22] a) R. Hernández, A. Rivera, J. A. Salazar, E. Suárez, *J. Chem. Soc., Chem. Commun* **1980**, 958-959; b) R. Carrau, R. Hernández, E. Suárez, C. Betancor, *J. Chem. Soc., Perkin Trans. 1* **1987**, 937-943.

- [23] R. L. Dorta, C. G. Francisco, E. Suárez, *J. Chem. Soc., Chem. Commun* **1989**, 1168-1169.
- [24] a) N. A. Romero, D. A. Nicewicz, *Chem. Rev.* **2016**, 116, 10075-10166; b) M. K. Bogdos, E. Pinard, J. A. Murphy, *Beilstein J. Org. Chem.* **2018**, 14, 2035-2064.
- [25] A. G. Condie, J. C. González-Gómez, C. R. J. Stephenson, *J. Am. Chem. Soc.* **2010**, 132, 1464-1465.
- [26] D. P. Hari, B. König, *Org. Lett.* **2011**, 13, 3852-3855.
- [27] Z. Li, C.-J. Li, *J. Am. Chem. Soc.* **2005**, 127, 3672-3673.
- [28] O. Basle, C.-J. Li, *Green Chem.* **2007**, 9, 1047-1050.
- [29] a) E. Hernando, R. R. Castillo, N. Rodriguez, R. Gomez Arrayas, J. C. Carretero, *Chem. Eur. J.* **2014**, 20, 13854-13859; b) S. J. S. Düsel, B. König, *J. Org. Chem.* **2018**, 83, 2802-2807.
- [30] H. Meerwein, E. Büchner, K. van Emster, *J. Prakt. Chem.* **1939**, 152, 237-266.
- [31] H. Cano-Yelo, A. Deronzier, *J. Chem. Soc., Perkin Trans. 2* **1984**, 1093-1098.
- [32] D. P. Hari, B. König, *Angew. Chem., Int. Ed.* **2013**, 52, 4734-4743.
- [33] P. Schroll, D. P. Hari, B. König, *ChemistryOpen* **2012**, 1, 130-133.
- [34] A. Wetzel, G. Pratsch, R. Kolb, M. R. Heinrich, *Chem. Eur. J.* **2010**, 16, 2547-2556.
- [35] I. Ghosh, T. Ghosh, J. I. Bardagi, B. König, *Science* **2014**, 346, 725-728.
- [36] I. Ghosh, B. König, *Angew. Chem., Int. Ed.* **2016**, 55, 7676-7679.
- [37] J. Roger, H. Doucet, *Adv. Synth. Cat.* **2009**, 351, 1977-1990.
- [38] R. S. Shaikh, S. J. S. Düsel, B. König, *ACS Catalysis* **2016**, 6, 8410-8414.
- [39] T. Hirao, T. Masunaga, Y. Ohshiro, T. Agawa, *Synthesis* **1981**, 56-57.
- [40] B. A. Arbuzov, *Pure Appl. Chem.* **1964**, 9, 307-335.
- [41] H.-J. Cristau, P. P. Cellier, J.-F. Spindler, M. Taillefer, *Eur. J. Org. Chem.* **2004**, 695-709.
- [42] J. Xu, K. Du, J. Shen, C. Shen, K. Chai, P. Zhang, *ChemCatChem* **2018**, 10, 3675-3679.
- [43] S. Fukuzumi, K. Ohkubo, *Org. Biomol. Chem.* **2014**, 12, 6059-6071.
- [44] N. A. Romero, K. A. Margrey, N. E. Tay, D. A. Nicewicz, *Science* **2015**, 349, 1326-1330.
- [45] S. Das, P. Natarajan, B. König, *Chem. Eur. J.* **2017**, 23, 18161-18165.
- [46] J. C. Tellis, C. B. Kelly, D. N. Primer, M. Jouffroy, N. R. Patel, G. A. Molander, *Acc. Chem. Res.* **2016**, 49, 1429-1439.
- [47] J. Twilton, C. Le, P. Zhang, M. H. Shaw, R. W. Evans, D. W. C. MacMillan, *Nat. Rev. Chem.* **2017**, 1, 0052.
- [48] K. L. Skubi, T. R. Blum, T. P. Yoon, *Chem. Rev.* **2016**, 116, 10035-10074.
- [49] K. Tamao, K. Sumitani, M. Kumada, *J. Am. Chem. Soc.* **1972**, 94, 4374-4376.

- [50] D. N. Primer, I. Karakaya, J. C. Tellis, G. A. Molander, *J. Am. Chem. Soc.* **2015**, *137*, 2195-2198.
- [51] O. Gutierrez, J. C. Tellis, D. N. Primer, G. A. Molander, M. C. Kozlowski, *J. Am. Chem. Soc.* **2015**, *137*, 4896-4899.
- [52] a) B. J. Shields, A. G. Doyle, *J. Am. Chem. Soc.* **2016**, *138*, 12719-12722; b) D. R. Heitz, J. C. Tellis, G. A. Molander, *J. Am. Chem. Soc.* **2016**, *138*, 12715-12718.
- [53] P. P. Singh, S. Gudup, S. Ambala, U. Singh, S. Dadhwal, B. Singh, S. D. Sawant, R. A. Vishwakarma, *Chem. Commun.* **2011**, *47*, 5852-5854.
- [54] a) A. S. Guram, S. L. Buchwald, *J. Am. Chem. Soc.* **1994**, *116*, 7901-7902; b) M. M. Heravi, Z. Kheilkordi, V. Zadsirjan, M. Heydari, M. Malmir, *J. Organomet. Chem.* **2018**, *861*, 17-104.
- [55] S. Ge, R. A. Green, J. F. Hartwig, *J. Am. Chem. Soc.* **2014**, *136*, 1617-1627.
- [56] E. B. Corcoran, M. T. Pirnot, S. Lin, S. D. Dreher, D. A. DiRocco, I. W. Davies, S. L. Buchwald, D. W. C. MacMillan, *Science* **2016**, *353*, 279-283.
- [57] P. Y. S. Lam, C. G. Clark, S. Saubern, J. Adams, M. P. Winters, D. M. T. Chan, A. Combs, *Tetrahedron Lett.* **1998**, *39*, 2941-2944.
- [58] J. C. Antilla, S. L. Buchwald, *Org. Lett.* **2001**, *3*, 2077-2079.
- [59] W.-J. Yoo, T. Tsukamoto, S. Kobayashi, *Angew. Chem., Int. Ed.* **2015**, *54*, 6587-6590.
- [60] A. Tlahuext-Aca, M. N. Hopkinson, B. Sahoo, F. Glorius, *Chem. Sci.* **2016**, *7*, 89-93.
- [61] R. Chinchilla, C. Nájera, *Chem. Soc. Rev.* **2011**, *40*, 5084-5121.
- [62] G. Fabrizi, A. Goggiamani, A. Sferrazza, S. Cacchi, *Angew. Chem., Int. Ed.* **2010**, *49*, 4067-4070.
- [63] A. L. J. Beckwith, G. F. Meijs, *J. Org. Chem.* **1987**, *52*, 1922-1930.
- [64] H. Peng, R. Cai, C. Xu, H. Chen, X. Shi, *Chem. Sci.* **2016**, *7*, 6190-6196.
- [65] a) M. C. Kohler, S. E. Wengryniuk, D. M. Coltart, in *Stereoselective Synthesis of Drugs and Natural Products* (Eds.: V. Andrushko, N. Andrushko), John Wiley & Sons, Inc, **2013**, pp. 183-213; b) R. Cano, A. Zakarian, G. P. McGlacken, *Angew. Chem., Int. Ed.* **2017**, *56*, 9278-9290.
- [66] a) D. Enders, H. Eichenauer, *Tetrahedron Lett.* **1977**, *18*, 191-194; b) A. Job, C. F. Janeck, W. Bettray, R. Peters, D. Enders, *Tetrahedron* **2002**, *58*, 2253-2329.
- [67] N. Vignola, B. List, *J. Am. Chem. Soc.* **2004**, *126*, 450-451.
- [68] a) D. A. Nicewicz, D. W. C. MacMillan, *Science* **2008**, *322*, 77-80; b) H.-W. Shih, M. N. Vander Wal, R. L. Grange, D. W. C. MacMillan, *J. Am. Chem. Soc.* **2010**, *132*, 13600-13603.
- [69] H. L. Tan, F. F. Abdi, Y. H. Ng, *Chem. Soc. Rev.* **2019**, *48*, 1255-1271.

2. Visible-light mediated nitration of protected anilines



The photocatalytic nitration of protected anilines proceeds with riboflavin tetraacetate as organic photoredox catalyst. Sodium nitrite serves as NO_2 -source in the visible-light driven room temperature reaction. Various nitroanilines are obtained in moderate to good yields without the addition of acid or stoichiometric oxidation agents. The catalytic cycle is closed by aerial oxygen as the terminal oxidant.

This Chapter has been published in:

S. J. S. Düsel, B. König, *J. Org. Chem.*, **2018**, 83, pp 2802–2807.

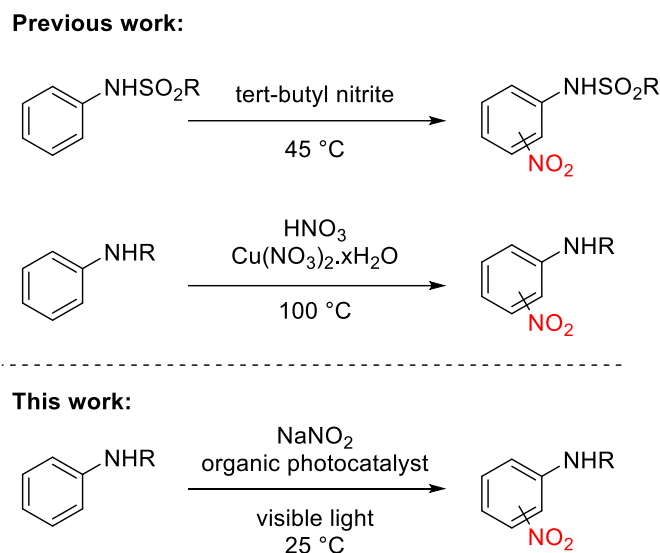
Reproduced with permission from *J. Org. Chem.*, **2018**, 83, pp 2802–2807. Copyright © 2018, American Chemical Society.

Author contributions:

SJSD discovered the reaction, carried out the experiments, and wrote the manuscript. BK supervised the project and is the corresponding author.

2.1 Introduction

Nitroanilines are an important class of compounds that are used as precursors in the synthesis of dyes, pigments and drugs.^[1] The classic nitration process of arenes requires harsh reaction conditions with high temperature and strong acids. Milder methods that allow the presence of sensitive functional groups were therefore developed.^[2] *Tert*-butyl nitrite was shown to be a potent nitration reagent at slightly elevated temperatures for the nitration of aromatic sulfonamides.^[3] However, differently protected anilines (e.g. amides) can only be obtained at high temperatures using copper catalysis.^[4] Many recently reported methods require transition metal catalysts or stoichiometric amounts of oxidants.^[5] Furthermore, nitration methods that work for a variety of functional groups are scarce. In this regard the work of Carretero is an exception, as they present a versatile copper catalyzed procedure for differently protected anilines with HNO_3 as NO_2 -source, though temperatures of 100 °C are required (Scheme 2-1).^[6] This motivated us to develop a room temperature nitration protocol that works for a broad range of differently protected anilines without the use of transition metals or acids. Many photoredox catalyzed reactions can be performed at room temperature.^[7] Moreover, such radical reactions open new pathways for substitution and for C-H functionalization reactions.^[8] Metal contamination can be avoided by using organic photocatalysts, which are typically of low cost.^[9]



Scheme 2-1. Recent methods for the nitration of protected anilines.^[3, 6]

2.2 Results and discussion

2.2.1 Synthesis

We started our investigations with sodium nitrite as NO_2 -source. To our delight, blue light irradiation with riboflavin tetraacetate (RFTA) as photocatalyst allowed the nitration of *N*-Boc-aniline.^[10] To solubilize the nitrite salt and the organic starting material, a 3 : 1 mixture of acetonitrile and water was used. The reaction progress was monitored by TLC and GC-FID analysis, showing that after complete conversion of the starting material slow degradation of the often colored products occurs. Therefore, the reaction time was adjusted for every compound. Anilines are typically protected as (PhNHR) carbamide (R = Boc, Cbz, Fmoc), sulfonamide (R = Ts, Ms) and amide (Ac, Bz). We therefore investigated our method on these substances (Table 2-1) and obtained moderate to good yields. The oxidation potentials of the anilines reside in the range of +1.7 V to +1.9 V (vs SCE in pure MeCN), but for the sulfonamide species a second oxidation peak (+1.91 V for **5a**; +1.89 V for **6a**) was measured indicating that further oxidation to an undesired species can be the origin of the diminished yield.^[11] The *para*-product was obtained as the major regioisomer in all experiments. Fmoc protected aniline (**7a**) is not suitable for this method, as this substrate is poorly soluble in the used solvent mixture. Furthermore, deprotection and undesired side reactions occur for this substrate.

Table 2-1. Photocatalytic nitration of differently protected anilines.

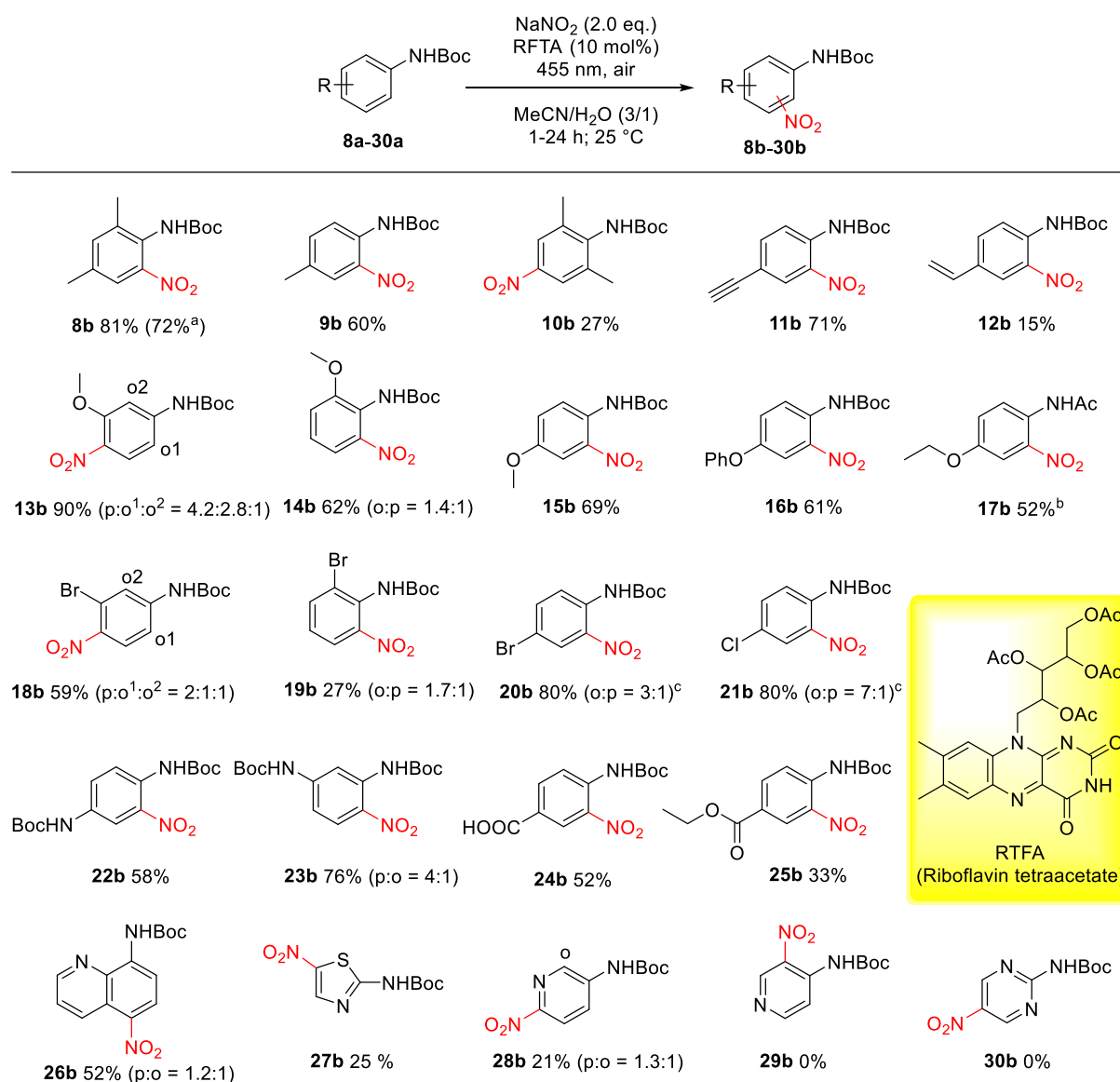
Entry	Compound	R =	E_{ox} (V)	Time (h)	Yield ^a (%)	
					1b-7b	1c-7c
1	1a	Boc	1.75	10	41	45
2	2a	Cbz	1.70	6	36	43
3	3a	Bz	1.83	8	28	41
4	4a	Ac	1.75	10	28	33
5	5a	Ts	1.77	5	37	50
6	6a	Ms	1.74	8	25	35
7	7a	Fmoc	1.87	8	>10	>10 ^b

Reaction conditions: Aniline **1a-7a** (0.2 mmol), sodium nitrite (0.4 mmol), RFTA (10 mol%) in a mixture of acetonitrile (3 mL) and water (1 mL) distributed over 4 glass vials irradiated from the bottom side with a blue LED at 25 °C. [a] Isolated yields. [b] Inseparable mixture, no full conversion.

The scope was expanded to differently *N*-Boc protected anilines (Table 2-2), as this class of compounds is, in contrast to sulfonamides, not well represented in the recent nitration literature. The reaction times vary between 1 h and 24 h. For electron-rich methoxy-substituted derivatives **13a-15a** good yields and complete conversion to the *ortho* and *para* regioisomers are achieved after a maximum of 6 h. Phenacetin (**17a**), a former used acetylated drug, is nitrated with a yield of 52% after 6 h, while for longer reaction times dinitration and degradation can be observed for this compound. Alkynes are tolerated, but vinyl anilines are not stable under the oxidative conditions. Partial oxidation of the double bond as well as vinylic NO₂ addition and polymerization were observed for **12a**. The reaction time for less activated anilines as halogenated anilines or aminobenzoic acid derivatives increases to 8 h - 10 h. Only for *para*-halogenated compounds **20b** and **21b** a small amount of *ipso*-substituted nitration product **1c** is obtained.^[12] The yield drastically decreases when this method is applied to very electron deficient heterocycles. For compound **29a** and **30a** more than 90% of the starting material can

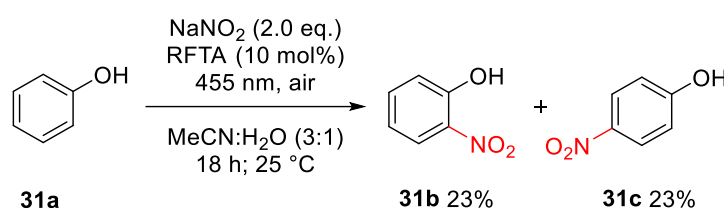
be reisolated. The oxidation potential of the excited catalyst is too low for the oxidation of these compounds.^[13] For compounds **8a-28a** neither large amounts of starting material nor any specific side products could be isolated. It is known that unprotected anilines easily polymerize upon oxidation.^[14] Related degradation pathways must be taken into account for the herein presented compounds that provided lower yield.

Table 2-2. Nitration of *N*-Boc-anilines.



Reaction conditions: Aniline **8a-30a** (0.2 mmol), sodium nitrite (0.4 mmol), RFTA (10 mol%) in a mixture of acetonitrile (3 mL) and water (1 mL) distributed over 4 glass vials irradiated from the bottom side with a blue LED at 25 °C for 1-24 h. Isolated yields. The major isomer is shown. [a] Reaction of **8a** (0.2 mmol) was performed in a single vial. [b] *N*-Acetylated starting material. [c] *para*-Isomer obtained by *ipso*-substitution of the halide atom.

Most of the obtained products absorb light in the same spectral region as the photocatalyst. A sufficient light input into the reaction mixture was achieved using a low concentration (0.05 M) of the aniline. For each compound four separate reaction vials were used in parallel and combined before workup to ensure a good light penetration into the reaction mixture. Applying a segmented flow system did not provide satisfying results. The herein described method was also used for the nitration of phenol (Scheme 2-2), yielding 46% of nitrophenol (**31b** + **31c**). A likely rational explanation for the diminished product yield is the known tendency of the intermediate phenoxyradicals to polymerize.^[15] (For the variation of the reaction conditions, see Chapter 2.4.2, Tables 2-4 and 2-5).



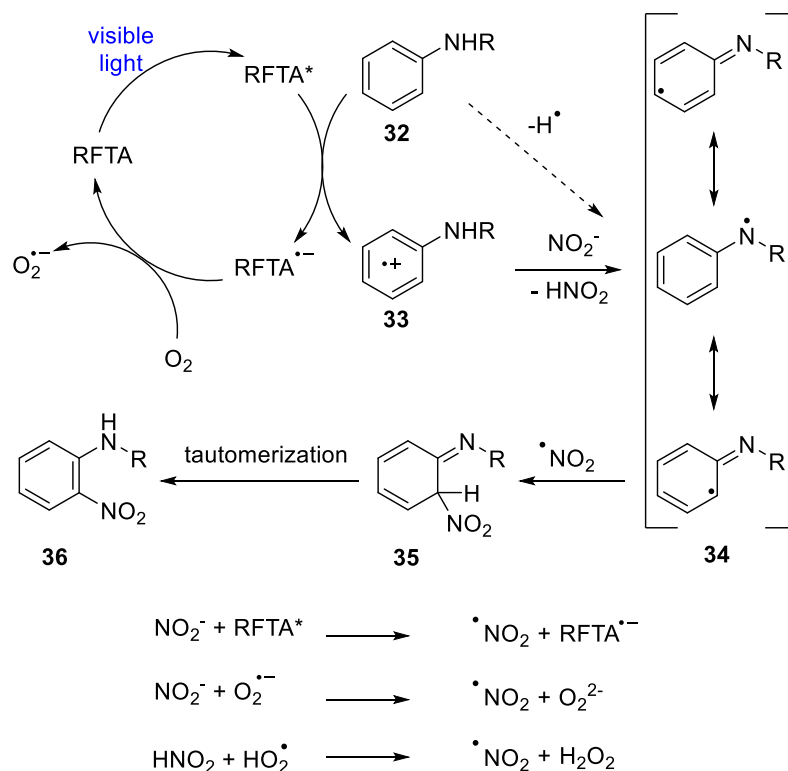
Scheme 2-2 Photocatalytic nitration of phenol.

Reaction conditions: Phenol (**31a**) (0.05 mmol), sodium nitrite (0.1 mmol), RFTA (10 mol%) in a mixture of acetonitrile (0.75 mL) and water (0.25 mL), irradiated with a blue LED at 25 °C. Yields determined by analytical HPLC with naphthalene as internal standard.

2.2.2 Mechanistic investigations

In Scheme 2-3 we propose a mechanism of the photo-nitration. The non-photocatalyzed parts of the mechanistic proposal are in agreement with literature reports.^[3, 4, 6] The photocatalyst, after excitation, oxidizes the aniline derivative **32**.^[16] The acidity of radical cations increases compared to the neutral compound and therefore the consecutive formation of the stabilized radical **34** via loss of a proton can occur.^[17] Nitrogen dioxide as a persistent radical species is formed via different pathways and is able to react with **34**.^[18] After rearomatization, the desired *para*- and *ortho*-regioisomeric substitution products are obtained. Direct H-abstraction from **32** by reactive oxygen species as alternative or additional route to the amidyl radical **34** cannot be excluded at this stage of the investigation. In 2010 Ivanov et al. reported a photo induced electron transfer from the nitrite anion to excited riboflavin, confirmed by fluorescence quenching experiments.^[19] We find emission quenching for the acetylated derivative of the dye by sodium nitrite. However, in contrast to Ivanov's observation, we observe dynamic quenching (Stern-Volmer constant $K_{SV} = 14.1 \text{ mol}^{-1}$) of the emission of RFTA upon addition of NaNO_2 in an acetonitrile-water solvent mixture (Figure 2-1). Dynamic emission quenching of RFTA by

aniline **1a** ($K_{SV} = 11.3 \text{ mol}^{-1}$) supports the oxidation of the arene as a key step of the proposed mechanism.



Scheme 2-3. Mechanistic proposal.

Carretero showed that *N,N*-disubstituted anilines do not react under their conditions, postulating Cu(II) as the oxidizing species, as the formation of the amidyl radical **34** is not possible.^[6] This was also observed during our investigations, *N,N*-disubstituted anilines do not yield nitration products. (See experimental part, Table 2-6)

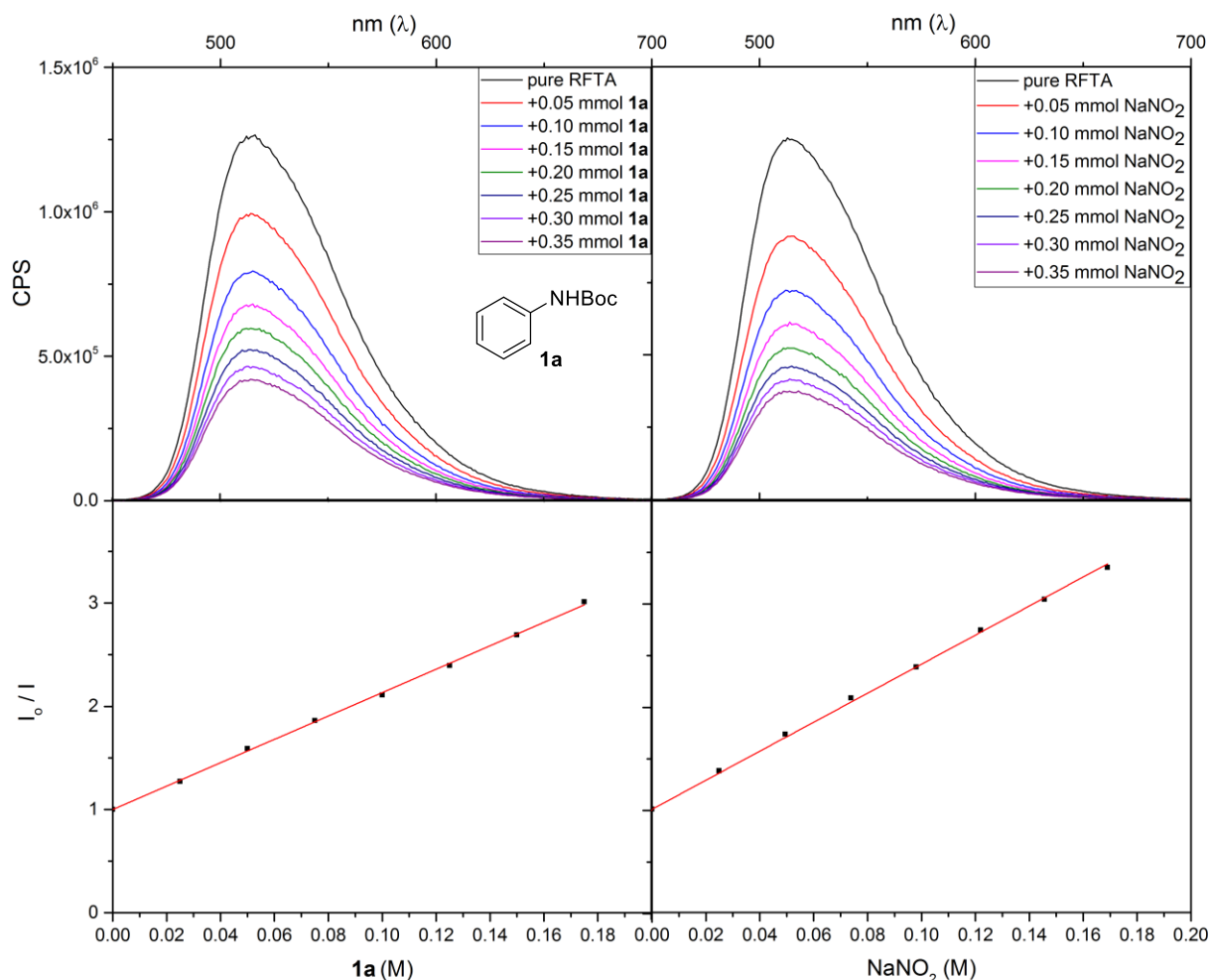
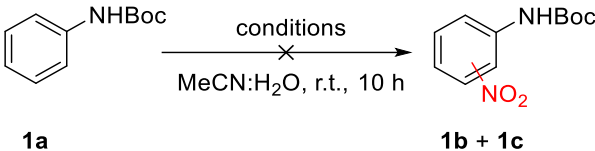


Figure 2-1. Fluorescence quenching of RFTA (10 μ M in a 3 : 1 mixture of MeCN : H₂O) upon titration with *N*-Boc-aniline (**1a**) and NaNO₂.

To confirm the postulated reaction mechanism, further experiments (Table 2-3) were performed. For entries 2-7 no product formation was detected by GC analysis. As oxygen is considered necessary to regenerate the ground state of the catalyst, the reaction was performed under inert atmosphere (entry 1), which drastically decreased the yield. Only traces (less than 5% of **1b** + **1c**) were detected. This can be explained as 10 mol% of the catalyst in its oxidized form are present at the beginning, which after reduction cannot be regenerated. The visible-light activated photocatalyst is essential, as the reaction does not proceed in the dark or without catalyst under blue light irradiation. The role of hydrogen peroxide (entry 4) was investigated, as this is the main byproduct of the described reaction. No product formation was observed upon addition of hydrogen peroxide. Nitration of the aniline derivative via peroxynitrite was not considered as relevant.^[20] The addition of TEMPO (entry 5) completely stops the reaction, indicating a radical mechanism. Nevertheless, it has to be noted that TEMPO itself can be photocatalytically oxidized.^[21] Pyrazole and Br⁻ were reported to be sufficient nucleophiles that can react with photocatalytically generated aromatic radical

cations.^[22] In our case only degradation of **1a** (which also occurs, if only **1a** and catalyst, but no NaNO₂ is present in the reaction mixture), but no formation of any adducts was observed. In difference to the mechanism postulated by Liang et al.,^[5c] direct nucleophilic addition of the nitrite anion to the aniline radical cation **33** is likely to be excluded for the herein reported process.

Table 2-3. Control experiments

 <p style="text-align: center;"> <chem>CC(C)(C)OC(=O)Nc1ccccc1</chem> $\xrightarrow[\text{MeCN:H}_2\text{O, r.t., 10 h}]{\text{conditions}}$ <chem>CC(C)(C)OC(=O)Nc1ccc(cc1)[N+](=O)[O-]</chem> </p> <p style="text-align: center;">1a 1b + 1c</p>	
Entry	Change from standard conditions ^a
1	under N ₂ atmosphere ^b
2	no light
3	no catalyst
4	no catalyst; with 3 eq. H ₂ O ₂
5	addition of 2 eq. TEMPO
6	2 eq. NaBr instead of NaNO ₂
7	2 eq. pyrazole instead of NaNO ₂

[a] Standard conditions: *N*-Boc-Aniline **1a** (0.05 mmol), sodium nitrite (0.1 mmol), RFTA (10 mol%) in a 3:1 mixture of MeCN : H₂O (1 mL) irradiated with 455 nm LED at 25 °C for 10 h. Analyzed by GC-FID; in general no product formation detected.

[b] minor traces of the desired product were detected.

2.3 Conclusion

In conclusion, protected anilines were photocatalytically nitrated. All reactions are performed at room temperature without the addition of transition metals or stoichiometric oxidation reagents. Sodium nitrite is used as a cost-effective nitration reagent that is easily stored and handled. The reactions were performed under air employing a mixture of acetonitrile and water as solvent. Many functional groups are tolerated by the reaction.

2.4 Experimental part

2.4.1 General information

Reagents, solvents and working methods

Unless stated differently, all reagents and solvents were purchased from commercial suppliers (Sigma Aldrich, Alfa Aesar, Acros, Fluka, VWR or TCI) and were used without further purification. Solvents were used as p.a. grade. Technical grade of solvents was used for automated flash column chromatography. Dry nitrogen or argon was used as inert gas atmosphere. Liquids were generally added with Gilson pipettes or syringe, needle and septum technique.

Nuclear magnetic resonance spectroscopy

All NMR spectra were measured at room temperature using a Bruker Avance 300 (300 MHz for ^1H , 75 MHz for ^{13}C) or a Bruker Avance 400 (400 MHz for ^1H , 101 MHz for ^{13}C) NMR spectrometer. All chemical shifts are reported in δ -scale as parts per million [ppm] (multiplicity, coupling constant J , number of protons) relative to the solvent residual peaks as the internal standard.^[23] The spectra were analyzed by first order and coupling constants J are given in Hertz [Hz]. Abbreviations used for signal multiplicity: ^1H -NMR: br = broad, s = singlet, d = doublet, t = triplet, q = quartet, dd = doublet of doublets, ddd = doublet of doublet of doublet, dt = doublet of triplets and m = multiplet.

Gas chromatography and gas chromatography coupled with mass spectrometry

Gas chromatography coupled with a flame ionization detector (GC-FID) was performed on an Agilent 7890 GC system. Data acquisition and evaluation was done with Agilent ChemStation Rev.C.01.04. Gas chromatography-mass spectrometry (GC-MS) was performed on a 7890A GC system from Agilent Technologies with an Agilent 5975 MSD Detector. Data acquisition and evaluation was done with MSD ChemStation E.02.02.1431. A capillary column HP-5MS (length: 30 m; diameter 0.25 mm; film thickness: 0.25 μm) and helium as carrier gas (flow rate of 1 mL/min) were used. The injector temperature (split injection: 40:1 split) was 300 °C and the detection temperature was 300 °C for the flame ionization detector (FID). GC measurements were performed and investigated *via* integration of the signals obtained. The GC oven temperature program was adjusted as follows: initial temperature 40 °C was kept for 3 min, the temperature was increased at a rate of 25 °C $\cdot\text{min}^{-1}$ over a period of 10.4 min until 300 °C was reached and kept for 5 min.

Mass spectrometry

High-resolution mass spectra (HRMS) were measured at the Central Analytical Laboratory of the University of Regensburg. All mass spectra were recorded on a Finnigan MAT 95, ThermoQuest Finnigan TSQ 7000, Finnigan MAT SSQ 710 A or an Agilent Q-TOF 6540 UHD instrument.

Thin layer chromatography

Analytical TLC was performed on silica gel coated alumina plates (MN TLC sheets ALUGRAM® Xtra SIL G/UV₂₅₄). Visualization was accomplished by UV light (254 or 366 nm). If necessary, potassium permanganate or phosphomolybdic acid was used for chemical staining.

Automated flash column chromatography

Automated flash chromatography was performed with a Biotage® Isolera™ Spektra One device. A mixture of petroleum ether (PE) and ethyl acetate (EE) as eluent and silica gel of type 60 M (40-63 µm, 230-440 mesh) by Merck as stationary phase were used.

Infrared spectroscopy

IR spectra were measured on an Agilent Cary 630 FTIR spectrometer at room temperature. The sample was applied as pure solid or liquid oil on the

UV-VIS absorption spectroscopy

UV-Vis absorption spectra were measured in acetonitrile on an Agilent Cary 100 spectrometer at 25 °C in MeCN with a quartz cuvette (4×10 mm).

Fluorescence spectroscopy

Fluorescence spectra were measured on a Horiba Scientific Fluoromax-4 spectrometer at room temperature with a quartz cuvette (10×10 mm), using 2 mL of a solution of RFTA (10 µM). Aliquots of pure solid compound **1a** or a solution of NaNO₂ (5.0 M; 10 µL) were added for quenching experiments.

Analytical high performance liquid chromatography

HPLC analysis was performed with an Agilent 1220 Infinity LC (column: Phenomenex Luna 3 µm C18(2) 100 Å, 150 x 2.00 mm; flow: 0.3 mL/min at 30 °C; solvent A: MilliQ water with 0.05 % vol. TFA; solvent B: MeCN) and naphthalene as internal standard.

Cyclic voltammetry

The cyclic voltammetry measurements were performed with a three-electrode setup "Potentiostat galvanostat PGSTAT302N" from Metrohm Autolab, using a glassy carbon

working electrode, a platinum wire counter electrode, and a silver wire quasi-reference electrode. Tetrabutylammonium tetrafluoroborate (0.1 M) was used as conduction salt and the ferrocene/ferrocenium (Fc/Fc^+) redox pair was used as internal standard. All measurements were performed in acetonitrile. The solution was degassed by argon purge and the baseline was recorded. The respective substrate was added (0.01 M) and the CV was recorded after subsequent argon purge. Afterwards ferrocene (ca. 2.2 mg, 12 μmol) was added and a final measurement was performed. The redox potentials vs. standard calomel electrode (SCE) were calculated by the commonly used method of Addison *et al.* ($E_{\text{vs SCE}} = E_{\text{sample}} - E_{\text{Ferrocene}} + 0.38 \text{ V}$).^[24]

Irradiation source

Photochemical reactions were performed with 455 nm LEDs (OSRAM Oslon SSL 80 LDCQ7P-2U3U; royal-blue. $\lambda_{\text{max}} = 455 \text{ nm}$ ($\pm 15 \text{ nm}$), 3.5 V, 700 mA).

Photoreaction setup

A custom-built cooling setup with six reaction slots was used for the conduction of the photo-reactions (Figure 2-2). The temperature was constantly maintained at 25°C ($\pm 1^\circ\text{C}$) by a water-cooled thermostat system.

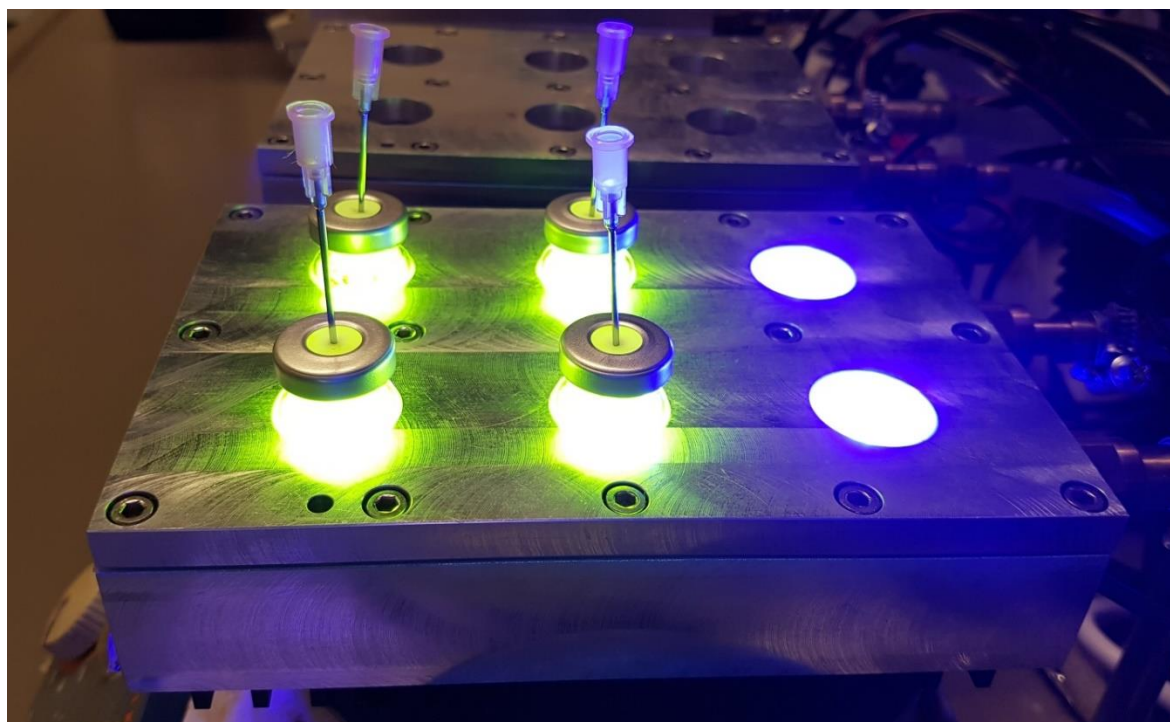


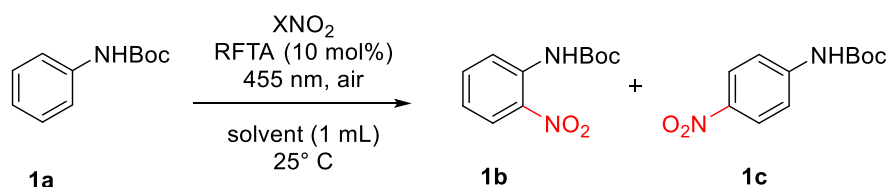
Figure2-2. Photoreaction setup

2.4.2 General experimental procedures

The aniline derivative **1a-30a** (0.05 mmol) and RFTA (2.7 mg, 0.005 mmol) were dissolved in acetonitrile (0.75 mL) and added to a glass vial (size 5 mL). A freshly prepared solution of sodium nitrite (6.9 mg, 0.1 mmol) in water (0.25 mL) was added. The vial was closed with a septum and a syringe needle ($\varnothing=1$ mm) was inserted to provide air supply. The reaction vial was placed in a custom-built cooling system at 25 °C and irradiated under stirring with a 455 nm LED through the glass bottom (0.5 cm distance to LED). The reaction progress was monitored by TLC or GC-FID and the reaction was stopped, when all starting material was consumed, or no further progress was detected. Four equal reaction mixtures were united and the solvent was removed at reduced pressure. Subsequently the products were purified by automated silica gel flash column chromatography.

Riboflavin tetraacetate (RFTA) was prepared by acetylation of riboflavin after a literature known procedure.^[25] Protected anilines were commercially available or prepared by standard procedures.^[5b, 26]

Table 2-4: Optimization of the photocatalytic nitration of **1a**.



Entry	Concentration of 1a	XNO ₂	Time [h]	Solvent ratio MeCN : H ₂ O	Yield [%] 1b	Yield [%] 1c
1	0.1	NEt ₄ NO ₂ (2 eq.)	18	pure MeCN	0	0
2	0.1	NaNO ₂ (2 eq.)	18	pure MeCN	10	14
3	0.1	NaNO ₂ (2 eq.)	18	9:1	40	46
4	0.1	NaNO ₂ (2 eq.)	18	3:1	41	44
5	0.1	NaNO ₂ (1 eq.)	18	3:1	29	33
6	0.2	NaNO ₂ (2 eq.)	18	3:1	16	21
7	0.05	NaNO ₂ (2 eq.)	18	3:1	40	44
8	0.05	NaNO₂ (2 eq.)	10	3:1	41	45

Table 2-5: Optimization of the photocatalytic nitration of phenol.

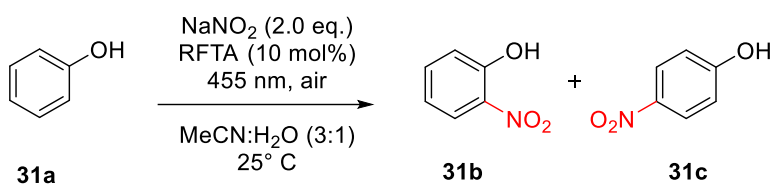
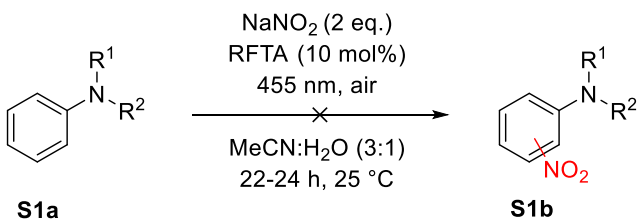
					
Entry	Concentration of Phenol [M]	Time [h]	Solvent [mL]	Yield [%] 31b	Yield [%] 31c
1	0.05	18	1	23	23
2	0.1	18	1	16	17
3	0.2	18	1	4	5
4	0.05	18	2	14	15
5	0.05	6	1	16	16
6	0.1	6	1	9	10

Table 2-6: Reactions of *N,N*-disubstituted anilines.

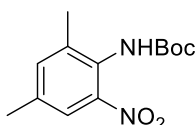
		
Entry ^a	R ¹	R ²
1	Me	Me
2	Et	Et
3	Ts	Me
4	Boc	Boc

[a] Formation of nitration products was not observed.

2.4.3 Product characterization

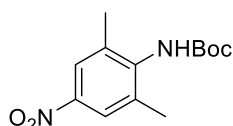
The product characterization data is listed for compounds that were first presented or fully characterized in the context of this work. The major isomer is shown. All other compounds that are displayed in Tables 2-1 and 2-2 were characterized by ^1H -NMR, ^{13}C -NMR, and HRMS.

***tert*-Butyl (2,4-dimethyl-6-nitrophenyl)carbamate (8b)**



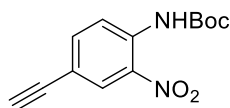
According to the general procedure, after 24 h **8b** was isolated as yellow solid (43.1 mg, 0.162 mmol, 81%) using a gradient of 2% to 10% EtOAc/PE for silica gel flash column chromatography. ^1H NMR (400 MHz, CDCl_3) δ 7.61 (s, 1H), 7.29 (s, 1H), 2.35 (s, 3H), 2.32 (s, 3H), 1.48 (s, 9H). ^{13}C NMR (101 MHz, CDCl_3) δ 152.7, 137.4, 136.8, 136.0, 127.7, 123.0, 81.3, 28.2, 20.7, 18.7. UV-Vis (ϵ , $\text{L}\cdot\text{mol}^{-1}\cdot\text{cm}^{-1}$): 268 nm (2949), 320 (1598). FT-IR (cm^{-1} , neat, ATR): 3118, 2978, 1700, 1532. HRMS (+ESI) m/z : Calcd for $\text{C}_{13}\text{H}_{18}\text{N}_2\text{O}_4\text{Na}$ 289.1159 $[\text{M} + \text{Na}]^+$; Found 289.1167. Mp: 140-142 $^\circ\text{C}$.

***tert*-Butyl (2,6-dimethyl-4-nitrophenyl)carbamate (10b)**



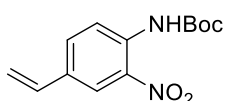
According to the general procedure, after 24 h **10b** was isolated as yellow solid (14.3 mg, 0.054 mmol, 27%) using a gradient of 2% to 9% EtOAc/PE for silica gel flash column chromatography. ^1H NMR (400 MHz, CDCl_3) δ 7.94 (s, 2H), 6.01 (s, 1H), 2.36 (s, 6H), 1.50 (s, 9H). ^{13}C NMR (101 MHz, CDCl_3) δ 145.7, 140.2, 136.8, 123.2, 81.1, 28.2, 18.8. UV-Vis (ϵ , $\text{L}\cdot\text{mol}^{-1}\cdot\text{cm}^{-1}$): 290 nm (7793). FT-IR (cm^{-1} , neat, ATR): 3244, 2926, 1685, 1502. HRMS (+ESI) m/z : Calcd for $\text{C}_{13}\text{H}_{18}\text{N}_2\text{O}_4\text{Na}$ 289.1159 $[\text{M} + \text{Na}]^+$; Found 289.1164.

***tert*-Butyl (4-ethynyl-2-nitrophenyl)carbamate (11b)**



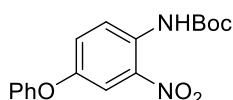
According to the general procedure, after 5.5 h **11b** was isolated as yellow solid (37.0 mg 0.141 mmol, 71%) using a gradient of 2% to 7% EtOAc/PE for silica gel flash column chromatography. ^1H NMR (400 MHz, CDCl_3) δ 9.71 (s, 1H), 8.56 (m, 1H), 8.31 (m, 1H), 7.66 (m, 1H), 3.10 (s, 1H), 1.54 (s, 9H). ^{13}C NMR (101 MHz, CDCl_3) δ 151.9, 138.8, 136.2, 135.3, 129.5, 120.6, 115.9, 82.3, 81.1, 78.4, 28.2. UV-Vis absorption (ϵ , $\text{L}\cdot\text{mol}^{-1}\cdot\text{cm}^{-1}$): 373 nm (3284). FT-IR (cm^{-1} , neat, ATR): 3388, 3287, 2983, 2929, 1729, 1503. HRMS (+ESI) m/z : Calcd for $\text{C}_{13}\text{H}_{14}\text{N}_2\text{O}_4\text{Na}$ 285.0846 $[\text{M} + \text{Na}]^+$; Found 285.0852. Mp: 112-113 $^\circ\text{C}$.

***tert*-Butyl (2-nitro-4-vinylphenyl)carbamate (**12b**)**



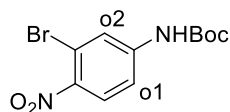
According to the general procedure, after 1 h **12b** was isolated as yellow solid (8.1 mg, 0.031 mmol, 15%) using a gradient of 2% to 5% EtOAc/PE for silica gel flash column chromatography. ^1H NMR (400 MHz, CDCl_3) δ 9.64 (s, 1H), 8.52 (m, 1H), 8.18 (m, 1H), 7.66 (m, 1H), 6.66 (dd, $J = 17.6, 10.9$ Hz, 1H), 5.77 (d, $J = 17.6$ Hz, 1H), 5.34 (d, $J = 10.9$ Hz, 1H), 1.54 (s, 9H). ^{13}C NMR (101 MHz, CDCl_3) δ 152.2, 136.0, 135.2, 134.2, 133.0, 131.8, 123.3, 120.8, 115.4, 80.0, 28.2. UV-Vis absorption (ϵ , $\text{L}\cdot\text{mol}^{-1}\cdot\text{cm}^{-1}$): 258 nm (25766), 380 (3016). FT-IR (cm^{-1} , neat, ATR): 3355, 2926, 1729, 1512. HRMS (+ESI) m/z : Calcd for $\text{C}_{13}\text{H}_{16}\text{N}_2\text{O}_4\text{Na}$ 287.1002 $[\text{M} + \text{Na}]^+$; Found 287.1003. Mp: 64-67 $^\circ\text{C}$.

***tert*-Butyl (2-nitro-4-phenoxyphenyl)carbamate (**16b**)**



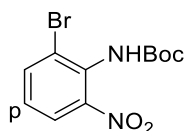
According to the general procedure, after 6 h **12b** was isolated as orange solid (40.2 mg, 0.122 mmol, 61%) using an isocratic mixture of 1% EtOAc/PE for silica gel flash column chromatography. ^1H NMR (300 MHz, CDCl_3) δ 9.49 (s, 1H), 8.52 (m, 1H), 7.78 (m, 1H), 7.41 – 7.29 (m, 3H), 7.20 – 7.12 (m, 1H), 7.00 (m, 2H), 1.54 (s, 9H). ^{13}C NMR (75 MHz, CDCl_3) δ 156.3, 152.4, 151.4, 136.5, 131.5, 130.1, 126.9, 124.2, 122.5, 118.9, 114.8, 81.8, 28.2. UV-Vis absorption (ϵ , $\text{L}\cdot\text{mol}^{-1}\cdot\text{cm}^{-1}$): 383 nm (3502). FT-IR (cm^{-1} , neat, ATR): 3369, 2926, 1726, 1510. HRMS (+ESI) m/z : Calcd for $\text{C}_{17}\text{H}_{18}\text{N}_2\text{O}_5\text{Na}$ 353.1108 $[\text{M} + \text{Na}]^+$; Found 353.1115. Mp: 81-81 $^\circ\text{C}$.

***tert*-Butyl (3-bromo-4-nitrophenyl)carbamate (18b-p), *tert*-Butyl (5-bromo-2-nitrophenyl)carbamate (18b-o¹) and *tert*-Butyl (3-bromo-2-nitrophenyl)carbamate (18b-o²)**



According to the general procedure, after 8 h **18b-p**, **18b-o¹** and **18b-o²** were isolated as yellow solids (**18b-p** 9.4 mg, 0.030 mmol, 15%. **18b-o¹** 9.4 mg, 0.030 mmol, 15%. **18b-o²** 18.3 mg, 0.058 mmol, 29%) using a gradient of 2% to 15% EtOAc/PE for silica gel flash column chromatography. Spectral data for **18b-p**: ¹H NMR (400 MHz, CDCl₃) δ 7.94 (d, *J* = 9.0 Hz, 1H), 7.90 (d, *J* = 2.3 Hz, 1H), 7.38 (dd, *J* = 9.0, 2.4 Hz, 1H), 6.74 (s, 1H), 1.53 (s, 9H). ¹³C NMR (101 MHz, CDCl₃) δ 151.60, 143.60, 143.09, 127.36, 123.35, 116.52, 116.45, 82.34, 28.20. HRMS (+ESI) *m/z*: Calcd for C₁₁H₁₃BrN₂O₄Na 338.9951 [M + Na]⁺; Found 338.9954. Spectral data for **18b-o**: ¹H NMR (400 MHz, CDCl₃) δ 9.73 (s, 1H), 8.85 (d, *J* = 2.1 Hz, 1H), 8.06 (d, *J* = 9.0 Hz, 1H), 7.21 (dd, *J* = 9.0, 2.1 Hz, 1H), 1.55 (s, 9H). ¹³C NMR (101 MHz, CDCl₃) δ 151.85, 136.83, 134.47, 131.35, 127.00, 125.10, 123.25, 82.46, 28.18. HRMS (+ESI) *m/z*: Calcd for C₁₁H₁₃BrN₂O₄Na 338.9951 [M + Na]⁺; Found 338.9948. Spectral data for **18b-o²**: ¹H NMR (400 MHz, CDCl₃) δ 8.15 (dd, *J* = 8.2, 1.5 Hz, 1H), 7.36 (dd, *J* = 8.0, 1.6 Hz, 1H), 7.34 – 7.31 (m, 1H), 1.51 (s, 9H). ¹³C NMR (101 MHz, CDCl₃) δ 151.8, 133.0, 132.2, 128.1, 121.3, 114.2, 82.3, 28.2. UV-Vis absorption (ε, L·mol⁻¹·cm⁻¹): 275 nm (2607). FT-IR (cm⁻¹, neat, ATR): 3417, 2929, 1737, 1490. HRMS (+ESI) *m/z*: Calcd for C₁₁H₁₃BrN₂O₄Na 338.9951 [M + Na]⁺; Found 338.9978.

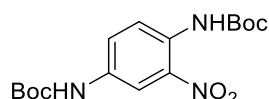
***tert*-Butyl (2-bromo-6-nitrophenyl)carbamate (19b-o) and *tert*-Butyl (2-bromo-4-nitrophenyl)carbamate (19b-p)**



According to the general procedure, after 10 h **19b-o** and **19b-p** were isolated as yellow solids (**19b-o** 10.5 mg, 0.033 mmol, 17%. **19b-p** 6.3 mg, 0.020 mmol, 10%) using a gradient of 3% to 5% EtOAc/PE for silica gel flash column chromatography. Spectral data for **19b-o**: ¹H NMR (400 MHz, CDCl₃) δ 8.46 – 8.39 (m, 2H), 8.18 (m, 1H), 7.32 (s, 1H), 1.56 (s, 9H). ¹³C NMR (101 MHz, CDCl₃) δ 151.5, 142.3, 142.3, 128.0, 124.2, 118.2, 111.0, 82.7, 28.2. UV-Vis absorption (L·mol⁻¹·cm⁻¹): ε₃₁₈ = 12161. FT-IR (cm⁻¹, neat, ATR): 3408, 2930, 1729, 1504. HRMS (+ESI) *m/z*: Calcd for C₁₁H₁₃BrN₂O₄Na 338.9951 [M + Na]⁺; Found 338.9949. Spectral

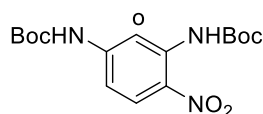
data for **19b-p**: ^1H NMR (400 MHz, CDCl_3) δ 7.88 (m, 1H), 7.82 (m, 1H), 7.18 (m, 1H), 6.95 (s, 1H), 1.49 (s, 9H). ^{13}C NMR (101 MHz, CDCl_3) δ 145.3, 137.1, 130.2, 125.9, 124.7, 120.9, 82.7, 28.1. UV-Vis absorption (ϵ , $\text{L}\cdot\text{mol}^{-1}\cdot\text{cm}^{-1}$): 307 nm (1787). FT-IR (cm^{-1} , neat, ATR): 3157, 2986, 1700, 1532. HRMS (+ESI) m/z : Calcd for $\text{C}_{11}\text{H}_{13}\text{BrN}_2\text{O}_4\text{Na}$ 338.9951 $[\text{M} + \text{Na}]^+$; Found 338.9952.

Di-*tert*-butyl (2-nitro-1,4-phenylene)dicarbamate (**22b**)



According to the general procedure, after 8.5 h **12b** was isolated as orange solid (41.2 mg, 0.117 mmol, 58%) using a gradient of 2% to 8% EtOAc/PE for silica gel flash column chromatography. ^1H NMR (300 MHz, Chloroform- d) δ 9.45 (s, 1H), 8.44 (m, 1H), 8.33 (d, J = 2.6 Hz, 1H), 7.51 (m, 1H), 6.68 (s, 1H), 1.52 (d, J = 3.6 Hz, 18H). ^{13}C NMR (75 MHz, CDCl_3) δ 152.5, 152.4, 136.1, 132.9, 131.0, 126.1, 121.5, 114.8, 81.7, 28.3, 28.2. UV-Vis absorption (ϵ , $\text{L}\cdot\text{mol}^{-1}\cdot\text{cm}^{-1}$): 248 nm (29040), 397 nm (2822). FT-IR (cm^{-1} , neat, ATR): 3386, 2978, 1726, 1517. HRMS (+ESI) m/z : Calcd for $\text{C}_{16}\text{H}_{23}\text{N}_3\text{O}_6\text{Na}$ 376.1479 $[\text{M} + \text{Na}]^+$; Found 376.1483. Mp: 160-162 $^\circ\text{C}$.

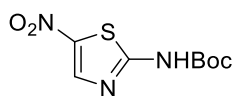
Di-*tert*-butyl (4-nitro-1,3-phenylene)dicarbamate (**23b-p**) and Di-*tert*-butyl (2-nitro-1,3-phenylene)dicarbamate (**23b-o**)



According to the general procedure, after 8.5 h **23b-p** and **23b-o** were isolated as yellow solids (**23b-p** 42.9 mg, 0.121 mmol, 61%. **23b-o** 10.8 mg, 0.031 mmol, 15%) using a gradient of 0% to 5% EtOAc/PE for silica gel flash column chromatography. Spectral data for **23b-p**: ^1H NMR (400 MHz, CDCl_3) δ 9.95 (s, 1H), 8.35 (m, 1H), 8.18 (d, J = 9.4 Hz, 1H), 7.43 (m, 1H), 6.99 (m, 1H), 1.52 (d, J = 7.2 Hz, 18H). ^{13}C NMR (101 MHz, CDCl_3) δ 152.3, 151.8, 145.8, 137.5, 130.5, 128.0, 111.1, 107.3, 81.9, 81.9, 28.2. UV-Vis absorption (ϵ , $\text{L}\cdot\text{mol}^{-1}\cdot\text{cm}^{-1}$): 253 nm (10153), 348 nm (13715). FT-IR (cm^{-1} , neat, ATR): 3322, 2985, 1737, 1704, 1543. HRMS (+ESI) m/z : Calcd for $\text{C}_{16}\text{H}_{23}\text{N}_3\text{O}_6\text{Na}$ 376.1479 $[\text{M} + \text{Na}]^+$; Found 376.1479. Spectral data for **23b-o**: ^1H NMR (400 MHz, CDCl_3) δ 8.51 (s, 2H), 7.91 (m, 2H), 7.46 (m, 1H), 1.51 (s, 18H). ^{13}C NMR (101 MHz, CDCl_3) δ 152.2, 134.5, 134.2, 130.9, 115.8, 81.9, 28.2. UV-Vis absorption (ϵ , $\text{L}\cdot\text{mol}^{-1}\cdot\text{cm}^{-1}$): 253 nm (10153), 348 nm (13715).

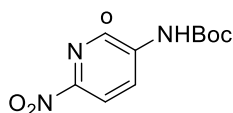
^1H -NMR (CDCl_3): 3.47 (s, 9H). FT-IR (cm^{-1} , neat, ATR): 3403, 2927, 1733, 1483. HRMS (+ESI) m/z : Calcd for $\text{C}_{16}\text{H}_{23}\text{N}_3\text{O}_6\text{Na}$ 376.1479 $[\text{M} + \text{Na}]^+$; Found 376.1480. Mp: 92-93 °C.

***tert*-Butyl (4-nitrothiazol-2-yl)carbamate (27b)**



According to the general procedure, after 24 h **27b** was isolated as yellow solid (12.3 mg, 0.050 mmol, 25%) using a gradient of 5% to 30% EtOAc/PE for silica gel flash column chromatography. ^1H NMR (400 MHz, CDCl_3) δ 8.21 (d, J = 0.8 Hz, 1H), 1.61 (s, 9H). ^{13}C NMR (101 MHz, CDCl_3) δ 164.7, 151.8, 143.0, 140.2, 84.7, 28.1. UV-Vis absorption (ϵ , $\text{L}\cdot\text{mol}^{-1}\cdot\text{cm}^{-1}$): 343 nm (14698), 433 nm (2121). FT-IR (cm^{-1} , neat, ATR): 3161, 2923, 1726, 1488. HRMS (+ESI) m/z : Calcd for $\text{C}_8\text{H}_{11}\text{N}_3\text{O}_4\text{SNa}$ 268.0362 $[\text{M} + \text{Na}]^+$; Found 268.0365. Mp: 148 °C (decomposition).

***tert*-Butyl (6-nitropyridin-3-yl)carbamate (28b-p) and *tert*-Butyl (2-nitropyridin-3-yl)carbamate (28b-o)**

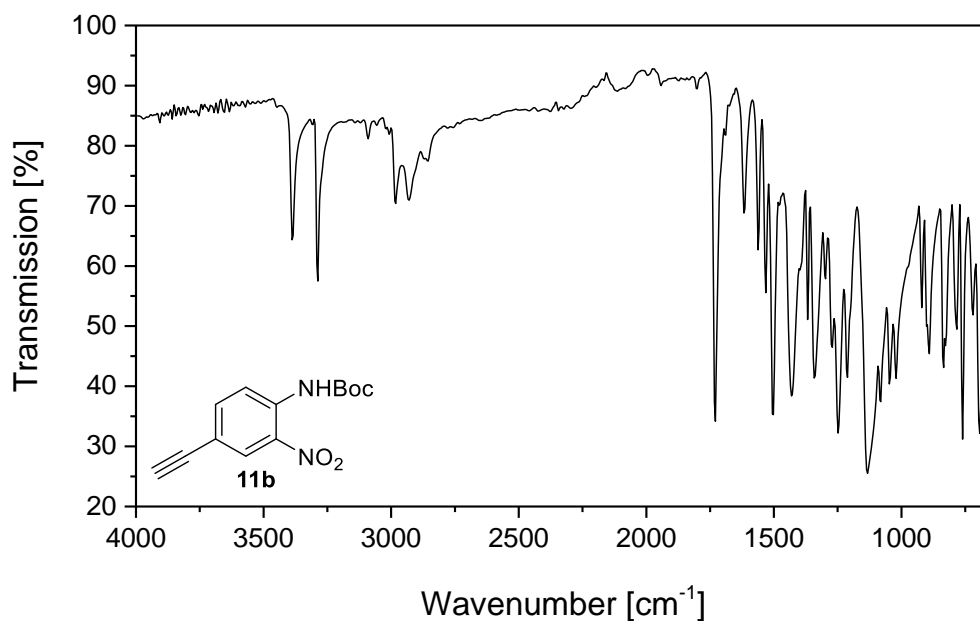


According to the general procedure, after 8.5 h **23b-p** and **23b-o** were isolated as pale yellow solids (**23b-p** 5.8 mg, 0.024 mmol, 12%. **23b-o** 4.3 mg, 0.018 mmol, 9%) using a gradient of 10% to 25% EtOAc/PE for silica gel flash column chromatography. Spectral data for **23b-o**: ^1H NMR (400 MHz, CDCl_3) δ 9.38 (s, 1H), 9.06 (dd, J = 8.6, 1.5 Hz, 1H), 8.23 (dd, J = 4.2, 1.5 Hz, 1H), 7.64 – 7.56 (m, 1H), 1.55 (s, 9H). ^{13}C NMR (101 MHz, CDCl_3) δ 152.0, 141.1, 132.2, 130.6, 130.1, 82.7, 28.2. UV-Vis absorption (ϵ , $\text{L}\cdot\text{mol}^{-1}\cdot\text{cm}^{-1}$): 310 nm (6607) FT-IR (cm^{-1} , neat, ATR): 3255, 2982, 1730, 1519. HRMS (+ESI) m/z : Calcd for $\text{C}_{10}\text{H}_{13}\text{N}_3\text{O}_4$ 240.0979 $[\text{M} + \text{H}]^+$; Found 240.0979. Spectral data for **23b-p**: ^1H NMR (400 MHz, CDCl_3) δ 8.40 (d, J = 2.6 Hz, 1H), 8.38 – 8.32 (m, 1H), 8.25 (d, J = 8.9 Hz, 1H), 7.04 (s, 1H), 1.54 (s, 9H). ^{13}C NMR (101 MHz, CDCl_3) δ 151.69, 140.47, 137.60, 126.62, 119.27, 82.78, 28.17. HRMS (+ESI) m/z : Calcd for $\text{C}_{10}\text{H}_{13}\text{N}_3\text{O}_4$ 240.0979 $[\text{M} + \text{H}]^+$; Found 240.0982.

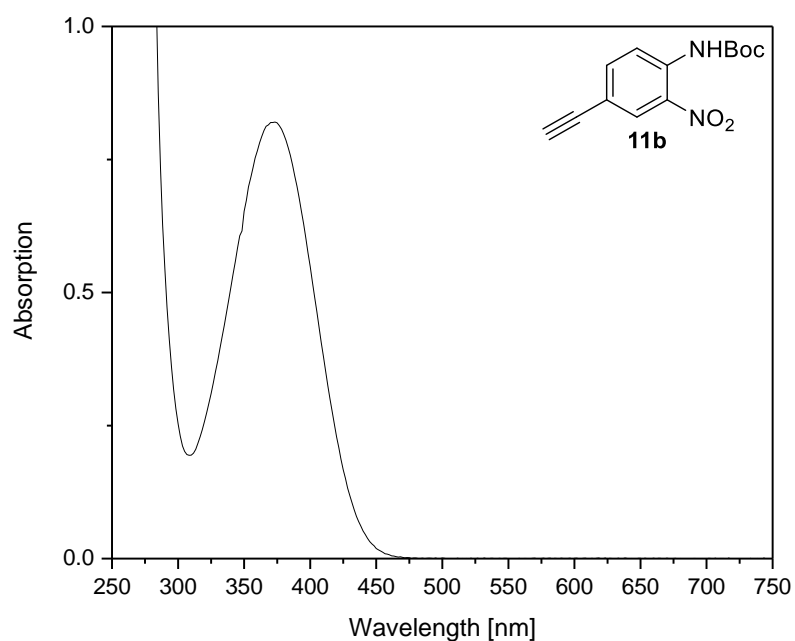
2.4.4 Spectroscopic characterization

All compounds that are characterized in Chapter 2.4.3 were spectroscopically analyzed as it is exemplarily shown for the compound *tert*-butyl (4-ethynyl-2-nitrophenyl)carbamate (**11b**).

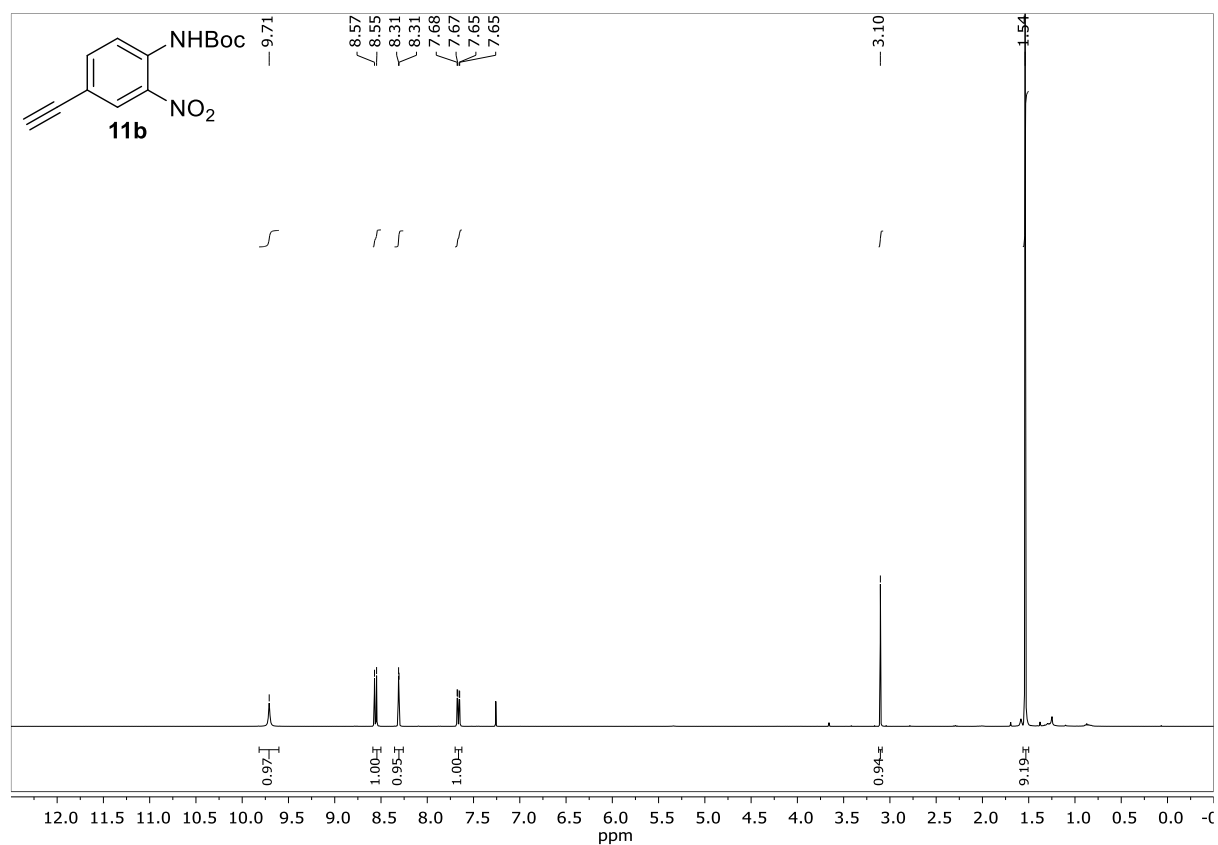
IR spectrum of **11b** (solid).



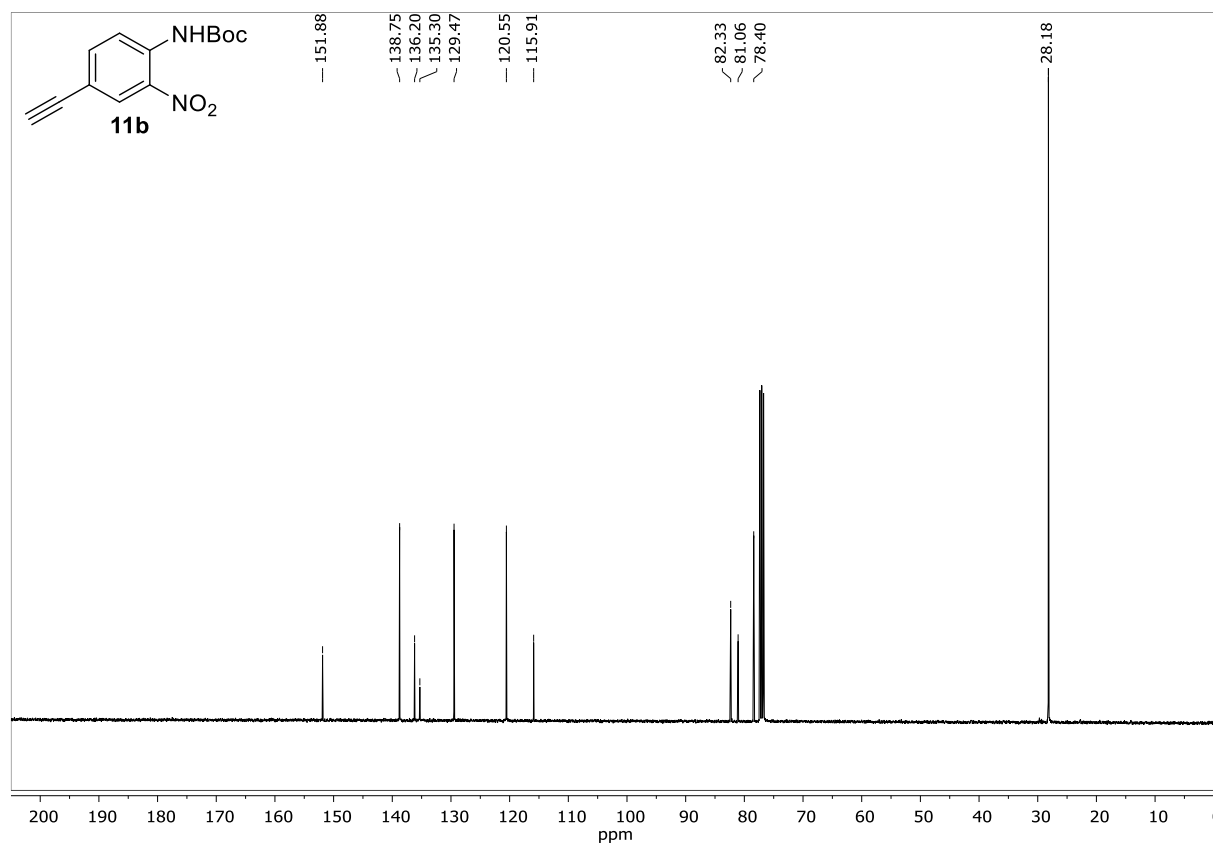
UV-VIS absorption spectrum of **11b** (in MeCN, $c = 624 \mu\text{mol}\cdot\text{L}^{-1}$).



¹H NMR spectrum of 11b (in CDCl₃, 400 MHz).



¹³C NMR spectrum of 11b (in CDCl₃, 101 MHz).

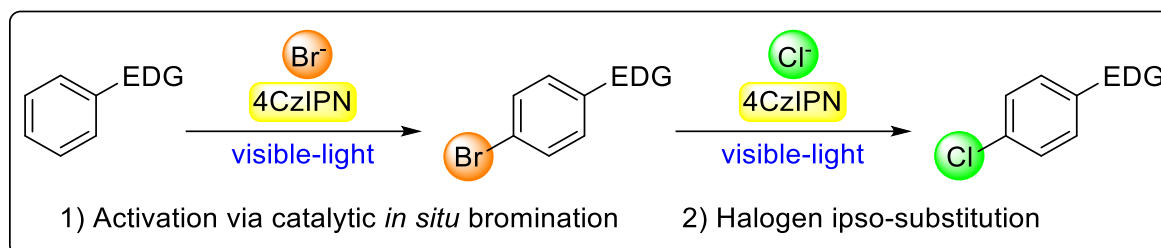


2.5 References

- [1] N. Ono, In *The Nitro Group in Organic Synthesis* (Ed.: H. Feuer); Wiley-VCH, New-York, **2001**.
- [2] G. Yan, M. Yang, *Org. Biomol. Chem.* **2013**, *11*, 2554.
- [3] B. Kilpatric, M. Heller, S. Arns, *Chem. Commun.* **2013**, *49*, 514.
- [4] Y.-F. Ji, H. Yan, Q.-B. Jiang, *Eur. J. Org. Chem.* **2015**, 2051.
- [5] a) X. Zhu, L. Qiao, P. Ye, B. Ying, J. Xu, C. Shen, P. Zhang, *RSC Adv.* **2016**, *6*, 89979; b) U. Kloeckner, B. J. Nachtsheim, *Chem. Commun.* **2014**, *50*, 10485; c) Y.-X. Li, L.-H. Li, Y.-F. Yang, H.-L. Hua, X.-B. Yan, L.-B. Zhao, J.-B. Zhang, F.-J Ji, Y.-M. Liang, *Chem. Commun.* **2014**, *50*, 9936; d) P. Sadhu, S. K. Alla, T. Punniyamurthy, *J. Org. Chem.* **2015**, *80*, 8245; e) G. G. Pawar, A. Brahmanandan, M. Kapur, *Org. Lett.* **2016**, *18*, 448; f) Y.-F. Liang, Li, X. Wang, Y. Yan, P. Feng, N. Jiao, *ACS Catal.* **2015**, *5*, 1956.
- [6] E. Hernando, R. R. Castillo, N. Rodriguez, R. Gomez Arrayas, J. C. C. Carretero, *Chem. Eur. J.* **2014**, *20*, 13854.
- [7] a) J. Xuan, W.-J. Xiao, *Angew. Chem., Int. Ed.* **2012**, *51*, 6828; b) M. Reckenthaeler, A. G. Griesbeck, *Adv. Synth. Catal.* **2013**, *355*, 2727; c) T. Hering, A. U. Meyer, B. König, *J. Org. Chem.* **2016**, *81*, 6927; d) J. Schwarz, B. König, *Green Chem.* **2016**, *18*, 4743; e) M. H. Shaw, J. Twilton, D. W. C. MacMillan, *J. Org. Chem.* **2016**, *81*, 6898.
- [8] a) J. Jin, D. W. C. MacMillan, *Nature* **2015**, *525*, 87; b) R. S. Shaikh, S. J. S. Düsel, B. König, *ACS Catal.* **2016**, *6*, 8410; c) I. Ghosh, L. Marzo, L.; A. Das, R. S. Shaikh, B. König, *B. Acc. Chem. Res.* **2016**, *49*, 1566; d) J. K. Matsui, D. N. Primer, G. A. Molander, *Chem. Sci.* **2017**, *8*, 3512.
- [9] Romero, N. A.; Nicewicz, D. A. *Chem. Rev.* **2016**, *116*, 10075.
- [10] a) B. Mühldorf, R. Wolf, *Chem. Comm.* **2015**, *51*, 8425; b) T. Hering, B. Mühldorf, R. Wolf, B. König, *Angew. Chem., Int. Ed.* **2016**, *55*, 5342; c) J. B. Metternich, R. Gilmour, *J. Am. Chem. Soc.* **2016**, *138*, 1040.
- [11] It has to be noted that in the used aqueous mixture the actual oxidation potentials differ as deprotonation of the anilines and proton-couplet transfers have to be considered (Ref. 20a and Ref. 20b). As the concentration of NO₂⁻, OH⁻ and HO₂⁻ are changing during the time of the reaction no exact potentials can be given.
- [12] For these compounds *ipso*-substituion of aryl hailides is observed. For photoredox catalyzed substitution of aromatatic methoxy groups see: N. E. S. Tay, D. A. Nicewicz, *J. Am. Chem. Soc.* **2017**, *139*, 16100.
- [13] The oxidation peak of **30a** could not be detected within the potential window of acetonitrile with the used cyclic voltammetry setup.

- [14] a) D. M. Mohilner, R. N. Adams, W. J. Argersinger, *J. Am. Chem. Soc.* **1962**, *84*, 3618; b) I. Sapurina, J. Stejskal, *Polym. Int.* **2008**, *57*, 1295.
- [15] a) D. Vione, V. Maurino, C. Minero, E. Pelizzetti, *Environ. Sci. Technol.* **2002**, *36*, 669; b) U. Al-Obaidi, R. B. Moodie, *J. Chem. Soc., Perkin Trans. 2* **1985**, 467; c) A. Kumar, R. Dutt Shukla, L. Kumar Gupta, D. Yadav, *RSC Adv.* **2015**, *5*, 52062; d) A. Eisenhofer, J. Hioe, R. M. Gschwind, B. König, *Eur. J. Org. Chem.* **2017**, 2194.
- [16] a) G. J. Choi, R. R. Knowles, *J. Am. Chem. Soc.* **2015**, *137*, 9226; b) D. C. Miller, G. J. Choi, H. S. Orbe, R. R. Knowles, *J. Am. Chem. Soc.* **2015**, *137*, 13492.
- [17] a) F. G. Bordwell, J. P. Cheng, *J. Am. Chem. Soc.* **1989**, *111*, 1792; b) J. W. Beatty, C. R. Stephenson, *J. Acc. Chem. Res.* **2015**, *48*, 1474.
- [18] a) P. S. Rao, E. Hayon, *J. Phys. Chem.* **1975**, *79*, 397; b) P. M. Wood, *Biochem. J.* **1988**, *253*, 287.
- [19] V. L. Ivanov, B. M. Uzhinov, S. Y. Lyashkevich, *Vestn. Mosk. Univ., Ser. 2: Khim.* **2010**, *51*, 279.
- [20] a) H. Gunaydin, K. N. Houk, *Chem. Res. Toxicol.* **2009**, *22*, 894; b) Z. Lin, W. Xue, H. Chen, J.-M. Lin, *Anal. Chem.* **2011**, *83*, 8245; c) K. M. Robinson, J. S. Beckman, *Synthesis of peroxyxynitrite from nitrite and hydrogen peroxide*. In *Methods Enzymol.* **2005**, *396*, pp. 207–214.
- [21] P. Schroll, B. König, *Eur. J. Org. Chem.* **2015**, 309.
- [22] a) N. A. Romero, K. A. Margrey, N. E. Tay, D. A. Nicewicz, *Science* **2015**, *349*, 1326; b) K. Ohkubo, K. Mizushima, R. Iwata, S. Fukuzumi, *Chem. Sci.* **2011**, *2*, 715; c) D. Petzold, B. König, *Adv. Synth. Catal.* **2018**, *360*, 626.
- [23] H.E. Gottlieb, V. Kotlyar, A. Nudelman, *J. Org. Chem.* **1997**, *62*, 7512.
- [24] V.V. Pavlishchuk, A. W. Addison, *Inorg. Chim. Acta* **2000**, *298*, 97.
- [25] R. A. Larson, P. L. Stackhouse, T. O. Crowley, *Environ. Sci. Technol.* **1992**, *26*, 1792.
- [26] a) P. Wipf, J. P. Maciejewski, *Org. Lett.* **2008**, *10*, 4383; b) I. Colomer, R. C. Barcelos, K. E. Christensen, T. J. Donohoe, *Org. Lett.* **2016**, *18*, 5880; c) M. B. Gawande, P. S. Branco, *Green Chem.* **2011**, *13*, 3355; d) L. Grehn, K. Gunnarsson, U. Ragnarsson, *Acta Chem. Scand., Ser. B* **1986**, *B40*, 745; e) S. Darnbrough, M. Mervic, S. M. Condon, C. J. Burns, *Synth. Commun.* **2001**, *31*, 3273.

3. Oxidative photochlorination of electron rich arenes via *in situ* bromination



Electron rich arenes are oxidatively photochlorinated in the presence of catalytic amounts of bromide ions, visible-light and 4CzIPN as organic photoredox catalyst. The substrates are *in situ* brominated in a first photoredox-catalyzed oxidation step, followed by a photocatalyzed *ipso*-chlorination yielding the target compounds in high *ortho*/*para* regioselectivity. Dioxygen serves as a green and convenient terminal oxidant. Aqueous hydrochloric acid serves as the chloride source, reducing the amount of saline by-products.

This Chapter has been published in:

S. J. S. Düsel, B. König, *Eur. J. Org. Chem.* **2019**. doi:10.1002/ejoc.201900411

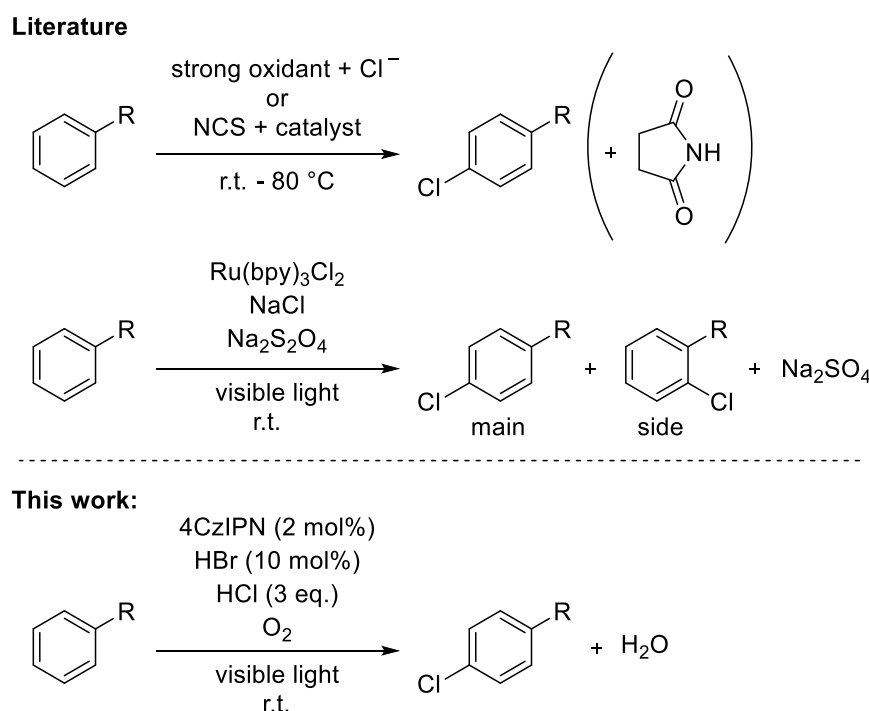
Reproduced with permission from Reproduced with permission from John Wiley and Sons.

Author contributions:

SJSD discovered the reaction, carried out the experiments, and wrote the manuscript. BK supervised the project and is the corresponding author.

3.1 Introduction

Chlorinated organic compounds are ubiquitously present in chemical synthesis, such as natural product synthesis, catalysis and material science.^[1] The robustness and electronic properties of the C-Cl bond enables the use of the halogenated compounds as pharmacophores and crop protection agents.^[2] Simple chlorinated arenes are produced in ton scales via chlorination by gaseous chlorine under harsh conditions, requiring elaborated safety conditions.^[3] In contrast, stoichiometric amounts of strong oxidants in combination with diverse chloride sources or preformed “Cl⁺”-species (e.g. *N*-chlorosuccinimide (NCS)) are utilized when compounds shall be obtained on smaller scale.^[4]



Scheme 3-1. Chlorine-free methods for the chlorination of arenes.^[4, 7a]

Visible-light photocatalysis has become an important tool for the promotion of new reaction pathways and overcoming energetic barriers at ambient temperature.^[5] Our group recently reported the visible-light driven bromination of aromatic systems.^[6] However, direct chlorination of arenes by photoredox-catalysis, starting from chloride ions, is challenging. The group of Hu described a synthetic visible-light driven protocol in 2017.^[7] The authors use Ru(bpy)₃Cl₂ in combination with Na₂S₂O₄ as oxidant, which is postulated to subsequently oxidize photocatalytically generated chlorine radicals to the reacting “Cl⁺”-species. Hu and coworkers present a wide substrate scope with high yields. However, strong oxidants are typically required for the formation of electrophilic Cl-species, and the generation of organic or saline byproducts (see Scheme 3-1) reduce the efficiency in terms of atom economy. Therefore, we investigated a metal-free oxidative chlorination under dioxygen atmosphere based on radical

chemistry, avoiding stoichiometric amounts of oxidants other than dioxygen in a visible-light mediated reaction. A key feature of the developed system is the presence of a catalytic amount of HBr for *in situ* bromination activation.

3.2 Results and discussion

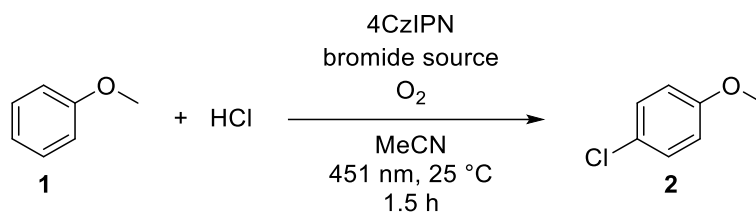
3.2.1 Synthesis

We observed the formation of 4-chloroanisole (**2**) with excellent regioselectivity upon blue-light irradiation of a mixture containing anisole, aqueous hydrochloric acid and 4CzIPN,^[8, 9] when a catalytic amounts of bromide ions was present (see Table 3-1). Light, oxygen and the organic photocatalyst (4CzIPN) are essential for the reaction to proceed, whereas the type bromide salt seemed to be less important. In order to achieve efficient reactivity with a decreased amount of saline byproducts, we decided to apply aqueous HBr as a simple bromide source for our standard conditions (Table 3-1, entry 4).^[10] The reaction proceeds well with aerial oxygen under open-air conditions (Table 3-1, entry 12). To create optimal oxidative conditions, the headspace of the closed reaction vials was saturated with oxygen. Other organic photocatalysts, chloride sources, solvents or an increased amount of catalyst did not provide higher yields (see Chapter 3.4.3, Tables 3-4 and 3-4).

We then investigated the scope of this reaction (Table 3-2) and observed that a variety of activated arenes and heteroarenes is chlorinated under the optimized reaction conditions. The mono-chloroarenes are generally obtained in moderate to good yields as single isomers. Only compound **4** was isolated as double-chlorinated benzene derivative, together with 5% of the mono-chlorinated starting material. Naphthalene derivatives **7-9** or unsubstituted pyrene (**11**) are functionalized, although oxidation of the triple bond of **8** is observed under the applied conditions. Anilides were *para*-chlorinated with yields up to 85% and benzanilide (**13**) was selectively chlorinated on the activated phenyl ring, whereas the second electron-deficient ring was unaffected. To our delight, the nitrile group of compound **15** remained stable under the acidic conditions and the protocol could also be applied to a more labile carbamate, to obtain **16** in reasonable yields. However, we noticed that for this compound and other molecules, such as the naproxen^[11] derivative **9**, the products degrade, if too long reaction times were applied. For that reason, the reaction time was adjusted for each compound (please see Chapter 3.4.4). The physiological active clofibrate^[12] **10** and heterocycles **17-18** remained stable and were therefore obtained in nearly quantitative yields. In contrast, the observed conversion of benzimidazole was very slow, which is why a high amount of starting material remained and **20** was only isolated in 35% yield. Its less activated derivative **21** showed even

lower conversion.^[13] For unsubstituted benzene (**30**) and more electron deficient arenes no, or only traces of product were detected.

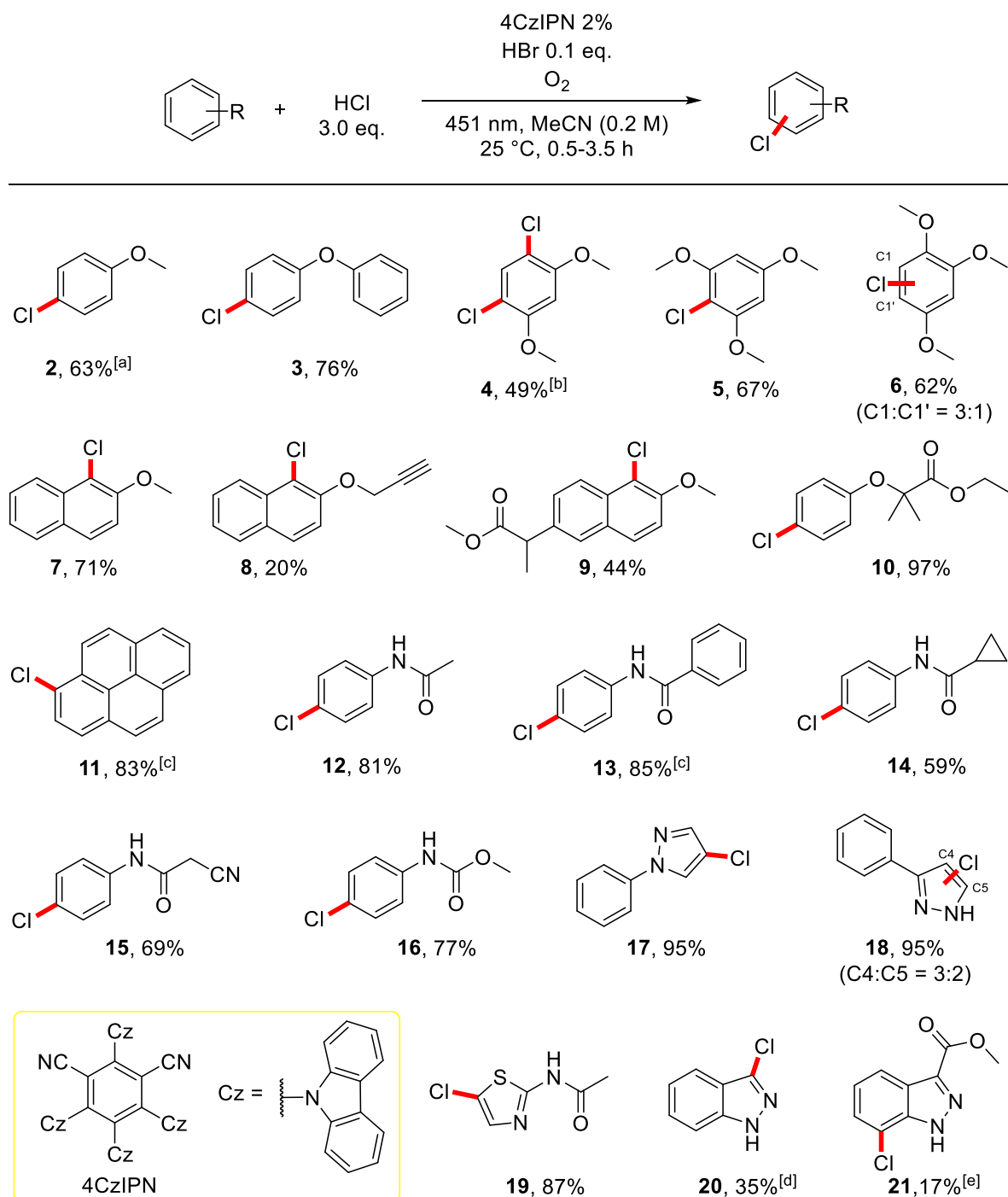
Table 3-1. Optimization table for the photocatalytic chlorination of anisole.



Entry	HCl [eq.]	Bromide source [eq.]	4CzIPN [mol%]	M [mol·L ⁻¹]	Yield ^[a] [%]
1 ^[b]	1.0	HBr (0.1)	2	0.1	37
2 ^[b]	2.0	HBr (0.1)	2	0.1	57
3 ^[b]	3.0	HBr (0.1)	2	0.1	57
4	3.0	HBr (0.1)	2	0.2	63
5 ^[b, c]	3.0	HBr (0.1)	2	0.2	56
6	3.0	HBr (0.1)	1	0.2	59
7	3.0	HBr (0.1)	3	0.2	58
8	3.0	NEt ₄ Br (0.1)	2	0.2	64
9	3.0	KBr (0.1)	2	0.2	30
10	3.0	HBr (0.05)	2	0.2	33
11	3.0	HBr (0.15)	2	0.2	61
12 ^[d]	3.0	HBr (0.1)	2	0.2	59
13	3.0	-	2	0.2	13
14	3.0	HBr (0.1)	0	0.2	0
15 ^[e]	3.0	HBr (0.1)	2	0.2	0
16 ^[f]	3.0	HBr (0.1)	2	0.2	0

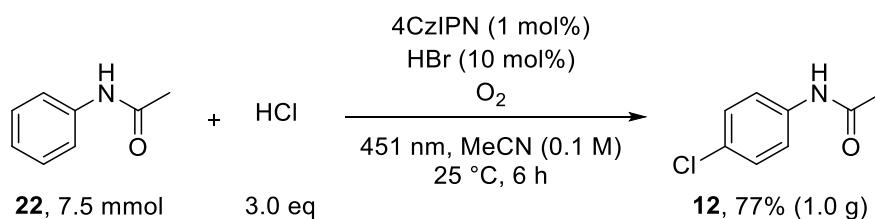
Reaction conditions: Anisole (0.1 mmol), HCl, 4CzIPN and bromide source in MeCN (0.5 mL), irradiated under oxygen atmosphere by 451 nm LEDs at 25 °C for 1.5h. [a] GC-yields with *tert*-butylbenzene as standard. [b] 1.0 mL of MeCN. [c] 0.2 mmol of anisole. [d] Absence of light. [e] Under nitrogen atmosphere.

Table 3-2. Scope of the photocatalytic chlorination reaction.



Reaction conditions: Substrate (0.1 mmol), HCl (3 eq.), HBr (10 mol%), 4CzIPN (2 mol%) in MeCN (0.5 mL), irradiated under oxygen atmosphere at 25 °C. Isolated yields. [a] GC-yield with *tert*-butylbenzene as standard. [b] The major product is shown. A mixture of **8** with 5% of the mono-chlorinated starting material was obtained. [c] Due to solubility, 1.0 mL of MeCN was used. [d] 43% of starting material reisolated. [e] 43% of starting material reisolated.

To demonstrate the application of the method to a larger scale, we performed a reaction with 7.5 mmol of acetanilide (**22**), with a reduced amount of catalyst. Due to the lower light output of the gram-scale photo-reactor, the reaction time was prolonged to 6 h, whereupon product **12** was isolated in 77% yield together with 8% of starting material and 4% of the respective *para*-brominated product (Scheme 3-2).



Scheme 3-2. Gram-scale reaction of acetanilide.

3.2.2 Mechanistic investigations

The kinetic reaction profile (see Figure 3-1) of the model reaction (see Table 3-1) provides a better understanding of processes occurring in the reaction mixture. Already after 5 minutes of irradiation, the bromide salts are consumed and have nearly quantitatively substituted the *para*-position of the methoxy group of anisole (**1**), whereas the formation of 4-chloroanisole (**2**) is delayed. During the next 20 minutes the amount of 4-bromoanisole (**27**) remains relatively constant and the concentration of 4-chloroanisole (**2**) is steadily increasing. After ca. 60 minutes, the consumption of starting material and the product formation slow down. The highest amount of **2** is obtained after ca. 90 minutes. For longer reaction times, increasing amounts of undesired degradation products are detected by GC-analysis for this compound.

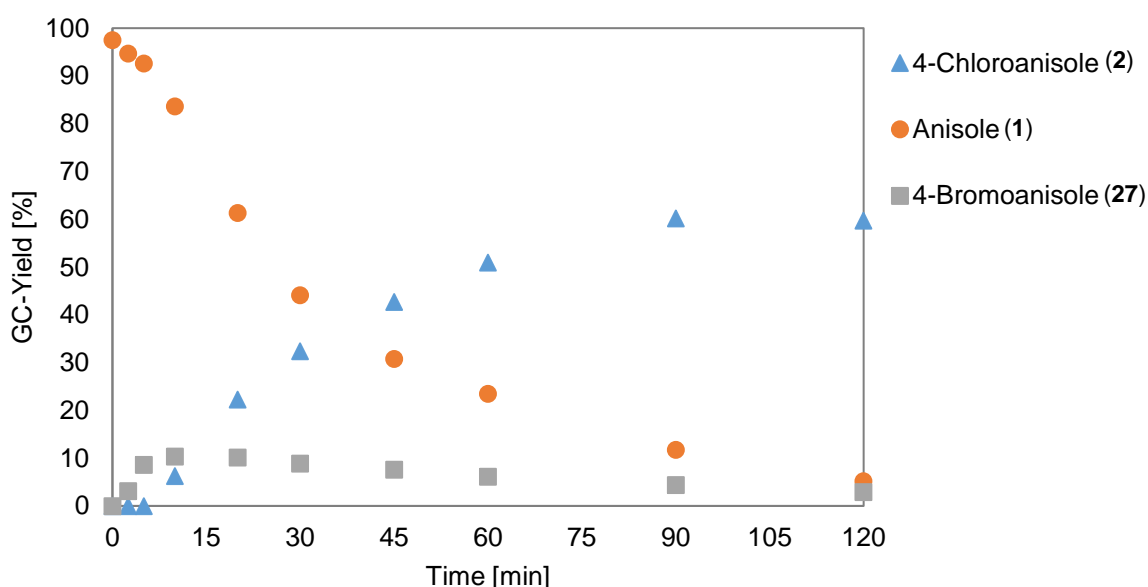
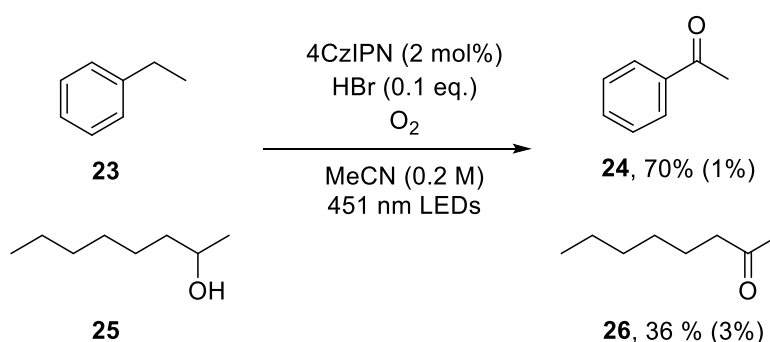


Figure 3-1. Kinetic reaction profile of the model reaction (see Table 3-1) under standard conditions: Anisole (0.1 mmol), HCl (3.0 eq.), HBr (10 mol%), and 4CzIPN (2 mol%) in MeCN (0.5 mL), irradiated under oxygen atmosphere by 451 nm LEDs at 25 °C. For each data point, 10 μ L of the reaction mixture were taken from the reaction vessel and analyzed with a GC-FID system after addition of *tert*-butylbenzene as standard.

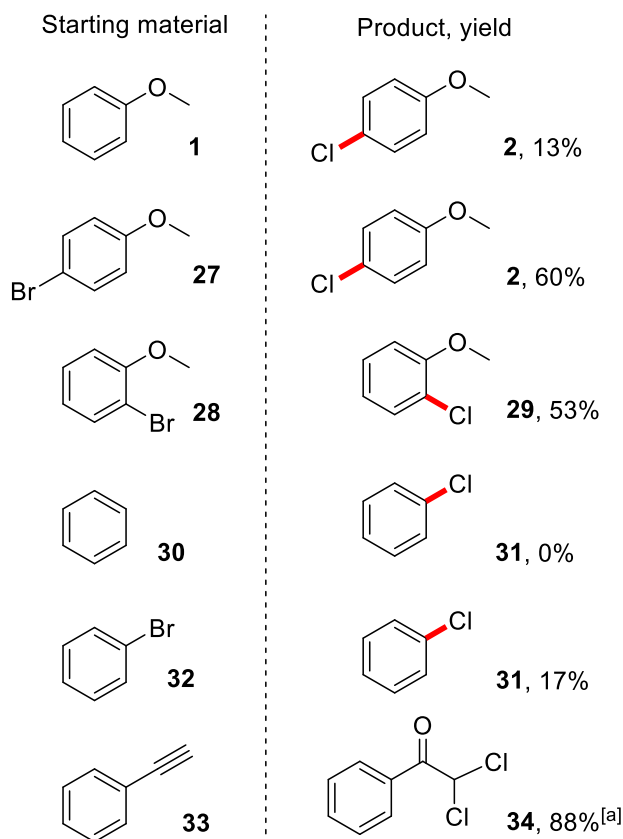
Upon investigating the scope of the reaction, we noticed that benzylic alkyl groups, as well as, benzylic and aliphatic alcohols were oxidized. As the reported oxidation potential of the excited catalyst ($E_{\text{ox}} = 1.35 \text{ V vs vs SCE}^{[9]}$) would not be sufficient for this process, we further investigated this phenomena, to get more insight into the whole reaction mechanism. We performed the reaction with ethylbenzene (**23**) and 2-octanol (**25**) in the presence of photocatalyst, oxygen, with and without 10 mol% of HBr (see Scheme 3-3). Whereas, the starting material was barely consumed in the absence of HBr, high conversion to the oxidized products was detected in the presence of bromide ions.^[14] It was previously reported that

bromine radicals are reasonable good hydrogen atom transfer (HAT) reagents and can be used in catalytic systems, developed for the generation of carbon radicals and the subsequent formation of new bonds.^[15] However, the reaction of carbon radicals with triplet oxygen (our conditions) will further oxidize the respective organic compounds. Whereas highly oxidizing photoredox catalysts can achieve the oxidation of aromatic systems, followed by the subsequent oxidation of benzylic positions, direct oxidation of unactivated aliphatic alcohols is less common.^[16]



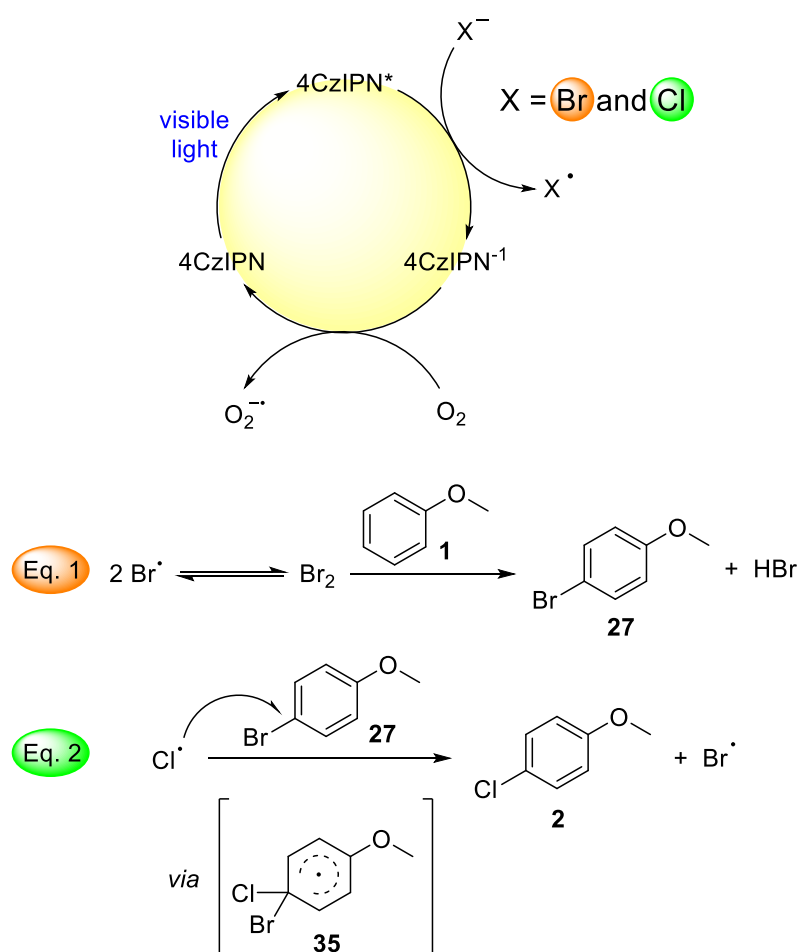
Scheme 3-3. Photocatalytic oxidation of organic compounds by generated bromine radicals via HAT. Yields without bromide source in parenthesis.

In 2014, the group of Chen postulated a FeCl_3 mediated halide exchange under UV-light conditions.^[17] They showed that liberated chlorine radicals readily react with aryl bromides, resulting in the formation of *ipso*-substituted chloroarenes. We assume that under our reaction conditions, chlorine radicals, generated by visible-light photoredox catalysis, may react in a comparable fashion. As the kinetic data (Figure 3-1) clearly demonstrates the initial formation of 4-bromoanisole (**27**) and its later consumption, we confirmed the consecutive chlorination step in the comparison experiments shown in Scheme 3-4.



Scheme 3-4. Halide exchange in the absence of a bromide source. Conditions: Starting material (0.1 mmol), HCl (3 eq.), and 4CzIPN (2 mol%) in MeCN (0.5 mL), irradiated under oxygen atmosphere by 451 nm LEDs at 25 °C for 1.5 h. GC-yields with *tert*-butylbenzene as standard. [a] Isolated yield.

When HCl, but no bromide source is present in the reaction mixture, anisole (**1**) is converted with a 13% yield of the desired product. However, 4-bromoanisole (**27**) as starting material will result in a 60% yield. Furthermore, 2-bromoanisole (**28**) as starting material yields 53% of *ipso*-substituted compound **29**, while only trace amounts of this *ortho*-product can be detected under standard reaction conditions. Moreover, less activated bromobenzene (**32**) can be converted, even if benzene itself is not halogenated under the photocatalytic conditions. All experiments support the proposed regioselective radical *ipso*-substitution of the bromine atom. To obtain further proof for the formation of an oxidized chlorine species, we exposed phenylacetylene (**33**) to our reaction conditions. As a result, we isolated **34** in high yield. Both, cationic and radical pathways are possible for the formation **34**.^[18]



Scheme 3-5. Mechanistic proposal for the visible-light mediated chlorination

Based on our observations and literature reports, we propose a mechanism for the described reaction (Scheme 3-5). The photoredox catalyst has a dual role, as it is oxidizing both, bromide and chloride anions, to their respective radical species. The formation of bromine radicals that can recombine to bromine as the active brominating agent, should occur faster. The *in situ* formed bromoarenes are subsequently attacked by chlorine radicals, yielding the desired chlorinated compounds.^[17, 19] In addition to the kinetic data, showing a fast consumption of bromide and quasi stoichiometric formation of bromoanisole (**27**), this assertion is supported by fluorescence quenching experiments (see Chapter 3.4.2.2, Figure 3-2). The interaction of the respective halide anions with the excited state of 4CzIPN is clearly demonstrated, whereas the observed quenching effect is stronger for the bromide ions. This observation also resembles the different oxidation potentials of Br⁻ ($E_{\text{ox}} = 0.74$ V vs SCE) and Cl⁻ ($E_{\text{ox}} = 1.05$ V vs SCE). Bromide can easier be oxidized by the catalyst ($E_{\text{ox}} = 1.35$ V vs SCE^[9]), which might result in a delayed oxidation of Cl⁻. The oxidation potential of our model substrate **1** ($E_{\text{ox}} = 1.75$ V vs SCE) exceeds the catalyst's excited state potential, consequently, the excited state quenching experiments show neglectable interaction of starting material with 4CzIPN*. As a result, and in contrast to reported photocatalytic brominations, we do not postulate the

formation of aryl radical cations as reaction intermediates.^[20] In the herein described process, the halogenation occurs with high regioselectivity due to the intermediary *para*-selective bromination step. The fate of the superoxide radicals, which are proposed to be generated from the reaction of O₂ with 4CzIPN^{•-}, is not completely clear yet. Often H₂O₂ is a final byproduct in photocatalytic reactions under aerial conditions.^[21] Yet, we could only detect low amounts of H₂O₂, as it is well known that hydrogen peroxide can be decomposed in the presence of bromide anions, whereupon elementary Br₂ is formed.^[22] This species can then further promote the described reaction pathway of the herein described reaction, as Br₂ readily reacts with electron rich arenes in the absence of light and catalyst,^[23] whereas unactivated benzene is not converted (for comparison experiments see Chapter 3.4.1, scheme 3-6).

3.3 Conclusion

In summary, a new visible-light mediated oxidative chlorination of electron rich arenes yielding chloroarenes is reported. The mechanistic investigations support a subsequent *in situ* bromination and halogen exchange pathway, yielding chloroarenes with high regioselectivity. The presence of 4CzIPN, an organic photoredox catalyst, light, and oxygen are crucial for the fast oxidation of bromide ions, as well as, for the chloride oxidation.

3.4 Experimental part

3.4.1 General information

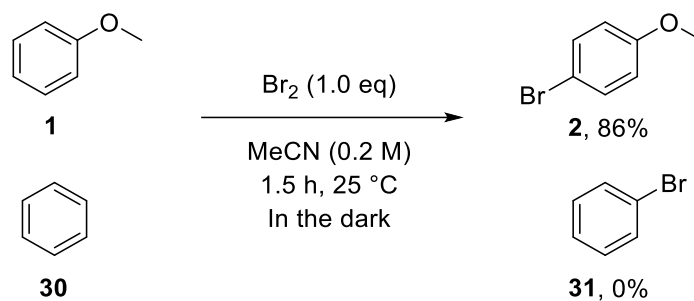
See Chapter 2.4.1

Additional information

Gas chromatography coupled with a flame ionization detector (GC-FID) was performed on an Agilent 7890 GC System with helium as carrier gas or an Agilent Intuvu 9000 GC system with hydrogen as carrier gas. Capillary column: length: 30 m; diam.: 0.25 mm; film: 0.25 μm .

3.4.2 Mechanistic investigations

3.4.2.1 Bromination of arenes by elementary bromine



Scheme 3-6: Bromination of anisole and benzene by elementary bromine in the absence of light and catalyst. Conditions: Anisole (0.1 mmol), Br_2 (0.1 mmol) in MeCN (0.5 mL) stirred in the dark for 1.5 h at 25 °C. GC-yields with *tert*-butylbenzene as standard.

3.4.2.2 Emission quenching experiments

All experiments were performed under argon atmosphere at room temperature with a gas-tight quartz cuvette (10×10 mm), containing 2 mL of a 2.5 μM solution of 4CzIPN in MeCN. Excitation wavelength $\lambda = 452$ nm.

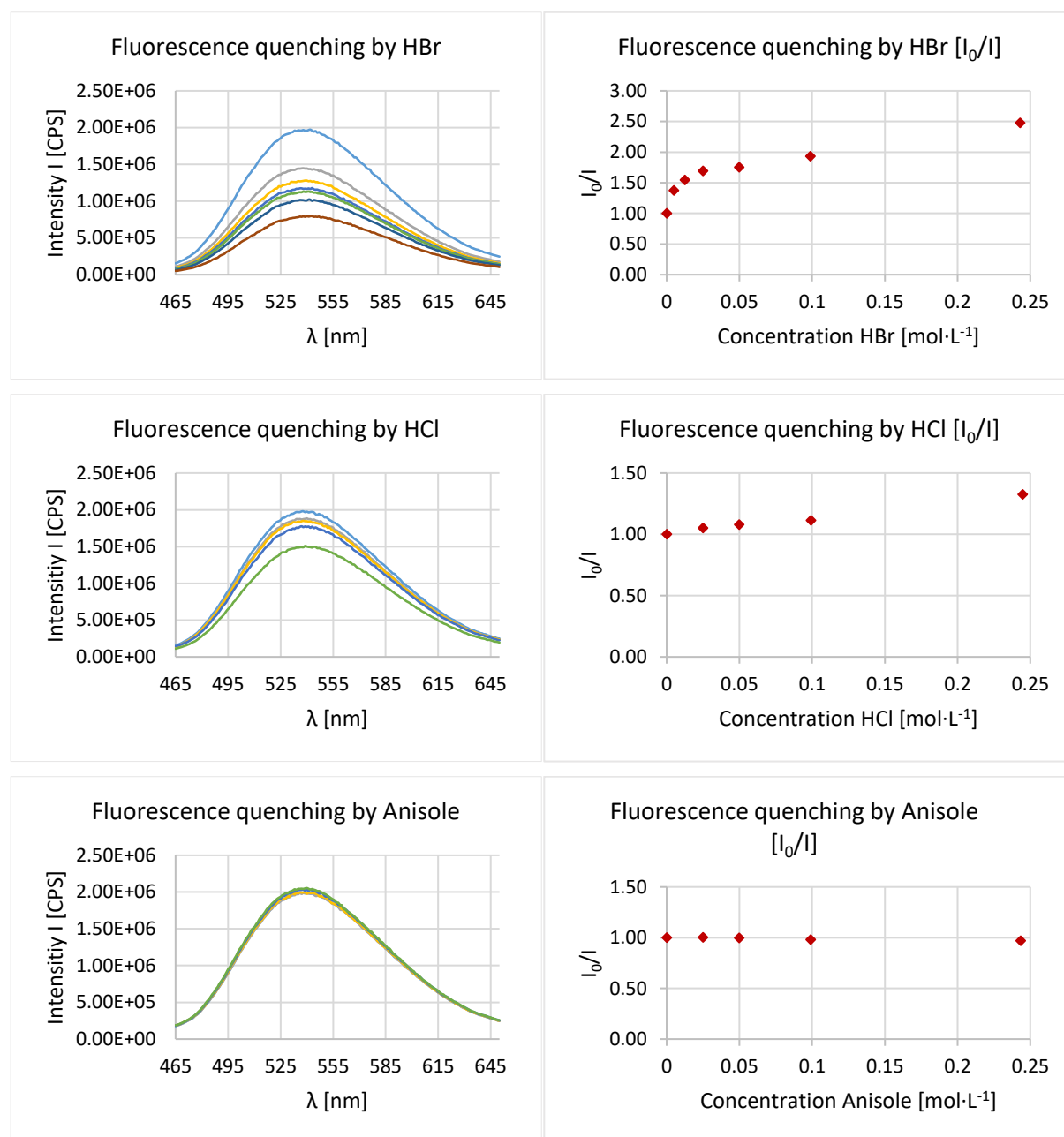


Figure 3-2: Fluorescence quenching experiments with 4CzIPN. Left: Fluorescence spectra (Signal intensity “I” in counts per second (CPS) vs the emission wavelength). Right: Plotting of I_0/I at $\lambda_{\text{max}} = 552$ nm vs the respective concentration of the quencher.

3.4.2.3 Cyclic voltammetry measurements

The scan rate for all measurements was $50 \text{ mV}\cdot\text{s}^{-1}$. The scan direction (start at 0 V) is indicated with a black arrow.

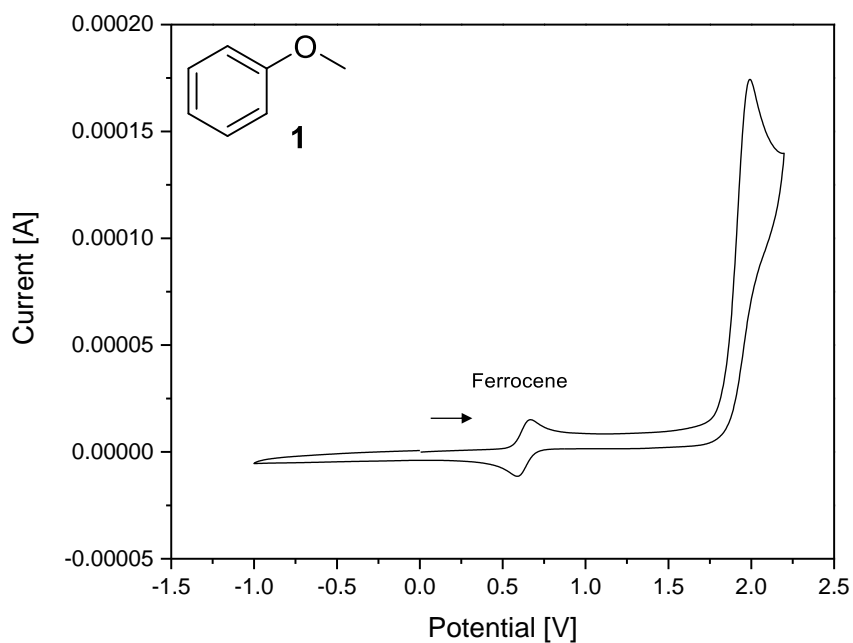


Figure 3-3: Oxidation of anisole (1).

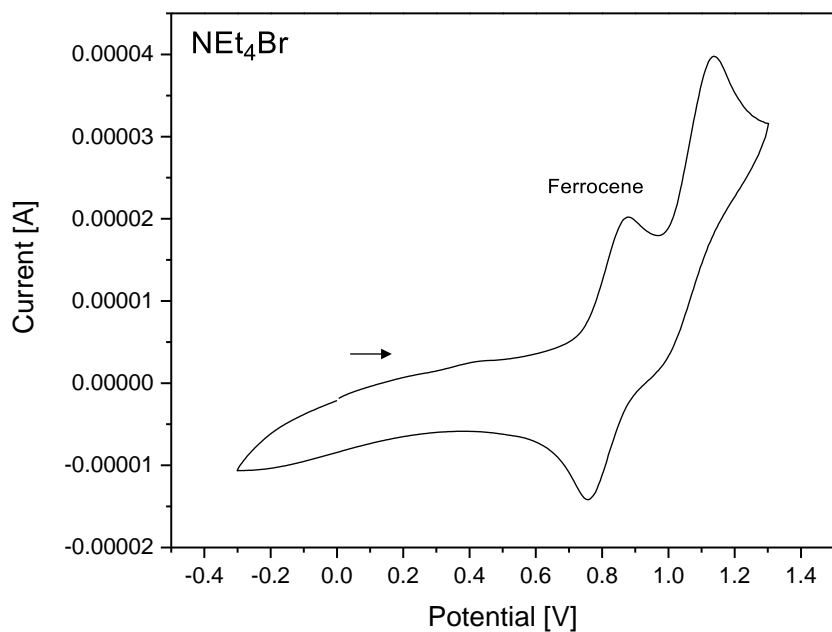


Figure 3-4: Oxidation of tetraethylammonium bromide.

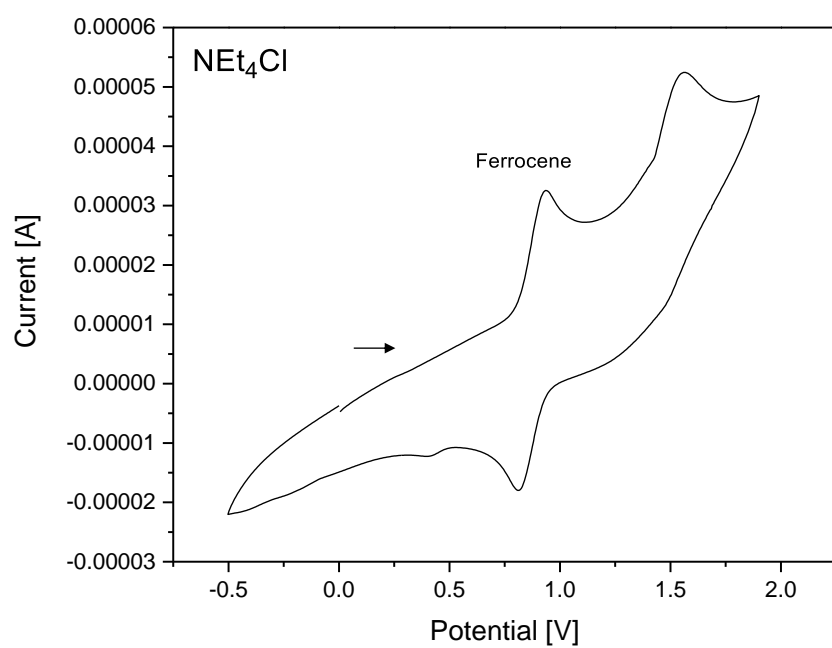
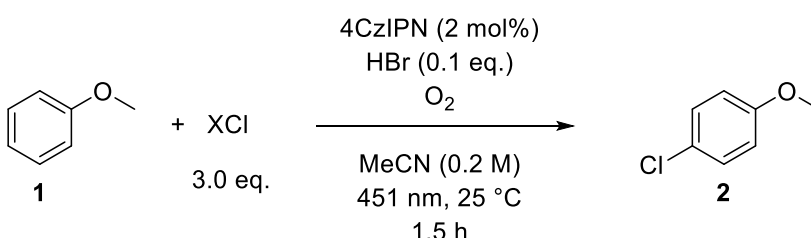


Figure 3-5: Oxidation of tetraethylammonium chloride.

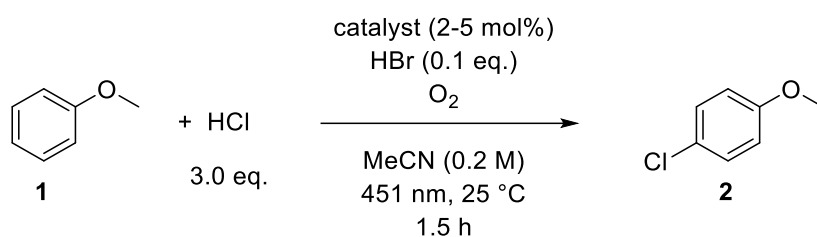
3.4.3 General experimental procedure

A 5 mL glass crimp vial was charged with 0.1 mmol of the respective substrate, 4CzIPN (1.6 mg, 2 mol%), MeCN (0.5 mL) and 27.4 μ L of a freshly prepared mixture of aqueous HCl and HBr (0.3 mmol, 3.0 eq. and 0.01 mmol, 0.1 eq.). The vial was closed with a septum and flushed two times with oxygen from a balloon connected to a syringe needle. The reaction vial was placed into a custom-built cooling system at 25 °C and irradiated under stirring by two 451 nm LEDs through the bottom side (ca. 5 mm distance to the LEDs). The reaction progress was monitored by TLC or GC-FID and the reaction was stopped after 0.5 - 3.5 h, when all starting material was consumed, or no further progress was detected. To obtain an average result, two reaction mixtures were united and the solvent was removed under reduced pressure after the addition of silica gel. The products were purified by automated silica gel flash column chromatography with a mixture of petrol ether and ethyl acetate as eluent

Table 3-3: Optimization of the chlorination of anisole - Screening of the chloride source.

<div style="text-align: center;">  </div>				
Entry	Chloride source	Light source (λ_{max})	Catalyst loading [mol%]	Yield [%]
1	HCl	451 nm	2	63
2	HCl + H ₂ O (14 eq.)	451 nm	5	55
3	NaCl	451 nm	5	0
9	NEt ₄ Cl	528 nm	5	0
10	NBu ₄ Cl	451 nm	5	1

Conditions: Anisole (0.1 mmol), XCl (3 eq.), HBr (0.1 eq.), and 4CzIPN (2 mol%) MeCN (0.5 mL), irradiated with 451 nm LEDs under oxygen atmosphere at 25 °C for 1.5 h. GC-yields with *tert*-butylbenzene as standard.

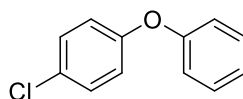
Table 3-4: Optimization of the chlorination of anisole - Screening of the Catalyst.

Entry	Catalyst	Light source (λ_{max}) ^[a]	Catalyst loading [mol%]	Yield ^[b] [%]
1	4CzIPN	451 nm	2	63
2	Riboflavin tetraacetate	451 nm	5	0
3	Rhodamine 6G	451 nm	5	0
4	Rhodamine 6G	528 nm	5	0
5	Rose bengal (disodium salt)	451 nm	2.5	15
6	Rose bengal (disodium salt)	528 nm	2.5	1
7	Triphenylpyrylium tetrafluoroborate	451 nm	5	12
8	Eosin Y (neutral form)	451 nm	5	16
9	Eosin Y (neutral form)	528 nm	5	4
10	9-Mesityl-10-methylacridinium perchlorate	451 nm	5	16

Conditions: Anisole (0.1 mmol), HCl (3 eq.), HBr (0.1 eq.), and catalyst in MeCN (0.5 mL), irradiated under oxygen atmosphere at 25 °C. [a] Irradiation by two 451 nm LEDs for 1.5 h or by a single 528 nm LED for 3 h. [b] GC-yields with *tert*-butylbenzene or 1-methylnaphthalene as standard.

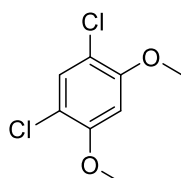
3.4.4 Product characterization

1-Chloro-4-phenoxybenzene (**3**)^[24]



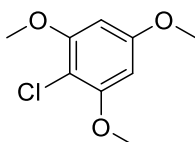
According to the general procedure, compound **3** was obtained after 3 h as a colorless oil (31.2 mg, 0.152 mmol, 76%). ¹H NMR (300 MHz, DMSO-*d*₆): δ 7.46 – 7.37 (m, 4H), 7.21 – 7.14 (m, 1H), 7.08 – 6.97 (m, 4H). ¹³C NMR (75 MHz, DMSO-*d*₆): δ 156.63, 156.15, 130.63, 130.33, 127.55, 124.37, 120.60, 119.33. HRMS: Calculated for C₁₂H₉ClO [M⁺] 204.0336; found 204.0329.

1,5-Dichloro-2,4-dimethoxybenzene (**4**)^[25]



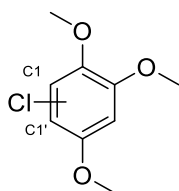
According to the general procedure, compound **4** was obtained after 2 h as a white solid (20.2 mg, 0.097 mmol, 49%), with 1-chloro-2,4-dimethoxybenzene (**4'**) as byproduct (NMR-yield 5%). ¹H NMR (400 MHz, DMSO-*d*₆): δ 7.48 (s, 1H), 6.88 (s, 1H), 3.89 (s, 6H). ¹³C NMR (101 MHz, DMSO-*d*₆): δ 154.89, 129.97, 112.71, 99.32, 57.06. HRMS: Calculated for C₈H₈Cl₂O₂ [M⁺] 205.9896; 205.9886; found 205.9886.

2-Chloro-1,3,5-trimethoxybenzene (**5**)^[26]



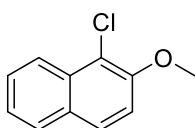
According to the general procedure, compound **5** was obtained after 1 h as an orange solid (27.3 mg, 0.135 mmol, 67%). ¹H NMR (400 MHz, DMSO-*d*₆): δ 6.34 (s, 2H), 3.85 – 3.77 (m, 9H). ¹³C NMR (101 MHz, DMSO-*d*₆): δ 159.79, 156.48, 101.36, 92.31, 56.62, 56.00. HRMS: Calculated for C₉H₁₁ClO₃ [M⁺] 202.0391; found 202.0377.

1-Chloro-2,3,5-trimethoxybenzene (**6**) and 1-Chloro-2,4,5-trimethoxybenzene (**6'**)^[27]



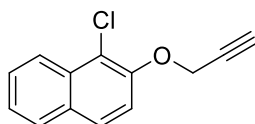
According to the general procedure, compounds **6** and **6'** were obtained after 2.5 h in a 3:1 (C1:C1') ratio (inseparable mixture) as an orange oil (25.1 mg, 0.124 mmol, 62%). Compound **6**: ¹H NMR (400 MHz, DMSO-*d*₆): δ 7.01 (s, 1H), 6.81 (s, 1H), 3.86 – 3.78 (m, 6H), 3.71 (s, 3H). Compound **6'**: ¹H NMR (400 MHz, DMSO-*d*₆): δ 7.12 (s, 1H), 6.80 (s, 1H), 3.86 – 3.78 (m, 6H), 3.71 (s, 3H). Compounds **6** and **6'** combined: ¹³C NMR (101 MHz, DMSO-*d*₆): δ 150.28, 149.62, 149.22, 148.99, 143.82, 143.47, 116.95, 114.37, 111.52, 100.08, 100.00, 99.95, 57.28, 57.16, 56.87, 56.83, 56.48, 56.43. HRMS: Calculated for C₉H₁₁ClO₃ [M⁺] 202.0391; found 202.0393.

1-Chloro-2-methoxynaphthalene (**7**)^[28]



According to the general procedure, compound **7** was obtained after 30 min as a white solid (27.4 mg, 0.142 mmol, 71%). ¹H NMR (300 MHz, DMSO-*d*₆): δ 8.12 – 8.04 (m, 1H), 8.00 – 7.91 (m, 2H), 7.67 – 7.59 (m, 1H), 7.59 – 7.52 (m, 1H), 7.51 – 7.40 (m, 1H), 3.99 (s, 3H). ¹³C NMR (75 MHz, DMSO-*d*₆): δ 152.86, 131.38, 129.41, 128.92, 128.75, 128.31, 124.74, 122.89, 115.19, 114.70, 57.15. HRMS: Calculated for C₁₁H₉ClO [M⁺] 192.0336; found 192.0346.

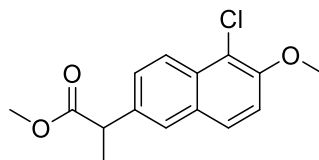
1-Chloro-2-(prop-2-yn-1-yloxy)naphthalene (**8**)^[29]



According to the general procedure, compound **8** was obtained after 30 min as a white solid (8.6 mg, 0.040 mmol, 20%). ¹H NMR (400 MHz, DMSO-*d*₆): δ 8.13 – 8.06 (m, 1H), 8.00 – 7.93 (m, 2H), 7.67 – 7.58 (m, 2H), 7.51 – 7.45 (m, 1H), 5.06 (d, *J* = 2.4 Hz, 2H), 3.62 (t, *J* = 2.4 Hz, 1H). ¹³C NMR (101 MHz, DMSO-*d*₆): δ 151.01, 131.39, 129.88, 128.77, 128.68, 128.41,

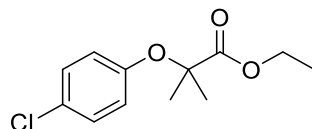
125.25, 123.12, 116.47, 116.14, 79.43, 79.35, 57.48. HRMS: Calculated for $C_{13}H_9ClO$ [M^{++}] 216.0336; found 216.0336.

Methyl 2-(5-chloro-6-methoxynaphthalen-2-yl)propanoate (9)^[30]



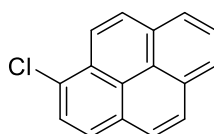
According to the general procedure, compound **9** was obtained after 30 min as a white solid (24.3 mg, 0.087 mmol, 44%). 1H NMR (400 MHz, $DMSO-d_6$): δ 8.08 – 8.00 (m, 1H), 7.97 – 7.91 (m, 1H), 7.85 – 7.79 (m, 1H), 7.58 – 7.51 (m, 2H), 4.03 – 3.91 (m, 4H), 3.59 (s, 3H), 1.47 (d, $J = 7.1$ Hz, 3H). ^{13}C NMR (101 MHz, $DMSO-d_6$): δ 174.65, 152.81, 137.00, 130.50, 129.41, 128.76, 128.23, 126.78, 123.43, 115.19, 115.03, 57.19, 52.33, 44.58, 18.75. HRMS: Calculated for $C_{15}H_{15}ClO_3$ [$M-H^+$] 279.0782; found 279.0784.

Ethyl 2-(4-chlorophenoxy)-2-methylpropanoate (10)^[31]



According to the general procedure, compound **10** was obtained after 2.5 h as a colorless oil (46.9 mg, 0.193 mmol, 97%). 1H NMR (400 MHz, $DMSO-d_6$): δ 7.34 – 7.22 (m, 2H), 6.85 – 6.75 (m, 2H), 4.15 (q, $J = 7.1$ Hz, 2H), 1.50 (s, 6H), 1.15 (t, $J = 7.1$ Hz, 3H). ^{13}C NMR (101 MHz, $DMSO-d_6$): δ 173.34, 154.37, 129.58, 126.26, 120.92, 79.52, 61.59, 25.37, 14.31. HRMS: Calculated for $C_{12}H_{15}ClO_3$ [$M-H^+$] 243.0782; found 243.0800.

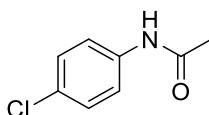
1-Chloropyrene (11)^[32]



According to the general procedure, but with 1.0 mL MeCN as solvent, compound **11** was obtained after 2.5 h as a white solid (39.2 mg, 0.166 mmol, 83%). 1H NMR (300 MHz, Chloroform- d): δ 8.51 – 8.39 (m, 1H), 8.25 – 8.12 (m, 3H), 8.10 – 7.93 (m, 5H). ^{13}C NMR (75

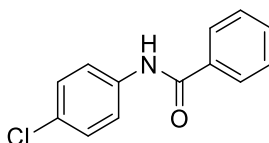
MHz, Chloroform-*d*): δ 131.20, 130.92, 130.03, 129.08, 128.97, 128.65, 128.08, 127.51, 127.05, 126.71, 126.47, 125.63, 125.49, 125.18, 124.11, 123.26. HRMS: Calculated for $C_{16}H_9Cl$ [M^{+}] 236.0387; found 236.0379.

***N*-(4-Chlorophenyl)acetamide (12)**^[33]



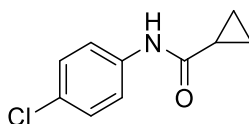
According to the general procedure, compound **12** was obtained after 1 h as a white solid (27.6 mg, 0.163 mmol, 81%). ¹H NMR (400 MHz, DMSO-*d*₆): δ 10.05 (s, 1H), 7.68 – 7.53 (m, 2H), 7.40 – 7.28 (m, 2H), 2.04 (s, 3H). ¹³C NMR (101 MHz, DMSO-*d*₆): δ 168.87, 138.72, 129.01, 126.92, 120.91, 24.44. HRMS: Calculated for C_8H_8ClNO [$M-H^+$] 170.0367; found 170.0369.

***N*-(4-Chlorophenyl)benzamide (13)**^[34]



According to the general procedure, but with 1.0 mL MeCN as solvent, compound **13** was obtained after 2.5 h as a white solid (39.4 mg, 0.170 mmol, 85%). ¹H NMR (400 MHz, DMSO-*d*₆): δ 10.36 (s, 1H), 8.00 – 7.90 (m, 2H), 7.85 – 7.79 (m, 2H), 7.63 – 7.56 (m, 1H), 7.56 – 7.49 (m, 2H), 7.44 – 7.37 (m, 2H). ¹³C NMR (101 MHz, DMSO-*d*₆): δ 166.11, 138.62, 135.17, 132.16, 128.98, 128.88, 128.14, 127.71, 122.30. HRMS: Calculated for $C_{13}H_{10}ClNO$ [$M-H^+$] 232.0524, found 232.0533.

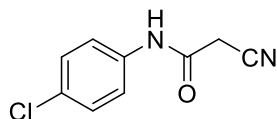
***N*-(4-Chlorophenyl)cyclopropanecarboxamide (14)**^[35]



According to the general procedure, compound **14** was obtained after 1.5 h as a white solid (23.0 mg, 0.118 mmol, 59%). ¹H NMR (400 MHz, DMSO-*d*₆): δ 10.30 (s, 1H), 7.67 – 7.55 (m, 2H), 7.39 – 7.28 (m, 2H), 1.83 – 1.70 (m, 1H), 0.85 – 0.74 (m, 4H). ¹³C NMR (101 MHz, DMSO-

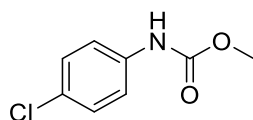
d_6): δ 172.20, 138.74, 129.03, 126.85, 120.92, 15.03, 7.74. HRMS: Calculated for $C_{10}H_{10}ClNO$ $[M-H^+]$ 196.0524, found 196.0549.

***N*-(4-Chlorophenyl)-2-cyanoacetamide (15)**^[36]



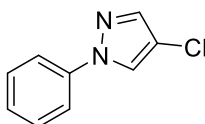
According to the general procedure, compound **15** was obtained after 2.5 h as a white solid (27.0 mg, 0.139 mmol, 69%). 1H NMR (400 MHz, $DMSO-d_6$): δ 10.43 (s, 1H), 7.63 – 7.54 (m, 2H), 7.46 – 7.34 (m, 2H), 3.91 (s, 2H). ^{13}C NMR (101 MHz, $DMSO-d_6$): δ 161.68, 137.77, 129.29, 127.94, 121.25, 116.24, 27.24. HRMS: Calculated for $C_9H_7ClN_2O$ $[M-H^+]$ 195.0320; found 195.0319.

Methyl (4-chlorophenyl)carbamate (16)^[37]



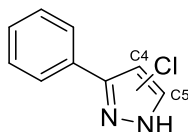
According to the general procedure, compound **16** was obtained after 75 min as a white solid (28.7 mg, 0.155 mmol, 77%). 1H NMR (400 MHz, $DMSO-d_6$): δ 9.77 (s, 1H), 7.50 – 7.43 (m, 2H), 7.36 – 7.27 (m, 2H), 3.65 (s, 3H). ^{13}C NMR (101 MHz, $DMSO-d_6$): δ 154.38, 138.63, 129.10, 126.44, 120.07, 52.21. HRMS: Calculated for $C_8H_8ClNO_2$ $[M-H^+]$ 186.0316; found 186.0325.

4-Chloro-1-phenyl-1H-pyrazole (17)^[38]



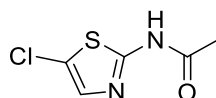
According to the general procedure, compound **17** was obtained after 2 h as a white solid (34.0 mg, 0.190 mmol, 95%). 1H NMR (400 MHz, $DMSO-d_6$): δ 8.85 – 8.74 (m, 1H), 7.98 – 7.84 (m, 1H), 7.84 – 7.76 (m, 2H), 7.58 – 7.46 (m, 2H), 7.39 – 7.29 (m, 1H). ^{13}C NMR (101 MHz, $DMSO-d_6$): δ 139.68, 139.64, 130.03, 127.26, 126.56, 118.76, 118.72, 111.47. HRMS: Calculated for $C_9H_7ClN_2$ $[M^+]$ 178.0292; found 178.0295.

4-Chloro-3-phenyl-1H-pyrazole (**18**) and 5-Chloro-3-phenyl-1H-pyrazole (**18'**)^[39]



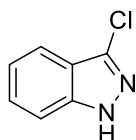
According to the general procedure, compounds **18** and **18'** were obtained after 2.5 h a 3:2(C4:C5) ratio (inseparable mixture) as a pale beige solid (34.1 mg, 0.191 mmol, 95%). Compound **18**: ¹H NMR (400 MHz, DMSO-*d*₆): δ 13.28 (s, 1H), 8.08 (s, 1H), 7.90 – 7.72 (m, 2H), 7.58 – 7.34 (m, 3H). Compound **18'**: ¹H NMR (400 MHz, DMSO-*d*₆): δ 13.55 (s, 1H), 7.90 – 7.72 (m, 2H), 7.68 (s, 1H), 7.58 – 7.34 (m, 3H). Compounds **18** and **18'** combined: ¹³C NMR (101 MHz, DMSO-*d*₆): δ 145.83, 139.36, 137.56, 132.37, 129.41, 129.21, 128.96, 128.85, 128.33, 127.52, 127.18, 127.06, 109.98, 106.37. HRMS: Calculated for C₉H₇ClN₂ [M⁺] 178.0292; found 178.0290.

N-(5-Chlorothiazol-2-yl)acetamide (**19**)^[40]



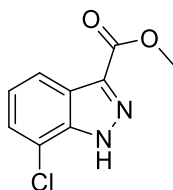
According to the general procedure, compound **19** was obtained after 1.5 h as a slightly yellow solid (30.6 mg, 0.173, 87%). ¹H NMR (300 MHz, DMSO-*d*₆) δ 12.34 (s, 1H), 7.48 (s, 1H), 2.14 (s, 3H). ¹³C NMR (75 MHz, DMSO-*d*₆): δ 169.34, 156.38, 135.93, 118.24, 22.66. HRMS: Calculated for C₅H₅ClN₂OS [M-H⁺] 176.9884, found 176.9883.

3-Chloro-1H-indazole (**20**)^[41]



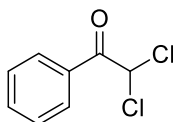
According to the general procedure, compound **20** was obtained after 2 h as a white solid (10.7, 0.070 mmol, 35%). ¹H NMR (400 MHz, DMSO-*d*₆): δ 13.28 (s, 1H), 7.69 – 7.64 (m, 1H), 7.59 – 7.54 (m, 1H), 7.49 – 7.43 (m, 1H), 7.27 – 7.19 (m, 1H). ¹³C NMR (101 MHz, DMSO-*d*₆): δ 141.56, 132.60, 127.94, 121.86, 119.87, 119.04, 111.42. HRMS: Calculated for C₇H₅ClN₂ [M⁺] 152.0136, found 152.0125.

Methyl 7-chloro-1H-indazole-3-carboxylate (21)^[42]



According to the general procedure, compound **21** was obtained after 3.5 h as a white solid (7.0, 0.033 mmol, 17%). ¹H NMR (400 MHz, DMSO-*d*₆): δ 14.46 (s, 1H), 8.08 – 7.98 (m, 1H), 7.61 – 7.52 (m, 1H), 7.34 – 7.27 (m, 1H), 3.93 (s, 3H). ¹³C NMR (101 MHz, DMSO-*d*₆) δ 162.76, 139.00, 136.60, 126.67, 124.46, 124.41, 120.52, 116.12, 52.31. HRMS: Calculated for C₉H₇ClN₂O₂ [M⁺] 210.0191, found 210.0193.

2,2-Dichloro-1-phenylethan-1-one (34)^[43]



According to the general procedure, but without HBr, compound **34** was obtained after 30 min as a colorless oil (33.1 mg, 0.018 mmol, 88%). ¹H NMR (400 MHz, DMSO-*d*₆): δ 8.12 – 8.05 (m, 2H), 7.92 (s, 1H), 7.80 – 7.71 (m, 1H), 7.67 – 7.57 (m, 2H). ¹³C NMR (101 MHz, DMSO-*d*₆): δ 186.79, 135.21, 132.03, 129.90, 129.58, 69.43. HRMS: Calculated for C₈H₇Cl₂O [M⁺] 187.9790; found 187.9761.

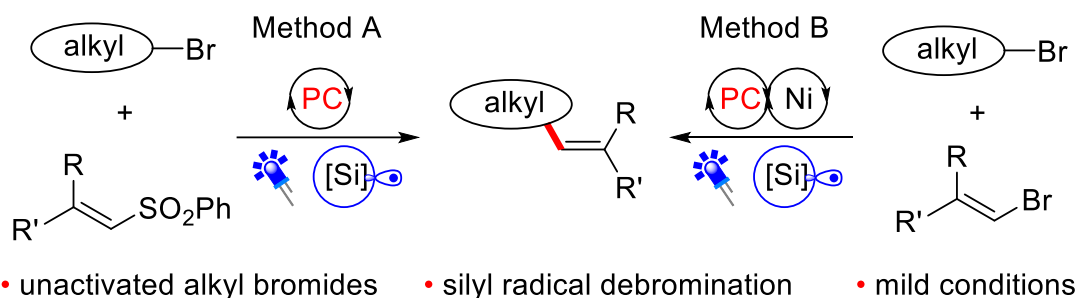
3.5 References

- [1] a) R. N. Wheeler, Jr., *Environ. Health Perspect.* **1981**, *41*, 123-128; b) A. F. Littke, G. C. Fu, *Angew. Chem., Int. Ed.* **2002**, *41*, 4176-4211; c) F. Ullmann, J. Bielecki, *Ber. Dtsch. Chem. Ges.* **1901**, *34*, 2174-2185; d) G. W. Gribble, *Environ. Sci. Technol.* **1994**, *28*, 310A-319A; e) Z.-X. Wang, Z., W.-J. Guo, In *Catalysis in C-Cl Activation - Homogeneous Catalysis for Unreactive Bond Activation* (Ed.: Z. Shi), John Wiley & Sons, Hoboken, N. J, **2015**, pp. 1-201.
- [2] a) R. Wilcken, M. O. Zimmermann, A. Lange, A. C. Jörger, F. M. Boeckler, *J. Med. Chem.* **2013**, *56*, 1363-1388; b) C. Lamberth, *Pest Manage. Sci.* **2013**, *69*, 1106-1114. Selected examples for common chlorinated crop protection agents: *Chlorothalonil*, *Atrazine*, *Imidacloprid*. Selected examples for common chlorinated pharmacophors: *Alprazolam*, *Losartan*, *Hydrochlorothiazide*, *Amlodipine*.
- [3] U. Beck, E. Löser in *Chlorinated Benzenes and Other Nucleus-Chlorinated Aromatic Hydrocarbons*. In *Ullmann's Encyclopedia of Industrial Chemistry*, Vol. 8 Wiley-VCH, Weinheim, **2011**, pp. 483-519; b) B. Galabov, D. Nalbantova, P. v. R. Schleyer, H. F. Schaefer, *Acc. Chem. Res.* **2016**, *49*, 1191-1199.
- [4] a) J. Chen, X. Xiong, Z. Chen, J. Huang, *Synlett* **2015**, *26*, 2831-2834; b) J. S. Yadav, B. V. S. Reddy, P. S. R. Reddy, A. K. Basak, A. V. Narsaiah, *Adv. Synth. Catal.* **2004**, *346*, 77-82; c) N. Narender, P. Srinivasu, S. J. Kulkarni, K. V. Raghavan, *Synth. Commun.* **2002**, *32*, 279-286.
- [5] Selected reviews: a) N. A. Romero, D. A. Nicewicz, *Chem. Rev.* **2016**, *116*, 10075-10166; b) L. Marzo, S. K. Pagire, O. Reiser, B. König, *Angew. Chem., Int. Ed.* **2018**, *57*, 10034-10072.
- [6] D. Petzold, B. König, *Adv. Synth. Catal.* **2018**, *360*, 626-630.
- [7] a) L. Zhang, X. Hu, *Chem. Sci.* **2017**, *8*, 7009-7013. For further work on photocatalytic chlorination please see: b) T. Hering, B. Mühlendorf, R. Wolf, B. König, *Angew. Chem., Int. Ed.* **2016**, *55*, 5342-5345; c) L. Candish, E. A. Standley, A. Gomez-Suarez, S. Mukherjee, F. Glorius, *Chem. Eur. J.* **2016**, *22*, 9971-9974; d) T. Hering, B. König, *Tetrahedron* **2016**, *72*, 7821-7825; e) K. Ohkubo, A. Fujimoto, S. Fukuzumi, *Chem. Asian J.* **2016**, *11*, 996-999.
- [8] 4CzIPN = 2,4,5,6-Tetra(9H-carbazol-9-yl)isophthalonitrile. The catalyst is depicted in Table 3-2.
- [9] J. Luo, J. Zhang, *ACS Catal.* **2016**, *6*, 873-877.
- [10] R. A. Sheldon, *Chem. Commun.* **2008**, *0*, 3352-3365.
- [11] X.-M. Wu, C. J. Branford-White, L.-M. Zhu, N. P. Chatterton, D.-G. Yu, *J. Mater. Sci.: Mater. Med.* **2010**, *21*, 2403-2411.

- [12] S. S. T. Lee, T. Pineau, J. Drago, E. J. Lee, J. W. Owens, D. L. Kroetz, P. M. Fernandez-Salguero, H. Westphal, F. J. Gonzalez, *Mol. Cell. Biol.* **1995**, *15*, 3012-3022.
- [13] Further prolonging of the reaction times did not reasonably increase the yield for compounds **20** and **21**.
- [14] Reactions in the absence of bromide ions, but with additional H₂O with and without TFA, for pH adjustment, delivered comparable results to reactions in the absence of HBr.
- [15] L. Capaldo, D. Ravelli, *Eur. J. Org. Chem.* **2017**, *2017*, 2056-2071.
- [16] S.-I. Hirashima, A. Itoh, *Green Chem.* **2007**, *9*, 318-320.
- [17] Y. Wang, L. Li, H. Ji, W. Ma, C. Chen, J. Zhao, *Chem. Commun.* **2014**, *50*, 2344-2346.
- [18] a) L. Finck, J. Brals, B. Pavuluri, F. Gallou, S. Handa, *J. Org. Chem.* **2018**, *83*, 7366-7372; b) J. Liu, W. Li, C. Wang, Y. Li, Z. Li, *Tetrahedron Lett.* **2011**, *52*, 4320-4323; c) C. Wu, X. Xin, Z.-M. Fu, L.-Y. Xie, K.-J. Liu, Z. Wang, W. Li, Z.-H. Yuan, W.-M. He, *Green Chem.* **2017**, *19*, 1983-1989.
- [19] K. Tanemura, T. Suzuki, Y. Nishida, T. Horaguchi, *Tetrahedron* **2010**, *66*, 2881-2888.
- [20] An anthraquinone derivate (estimated excited state oxidation potential up to 2.3 V vs SCE) was used as catalyst for the photocatalytic bromination. Please see reference 6.
- [21] a) S. Fukuzumi, K. Ohkubo, *Organic & Biomolecular Chemistry* **2014**, *12*, 6059-6071; b) S. J. S. Düsel, B. König, *J. Org. Chem.* **2018**, *83*, 2802-2807; c) K. Sahel, L. Elsellami, I. Mirali, F. Dappozze, M. Bouhent, C. Guillard, *Appl. Catal., B* **2016**, *188*, 106-112.
- [22] A. Podgorsek, S. Stavber, M. Zupan, J. Iskra, *Tetrahedron* **2009**, *65*, 4429-4439.
- [23] T. Kesharwani, C. Kornman, A. Tonnaer, A. Hayes, S. Kim, N. Dahal, R. Romero, A. Royappa, *Tetrahedron* **2018**, *74*, 2973-2984.
- [24] J. Zhang, Z. Zhang, Y. Wang, X. Zheng, Z. Wang, *Eur. J. Org. Chem.* **2008**, 5112-5116.
- [25] L. Testaferri, M. Tiecco, M. Tingoli, D. Chianelli, M. Montanucci, *Tetrahedron* **1983**, *39*, 193-197.
- [26] K. Yonehara, K. Kamata, K. Yamaguchi, N. Mizuno, *Chem. Commun.* **2011**, *47*, 1692-1694.
- [27] A. Oliverio, G. Castelfranchi, *Gazz. Chim. Ital.* **1950**, *80*, 276-280.
- [28] P. D. Nahide, V. Ramadoss, K. A. Juarez-Ornelas, Y. Satkar, R. Ortiz-Alvarado, J. M. J. Cervera-Villanueva, A. J. Alonso-Castro, J. R. Zapata-Morales, M. A. Ramirez-Morales, A. J. Ruiz-Padilla, M. A. Deveze-Alvarez, C. R. Solorio-Alvarado, *Eur. J. Org. Chem.* **2018**, *2018*, 485-493.
- [29] N. Sarcevic, J. Zsindely, H. Schmid, *Helv. Chim. Acta* **1973**, *56*, 1457-1476.

- [30] O. Piccolo, F. Spreafico, G. Visentin, E. Valoti, *J. Org. Chem.* **1987**, *52*, 10-14.
- [31] S. S. T. Lee, T. Pineau, J. Drago, E. J. Lee, J. W. Owens, D. L. Kroetz, P. M. Fernandez-Salguero, H. Westphal, F. J. Gonzalez, *Mol. Cell. Biol.* **1995**, *15*, 3012-3022.
- [32] J. Aguilera-Sigalat, J. Sanchez-SanMartin, C. E. Agudelo-Morales, E. Zaballos, R. E. Galian, J. Perez-Prieto, *ChemPhysChem* **2012**, *13*, 835-844.
- [33] T. Hering, B. Mühldorf, R. Wolf, B. König, *Angew. Chem., Int. Ed.* **2016**, *55*, 5342-5345.
- [34] Y. Wu, S. Wang, L. Zhang, G. Yang, X. Zhu, Z. Zhou, H. Zhu, S. Wu, *Eur. J. Org. Chem.* **2010**, 326-332.
- [35] J. K. Augustine, R. Kumar, A. Bombrun, A. B. Mandal, *Tetrahedron Lett.* **2011**, *52*, 1074-1077.
- [36] R. Adhikari, D. A. Jones, A. J. Liepa, R. H. Nearn, *Aust. J. Chem.* **2005**, *58*, 882-890.
- [37] M. Iinuma, K. Moriyama, H. Togo, *Tetrahedron* **2013**, *69*, 2961-2970.
- [38] D. Kalyani, A. R. Dick, W. Q. Anani, M. S. Sanford, *Tetrahedron* **2006**, *62*, 11483-11498.
- [39] K. L. Olsen, M. R. Jensen, J. A. MacKay, *Tetrahedron Lett.* **2017**, *58*, 4111-4114.
- [40] Z. Lu, Q. Li, M. Tang, P. Jiang, H. Zheng, X. Yang, *Chem. Commun.* **2015**, *51*, 14852-14855.
- [41] G. Luo, L. Chen, G. Dubowchik, *J. Org. Chem.* **2006**, *71*, 5392-5395.
- [42] I. P. Buchler, M. J. Hayes, S. G. Hedge, S. L. Hockerman, D. E. Jones, S. W. Kortum, J. G. Rico, R. E. Tenbrink, K. K. Wu. (Pfizer Inc., USA). Indazole derivatives as CB1 receptor modulators and their preparation and use in the treatment of CB1-mediated diseases. Patent WO2009106982, 2009.
- [43] L. Finck, J. Brals, B. Pavuluri, F. Gallou, S. Handa, *J. Org. Chem.* **2018**, *83*, 7366-7372.

4. Alkenylation of unactivated alkyl bromides through visible-light photocatalysis



Two visible-light driven alkenylation reactions of unactivated alkyl bromides, which were enabled by the use of $\text{Ir}(\text{dF}(\text{CF}_3)\text{ppy})_2(\text{dtbbpy})\text{PF}_6$ as photocatalyst and $(\text{TMS})_3\text{SiH}$ as atom transfer reagent to activate the alkyl bromides, were described for the first time. These protocols can produce a variety of alkenes from easily available feedstock with good reaction efficiency and high chemoselectivity under mild reaction conditions. To further demonstrate the applicability of present strategy, the alkenylation of bioactive molecules and glycosyl bromides, as well as the alkynylation of unactivated alkyl bromides, were proven to be feasible.

This Chapter has been published in:

Q.-Q. Zhou, S. J. S. Düsel, L.-Q. Lu, B. König, W.-J. Xiao, *Chem. Commun.*, 2019, **55**, pp. 107-110.

Adapted from *Chem. Commun.*, 2019, **55**, 107 with permission from The Royal Society of Chemistry.

Author contributions:

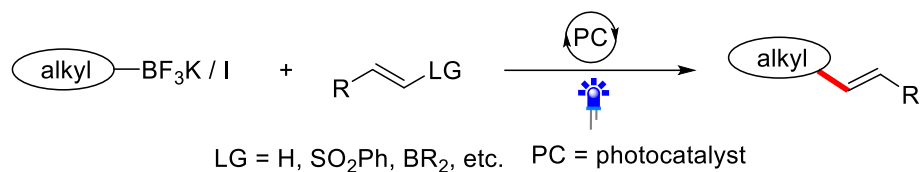
SJSD and QQZ contributed equally to this work. QQZ discovered the reaction, optimized the reaction conditions, carried out the dual-catalytic reactions, and the reactions shown in Scheme 4-2 and Eq. 1+2. SJSD and QQZ carried out the reactions with vinyl sulfones (Table 4-1). SJSD wrote the initial manuscript and carried out the mechanistic studies described in Chapter 4.4.2. QQZ shortened the manuscript for the submission to *Chemical Communications*. LQL, BK and WJX supervised this project. BK and WJX are the corresponding authors.

4.1 Introduction

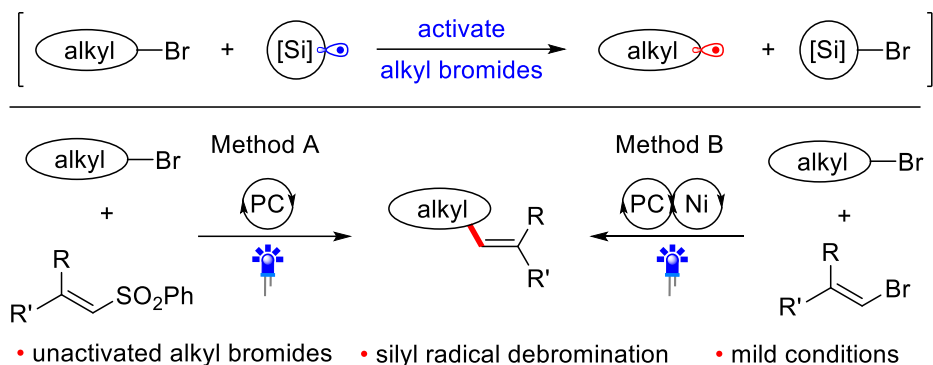
Alkenes are a class of fundamentally important compounds, as they are broadly applied in synthetic chemistry and material science.^[1] Tremendous research efforts have been devoted to the synthesis of alkenes, including well-known Wittig-type reactions,^[2] semi-reduction of alkynes,^[3] Heck-type reactions^[4] and many others.^[5] Inherently, cross coupling of an alkene moiety with the pre-functionalized alkane partner through transition metal catalysis has been considered as an ideal tool for this purpose with anticipated chemo- and regioselectivity.^[4, 5] Though great achievement, this valuable protocol still entails some drawbacks. For example, organometallic reagents, which are widely used in these reactions, are usually sensitive to water and air.^[6] Additionally, the oxidative addition of alkyl halides to the metal catalyst is difficult and the generated transient species might undergo undesired β -hydride elimination.^[4, 5] Moreover, elevated temperatures are frequently required.

Visible light photocatalysis has attracted increasing interest from the synthetic community, because it enables the generation of reactive intermediates under mild conditions.^[7] This strategy has been gradually applied in alkenylation reactions during the last decade.^[8] In this context, alkyl fluoroborate salts, which inherit a photocatalytically addressable oxidation potential, have been widely used as potent radical precursors for many coupling reactions,^[9] including the alkenylation with alkenyl sulfones (Scheme 4-1a).^[9a] However, the preparation of this reagent produces stoichiometric amounts of byproducts and usually requires three consecutive steps, including reactions using an oxygen- and water-sensitive organometallic reagents at low temperatures, somewhat limiting its application. Thus, many other alkyl precursors have been developed to improve the photocatalytic alkenylation reaction.^[8] Among them, easily available halides¹⁰ have been proven an efficient feedstock for the alkenylation. Usually activated alkyl halides, such as alkyl iodides or electron-deficient alkyl bromides, were required due to their higher reduction potential, which favors the generation of alkyl radicals via photocatalytic SET processes. Hence, the direct use of unactivated alkyl bromides in alkenylation reactions through visible light photocatalysis remains a challenge, albeit their advantage of low price, bench stability and easy availability.^[11] Inspired by the well-established process using organosilicon radicals to activate alkyl bromides,^[12] we therefore envision that alkyl bromides can also be utilized as efficient alkyl radical precursors to participate in new alkenylation reactions through the combination of visible light photocatalysis and silicon radical debromination. In this work, we plan to develop two kinds of coupling reactions of non-activated alkyl bromides with phenyl vinyl sulfones (method A) or bromides (method B) as shown in Scheme 4-1b. If successful, these protocols will provide two competitive and alternative methods for the preparation of alkenes from easily available chemicals under the mild conditions.

a) Previous work on visible light photocatalytic alkenylations



b) This work: photocatalytic alkenylation of unactivated alkyl bromides



Scheme 4-1 Reaction design: intermolecular alkyl-alkenyl coupling reactions via visible light photocatalysis.

4.2 Results and discussion

4.2.1 Synthesis

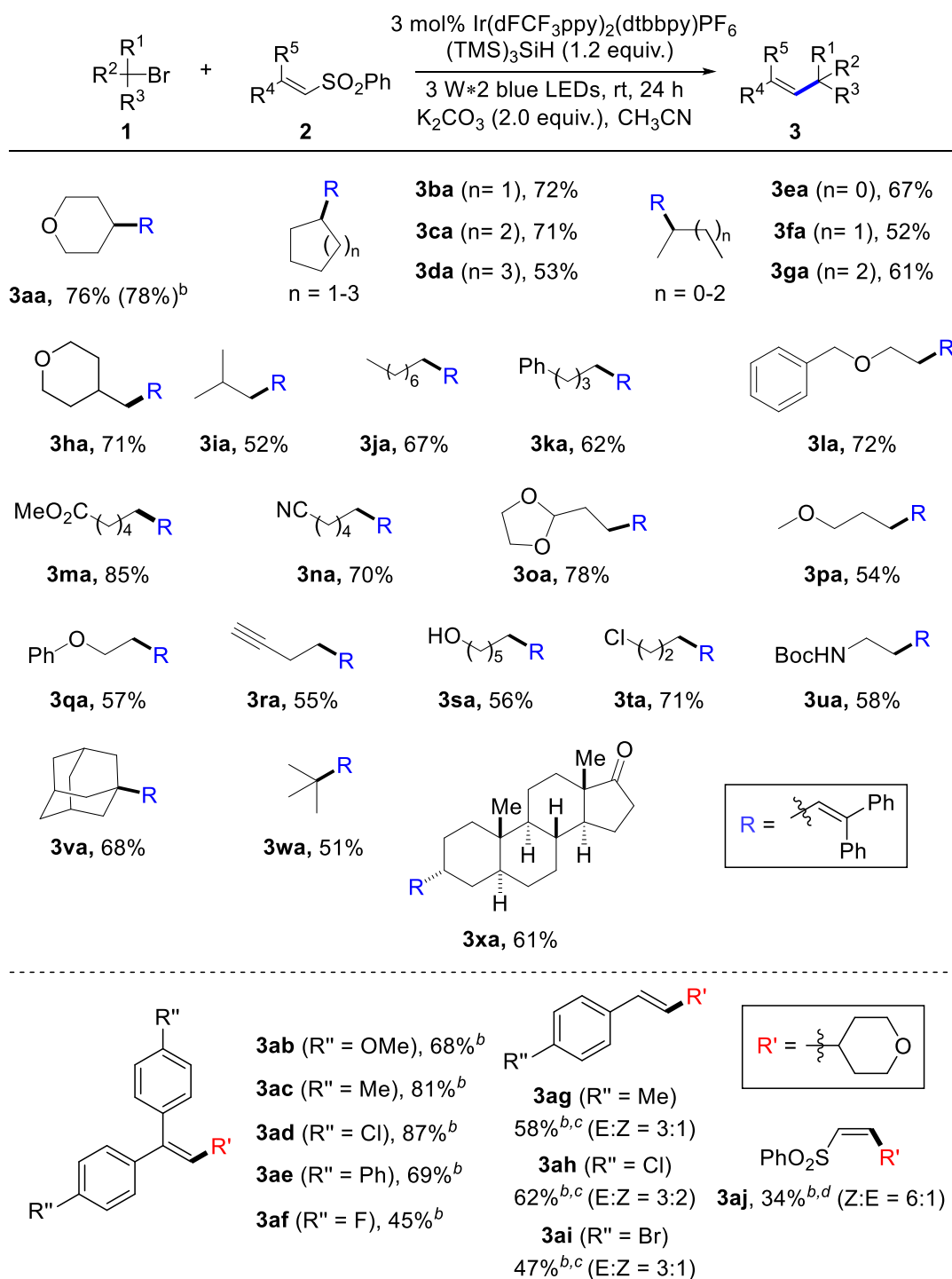
Initially, we started our investigations with the coupling of bromotetrahydropyran (**1a**) and diphenyl vinyl sulfone (**2a**) as the model reaction.^[13] In the presence of photocatalyst Ir(dFCF₃ppy)₂(dtbbpy)PF₆, silicon radical precursor tris(trimethylsilyl)silane (TTMSS) and inorganic base Na₂CO₃, a high amount of the desired alkene product **3aa** was detected after blue light irradiation at room temperature (rt) for 24 hours. Then, Routine optimization of reaction parameters including bases, solvents, hydrosilanes and concentration improved the result, in which the combination of K₂CO₃ and CH₃CN (0.05 M) stood out as the best choice (for optimal condition see the footnote in Table 4-1, optimization shown in Chapter 4.4.3, Table 4-3). Moreover, the reaction efficiency was not obviously affected by air atmosphere (Table 4-3, entry 23). Control experiments showed that visible light and a suitable photoredox catalyst were necessary for the transformation.^[13]

Having established the optimal reaction conditions, we started to examine the generality of this photocatalytic alkenylation reaction. As highlighted in Table 4-1, the mild protocol enables the alkenylation of different unactivated bromides. The coupling with secondary cyclic alkyl bromides proceeded smoothly, providing the corresponding alkene products in good yields (**3aa-3da**: 53-78% yields). Acyclic secondary alkyl bromides can readily undergo this

transformation, too; alkenylation products were obtained in 52-67% yields (**3ea-3ga**). In addition, primary and tertiary alkyl bromides were also converted into the desired products with satisfied results (**3ha-3xa**: 51-85% yields). To our delight, this protocol shows good functional group tolerance. Many alkyl bromides bearing ether, ester, alkyne, acetal and several other moieties can well participate in the photocatalytic alkenylation (**1l-1r**). More specially, the reaction with substrate **1s** containing a free hydroxyl group also proceeds smoothly with moderate yield. Besides, the reaction with dihalide **1t** showed an excellent chemoselectivity between bromide and chloride. Moreover, this protocol allows the debrominative alkenylation of bioactive molecule **1x** under mild reaction conditions, delivering product **3xa** in a good yield.

Next, we probed the scope of phenyl vinyl sulfones under the photocatalysis conditions. As summarized in Table 4-1, a variety of 2,2'-diaryl-substituted vinylsulfones can be applied as efficient substrates and the electronic character of aryls somewhat affect the reaction results. In the case of the chlorinated product **3ad**, a high yield of 87% was obtained and the phenyl chloride moieties were not affected by the silyl radical. In addition to 2,2'-diaryl-substituted vinylsulfones, styrene-substituted sulfones can participate in this photochemical transformation well. For example, when *para*-Me-, Cl-, or Br-substituted styrene sulfones were subjected to the standard reaction conditions, the desired alkenylation products **3ag-3ai** were achieved in good yields with modest E/Z ratios. Moreover, this protocol can be successfully extended to the alkenylation of alkyl-substituted vinylsulfones (**3aj**, Z:E = 6:1), albeit in 34% yield.

Table 1 Generality of the photocatalytic alkenylation of unactivated alkyl bromides with vinyl sulfones^a.

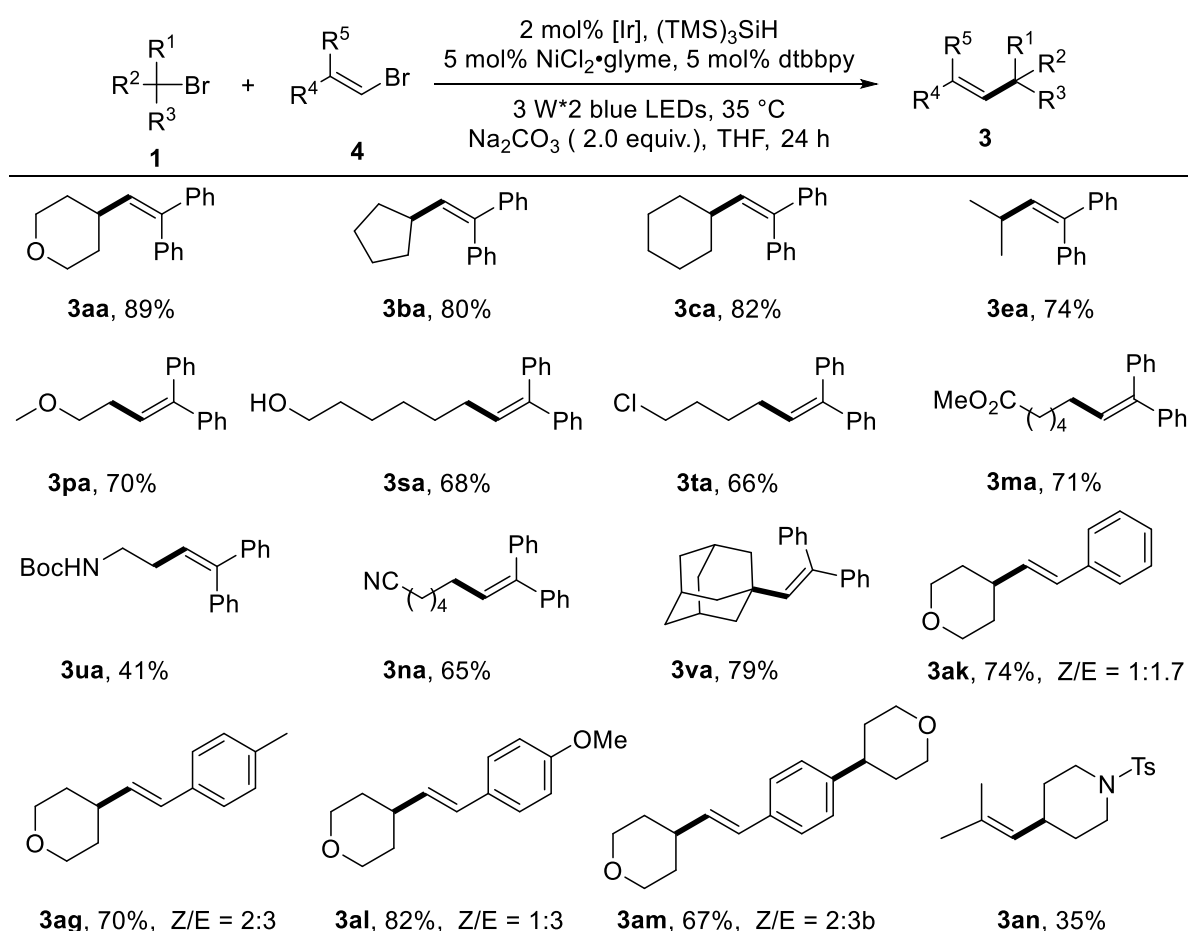


[a] Reaction conditions: **1** (0.6 mmol), **2** (0.2 mmol), TTMSS (0.24 mmol) Ir(dFCF₃ppy)₂(dtbbpy)PF₆ (3 mol%), K₂CO₃ (2.0 equiv) in CH₃CN (4.0 mL) at rt under irradiation of 3 W*2 blue LEDs for 24 h, isolated yield. [b] 1.5 equiv. of TTMSS. [c] (*E*)-Phenyl vinyl sulfone was used. [d] *cis*-1,2-Bis(phenylsulfonyl)ethane was used.

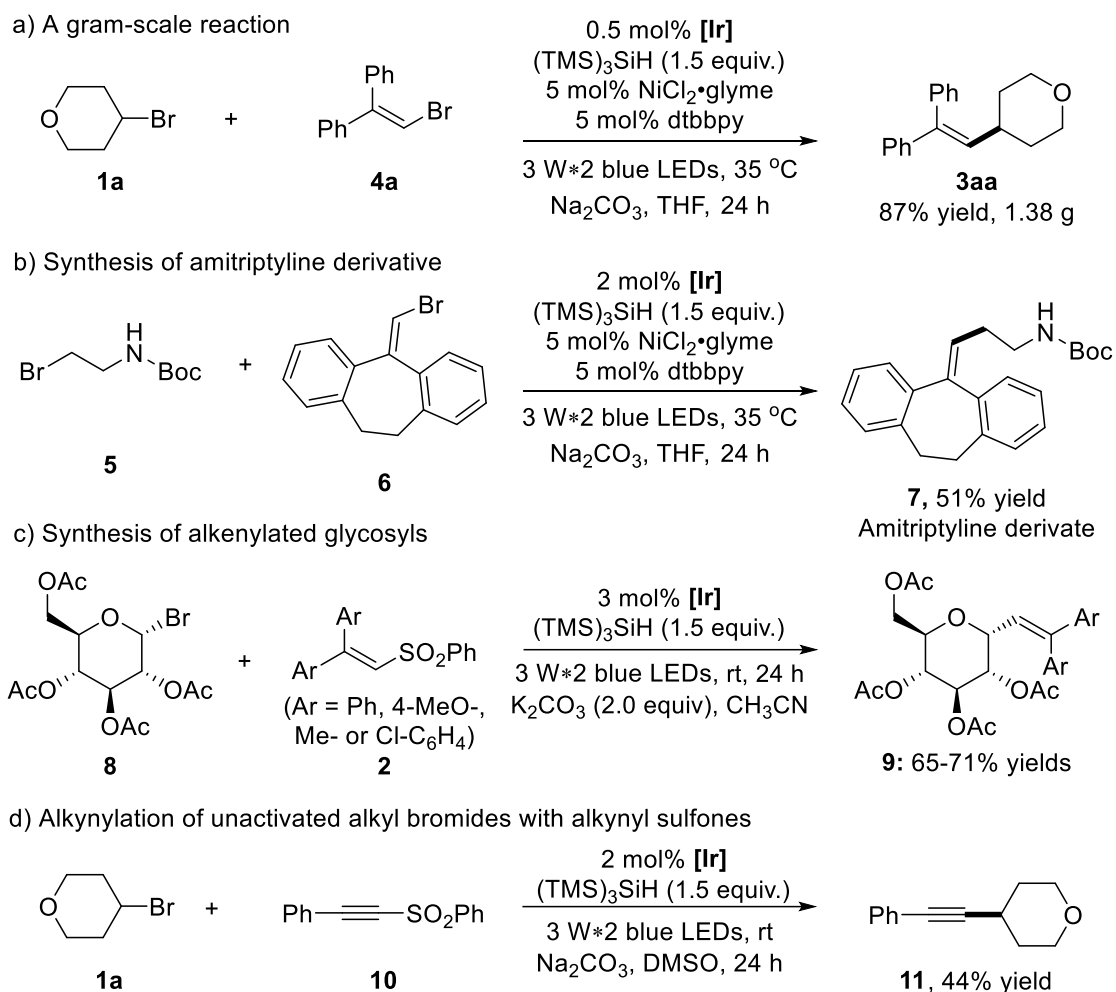
Recently, the use of nickel catalysis in combination with photoredox catalysis has been proven feasible for the coupling reaction of aryl halides.^[14] However, examples for the dual catalytic

coupling reactions of vinyl halides are rare.^[15] In order to be more comprehensive, we present an additional method for the reaction of unactivated alkyl bromides with vinyl bromides through a dual photoredox/nickel catalysis. With a slight alteration of the reaction conditions of the first alkenylation method, we established the optimal reaction conditions for the dual catalytic alkenylation of unactivated alkyl bromides with vinyl bromides. As highlighted in Table 4-2, the transformation under the dual catalysis system generally provided the corresponding alkene products in good yields (Table 4-2, 41-89% yields). In addition, it is general for alkyl bromides and shows good function group compatibility. Furthermore, this protocol can also be extended to non-aromatic alkenes (**3an**, Table 4-2). Different from the formation of the mono-alkylated product **3ai** using method A, the double alkylated compound **3am** was obtained in a good yield under the conditions of method B, demonstrating the different characteristics of the two presented methods.

Table 4-2 Generality of the alkenylation of unactivated alkyl bromides with vinyl bromides via dual photoredox/nickel catalysis^a.



[a] Reaction conditions: alkyl bromides **1** (0.6 mmol), **6** (0.2 mmol), Na₂CO₃ (2.0 equiv.), (TMS)₃SiH (0.24 mmol), [Ir] = Ir(dFCF₃ppy)₂(dtbbpy)PF₆ (2 mol%), NiCl₂•glyme (5 mol%), dtbbpy (5 mol%), THF (2.0 mL), Ar atmosphere, 3 W×2 blue LEDs, 35 °C for 24 h; isolated yields. [b] 6.0 equiv. of **1a** was used, DME as solvent.

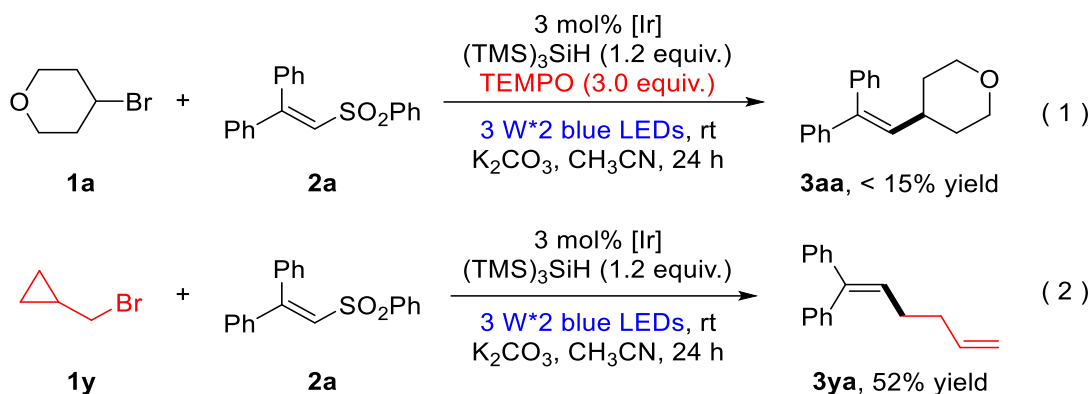


Scheme 4-2 Demonstration of the synthetic utility of the methodology.

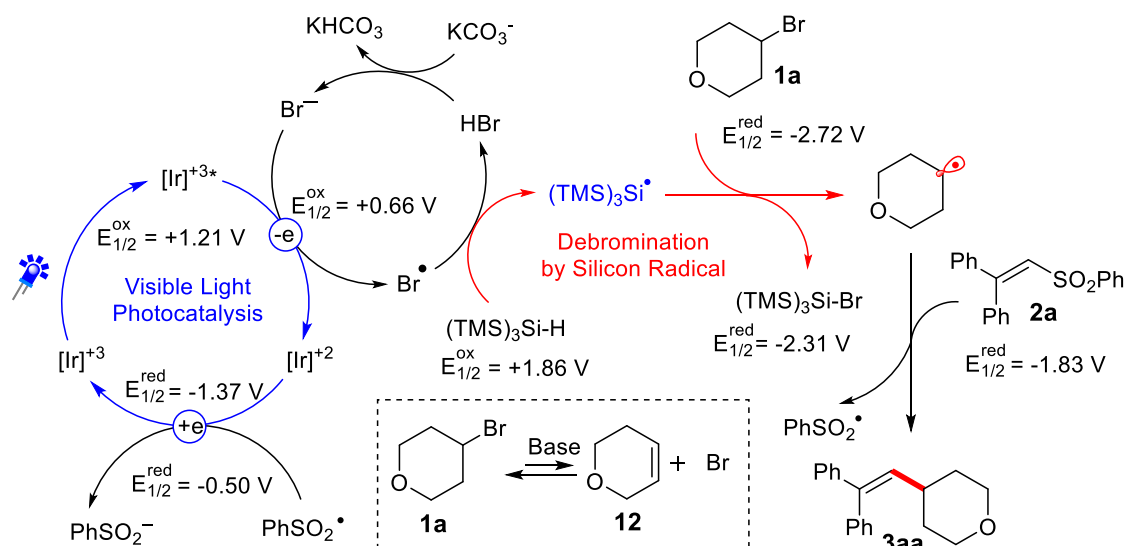
To show the applicability of the dual photoredox/nickel catalysis systems, a gram-scale alkenylation reaction of alkyl bromide **1a** and vinyl bromide **4a** was conducted, for which the loading of the photocatalyst could be lowered to 0.5 mol% without affecting the reaction efficiency (Scheme 4-2a: 1.38 g, 87% yield). Moreover, the pharmacophore amitriptyline derivative **7** was prepared from the *tert*-butyl (2-bromoethyl) carbamate **5** in 51% yield, which could be easily transferred to the antidepressant drug amitriptyline.^[1d] Considering the significance of utilizing renewable starting materials from nature,^[16] herein we realized the first photocatalytic alkenylation of glycosyl bromides with good efficiency and selectivity (Scheme 2c, **9aa-9ad**, 65-71% yields). Furthermore, this strategy of visible light photocatalysis and silicon radical debromination was successfully extended to the alkynylation of alkynyl phenylsulfone **10**, albeit with a moderate yield of 44% (Scheme 4-2d).

4.2.2 Mechanistic investigations

As shown in Eq. 1, the formation of **3aa** was nearly completely inhibited by the addition of the radical scavenger TEMPO. Yet, we were able to detect the trapping product of the free alkyl radical. To further verify the presence of free alkyl radicals, a “radical-clock” experiment was performed with bromide **1y** (Eq. 2); as a result, an 1,5-diene product **3ya** could be isolated in 52% yield via a radical-induced ring opening process.



Based on these observations and related literature reports,^[8b,12] we proposed a possible mechanism for the coupling of unactivated alkyl bromides and vinyl phenyl sulfones (Scheme 4-3).^[17] Upon stirring a mixture of the bromide **1a** with carbonate base for 6 h, small amounts of the unsaturated compound **12** were detected. The generated Br⁻ can be oxidized by a photoredox catalyst, whereas the formed bromine radical can abstract a hydrogen atom from (TMS)₃SiH.^[12e] The generated silyl radical will abstract a bromine atom from **1a**, and thereby the created alkyl radical adds to the double bond of **2a**. A consecutive cleavage of the C-S bond will release the desired product and an open shell phenyl sulfonyl radical. Finally, the phenyl sulfonyl radical then undergoes a SET with the reduced photocatalyst to close the catalytic cycle. It has to be noted that only trace amounts of product were formed without the addition of base. However, product formation was observed when LiBr was added as a bromide source instead of the carbonate base. Moreover, the yield could be further increased a little by supplemental addition of LiBr, demonstrating the necessity of the presence of bromide species for the photocatalytic cycle.



Scheme 3 Proposed mechanism for the photocatalytic alkenylation of alkyl bromide with vinyl phenyl sulfone.

4.3 Conclusion

In summary, we developed two photocatalytic alkenylation reactions of unactivated alkyl bromides with vinyl phenyl sulfones or vinyl bromides. The combination of visible light photocatalysis and silicon radical debromination was the key of this success. Moreover, this strategy was proven feasible for the alkenylation of bioactive molecules and glycosyl bromides, as well as the alkynylation of unactivated alkyl bromides.

4.4 Experimental part

4.4.1 General information

See Chapter 2.4.1

Additional information

The synthetic part of this project was carried out at the College of Chemistry, Key Laboratory of Pesticide & Chemical Biology, Ministry of Education, Central China Normal University, 152 Luoyu Road, Wuhan, Hubei, China, 430079.

^1H NMR spectra were recorded on 400 or 600 MHz spectrophotometers. Chemical shifts (δ) are reported in ppm from the resonance of tetramethyl silane as the internal standard. ^{13}C NMR spectra were recorded on 100 MHz spectrometers. HRMS was recorded on Waters *Micromass* GCT mass spectrometer, Bruker micrOTOF-Q II mass spectrometer or Bruker ultrafleXtreme MALDI-TOF/TOF mass spectrometer. The photoreactions were performed in with blue LEDs ($\lambda_{\text{max}} = 450 \text{ nm } (\pm 15 \text{ nm})$, 3 W electrical power)

Lifetime measurements were performed with a HORIBA DeltaPro lifetime fluorimeter at room temperature.

4.4.2 Mechanistic investigations

4.4.2.1 Steady-state and time-resolved emission quenching experiments

Fluorescence spectra were measured on a Horiba Scientific Fluoromax 4 spectrometer. Lifetimes were determined with a HORIBA DeltaPro lifetime fluorimeter. A mono-exponential fit function was applied. The same sample was used for the steady-state and time-resolved quenching experiments. All experiments were performed under argon atmosphere with a gas-tight quartz cuvette (10×10 mm) containing 2 mL of iridium catalyst solution (2.5 μ M) at room temperature. Excitation wavelength $\lambda = 452$ nm. Lifetimes without quencher: $\tau_0 = 2.2 - 2.3$ μ s.

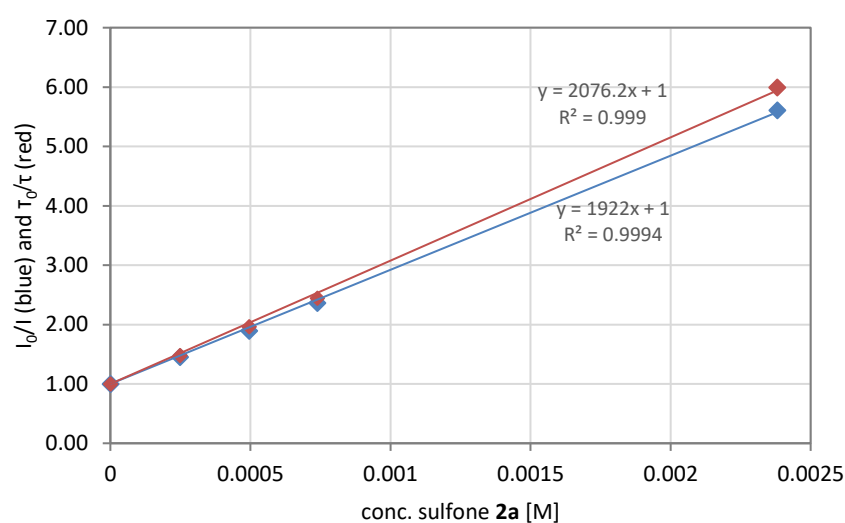


Figure 4-1. Stern-Volmer plot of the steady-state (blue) and time-resolved fluorescence quenching (red), upon the addition of sulfone **2a**.

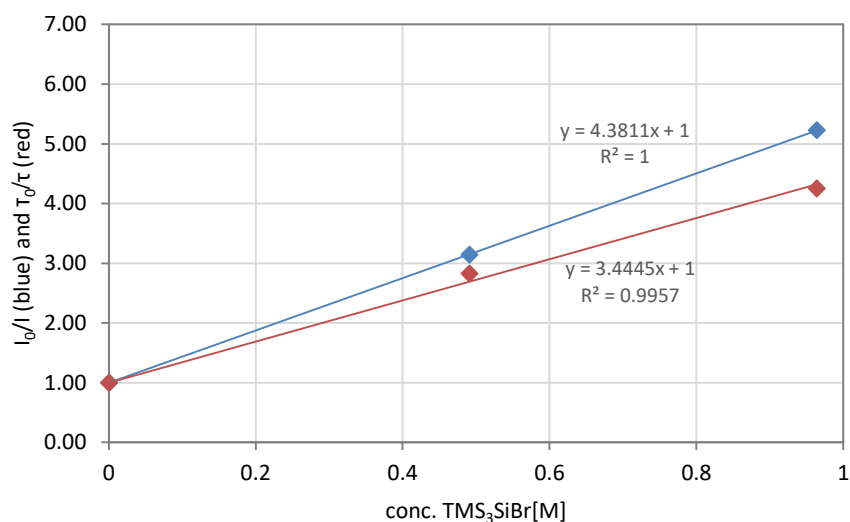


Figure 4-2. Stern-Volmer plot of the steady-state (blue) and time-resolved fluorescence quenching (red), upon the addition of sulfone $(\text{TMS})_3\text{SiBr}$.

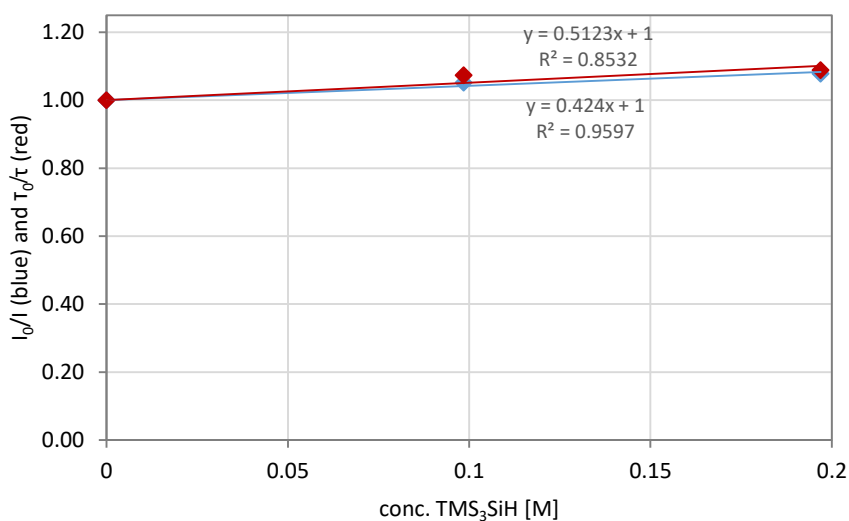


Figure 4-3. Stern-Volmer plot of the steady-state (blue) and time-resolved fluorescence quenching (red), upon the addition of sulfone $(\text{TMS})_3\text{SiH}$. Note: No significant quenching effects are noticed, therefore no linear quenching behavior present.

4.4.2.2 Quantum yield measurements

The quantum yield was measured with a custom-made quantum yield determination setup.^[18] Translation stages (horizontal and vertical): Thorlabs DT 25/M or DT S25/M; photographic lens “Nikkor AF 50/1,4 D” with $f = 50$ mm; magnetic stirrer: Faulhaber motor (1524B024S R) with 14:1 gear (15A); PS19Q power sensor from Coherent; PowerMax software; adjustable power supply “Basetech BT-153 0–15 V/DC 0–3 A 45 W”.^[18]

For the determination of the quantum yield a gas-tight quartz cuvette (10×10 mm) was charged with Ir(dFCF₃ppy)₂(dtbbpy)PF₆ (3.4 mg, 0.003 mmol), K₂CO₃ (27.6 mg, 0.2 mmol), sulfone **2a** (32.0 mg, 0.1 mmol), bromide **1a** (33.7 μL, 0.3 mmol), TTMSS (37.0 μL, 0.12 mmol), a magnetic stirring bar and 2 mL MeCN. The oxygen was removed by purging with argon for 3 minutes.

The quantum yield was measured in the covered apparatus to minimize the ambient light. The cuvette with the pure solvent was placed in the beam of a 455 (±15) nm LED and the transmitted power P_{ref} was measured by a calibrated photodiode horizontal to the cuvette. The content of the cuvette was changed to the reaction mixture and the transmitted power P_{sample} was measured analogously to the blank solution. The sample was further irradiated and the transmitted power as well as the respective yield of photocatalytic product (measured by quantitative GC using 1-methylnaphthalene as an internal standard) were recorded after different times.

The quantum yield was calculated by using the following equation:

$$\Phi = \frac{N_{product}}{N_{ph}} = \frac{N_A \cdot n_{product}}{\frac{E_{light}}{E_{ph}}} = \frac{N_A \cdot n_{product}}{\frac{P_{abs} \cdot t}{\frac{h \cdot c}{\lambda}}} = \frac{N_A \cdot n_{product} \cdot h \cdot c}{(P_{ref} - P_{sample}) \cdot t \cdot \lambda}$$

Φ is the quantum yield; $N_{product}$ is the number of product molecules created; N_{ph} is the number of photons absorbed; N_A is Avogadro's constant in mol⁻¹; $n_{product}$ is the molar amount of molecules created; E_{light} is the energy of light absorbed in joule; E_{ph} is the energy of a single photon in joule; P_{abs} is the radiant power absorbed in watt; t is the irradiation time in seconds; h is the Planck's constant in J s; c is the speed of light in m s⁻¹; λ the wavelength of irradiation source (455 nm) in meters; P_{ref} is the radiant power transmitted by a blank vial in watt and P_{sample} is the radiant power transmitted by the vial with reaction mixture in watt.

The calculated quantum yield for the described model reaction is 0.006 (i.e. 0.6%).

4.4.2.3 Cyclic voltammetry measurements

The cyclic voltammetry measurements were performed in MeCN with a scan rate of $50 \text{ mV}\cdot\text{s}^{-1}$. The measured peak potentials (E_p) and the ferrocene peaks are displayed for each substance.

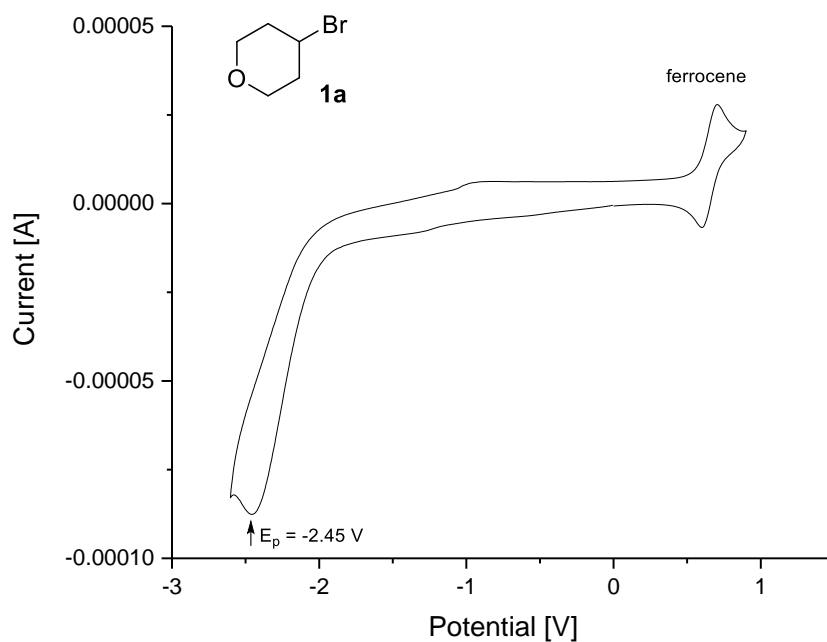


Figure 4-4. Reduction of alkyl bromide **1a**.

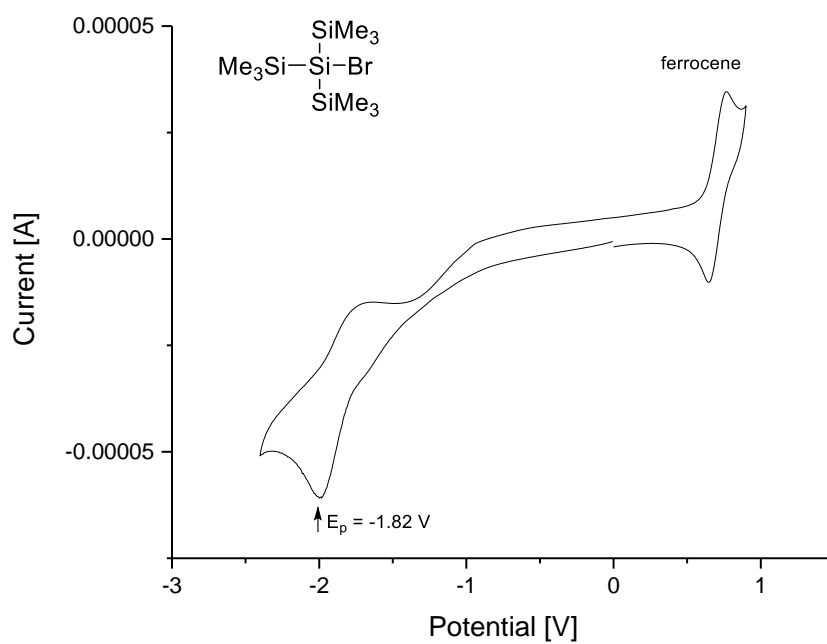


Figure 4-5. Reduction of $(\text{TMS})_3\text{SiBr}$

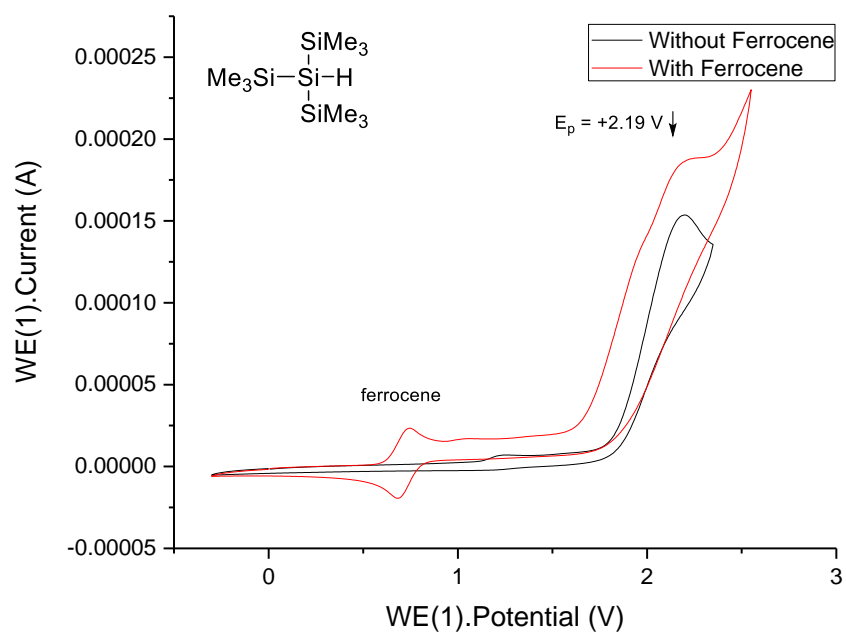


Figure 4-6. Oxidation of $(\text{TMS})_3\text{SiH}$. (Note: Upon the addition of ferrocene, the shape of the cyclic voltammogram slightly altered, but the peak potential stayed constant.)

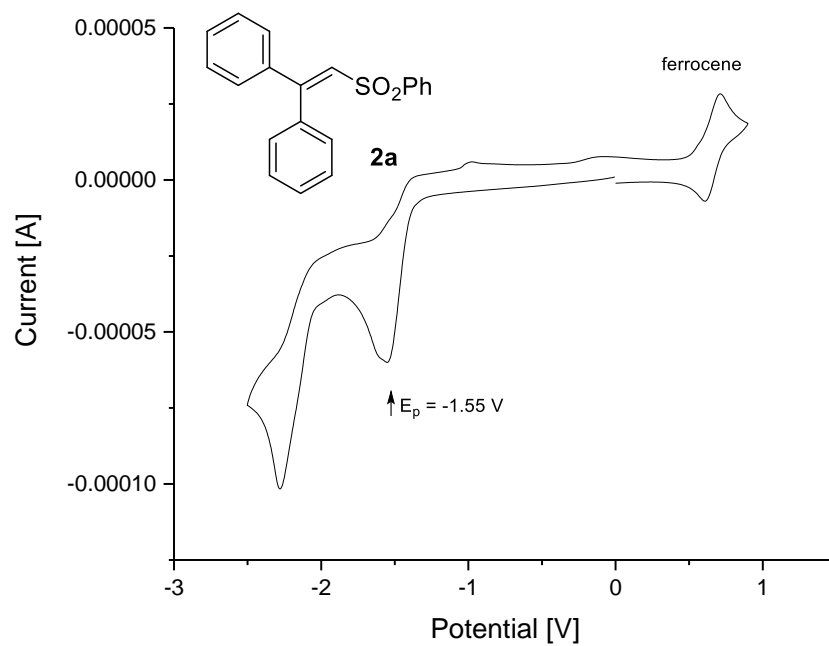


Figure 4-7. Reduction of sulfone **2a**.

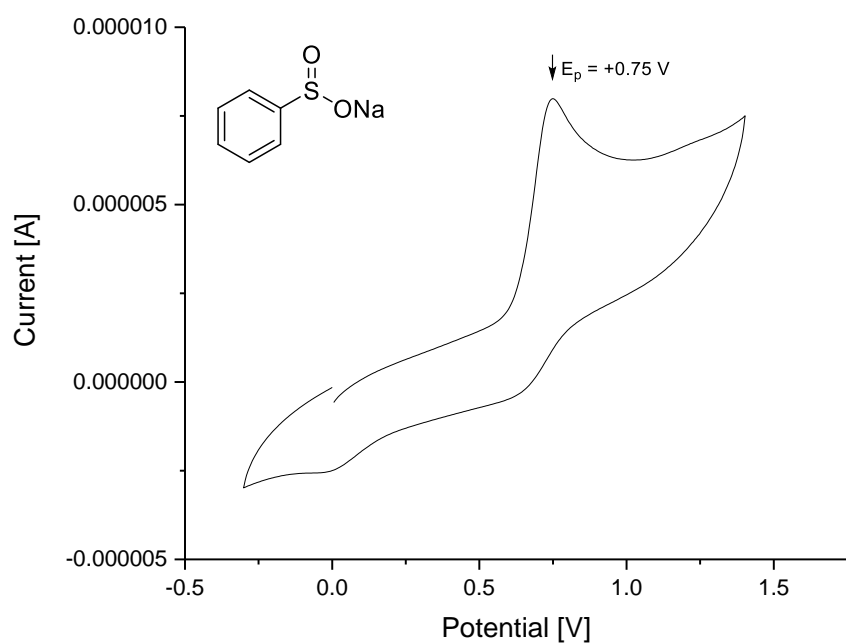


Figure 4-8. Oxidation of sodium benzenesulfinate. (Note: A comparison experiment with the addition of ferrocene as internal standard was performed. The oxidation potential of sodium benzenesulfinate and ferrocene lie in same range, whereas herein the CV without ferrocene is shown.)

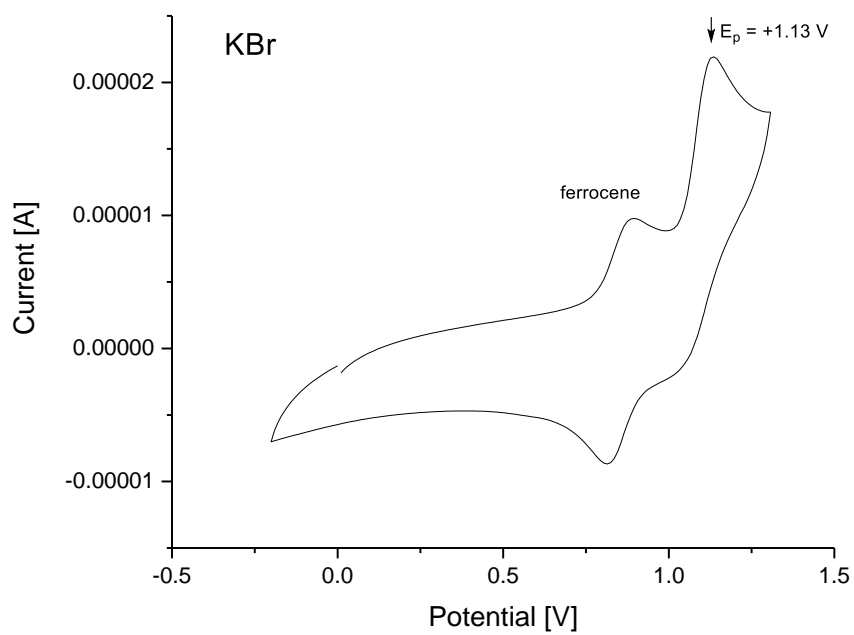


Figure 4-9. Oxidation of potassium bromide

4.4.3 General experimental procedures

General procedure for photocatalytic alkenylation of alkyl bromides with alkenyl sulfone **2a**

General procedure A: To a 10 mL Schlenk tube equipped with a magnetic stirrer bar was added **2a** (0.2 mmol), K_2CO_3 (0.4 mmol), $Ir(dFCF_3ppy)_2(dtbbpy)PF_6$ (0.006 mmol) and 4 mL CH_3CN . The reaction mixture was degassed using a freeze-pump-thaw procedure (3 times), then **1** (0.6 mmol) and $(TMS)_3SiH$ (0.24 mmol) were added. The mixture was stirred at room temperature under irradiation of 3 W*2 blue LEDs. Upon the completion of the reaction (about 24h), monitored by TLC, 5 g of KF on Alumina (37 wt%) were added and it was subsequently stirred for 30 min. The solid was filtered off and washed with ethyl acetate. The residue was purified by flash chromatography on silica gel to provide pure product **3**.

General procedure for photocatalytic alkenylation of alkyl bromide **1a** with alkenyl sulfones **2**

General procedure B: To a 10 mL Schlenk tube equipped with a magnetic stirrer bar was added **2** (0.2 mmol), K_2CO_3 (0.4 mmol), $Ir(dFCF_3ppy)_2(dtbbpy)PF_6$ (0.006 mmol) and 4 mL CH_3CN . The reaction mixture was degassed using a freeze-pump-thaw procedure (3 times), then **1a** (0.6 mmol) and $(TMS)_3SiH$ (0.30 mmol) were added. The mixture was stirred at room temperature under irradiation of 3 W*2 blue LEDs. Upon the completion of the reaction (about 24h), monitored by TLC, 5 g of KF on Alumina (37 wt%) were added and it was subsequently stirred for 30 min. The solid was filtered off and washed with ethyl acetate. The residue was purified by flash chromatography on silica gel to provide pure product **3**.

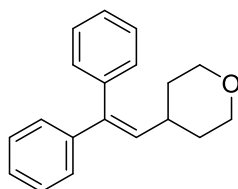
General procedure for Ir/Ni dual catalysis of alkyl bromides with vinyl bromides

General procedure C: To a 10 mL Schlenk tube equipped with a magnetic stirrer bar was added $NiCl_2 \cdot glyme$ (0.01 mmol), 4,4'-di-tert-butyl-2,2'-bipyridine (0.01 mmol), and 2 mL THF. The mixture was stirred for 30 minutes under an Ar atmosphere. Then **4** (0.2 mmol), Na_2CO_3 (0.4 mmol) and $Ir(dFCF_3ppy)_2(dtbbpy)PF_6$ (0.006 mmol) were added and the reaction mixture was degassed using a freeze-pump-thaw procedure (3 times), then **1** (0.6 mmol) in 1mL THF and the $(TMS)_3SiH$ (0.24 mmol) were added. The mixture was stirred at room temperature under irradiation of 3W*2 blue LEDs. Upon the completion of the reaction, monitored by TLC, 5 g of KF on Alumina (37 wt%) were added and it was subsequently stirred for 30 min. The solid was filtered off and washed with ethyl acetate. The residue was purified by flash chromatography on silica gel or automatic flash chromatography machine (SepaBean machine) to provide pure product **3**.

4.4.4 Product characterization

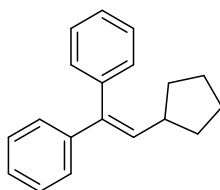
The product characterization data is listed for compounds that were prepared following procedure A and B.

4-(2,2-Diphenylvinyl)tetrahydro-2H-pyran (**3aa**)^[19]



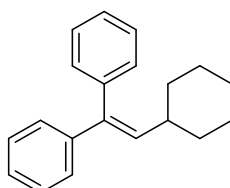
Compound **3aa** was prepared following the procedure A. 76% isolated yield. ¹H NMR (600 MHz, CDCl₃) δ 7.35 – 7.33 (m, 2H), 7.30 – 7.27 (m, 1H), 7.25 – 7.01 (m, 7H), 5.88 (d, *J* = 9.8 Hz, 1H), 3.87 (d, *J* = 11.7 Hz, 2H), 3.26 – 3.23 (m, 2H), 2.38 – 2.34 (m, 1H), 1.60 – 1.11 (m, 4H). ¹³C NMR (100 MHz, CDCl₃) δ 142.3, 141.0, 140.1, 133.5, 129.5, 128.2, 128.0, 127.0, 126.9, 126.9, 67.2, 35.5, 32.8. HRMS (ESI) for: C₁₉H₂₁O [M+H]⁺: calcd 265.1587, found 265.1585.

(2-Cyclopentylethene-1,1-diyl) dibenzene (**3ba**)^[20]



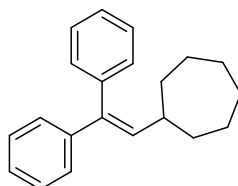
Compound **3ba** was prepared following the procedure A. 72% isolated yield. ¹H NMR (600 MHz, CDCl₃) δ 7.38 – 7.29 (m, 2H), 7.28 – 7.07 (m, 8H), 5.96 (d, *J* = 9.8 Hz, 1H), 2.59 – 2.48 (m, 1H), 1.84 – 1.61 (m, 4H), 1.54 – 1.33 (m, 4H). ¹³C NMR (100 MHz, CDCl₃) δ 142.9, 140.6, 140.1, 135.3, 130.0, 128.0, 128.0, 127.2, 126.7, 126.6, 40.4, 34.2, 25.6. HRMS (ESI) for: C₁₉H₂₁ [M+H]⁺: calcd 249.1638, found 249.1634.

(2-Cyclopentylethene-1,1-diyl)dibenzene (**3ca**)^[20]



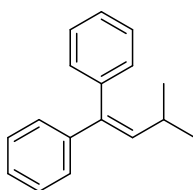
Compound **3ca** was prepared following the procedure A. 71% isolated yield. ^1H NMR (600 MHz, CDCl_3) δ 7.41 – 7.28 (m, 3H), 7.27 – 7.14 (m, 7H), 5.90 (d, J = 10.1 Hz, 1H), 2.15 – 2.08 (m, 1H), 1.77 – 1.57 (m, 5H), 1.24 – 1.08 (m, 5H). ^{13}C NMR (100 MHz, CDCl_3) δ 142.9, 140.5, 139.5, 136.0, 129.8, 128.1, 128.0, 127.2, 126.7, 126.7, 38.3, 33.3, 26.0, 25.6. HRMS (ESI) for: $\text{C}_{20}\text{H}_{23} [\text{M}+\text{H}]^+$: calcd 263.1794, found 263.1798.

(2,2-Diphenylvinyl)cycloheptane (3da)



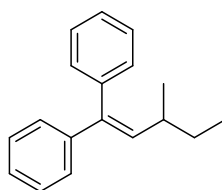
Compound **3da** was prepared following the procedure A. 53% isolated yield. ^1H NMR (600 MHz, CDCl_3) δ 7.25 (t, J = 7.3 Hz, 2H), 7.20 (d, J = 7.1 Hz, 1H), 7.16 – 7.04 (m, 7H), 5.92 (d, J = 10.4 Hz, 1H), 2.26 – 2.21 (m, 1H), 1.70 – 1.60 (m, 2H), 1.60 – 1.49 (m, 2H), 1.47 – 1.36 (m, 4H), 1.36 – 1.20 (m, 4H). ^{13}C NMR (100 MHz, CDCl_3) δ 142.3, 141.0, 140.1, 133.5, 129.5, 128.2, 128.0, 127.0, 126.9, 126.9, 67.2, 35.5, 32.8. HRMS (ESI) for: $\text{C}_{21}\text{H}_{25} [\text{M}+\text{H}]^+$: calcd 277.1951, found 277.1949.

(3-Methylbut-1-ene-1,1-diyl)dibenzene (3ea)^[21]



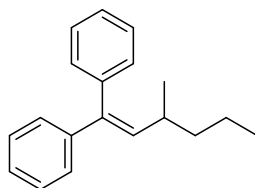
Compound **3ea** was prepared following the procedure A. 67% isolated yield. ^1H NMR (600 MHz, CDCl_3) δ 7.24 (dd, J = 8.1, 6.5 Hz, 2H), 7.20 – 7.16 (m, 1H), 7.14 – 7.00 (m, 7H), 5.78 (d, J = 10.1 Hz, 1H), 2.43 – 2.24 (m, 1H), 0.90 (d, J = 6.6 Hz, 6H). ^{13}C NMR (100 MHz, CDCl_3) δ 142.9, 140.6, 140.0, 135.4, 130.0, 128.0, 128.0, 127.2, 126.7, 126.6, 40.4, 34.2, 25.6. HRMS (ESI) for: $\text{C}_{17}\text{H}_{19} [\text{M}+\text{H}]^+$: calcd 223.1481, found 223.1488.

(3-Methylpent-1-ene-1,1-diyl)dibenzene (3fa)^[21]



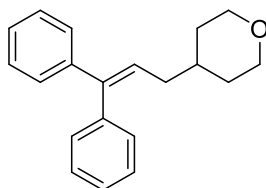
Compound **3fa** was prepared following the procedure A. 52% isolated yield. ^1H NMR (400 MHz, CDCl_3) δ 7.36 – 7.26 (m, 4H), 7.24 – 7.16 (m, 6H), 5.90 – 5.82 (m, 1H), 2.27 – 2.15 (m, 1H), 1.40 – 1.29 (m, 2H), 1.04 – 0.97 (m, 3H), 0.89 – 0.78 (m, 3H). ^{13}C NMR (100 MHz, CDCl_3) δ 142.8, 140.7, 140.3, 136.2, 129.8, 128.2, 128.1, 128.1, 127.1, 126.7, 126.7, 35.5, 30.4, 21.0, 12.0. HRMS (ESI) for: $\text{C}_{18}\text{H}_{21}$ $[\text{M}+\text{H}]^+$: calcd 237.1638, found 237.1630.

(3-Methylhex-1-ene-1,1-diyl)dibenzene (3ga) ^[22]



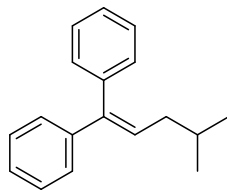
Compound **3ga** was prepared following the procedure A. 61% isolated yield. ^1H NMR (400 MHz, CDCl_3) δ 7.39 – 7.33 (m, 2H), 7.33 – 7.28 (m, 1H), 7.28 – 7.24 (m, 2H), 7.24 – 7.22 (m, 3H), 7.22 – 7.20 (m, 1H), 7.19 – 7.17 (m, 1H), 7.17 – 7.15 (m, 1H), 5.85 (d, J = 10.3 Hz, 1H), 2.38 – 2.20 (m, 1H), 1.40 – 1.23 (m, 4H), 1.24 – 1.13 (m, 1H), 1.00 (d, 3H), 0.82 – 0.76 (m, 3H). ^{13}C NMR (100 MHz, CDCl_3) δ 140.6, 140.1, 136.4, 129.8, 128.1, 128.1, 127.1, 126.7, 40.0, 33.6, 21.4, 20.7, 14.2. HRMS (ESI) for: $\text{C}_{19}\text{H}_{22}\text{Na}$ $[\text{M}+\text{Na}]^+$: calcd 273.1614, found 273.1610.

4-(3,3-Diphenylallyl) tetrahydro-2H-pyran (3ha)



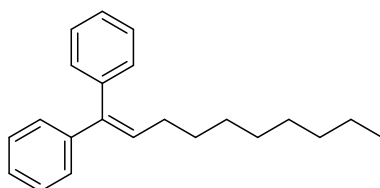
Compound **3ha** was prepared following the procedure A. 71% isolated yield. ^1H NMR (400 MHz, CDCl_3) δ 7.41 – 7.34 (m, 2H), 7.34 – 7.30 (m, 1H), 7.27 – 7.20 (m, 5H), 7.18 – 7.13 (m, 2H), 6.10 (t, J = 7.5 Hz, 1H), 4.02 – 3.86 (m, 2H), 3.47 – 3.29 (m, 2H), 2.17 – 2.02 (m, 2H), 1.72 – 1.54 (m, 3H), 1.32 – 1.23 (m, 2H). ^{13}C NMR (100 MHz, CDCl_3) δ 142.8, 142.7, 140.1, 129.9, 128.2, 128.1, 127.5, 127.1, 126.9, 68.1, 36.7, 35.9, 32.9. HRMS (ESI) for: $\text{C}_{20}\text{H}_{23}\text{O}$ $[\text{M}+\text{H}]^+$: calcd 279.1743, found 279.1740.

(4-Methylpent-1-ene-1,1-diyl) dibenzene (3ia)



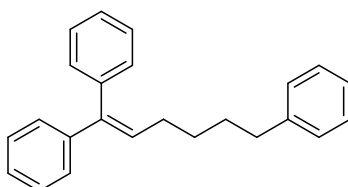
Compound **3ia** was prepared following the procedure A. 52% isolated yield. ^1H NMR (400 MHz, CDCl_3) δ 7.39 – 7.33 (m, 2H), 7.33 – 7.28 (m, 1H), 7.28 – 7.23 (m, 3H), 7.23 – 7.19 (m, 2H), 7.19 – 7.14 (m, 2H), 6.11 (t, J = 7.4 Hz, 1H), 2.04 – 1.97 (m, 2H), 1.79 – 1.66 (m, 1H), 0.91 (s, 3H), 0.89 (s, 3H). ^{13}C NMR (101 MHz, CDCl_3) δ 143.0, 142.0, 140.4, 130.0, 129.2, 128.06, 128.04, 127.2, 126.72, 126.72, 38.7, 29.1, 22.5. HRMS (ESI) for: $\text{C}_{18}\text{H}_{21}$ $[\text{M}+\text{H}]^+$: calcd 237.1638, found 237.1630.

Dec-1-ene-1,1-diyl dibenzene (3ja)



Compound **3ja** was prepared following the procedure A. 67% isolated yield. ^1H NMR (400 MHz, CDCl_3) δ 7.40 – 7.32 (m, 2H), 7.32 – 7.26 (m, 1H), 7.26 – 7.13 (m, 7H), 6.08 (t, J = 7.5 Hz, 1H), 2.15 – 2.05 (m, 2H), 1.47 – 1.38 (m, 2H), 1.32 – 1.18 (m, 11H), 0.87 (t, J = 6.7 Hz, 3H). ^{13}C NMR (100 MHz, CDCl_3) δ 142.9, 141.4, 140.4, 130.4, 130.0, 128.1, 128.0, 127.2, 126.8, 126.7, 31.9, 30.0, 29.8, 29.5, 29.3, 29.3, 22.7, 14.1. HRMS (ESI) for: $\text{C}_{22}\text{H}_{29}$ $[\text{M}+\text{H}]^+$: calcd 293.2264, found 293.2260.

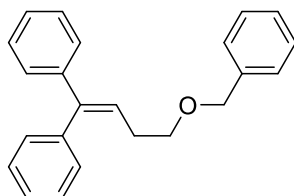
Hex-1-ene-1,1,6-triyltribenzene (3ka)



Compound **3ka** was prepared following the procedure A. 62% isolated yield. ^1H NMR (400 MHz, CDCl_3) δ 7.39 – 7.31 (m, 2H), 7.31 – 7.19 (m, 7H), 7.18 – 7.02 (m, 7H), 6.09 – 5.99 (m, 1H), 2.60 – 2.48 (m, 2H), 2.18 – 2.05 (m, 2H), 1.67 – 1.55 (m, 2H), 1.51 – 1.42 (m, 2H). ^{13}C NMR (100 MHz, CDCl_3) δ 142.8, 142.6, 141.7, 140.3, 129.9, 128.4, 128.2, 128.1, 128.1, 127.2,

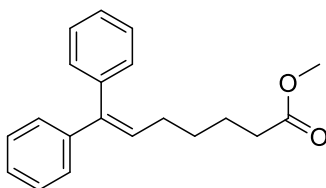
126.9, 126.8, 125.6, 35.7, 31.0, 29.6, 29.5. HRMS (ESI) for: C₂₄H₂₅ [M+H]⁺: calcd 313.1951, found 313.1948.

(4-(Benzyloxy)but-1-ene-1,1-diyl)dibenzene (3la)



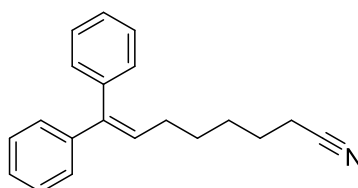
Compound **3la** was prepared following the procedure A. 72% isolated yield. ¹H NMR (400 MHz, CDCl₃) δ 7.39 – 7.30 (m, 4H), 7.30 – 7.24 (m, 4H), 7.25 – 7.21 (m, 2H), 7.22 – 7.13 (m, 5H), 6.20 – 6.03 (m, 1H), 4.51 – 4.48 (m, 1H), 4.47 – 4.41 (m, 1H), 3.60 – 3.46 (m, 2H), 2.50 – 2.34 (m, 2H). ¹³C NMR (100 MHz, CDCl₃) δ 143.3, 142.6, 140.0, 139.5, 129.9, 128.4, 128.2, 128.1, 127.6, 127.5, 127.3, 126.99, 126.95, 125.8, 72.8, 70.0, 30.5. HRMS (ESI) for: C₂₃H₂₂NaO [M+Na]⁺: calcd 337.1563, found 337.1559.

Methyl 7,7-diphenylhept-6-enoate (3ma)



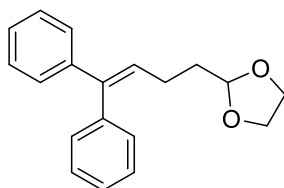
Compound **3ma** was prepared following the procedure A. 85% isolated yield. ¹H NMR (600 MHz, CDCl₃) δ 7.49 – 7.38 (m, 2H), 7.37 – 7.32 (m, 1H), 7.32 – 7.09 (m, 7H), 6.11 (s, 1H), 3.70 (s, 3H), 2.35 – 2.26 (m, 2H), 2.22 – 2.12 (m, 2H), 1.74 – 1.63 (m, 2H), 1.57 – 1.47 (m, 2H). ¹³C NMR (100 MHz, CDCl₃) δ 173.9, 142.7, 142.0, 140.1, 129.8, 129.3, 128.1, 128.0, 127.1, 126.8, 126.8, 51.3, 33.8, 29.3, 29.3, 24.5. HRMS (ESI) for: C₂₀H₂₃O₂ [M+H]⁺: calcd 295.1693, found 295.1688.

8,8-Diphenyloct-7-enenitrile (3na)



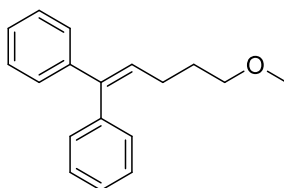
Compound **3na** was prepared following the procedure A. 70% isolated yield. ^1H NMR (400 MHz, CDCl_3) δ 7.41 – 7.34 (m, 2H), 7.34 – 7.29 (m, 1H), 7.27 – 7.23 (m, 2H), 7.23 – 7.18 (m, 3H), 7.18 – 7.13 (m, 2H), 6.05 (t, J = 7.4 Hz, 1H), 2.32 – 2.23 (m, 2H), 2.17 – 2.08 (m, 2H), 1.64 – 1.56 (m, 2H), 1.50 – 1.39 (m, 4H). ^{13}C NMR (100 MHz, CDCl_3) δ 142.6, 142.2, 140.1, 129.8, 129.1, 128.2, 128.1, 127.2, 127.0, 126.9, 119.7, 29.3, 29.0, 28.2, 25.2, 17.1. HRMS (ESI) for: $\text{C}_{20}\text{H}_{21}\text{NNa}$ $[\text{M}+\text{Na}]^+$: calcd 298.1566, found 298.1558.

2-(4,4-Diphenylbut-3-en-1-yl)-1,3-dioxolane (3oa)



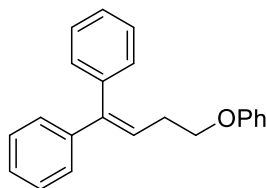
Compound **3oa** was prepared following the procedure A. 78% isolated yield. ^1H NMR (400 MHz, CDCl_3) δ 7.40 – 7.33 (m, 2H), 7.32 – 7.29 (m, 1H), 7.26 – 7.19 (m, 5H), 7.19 – 7.15 (m, 2H), 6.09 (t, J = 7.4 Hz, 1H), 4.85 (t, J = 4.7 Hz, 1H), 3.96 – 3.88 (m, 2H), 3.86 – 3.78 (m, 2H), 2.31 – 2.20 (m, 2H), 1.86 – 1.75 (m, 2H). ^{13}C NMR (100 MHz, CDCl_3) δ 142.7, 142.0, 140.0, 129.9, 128.9, 128.2, 128.1, 127.3, 127.0, 126.9, 104.1, 64.9, 34.1, 24.5. HRMS (ESI) for: $\text{C}_{19}\text{H}_{21}\text{O}_2$ $[\text{M}+\text{H}]^+$: calcd 281.1536, found 281.1536.

(5-Methoxypent-1-ene-1,1-diyl)dibenzene (3pa)



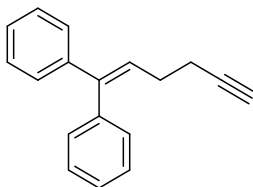
Compound **3pa** was prepared following the procedure A. 54% isolated yield. ^1H NMR (400 MHz, CDCl_3) δ 7.40 – 7.33 (m, 2H), 7.33 – 7.29 (m, 1H), 7.27 – 7.19 (m, 5H), 7.19 – 7.14 (m, 2H), 6.08 (t, J = 7.5 Hz, 1H), 3.36 (t, J = 6.7 Hz, 2H), 3.29 (s, 3H), 2.21 – 2.15 (m, 2H), 1.76 – 1.66 (m, 2H). ^{13}C NMR (100 MHz, CDCl_3) δ 142.7, 142.0, 140.1, 129.9, 129.3, 128.2, 128.1, 127.2, 126.9, 126.9, 72.3, 58.5, 29.9, 26.4. HRMS (ESI) for: $\text{C}_{18}\text{H}_{20}\text{NaO}$ $[\text{M}+\text{Na}]^+$: calcd 275.1406, found 275.1407.

(4-Phenoxybut-1-ene-1,1-diyl) dibenzene (3qa)



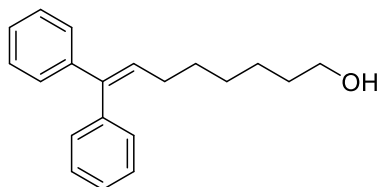
Compound **3qa** was prepared following the procedure A. 57% isolated yield. ^1H NMR (600 MHz, CDCl_3) δ 7.50 – 7.40 (m, 2H), 7.40 – 7.20 (m, 10H), 7.01 – 6.89 (m, 3H), 6.31 – 6.22 (m, 1H), 4.09 (t, J = 6.8 Hz, 2H), 2.72 – 2.62 (m, 2H). ^{13}C NMR (150 MHz, CDCl_3) δ 158.9, 144.0, 142.4, 139.9, 129.8, 129.4, 128.3, 128.1, 127.3, 127.1, 124.9, 120.7, 114.6, 67.4, 30.0. HRMS (ESI) for: $\text{C}_{22}\text{H}_{20}\text{NaO}$ $[\text{M}+\text{Na}]^+$: calcd 323.1406, found 323.1410.

Hex-1-en-5-yne-1,1-diyl dibenzene (3ra)



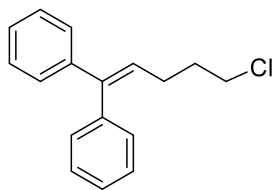
Compound **3ra** was prepared following the procedure A. 55% isolated yield. ^1H NMR (400 MHz, CDCl_3) δ 7.32 - 7.28 (m, 2H), 7.26 - 7.24 (m, 2H), 7.21 – 7.14 (m, 5H), 7.13 - 7.10 (m, 2H), 6.08 (t, J = 7.0 Hz, 1H), 2.31 – 2.21 (m, 4H), 1.90 (t, J = 2.5 Hz, 1H). ^{13}C NMR (101 MHz, CDCl_3) δ 143.0, 142.4, 139.9, 129.9, 128.3, 128.1, 127.5, 127.1, 127.1, 127.1, 83.9, 68.9, 28.7, 19.0. HRMS (ESI) for: $\text{C}_{18}\text{H}_{17}$ $[\text{M}+\text{H}]^+$: calcd 233.1325, found 233.1318.

8,8-Diphenyloct-7-en-1-ol (3sa)



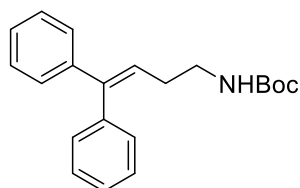
Compound **3sa** was prepared following the procedure A. 56% isolated yield. ^1H NMR (400 MHz, CDCl_3) δ 7.31 – 7.27 (m, 2H), 7.26 – 7.22 (m, 1H), 7.19 – 7.12 (m, 5H), 7.12 – 7.08 (m, 2H), 6.00 (t, J = 7.5 Hz, 1H), 3.60 – 3.46 (m, 2H), 2.07 - 2.01 (m, 2H), 1.48 – 1.40 (m, 2H), 1.38 (t, J = 7.3 Hz, 2H), 1.24 (m, 4H), 1.15 (s, 1H). ^{13}C NMR (100 MHz, CDCl_3) δ 142.8, 141.5, 140.3, 130.1, 129.9, 128.1, 128.1, 127.2, 126.8, 126.8, 63.0, 32.7, 29.9, 29.6, 29.0, 25.6. HRMS (ESI) for: $\text{C}_{20}\text{H}_{25}\text{O}$ $[\text{M}+\text{H}]^+$: calcd 281.1900, found 281.1891.

(5-Chloropent-1-ene-1,1-diyl)dibenzene (3ta)



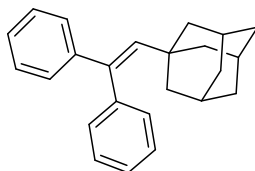
Compound **3ta** was prepared following the procedure A. 71% isolated yield. ^1H NMR (400 MHz, CDCl_3) δ 7.40 – 7.35 (m, 2H), 7.33 – 7.30 (m, 1H), 7.27 – 7.20 (m, 5H), 7.19 – 7.11 (m, 2H), 6.05 (t, J = 7.5 Hz, 1H), 3.51 (t, J = 6.8 Hz, 2H), 2.29 – 2.24 (m, 2H), 1.93 – 1.89 (m, 2H). ^{13}C NMR (100 MHz, CDCl_3) δ 143.0, 142.4, 139.9, 129.8, 128.3, 128.1, 127.7, 127.2, 127.1, 127.1, 44.5, 32.9, 27.2. HRMS (ESI) for: $\text{C}_{17}\text{H}_{18}\text{Cl}$ $[\text{M}+\text{H}]^+$: calcd 257.1092, found 257.1103.

(5-Chloropent-1-ene-1,1-diyl)dibenzene (3ua)



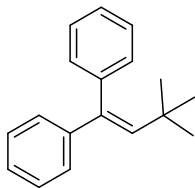
Compound **3ua** was prepared following the procedure A. 58% isolated yield. ^1H NMR (400 MHz, CDCl_3) δ 7.39 – 7.35 (m, 2H), 7.34 – 7.30 (m, 1H), 7.26 – 7.21 (m, 5H), 7.18 - 1.15 (m, 2H), 6.05 (t, J = 7.5 Hz, 1H), 4.51 (s, 1H), 3.22 (t, J = 6.7 Hz, 2H), 2.32-2.27 (m, 2H), 1.42 (s, 9H). ^{13}C NMR (100 MHz, CDCl_3) δ 143.0, 142.4, 139.9, 129.8, 128.3, 128.1, 127.7, 127.2, 127.1, 127.1, 44.5, 32.9, 27.2. HRMS (ESI) for: $\text{C}_{21}\text{H}_{26}\text{NO}_2$ $[\text{M}+\text{H}]^+$: calcd 324.1958, found 324.1951.

1-(2,2-Diphenylvinyl)adamantine (3va)



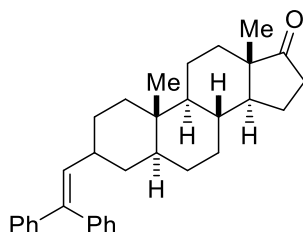
Compound **3va** was prepared following the procedure A. 68% isolated yield. ^1H NMR (400 MHz, CDCl_3) δ 7.36 – 7.27 (m, 3H), 7.25 – 7.13 (m, 7H), 5.84 (s, 1H), 1.89 – 1.80 (m, 3H), 1.65 – 1.50 (m, 12H). ^{13}C NMR (100 MHz, CDCl_3) δ 144.3, 141.0, 140.6, 138.7, 130.4, 127.9, 127.6, 126.8, 126.7, 126.5, 43.2, 36.7, 36.3, 28.6. HRMS (ESI) for: $\text{C}_{24}\text{H}_{27}$ $[\text{M}+\text{H}]^+$: calcd 315.2107, found 315.2112.

(3,3-Dimethylbut-1-ene-1,1-diyl)dibenzene (3wa)



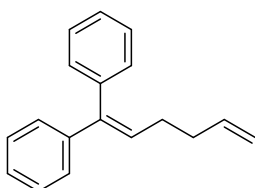
Compound **3wa** was prepared following the procedure A. 51% isolated yield. ^1H NMR (600 MHz, CDCl_3) δ 7.48 – 7.37 (m, 3H), 7.37 – 7.22 (m, 7H), 6.20 (s, 1H), 1.07 (s, 9H). ^{13}C NMR (100 MHz, CDCl_3) δ 142.3, 141.0, 140.1, 133.5, 129.5, 128.2, 128.0, 127.0, 126.9, 126.9, 67.2, 35.5, 32.8. HRMS (ESI) for: $\text{C}_{18}\text{H}_{20}\text{Na}$ $[\text{M}+\text{Na}]^+$: calcd 259.1457, found 259.1463.

(3S,5S,8R,9S,10S,13S,14S)-3-(2,2-Diphenylvinyl)-10,13-dimethylhexadecahydro-17H-cyclopenta[a]phenanthren-17-one (3xa)



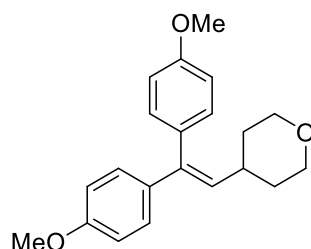
Compound **3xa** was prepared following the procedure A. 61% isolated yield. ^1H NMR (400 MHz, CDCl_3) δ 7.38 – 7.34 (m, 2H), 7.33 – 7.28 (m, 1H), 7.27 – 7.15 (m, 7H), 5.89 (d, J = 10.0 Hz, 1H), 2.42 (dd, J = 19.2, 8.8 Hz, 1H), 2.24 – 2.10 (m, 2H), 2.09 – 2.00 (m, 1H), 1.94 -1.84 (m, 1H), 1.79 – 1.73 (m, 2H), 1.68 – 1.63 (m, 2H), 1.57 – 1.37 (m, 4H), 1.23 (dt, J = 15.4, 11.0 Hz, 7H), 1.06 – 1.01 (m, 1H), 0.99 – 0.93 (m, 2H), 0.91- 0.83 (m, 6H), 0.68 – 0.61 (m, 1H). ^{13}C NMR (100 MHz, CDCl_3) δ 142.8, 140.5, 139.9, 135.6, 129.7, 128.1, 128.0, 127.1, 126.8, 126.7, 54.6, 51.5, 47.8, 45.7, 38.8, 37.8, 35.8, 35.7, 35.5, 35.1, 31.6, 30.7, 28.7, 28.5, 21.7, 20.2, 13.8, 12.3. ^{13}C NMR-DEPT135 (100 MHz, CDCl_3) δ 148.2, 135.6, 129.8, 128.2, 128.0, 127.2, 126.8, 126.6, 54.6, 51.5, 45.7, 38.8, 37.8, 35.9, 35.5, 35.1, 31.6, 30.9, 28.8, 28.5, 21.7, 20.2, 13.8, 12.3. HRMS (ESI) for: $\text{C}_{33}\text{H}_{41}\text{O}$ $[\text{M}+\text{H}]^+$: calcd 453.3152, found 453.3142.

Hexa-1,5-diene-1,1-diylidibenzene (3ya)



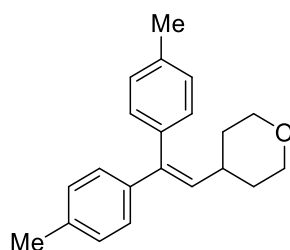
Compound **3ya** was prepared following the procedure A. 52% isolated yield. ^1H NMR (400 MHz, CDCl_3) δ 7.42 – 7.34 (m, 2H), 7.33 – 7.29 (m, 1H), 7.27 – 7.15 (m, 8H), 6.08 (t, J = 6.9 Hz, 1H), 5.87 – 5.73 (m, 1H), 5.08 – 4.92 (m, 2H), 2.26 – 2.15 (m, 4H). ^{13}C NMR (101 MHz, CDCl_3) δ 142.8, 142.0, 140.2, 138.1, 129.9, 129.2, 128.2, 128.1, 127.3, 126.9, 126.9, 114.9, 34.1, 29.1. HRMS (ESI) for: $\text{C}_{18}\text{H}_{19}$ $[\text{M}+\text{H}]^+$: calcd 235.1481, found 235.1472.

4-(2,2-Bis(4-methoxyphenyl)vinyl)tetrahydro-2H-pyran (**3ab**)



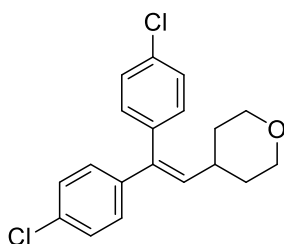
Compound **3ab** was prepared following the procedure B. 68% isolated yield. ^1H NMR (400 MHz, CDCl_3) δ 7.06 (d, J = 8.9 Hz, 2H), 7.00 (d, J = 8.7 Hz, 2H), 6.83 (d, J = 8.7 Hz, 2H), 6.71 (d, J = 8.9 Hz, 2H), 5.67 (d, J = 9.8 Hz, 1H), 3.88 – 3.80 (m, 2H), 3.77 (s, 3H), 3.70 (s, 3H), 3.28 – 3.18 (m, 2H), 2.38 – 2.23 (m, 1H), 1.54 – 1.42 (m, 4H). ^{13}C NMR (100 MHz, CDCl_3) δ 158.8, 158.6, 140.0, 135.5, 132.7, 131.9, 130.71, 128.3, 113.6, 113.5, 67.4, 55.3, 55.2, 35.6, 33.1. HRMS (ESI) for: $\text{C}_{21}\text{H}_{24}\text{NaO}_3$ $[\text{M}+\text{Na}]^+$: calcd 347.1618, found 347.1614.

4-(2,2-Di-p-tolylvinyl)tetrahydro-2H-pyran (**3ac**)



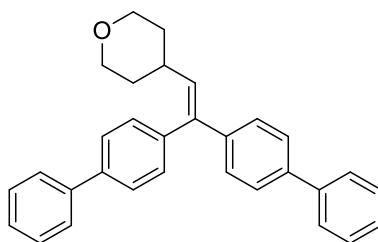
Compound **3ac** was prepared following the procedure B. 81% isolated yield. ^1H NMR (400 MHz, CDCl_3) δ 7.22 – 7.14 (m, 2H), 7.13 – 7.01 (m, 6H), 5.82 (d, J = 9.8 Hz, 1H), 3.91 (d, J = 11.4 Hz, 2H), 3.41 – 3.24 (m, 2H), 2.39 (s, 3H), 2.32 (s, 3H), 1.65 – 1.51 (m, 5H). ^{13}C NMR (101 MHz, CDCl_3) δ 140.7, 139.9, 137.3, 136.7, 136.6, 132.7, 129.5, 128.9, 128.8, 127.1, 67.4, 35.5, 33.0, 21.3, 21.1. HRMS (ESI) for: $\text{C}_{21}\text{H}_{24}\text{NaO}$ $[\text{M}+\text{Na}]^+$: calcd 315.1719, found 315.1715.

4-(2,2-Bis(4-chlorophenyl)vinyl)tetrahydro-2H-pyran (3ad)



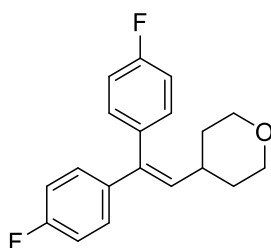
Compound **3ad** was prepared following the procedure B. 87% isolated yield. ^1H NMR (400 MHz, CDCl_3) δ 7.43 – 7.33 (m, 2H), 7.29 – 7.18 (m, 3H), 7.12 – 7.06 (m, 3H), 5.88 (d, J = 9.9 Hz, 1H), 4.00 – 3.85 (m, 2H), 3.38 – 3.23 (m, 2H), 2.42 – 2.25 (m, 1H), 1.59 – 1.49 (m, 4H). ^{13}C NMR (101 MHz, CDCl_3) δ 140.4, 138.8, 138.1, 134.6, 133.3, 133.1, 130.9, 128.7, 128.4, 128.3, 67.2, 35.7, 32.7. HRMS (ESI) for: $\text{C}_{19}\text{H}_{19}\text{Cl}_2\text{O}$ $[\text{M}+\text{H}]^+$: calcd 333.0807, found 333.0810

4-(2,2-Di([1,1'-biphenyl]-4-yl)vinyl)tetrahydro-2H-pyran (3ae)



Compound **3ae** was prepared following the procedure B. 69% isolated yield. ^1H NMR (400 MHz, CDCl_3) δ 7.63 – 7.53 (m, 4H), 7.49 (m, 2H), 7.47 – 7.31 (m, 6H), 7.31 – 7.12 (m, 6H), 5.90 (d, J = 9.8 Hz, 1H), 3.86 (d, J = 11.4 Hz, 2H), 3.25 (s, 2H), 2.39 (d, J = 9.2 Hz, 1H), 1.53 (m, 4H). ^{13}C NMR (101 MHz, CDCl_3) δ 141.3, 140.7, 140.7, 140.2, 139.9, 139.9, 139.1, 133.9, 130.1, 128.8, 128.7, 127.6, 127.3, 127.2, 127.0, 126.9, 126.8, 67.3, 35.7, 32.9. HRMS (ESI) for: $\text{C}_{31}\text{H}_{29}\text{O}$ $[\text{M}+\text{H}]^+$: calcd 417.2213, found 417.2206.

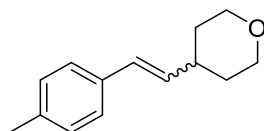
4-(2,2-Bis(4-fluorophenyl)vinyl)tetrahydro-2H-pyran (3af)



Compound **3af** was prepared following the procedure B. 45% isolated yield. ^1H NMR (400 MHz, CDCl_3) δ 7.19 – 7.02 (m, 6H), 7.01 – 6.88 (m, 2H), 5.82 (d, J = 9.8 Hz, 1H), 4.00 – 3.84 (m, 2H), 3.37 – 3.21 (m, 2H), 2.39 – 2.25 (m, 1H), 1.62 – 1.50 (m, 4H). ^{13}C NMR (100 MHz,

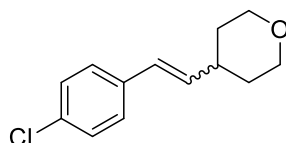
CDCl₃) δ 163.3 (d, J_{C-F} = 13 Hz), 160.8 (d, J_{C-F} = 13 Hz), 139.0, 138.3 (d, J_{C-F} = 3 Hz), 135.8 (d, J_{C-F} = 3 Hz), 133.8, 131.1 (d, J_{C-F} = 8 Hz), 128.7 (d, J_{C-F} = 8 Hz), 115.4 (d, J_{C-F} = 21 Hz), 115.0 (d, J_{C-F} = 22 Hz), 67.3, 35.7, 32.8. HRMS (ESI) for: C₁₉H₁₈F₂NaO [M+Na]⁺: calcd 323.1218, found 323.1227.

4-(4-Methylstyryl)tetrahydro-2H-pyran (**3ag**)



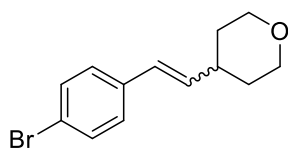
Compound **3ag** was prepared following the procedure B. 58% isolated yield, E:Z= 3:1. ¹H NMR (400 MHz, CDCl₃) δ 7.17 (d, J = 7.9 Hz, 2H), 7.07 – 6.99 (m, 2H), 6.27 (d, J = 16.4 Hz, 1H), 6.02 (dd, J = 16.0, 6.8 Hz, 1H, E isomer), 5.36 (dd, J = 11.7, 9.9 Hz, 1H, Z isomer), 3.97 – 3.83 (m, 2H), 3.41 – 3.30 (m, 2H), 2.79 – 2.69 (m, 1H, Z isomer), 2.33 – 2.30 (m, 1H, E isomer), 2.26 (d, J = 11.6 Hz, 3H), 1.67 – 1.57 (m, 2H), 1.54 – 1.45 (m, 2H). ¹³C NMR (100 MHz, CDCl₃) δ 136.8 (E isomer), 136.4 (Z isomer), 136.1, 134.7 (E isomer), 134.6 (Z isomer), 133.5, 129.2 (E isomer), 128.9 (Z isomer), 128.4, 128.04 (E isomer), 128.02 (Z isomer), 125.9, 67.7 (E isomer), 67.4 (Z isomer), 38.3 (E isomer), 34.1 (Z isomer), 32.84 (Z isomer), 32.7 (E isomer), 21.12 (Z isomer), 21.09 (E isomer). HRMS (ESI) for: C₁₄H₁₉O [M+H]⁺: calcd 203.1430, found 203.1426. ¹³C NMR-DEPT135 (100 MHz, CDCl₃) δ 136.2, 133.6, 129.2, 129.0, 128.4, 128.11, 128.08, 125.9, 67.8, 67.4, 38.4, 34.2, 32.9, 32.7, 21.19, 21.16.

4-(4-Chlorostyryl) tetrahydro-2H-pyran (**3ah**)



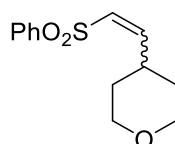
Compound **3ah** was prepared following the procedure B. 62% isolated yield, E:Z= 3:2. ¹H NMR (400 MHz, CDCl₃) δ 7.28 (d, J = 11.9 Hz, 3H), 7.16 (d, J = 8.4 Hz, 1H), 6.38 – 6.28 (m, 1H), 6.13 (dd, J = 16.0, 6.8 Hz, 1H, E isomer), 5.50 (dd, J = 11.7, 9.9 Hz, 1H, Z isomer), 4.06 – 3.91 (m, 2H), 3.52 – 3.36 (m, 2H), 2.81 – 2.67 (m, 1H, Z isomer), 2.37 (td, J = 7.6, 4.0 Hz, 1H, E isomer), 1.72 – 1.67 (m, 4H, Z isomer), 1.60 – 1.47 (m, 4H, E isomer). ¹³C NMR (100 MHz, CDCl₃) δ 137.4, 136.0 (E isomer), 135.9 (Z isomer), 135.3, 132.6 (E isomer), 132.5 (Z isomer), 129.7, 128.6 (E isomer), 128.4 (Z isomer), 127.2, 127.1 (E isomer), 127.0 (Z isomer), 67.7 (E isomer), 67.29 (Z isomer), 38.3 (E isomer), 34.1 (Z isomer), 32.7 (Z isomer), 32.52 (E isomer). HRMS (ESI) for: C₁₃H₁₆ClO [M+H]⁺: calcd 223.0884, found 223.0875.

4-(4-Bromostyryl)tetrahydro-2H-pyran (3ai)



Compound **3ai** was prepared following the procedure B. 47% isolated yield, E:Z= 3:1. ^1H NMR (400 MHz, CDCl_3) δ 7.48 – 7.43 (m, 2H), 7.12 – 7.07 (m, 2H), 6.32 (d, J = 11.7 Hz, 1H), 5.51 (dd, J = 11.6, 10.0 Hz, 1H), 4.02 – 3.88 (m, 2H), 3.98 – 3.93 (m, 2H), 2.79 – 2.69 (m, 1H), 1.55 – 1.48 (m, 2H). ^{13}C NMR (100 MHz, CDCl_3) δ 137.5, 136.4, 131.4, 130.1, 127.1, 120.6, 67.3, 34.2, 32.7. HRMS (ESI) for: $\text{C}_{13}\text{H}_{16}\text{BrO}$ $[\text{M}+\text{H}]^+$: calcd 263.0379, found 263.0381.

4-(2-(Phenylsulfonyl)vinyl)tetrahydro-2H-pyran (3aj)



Compound **3aj** was prepared following the procedure B. 34% isolated yield, Z: E = 6:1. The pure Z product was separated by flash chromatography on silica gel. ^1H NMR (400 MHz, CDCl_3) δ 7.88 (dd, J = 7.4, 1.8 Hz, 2H), 7.63 (dd, J = 8.6, 6.6 Hz, 1H), 7.55 (dd, J = 8.5, 6.8 Hz, 2H), 6.95 (dd, J = 15.2, 6.2 Hz, 1H), 6.30 (dd, J = 15.2, 1.6 Hz, 1H), 4.0 – 3.96 (m, 2H), 3.45 – 3.38 (m, 2H), 2.48 – 2.41 (m, 1H), 1.70 – 1.65 (m, 2H), 1.56 – 1.46 (m, 2H). ^{13}C NMR (100 MHz, CDCl_3) δ 140.6, 140.1, 136.4, 129.8, 128.1, 128.1, 127.1, 126.7, 40.0, 33.6, 21.4, 20.7, 14.2. HRMS (ESI) for: $\text{C}_{13}\text{H}_{17}\text{O}_3\text{S}$ $[\text{M}+\text{H}]^+$: calcd 253.0893, found 253.0895.

4.5 References

- [1] a) M. B. Smith, J. March, in *March's Advanced Organic Chemistry: Reactions, Mechanisms, and Structure*; John Wiley & Sons: Hoboken, NJ, 2013; b) R. Álvarez, B. Vaz, H. Gronemeyer, A. R. de Lera, *Chem. Rev.*, **2014**, 114, 1; c) M. Hassam, A. Taher, G. E. Arnott, I. R. Green, W. A. L. Van Otterlo, *Chem. Rev.*, **2015**, 115, 5462; d) N. A. McGrath, M. Brichacek, J. T. Njardarson, *J. Chem. Educ.*, **2010**, 87, 1348.
- [2] a) B. E. Maryanoff, A. B. Reitz, *Chem. Soc. Rev.*, **1989**, 89, 863; b) P. A. Byrne, D. G. Gilheany, *Chem. Soc. Rev.*, **2013**, 42, 6670.
- [3] a) H.-T. Chang, T. T. Jayanth, C.-C. Wang, C.-H. Cheng, *J. Am. Chem. Soc.*, **2007**, 129, 12032; b) C. W. Cheung, F. E. Zhurkin, X. Hu, *J. Am. Chem. Soc.*, **2015**, 137, 4932.
- [4] a) R. F. Heck, *Acc. Chem. Res.*, **1979**, 12, 146; b) I. P. Beletskaya, A. V. Cheprakov, *Chem. Rev.*, **2000**, 100, 3009; c) Y. Ikeda, T. Nakamura, H. Yorimitsu, K. Oshima, *J. Am. Chem. Soc.*, **2002**, 124, 6514; d) W. Affo, H. Ohmiya, T. Fujioka, Y. Ikeda, T. Nakamura, H. Yorimitsu, K. Oshima, Y. Imamura, T. Mizuta, K. Miyoshi, *J. Am. Chem. Soc.*, **2006**, 128, 8068; e) L. Firmansjah, G. C. Fu, *J. Am. Chem. Soc.*, **2007**, 129, 11340; f) A. C. Bissember, A. Levina, G. C. Fu, *J. Am. Chem. Soc.*, **2012**, 134, 14232; g) Y. Zou, J. Zhou, *Chem. Commun.*, **2014**, 50, 3725; h) C. M. McMahon, E. J. Alexanian, *Angew. Chem., Int. Ed.*, **2014**, 53, 5974.
- [5] a) E. Negishi, X. Zeng, Z. Tan, M. Qian, Q. Hu, Z. Huang, in *Metal-Catalyzed Cross-Coupling Reactions* (Eds. A. de Meijere, F. Diederich), Wiley-VCH Verlag GmbH: Weinheim, **2008**; 815; b) G. C. Vougioukalakis, R. H. Grubbs, *Chem. Rev.*, **2010**, 110, 174; c) S. H. Cho, J. Y. Kim, J. Kwak, S. Chang, *Chem. Soc. Rev.*, **2011**, 40, 5068; d) N. Kambe, T. Iwasaki, J. Terao, *Chem. Soc. Rev.*, **2011**, 40, 4937; e) K. Zhu, J. Dunne, M. P. Shaver, S. P. Thomas, *ACS Catal.*, **2017**, 7, 2353; f) S. J. Meek, R. V. O'Brien, J. Liaveria, R. R. Schrock, *Nature*, **2011**, 471, 461; g) T. Di Franco, A. Epenoy, X. Hu, *Org. Lett.*, **2015**, 17, 4910; h) Q. Liu, X. Dong, J. Li, J. Xiao, Y. Dong, H. Liu, *ACS Catal.*, **2015**, 5, 6111.
- [6] a) P. Knochel in *Handbook of Functionalized Organometallics: Applications in Synthesis*, Wiley-VCH, Weinheim, **2005**; b) R. Jana, T. P. Pathak, M. S. Sigman, *Chem. Rev.*, **2011**, 111, 1417; c) M. Movsisyan, E. I. P. Delbeke, J. K. E. T. Berton, C. Battilocchio, S. V. Ley, C. V. Stevens, *Chem. Soc. Rev.*, **2016**, 45, 4892.
- [7] For selected reviews on visible light photocatalysis, see: a) J. M. R. Narayanam, C. R. J. Stephenson, *Chem. Soc. Rev.*, **2011**, 40, 102; b) J. Xuan, W.-J. Xiao, *Angew. Chem., Int. Ed.*, **2012**, 51, 6828; c) C. K. Prier, D. A. Rankic, D. W. C. MacMillan, *Chem.*

- Rev., **2013**, 113, 5322; d) Y. Xi, H. Yi, A. Lei, *Org. Biomol. Chem.*, **2013**, 11, 2387; e) T. P. Yoon, M. A. Ischay, J. Du, *Nat. Chem.*, **2010**, 2, 527; f) D. Ravelli, S. Protti, M. Fagnoni, *Chem. Rev.*, **2016**, 116, 9850; g) Q. Liu, L.-Z. Wu, *Natl. Sci. Rev.*, **2017**, 4, 359; h) L. Marzo, S. Pagire, O. Reiser, B. König, *Angew. Chem., Int. Ed.*, **2018**, 57, 10034.
- [8] For selected works on photocatalytic alkenylation reactions, see: a) S. F. Wnuk, P. I. Garcia, Z. Wang, *Org. Lett.*, **2004**, 6, 2047; b) A. Noble, D. W. C. MacMillan, *J. Am. Chem. Soc.*, **2014**, 136, 11602; c) V. Corce, L.-M. Chamoreau, E. Derat, J.-P. Goddard, C. Ollivier, L. Fensterbank, *Angew. Chem., Int. Ed.*, **2015**, 54, 11414; d) H. Huang, K. Jia, Y. Chen, *Angew. Chem., Int. Ed.*, **2015**, 54, 1881; e) J. Li, J. Zhang, H. Tan, D. Z. Wang, *Org. Lett.*, **2015**, 17, 2522; f) J. Xie, J. Li, V. Weingand, M. Rudolph, A. S. K. Hashmi, *Chem. Eur. J.*, **2016**, 22, 12646; g) K. Xu, Z. Tan, H. Zhang, J. Liu, S. Zhang, Z. Wang, *Chem. Commun.*, **2017**, 53, 10719; h) G.-Z. Wang, R. Shang, W.-M. Cheng, Y. Fu, *J. Am. Chem. Soc.*, **2017**, 139, 18307; i) S. Paul, J. Guin, *Green Chem.*, **2017**, 19, 2530; j) G.-Z. Wang, R. Shang, Y. Fu, *Org. Lett.*, **2018**, 20, 888.
- [9] For selected examples on photocatalytic transformations of alkyl fluoroborate salts, see: a) D. R. Heitz, K. Rizwan, G. A. Molander, *J. Org. Chem.*, **2016**, 81, 7308; b) J. K. Matsui, S. B. Lang, D. R. Heitz, G. A. Molander, *ACS Catal.*, **2017**, 7, 2563; c) Y. Yasu, T. Koike, M. Akita, *Adv. Synth. Catal.*, **2012**, 354, 3414; d) D. N. Primer, I. Karakaya, J. C. Tellis, G. A. Molander, *J. Am. Chem. Soc.*, **2015**, 137, 2195; e) M. El Khatib, R. A. Serafim, G. A. Molander, *Angew. Chem., Int. Ed.*, **2016**, 55, 254.
- [10] For selected reviews on coupling reactions of alkyl halides, see: a) A. C. Frisch, M. Beller, *Angew. Chem., Int. Ed.*, **2005**, 44, 674; b) A. Rudolph, M. Lautens, *Angew. Chem., Int. Ed.*, **2009**, 48, 2656; c) X. Hu, *Chem. Sci.*, **2011**, 2, 1867; d) N. Kambe, T. Iwasaki, J. Terao, *Chem. Soc. Rev.*, **2011**, 40, 4937.
- [11] a) J. D. Nguyen, E. M. D'Amato, J. M. R. Narayanam, C. R. J. Stephenson, *Nat. Chem.*, **2012**, 4, 854; b) D. Fernandez Reina, A. Ruffoni, Y. S. S. Al-Faiyz, J. J. Douglas, N. S. Sheikh, D. Leonori, *ACS Catal.*, **2017**, 7, 4126; c) Y. Shen, J. Cornella, F. Julia-Hernandez, R. Martin, *ACS Catal.*, **2017**, 7, 409; d) S. Sumino, M. Uno, H.-J. Huang, Y.-K. Wu, I. Ryu, *Org. Lett.*, **2018**, 20, 1078; e) D. Kurandina, M. Rivas, M. Radzhabov V. Gevorgyan, *Org. Lett.*, **2018**, 20, 357.
- [12] a) C. Chatgililoglu, A. Alberti, M. Ballestri, D. Macciantelli, D. P. Curran, *Tetrahedron Lett.*, **1996**, 37, 6391; b) C. Chatgililoglu, *Chem. Eur. J.*, **2008**, 14, 2310; c) G. Rouquet, F. Robert, R. Mereau, F. Castet, Y. Landais, *Chem. Eur. J.*, **2011**, 17, 13904; d) J. J. Devery, J. D. Nguyen, C. Dai, C. R. J. Stephenson, *ACS Catal.*, **2016**, 6, 5962; e) P. Zhang, C. C. Le, D. W. C. MacMillan, *J. Am. Chem. Soc.*, **2016**, 138, 8084; f) C. Le, T. Q. Chen, T. Liang, P. Zhang, D. W. C. MacMillan, *Science*, **2018**, 360, 1010.

- [13] For details, see Chapter 4.4.3 or Q.-Q. Zhou, S. J. S. Düsel, L.-Q. Lu, B. König, W.-J. Xiao, *Chem. Commun.*, **2019**, 55, 107.
- [14] For selected reviews and examples on photoredox/nickel dual catalytic transformations, see: a) J. Twilton, C. Le, P. Zhang, M. H. Shaw, R. W. Evans, D. W. C. MacMillan, *Nat. Rev. Chem.*, **2017**, 1, 0052; b) K. L. Skubi, T. R. Blum, T. P. Yoon, *Chem. Rev.*, **2016**, 116, 10035; c) Z. Zuo, D. T. Ahneman, L. Chu, J. A. Terrett, A. G. Doyle, D. W. C. MacMillan, *Science*, **2014**, 345, 437; d) J. C. Tellis, D. N. Primer, G. A. Molander, *Science*, **2014**, 345, 433.
- [15] a) A. Noble, S. J. McCarver, D. W. C. MacMillan, *J. Am. Chem. Soc.*, **2015**, 137, 624; b) H. Yue, C. Zhu, M. Rueping, *Angew. Chem., Int. Ed.*, **2018**, 57, 1371.
- [16] a) Y. Yang, B. Yu, *Chem. Rev.*, **2017**, 117, 12281; b) R. S. Andrews, J. J. Becker, M. R. Gagne, *Angew. Chem., Int. Ed.*, **2010**, 49, 7274; c) S. O. Badir, A. Dumoulin, J. K. Matsui, G. A. Molander, *Angew. Chem., Int. Ed.*, **2018**, 57, 6610.
- [17] For more information about the mechanistic investigations, see Chapter 4.4.2.
- [18] U. Megerle, R. Lechner, B. König, E. Riedle, *Photochem. Photobiol. Sci.* **2010**, 9, 1400.
- [19] G.-Z. Wang, R. Shang and Y. Fu, *Org. Lett.* **2018**, 20, 888.
- [20] Gu, H.; Wang, C. *Org. Biomol. Chem.* **2015**, 13, 5880.
- [21] M. Brown, R. Kumar, J. Rehbein, T. Wirth, *Chem. Eur. J.* **2016**, 22, 4030.
- [22] Q.-Q. Zhou, W. Guo, W. Ding, X. Xu, X. Chen, L.-Q. Lu, W.-J. Xiao, *Angew. Chem., Int. Ed.* **2015**, 54, 11196.

5. Visible-light photo-Arbuzov reaction of aryl bromides and trialkyl phosphites yielding aryl phosphonates



Aryl phosphonates are functional groups frequently found in pharmaceutical and crop protection agents. For their synthesis via C-P bond formation typically transition metal catalyzed reactions are used. We report a visible light photo-Arbuzov reaction as an efficient, mild and metal-free alternative. Rhodamine 6G (Rh.6G) is used as photocatalyst generating aryl radicals under blue light. Coupling of the radicals with a wide range of trivalent phosphites gives aryl phosphonates in good to excellent isolated yields. The mild reaction conditions allow the introduction of a phosphonate group into complex and sensitive pharmaceutically active molecules, such as benzodiazepams or Nicergoline by the activation of a carbon halogen bond.

This Chapter has been published in:

R. S. Shaikh, S. J. S. Düsel, B. König, *ACS Catal.*, **2016**, 6, pp 8410–8414.

Reproduced with permission from *ACS Catal.*, **2016**, 6, pp 8410–8414. Copyright © 2016, American Chemical Society.

Author contributions:

RSR discovered the reaction, wrote the manuscript, and synthesized most of the heterocyclic products (Schme 5-3) and compounds 14 + 16. Both RSR and SJSD synthesized the products with P(OEt)₃ as reactant and contributed to the optimization (Table 5-1). SJSD synthesized the products with P(OMe)₃, P(OPh)₃, and P(OⁱPr)₃ as reactant and the products with triflates as starting material. BK supervised the project and is the corresponding author.

5.1 Introduction

Aryl phosphonates and phosphine oxides are structural motifs found in many pharmaceutically active molecules. In addition, they find applications in organic materials and as synthetic intermediates.^[1] The phosphorous containing moiety act as ligand coordinating to transition metals or binding to biological receptors and thereby regulating physiological processes or material functions.^[2] The broad use of organophosphorus compounds in different areas of science triggered the development of many methods for their preparation. Classic synthesis of aryl phosphonates involves transition metal catalyzed cross coupling of $R_2P(O)H$ with a coupling partner via P-H bond activation.^[3] Palladium-catalysed C-P coupling has been well established using various precursors such as aryl halides,^[4] triflates,^[5] boronic acids,^[6] aryl sulfonates,^[7] and triaryl bismuth,^[8] Other methods involve nickel and copper catalysed C-P bond formation.^[9] Recently, a combination of transition metal and visible light catalysis were used for the synthesis of aryl phosphonates via C-X bond activation, which require expensive metal complexes.^[10] However, most transition metal catalysed methods require harsh reaction conditions or have a limited substrate scope calling for the development of new routes for the synthesis of aryl phosphonates.

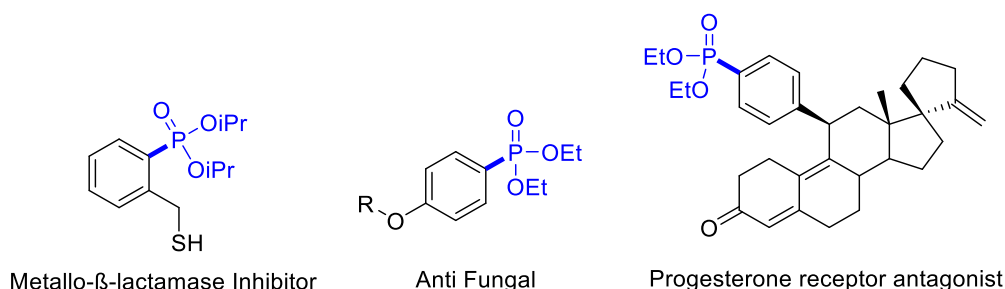
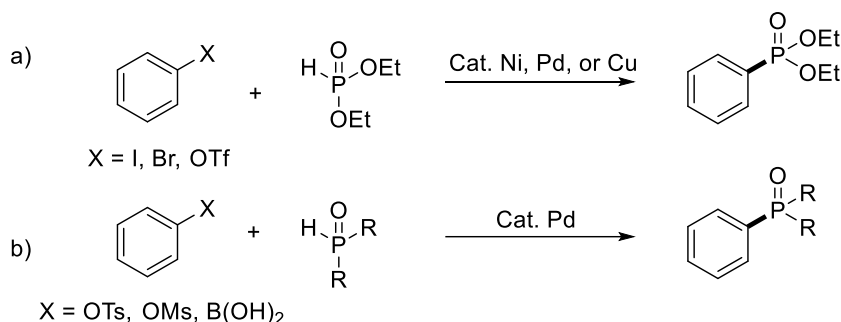


Figure 5-1. Aryl phosphonates in commercial pharmaceutical agents.

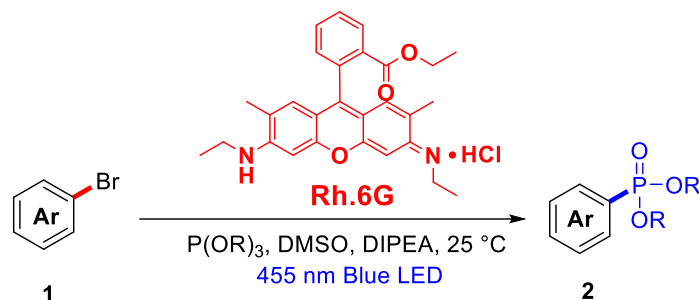
In recent years, visible light photoredox catalysis has emerged as a useful tool for the C-X bond activation by functionalization via photoinduced electron transfer (PET) processes.^[11, 12, 13] A highly anticipated application of visible light catalysis is the generation of reactive aryl radicals, which serve as arylating agents to suitable precursors. We have recently introduced the photoredox catalyzed generation of transient aryl radicals from electron deficient arenes, such as diazonium salts^[14] or perfluorophenyl bromide^[15] by a visible light PET process. Using a consecutive photoinduced electron transfer process (conPET)^[16] the scope of starting materials for the generation of aryl radicals was extended to less reactive aryl bromides or aryl chlorides bearing very negative reduction potentials.^[17] The xanthene dye rhodamine 6G (Rh.6G)^[18] is a particular useful conPET photocatalyst allowing the chromo-selective C-X bond activation.^[19]

Upon irradiation with blue light (455 nm) in the presence of an electron donor under nitrogen atmosphere Rh.6G yields the corresponding excited radical anion ($\text{Rh.6G}^{\bullet-}$),^[20, 21] which has a reduction potential of ca. -2.4 V vs SCE^[19] that is sufficient to activate aryl halides.^[16, 22] The initial aryl halide radical anion may cleave into a halide anion and an aryl radical, which can further react with different coupling partners.

Previous work



This work



Scheme 5-1. Rh.6G catalyzed mild C-P bond formation via C-Br bond activation.

As a part of our efforts towards the development of mild methods for C-X bond activation, we report here the visible light photoredox catalyzed synthesis of aryl phosphonates via photo-Arbuzov reaction. The photo-Arbuzov reaction is a variation of the classical Michaelis-Arbuzov reaction,^[23] and was first demonstrated in 1966 using UV light (quartz mercury vapor lamp) at low temperature and mostly aryl iodides as substrates. The obtained product yields were low to good in the range of 34-90%.^[23] To improve the method we aimed to develop a more broadly applicable radical phosphonylation reaction employing visible light photocatalysis using Rh.6G and commercially available bench stable aryl halides.

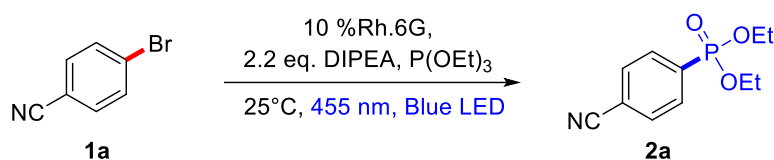
5.2 Results and discussion

5.2.1 Synthesis

We began the investigations towards a visible light mediated photo-Arbuzov reaction with irradiating 4-bromobenzonitrile in DMSO in the presence of Rh.6G and *N,N*-

diisopropylethylamine (DIPEA), as sacrificial electron donor, under nitrogen atmosphere to generate a highly reactive *p*-cyano phenyl radical. Trapping of the radical with triethyl phosphite delivered the corresponding diethyl (4-cyanophenyl) phosphonate (**2a**) in 71% (see table 5-1, entry 3, 4). Reactions were also performed in presence of oxygen atmosphere, but it did not show promising results. In addition, the reactions can be performed on large scale by using the constant flow reactor. The same reaction conditions with different triethyl phosphite concentrations did not show much influence on the isolated yield. The reaction in CH₃CN showed excellent conversion, but it was limited to the standard substrate. In the absence of DIPEA only traces of the desired product were observed. This might be rationalized by a single electron transfer from the trapping reagent to the excited photocatalyst, but the reaction proceeds very sluggish with minor amounts of product formed.

Table 5-1. Optimization of the reaction conditions.

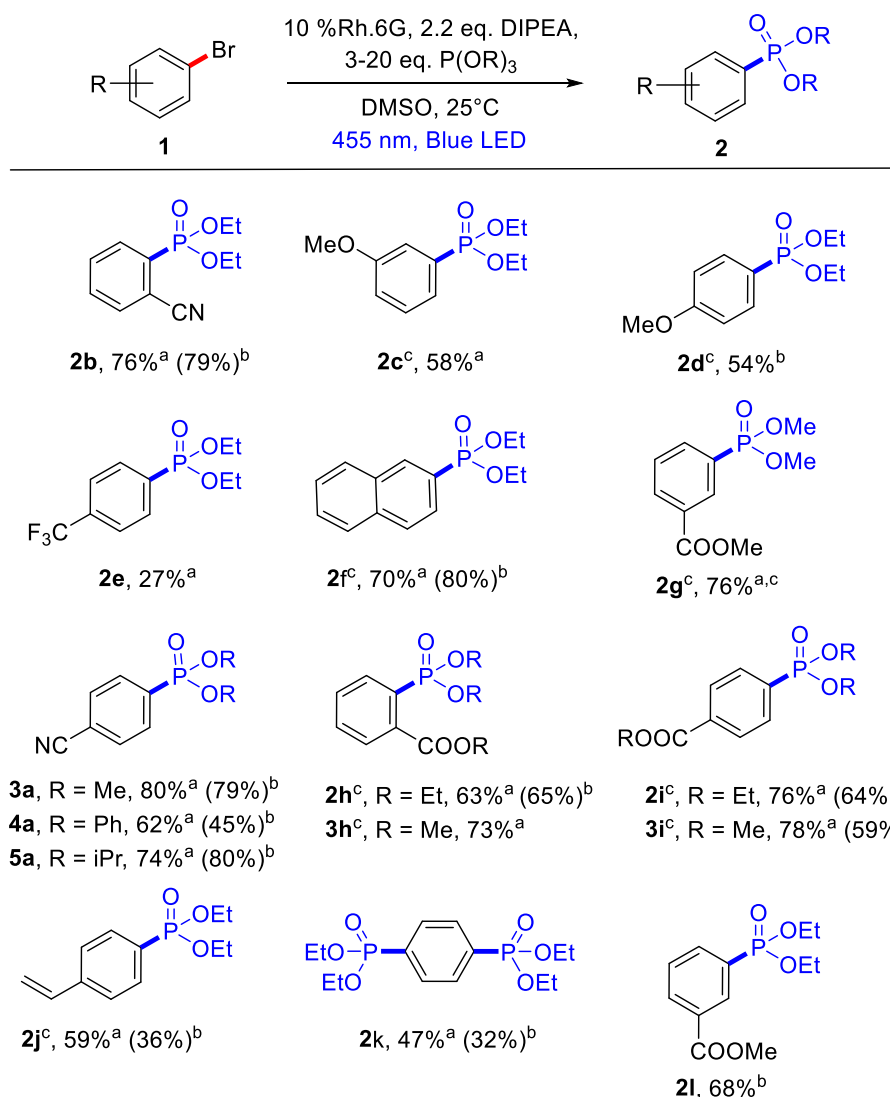


Entry	Solvent	Time [h]	P(OEt) ₃	Yield [%] ^[a]
1	DMSO	6	20 eq.	[e]
2	DMSO	12	20 eq.	[e]
3	DMSO	17	20 eq.	71
4	DMSO	17	3 eq.	76
5	DMSO	18	5 eq.	76
5	CH ₃ CN ^[b]	18	20 eq.	93
6 ^[c]	DMSO	18	20 eq.	34
7 ^[d]	DMSO	18	20 eq.	0
8 ^[f]	DMSO	18	3 eq.	36
9 ^[g]	DMSO	18	3 eq.	Traces
10 ^[h]	DMSO	8	3 eq.	76

[a] Isolated yield. [b] Substrate specific. [c] Reactions performed in the absence of DIPEA. [d] Reactions performed in the absence of light. [e] Product was not isolated based on GC observation. [f] Without degassing. [g] Under O₂ atmosphere. [h] In PTFE flow reactor. P(OEt)₃ = triethyl phosphite. Reactions were monitored using gas chromatography.

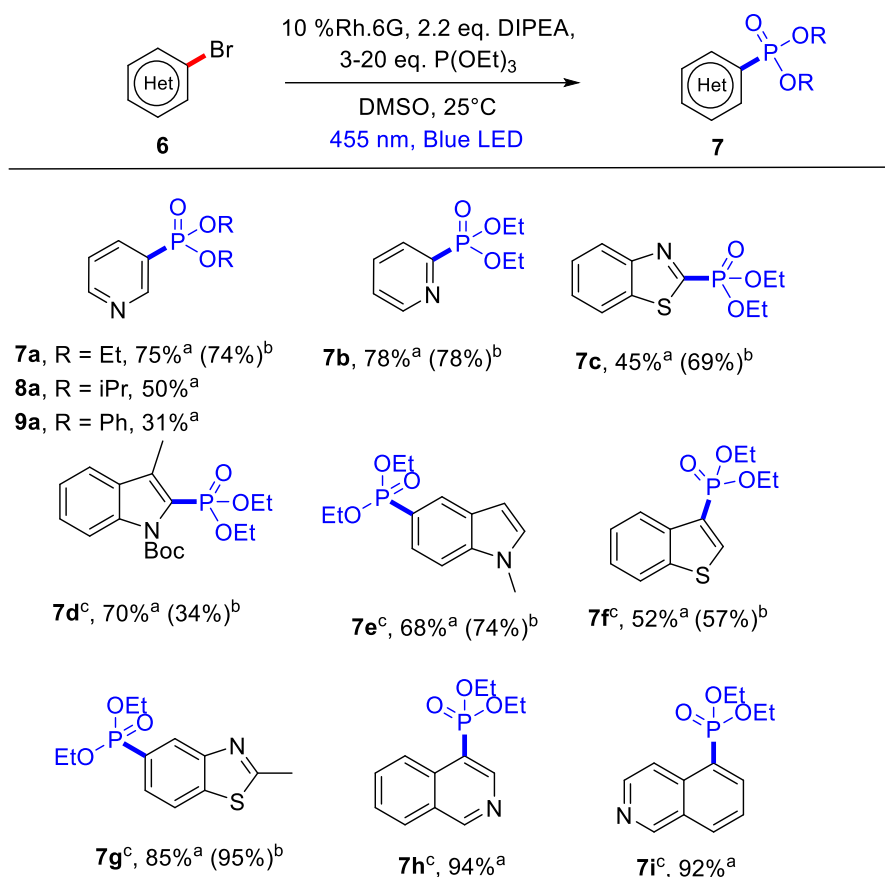
Based on the optimized reaction conditions, we explored the scope of visible light induced phosphonylation of aryl bromides further. The reaction proceeds smoothly with a wide functional group tolerance. Mostly, 10-15 mol% loading of the catalyst was required for a complete conversion of the substrate. Precursors bearing nitrile, ester, methoxy, vinyl functionality (**1a-1l**) gave the phosphonylated product in good yield. In general, electron deficient arenes (**1a**, **1b**, **1g**, **1h**, **1i**) showed higher conversion to the corresponding phosphonylated product than electron-rich arenes (**1c**, **1d**, **1j**). Contradictory to the observation, 4-bromobenzotrifluoride (**1e**) gave the corresponding phosphonate in a yield of only 27%. One-pot conversion of 1,4-dibromobenzene (**1k**) to the corresponding di-phosphonate was achieved in moderate yield. Also, 4-bromostyrene (**1j**) gave the interesting building block **2j** in good yield. Apparently, bromobenzonitriles (**1a**, **1b**) are more reactive substrates in the photocatalytic phosphonylation reaction, with comparatively shorter reaction time (17h) required for a complete conversion.

A variety of different phosphites, such as P(OMe)_3 , P(OPh)_3 and P(OiPr)_3 , were coupled with aryl bromides under the optimized reaction conditions (Scheme 5-2, entry **2g**, **3a-5a**, **3h**, **3i**, **2l**). Varying electronic properties and steric bulk were tolerated: aryl-dimethyl, diphenyl and diisopropyl phosphonates were synthesised in 62 to 80% yield.



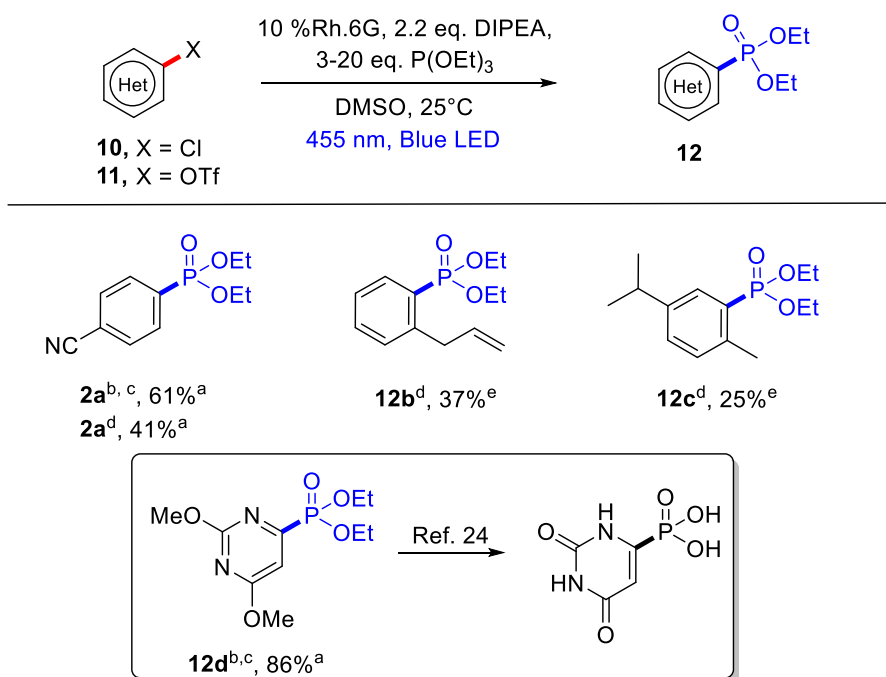
Scheme 5-2. Scope of aryl bromides for the photo-Arbuzov reaction: Starting material in all the cases 0.1–0.3 mmol, reaction time 15–40 h. [a] Yield of product with 20 eq. of the trapping reagent. [b] Yield of the product with 3 eq. of the trapping reagent. [c] 15% of the Rh.6G used. For detailed information on the reaction conditions, see Chapter 5.4.3.

Subsequently, we explored the use of heteroaryl bromides in this photo-Arbuzov reaction protocol. To our delight, a range of six membered and fused heterocyclic bromides were suitable for the coupling with triethyl phosphite as well as other trialkyl phosphites (Scheme 5-3) in moderate to excellent yield. The ability of the catalytic system to activate electron-rich as well as electron-deficient heteroarenes demonstrates a remarkable generous scope of the reaction conditions. Bromopyridine analogues **6a** and **6b** showed fast conversion to the corresponding phosphonates (14 h) with 75–78% yield. In addition, electron rich heterocycles such as **6d**, **6e**, **6f**, and **6g** gave excellent conversion. Moreover, isoquinoline derived substrates such as **6h** and **6i** showed exceptionally good conversion to the corresponding phosphonates **7h** and **7i** giving 94 and 92% yield, respectively, in 33 h. (Scheme 5-3).



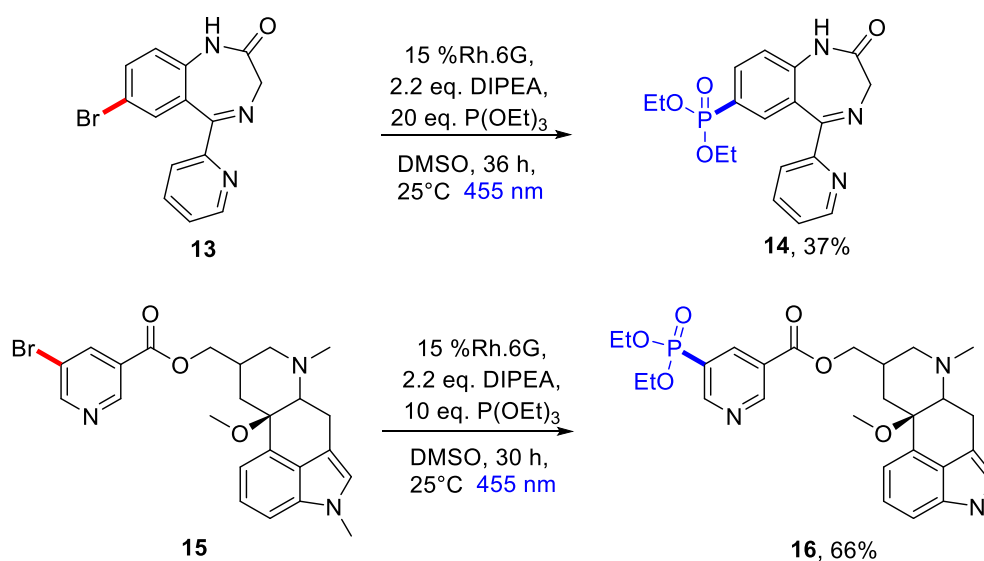
Scheme 5-3. Visible light induced phosphonylation of heteroaryl bromides: Starting material in all the cases 0.1 – 0.3 mmol, reaction time 15-33 h. [a] Yield of product with 20 eq. of trapping reagent. [b] Yield of the product with 3 eq. of the trapping reagent. [c] 15% of the Rh.6G used. For detailed information on the reaction conditions, see Chapter 5.4.3.

Next, we examined aryl chloride and aryl triflates as aryl radical precursors under the optimized conditions (Scheme 5-4). A longer reaction time was required for the conversion of *p*-chlorobenzonitrile (**10a**) to the corresponding phosphonate, because of the more negative reduction potential of the substrate.^[16, 21] The reaction with aryl chlorides and aryl triflates gave the corresponding phosphonate **12a**^c in 61% and **12a**^d in 41% yield. A triflate derivative of the natural product carvacrol (**11c**) was converted to its diethyl phosphonate analogue **12c**^d. The dimethoxy-protected uracil **10d** gave the expected product **12d** in 86% yield. This compound can be further converted to the phosphoric acid analogue of uracil.^[24]



Scheme 5-4. Scope of aryl chlorides and aryl triflates: Amount of starting material in all cases 0.1 – 0.3 mmol, reaction time 24-68 h. [a] Yield of product with 20 eq. of trapping reagent. [b] 15% of the Rh.6G used. [c] Aryl chloride as a substrate. [d] Aryl triflate as substrate. [e] Yield of product with 3 eq. of trapping reagent. For detailed information on the reaction conditions, see Chapter 5.4.3.

Encouraged by the results we applied the developed conditions to the late stage metal-free phosphonylation of pharmaceutically active molecules (Scheme 5-5). We chose Bromazepam, a benzodiazepine derivative and anti-anxiety agent and Nicergoline, an ergot alkaloid used for the treatment of metabolic vascular disorders, both containing a bromide group in the aryl ring.

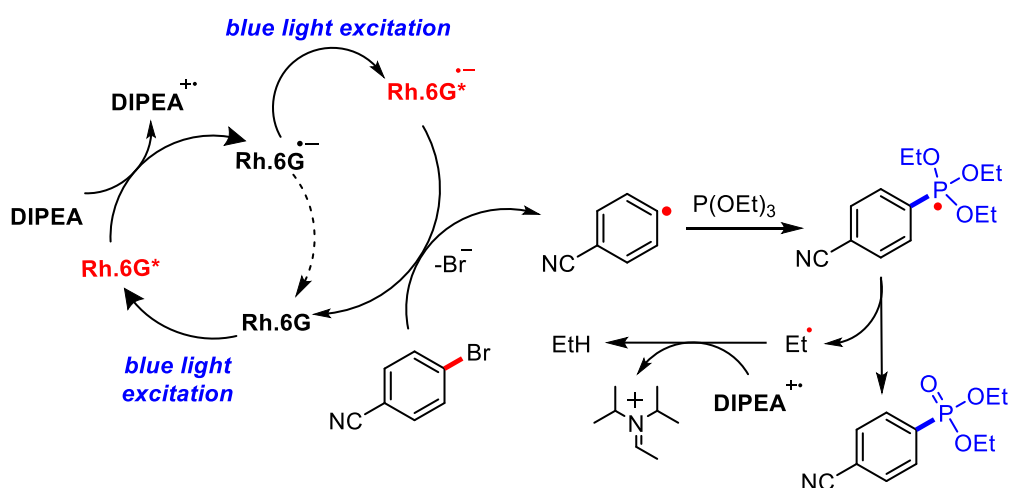


Scheme 5-5. Late stage phosphonylation of biologically active compounds.

The phosphorylation of bromazepam **13** gave the respective azepam phosphonate (**14**) in 37% isolated yield, tolerating the amide and imine functional groups. Likewise, the reaction of highly functionalized Nicergoline **15** yielded the phosphorylated product in 66%.

5.2.2 Mechanistic investigations

A proposed mechanism for the visible light induced Rh.6G catalysed photo-Arbuzov reaction is outlined in Scheme 5-6. Upon blue light photoexcitation Rh.6G photooxidizes DIPEA giving the radical anion $\text{Rh.6G}^{\bullet-}$ and the radical cation of DIPEA $^{\bullet+}$. Continuous irradiation of the radical anion $\text{Rh.6G}^{\bullet-}$ with blue light triggers a single electron transfer from the excited $\text{Rh.6G}^{\bullet-}$ [17, 19, 20] to the aryl halide producing the transient $\text{Ar-Br}^{\bullet-}$ radical anion and regenerating the neutral Rh.6G completing the catalytic cycle. Further, $\text{Ar-Br}^{\bullet-}$ undergoes fragmentation to release an aryl radical and a bromide anion; this process is in competition with a non-productive back electron transfer. The aryl radical reacts with trivalent phosphorous forming a C-P bond and the unstable phosphoranyl radical.^[25] Release of an ethyl radical and rearrangement results in the formation of the target aryl phosphonate. The reactive ethyl radical may abstract a hydrogen atom from DIPEA $^{\bullet+}$ or the solvent. In competition with the desired C-P bond forming reaction, the aryl radical can abstract a hydrogen atom from DIPEA $^{\bullet+}$ or the solvent giving the respective reduced product. This process is confirmed by the gas chromatography mass spectrometry (GS-MS) data showing the formation of diisopropylamine and the dehalogenated arenes as by-products in the reaction mixture.



Scheme 5-6. Proposed mechanism for the visible light photo-Arbuzov reaction.

5.3 Conclusion

In conclusion, we have demonstrated the metal-free visible light driven phosphorylation of aryl halides to their corresponding phosphonates. The mild reaction conditions are compatible with many functional groups and the scope of trialkyl phosphites and halogenated heteroarenes is broad providing various phosphonates with consistent yields. Furthermore, the method allows a late stage functionalization of biological active aryl halides that can be converted into the phosphoric acid analogues. We believe this new photoredox C-P bond formation via a visible light photo-Arbuzov reaction will find applications in pharmaceutical and academic research.

5.4 Experimental part

5.4.1 General Information

See Chapter 2.4.1

5.4.2 Cyclic voltammetry measurements

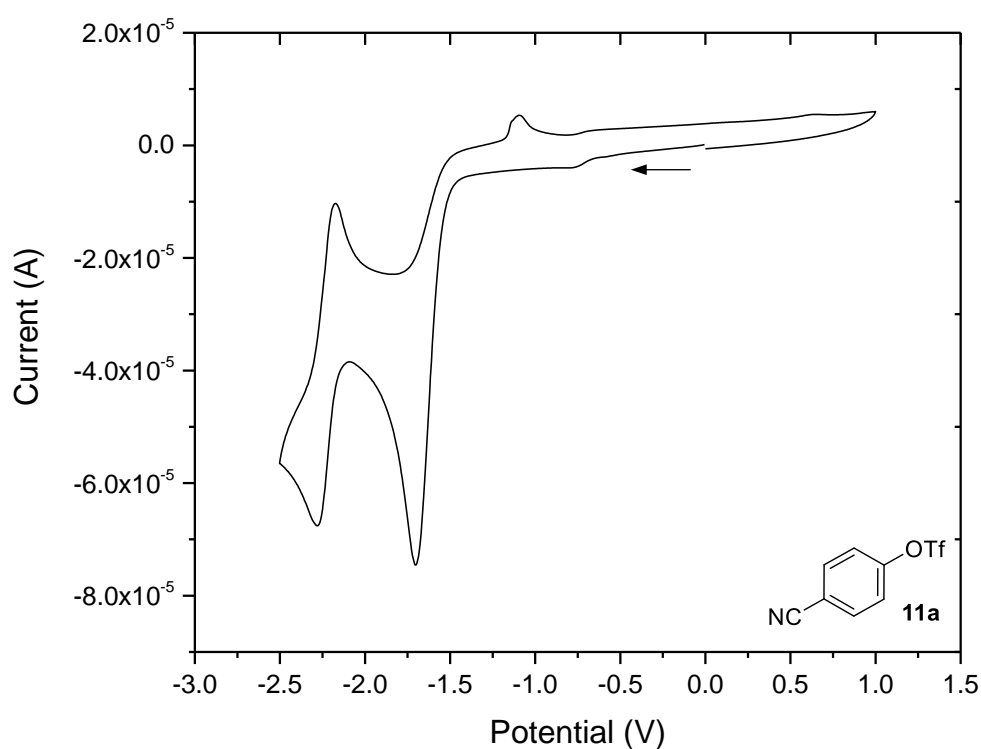


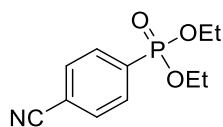
Figure 5-2 Cyclic voltammogram of 4-cyanophenyl trifluoromethanesulfonate (**11a**) in acetonitrile (0.01 M) under argon atmosphere. The irreversible reduction peak for the triflate is observed at -1.71 V. The reversible reduction of the benzonitrile moiety is observed at -2.13 V. (The arrow indicates the scan direction, starting from 0 V)

5.4.3 General experimental procedure

A 5 mL crimp vial was charged with a magnetic stirring bar, the respective aryl halide (0.1 mmol, 1 eq.) and Rh.6G (0.01 mmol, 0.1 eq.) and degassed by syringe needle. To the vial (0.3 - 2.0 mmol) trialkyl phosphite was added, degassed and refilled with N₂ (× 3). Dry DMSO (1 mL) was added *via* syringe and the reaction mixture was again degassed and refilled with N₂. DIPEA (0.22 mmol, 2.2 eq.) was added under N₂ atmosphere and the reaction mixture was irradiated through the plane bottom side of the crimp vial using a 455 nm LED at 25°C. (Note: For catalytic transformation that required 15 mol% catalyst loading, Rh.6G was added in two batches 10% and 5%) The reaction progress was monitored by GC analysis. For work up, the reaction mixture was diluted with 20 mL of distilled water and extracted with DCM (3 × 10 mL). The combined organic layers were dried over MgSO₄, filtered and concentrated in vacuum. Purification of the crude product was achieved by silica gel flash column chromatography using petrol ether/ethyl acetate (in some cases DCM/MeOH) as eluents.

5.4.4 Product characterization

Diethyl (4-cyanophenyl)phosphonate (**2a**)^[26]



According to the general procedure, 4-bromobenzonitrile (20 mg, 0.109 mmol, 1 eq.), Rh.6G (5.22 mg, 0.011 mmol, 0.1 eq.), triethyl phosphite (55 µl, 0.327 mmol, 3 eq.) and DIPEA (44 µl, 0.234 mmol, 2.2 eq.) were reacted in 1 mL of DMSO. The reaction mixture was irradiated for 17 h. Four reactions were run in parallel. After 17 h, the combined reaction mixture was subjected to the workup protocol outlined in the general procedure and purified by flash chromatography (ethyl acetate/petroleum ether) to provide the title compound as a yellowish liquid (79.7 mg, 76% yield). (Note: 74.5 mg, 71% yield was observed with 20 eq. of triethyl phosphite.)

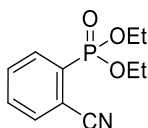
Phosphonate **2a** was prepared from 4-chlorobenzonitrile (13.8 mg, 0.1 mmol, 1 eq.), Rh.6G (4.8 mg, 0.01 mmol, 0.1 eq.), trimethyl phosphite (342.6 µl, 2.0 mmol, 20 eq) and DIPEA (37.4 µl, 0.22 mmol, 2.2 eq.) in 1 ml of DMSO. After 48 h of irradiation additional Rh.6G (2.4 mg, 0.005 mmol, 0.05 eq.) dissolved in 80 µl of DMSO was added via a glass syringe and the reaction mixture was further irradiated for 17 h. Four reactions were run in parallel. After a total reaction time of 65 h the combined reaction mixture was subjected to the workup outlined in

the general procedure and purified by flash chromatography (ethyl acetate/petroleum ether) to provide the title compound as viscous oil (53.1 mg, 61%).

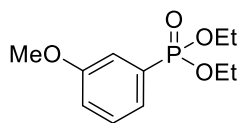
Phosphonate **2a** was synthesized from 4-cyanophenyl trifluoromethanesulfonate (25.1 mg, 0.1 mmol, 1 eq.), Rh.6G (4.8 mg, 0.01 mmol, 0.1 eq.), triethyl phosphite (51.4 μ l, 0.3 mmol, 3 eq.) and DIPEA (37.4 μ l, 0.22 mmol, 2.2 eq.) in 1 mL of DMSO. Two reactions were irradiated for 36 h in parallel. Afterwards the combined reaction mixture was subjected to the workup protocol outlined in the general procedure and purified by flash chromatography (ethyl acetate/petroleum ether) to provide the title compound as viscous oil (12.6 mg, 26%). (Note: 38.9 mg, 41% yield was observed with 20 eq. of triethyl phosphite, when four vials were irradiated in parallel for 28 h)

^1H NMR (600 MHz, CDCl_3): δ 7.92 (dd, J = 13.1 Hz, 8.3 Hz, 2H), 7.79 – 7.73 (m, 2H), 4.25 – 4.05 (m, 4H), 1.34 (t, J = 7.1 Hz, 6H). ^{13}C NMR (151 MHz, CDCl_3): δ 132.9 (d, J = 187.7 Hz), 131.2 (d, J = 9.8 Hz), 130.9 (d, J = 15.0 Hz), 116.8 (s), 115.0 (d, J = 3.5 Hz), 61.6 (d, J = 5.7 Hz), 15.3 (d, J = 6.3 Hz). ^{31}P NMR (162 MHz, CDCl_3): δ 16.0 (s). HRMS: calculated for $\text{C}_{11}\text{H}_{14}\text{NO}_3\text{P}$ [(M+H) $^+$] 240.0790; found 240.0180.

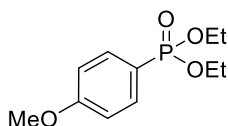
Diethyl (2-cyanophenyl)phosphonate (**2b**)^[27]



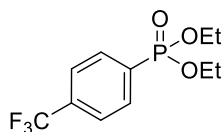
According to the general procedure, 2-bromobenzonitrile (20 mg, 0.109 mmol, 1 eq.), Rh.6G (5.22 mg, 0.0109 mmol, 0.1 eq.), triethyl phosphite (56 μ l, 0.327 mmol, 20 eq.) and DIPEA (44 μ l, 0.234 mmol, 2.2 eq.) were reacted in 1 mL of DMSO. The reaction mixture was irradiated for 17 h. Four reactions were run in parallel. After 17 h, the combined reaction mixture was worked up according to the protocol outlined in the general procedure and purified by flash chromatography (ethyl acetate/petroleum ether) to provide the title compound as a yellowish liquid (83 mg, 79% yield). (Note. 79 mg, 76% yield was observed with 20 eq. of triethyl phosphite). ^1H NMR (600 MHz, CDCl_3): δ 8.07 – 8.03 (m, 1H), 7.76 – 7.72 (m, 1H), 7.64 – 7.60 (m, 1H), 7.58 (tt, J = 7.6 Hz, 1.4 Hz, 1H), 4.25 – 4.09 (m, 4H), 1.33 – 1.29 (m, 6H). ^{13}C NMR (151 MHz, CDCl_3): δ 133.5 (d, J = 8.7 Hz), 133.4 (d, J = 11.2 Hz), 131.3 (d, J = 2.7 Hz), 131.2 (d, J = 188 Hz), 131.1 (d, J = 14.1 Hz), 116.0 (d, J = 5.9 Hz), 113.6 (d, J = 4.8 Hz), 62.1 (d, J = 5.9 Hz), 15.2 (d, J = 6.3 Hz). ^{31}P NMR (162 MHz, CDCl_3): δ 13.3 (s). HRMS: calculated for $\text{C}_{11}\text{H}_{14}\text{NO}_3\text{P}$ [(M+H) $^+$] 240.0790; found 240.0788.

Diethyl (3-methoxyphenyl)phosphonate (2c)^[28]

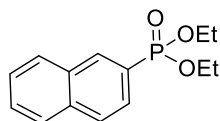
According to the general procedure, 3-bromoanisole (12.6 μ l, 0.1 mmol, 1 eq.), Rh.6G (4.8 mg, 0.01 mmol, 0.1 eq.), triethyl phosphite (342.6 μ l, 2.0 mmol, 20 eq.) and DIPEA (37.4 μ l, 0.22 mmol, 2.2 eq.) were reacted in 1 mL of DMSO. After 20 h of irradiation additional Rh.6G (2.4 mg, 0.005 mmol, 0.05 eq.) dissolved in 80 μ l DMSO was added via a glass syringe and the reaction mixture was further irradiated for 13 h. Four reactions were run in parallel. After a total reaction time of 33 h the combined reaction mixture was subjected to the workup outlined in the general procedure and purified by flash chromatography (ethyl acetate/petroleum ether) to provide the title compound as viscous oil (52.2 mg, 58%). ¹H NMR (300 MHz, CDCl₃): δ 7.42 – 7.29 (m, 3H), 7.12 – 7.03 (m, 1H), 4.23 – 3.97 (m, 4H), 3.84 (s, 3H), 1.35 – 1.29 (m, 6H). ¹³C NMR (75 MHz, CDCl₃): δ 159.4 (d, J = 18.8 Hz), 129.7 (d, J = 17.6 Hz), 129.5 (d, J = 186.7 Hz), 123.9 (d, J = 9.3 Hz), 118.8 (d, J = 3.3 Hz), 116.3 (d, J = 11.4 Hz), 62.2 (d, J = 5.3 Hz), 55.44, 16.35 (d, J = 6.6 Hz). ³¹P NMR (121 MHz, CDCl₃): δ 19.34. LRMS: calculated for C₁₁H₁₇O₄P [(M+H)⁺] 245.0943; found 245.0941.

Diethyl (4-methoxyphenyl)phosphonate (2d)^[26]

4-Bromoanisole (13.0 μ l, 0.1 mmol, 1 eq.), Rh.6G (4.8 mg, 0.01 mmol, 0.1 eq.), triethyl phosphite (51.4 μ l, 0.3 mmol, 3 eq.) and DIPEA (37.4 μ l, 0.22 mmol, 2.2 eq.) were reacted in 1 mL of DMSO according to the general procedure. Two reaction batches were irradiated for 36 h in parallel. Afterwards the combined reaction mixture was subjected to the workup protocol outlined in the general procedure and purified by flash chromatography (ethyl acetate/petroleum ether) to provide the title compound as viscous oil (26.2 mg, 54%). ¹H NMR (300 MHz, CDCl₃): δ 7.81 – 7.66 (m, 2H), 7.02 – 6.90 (m, 2H), 4.20 – 3.94 (m, 4H), 3.84 (s, 3H), 1.33 – 1.26 (m). ¹³C NMR (75 MHz, CDCl₃): δ 162.8 (d, J = 3.4 Hz), 133.7 (d, J = 11.4 Hz), 119.4 (d, J = 194.7 Hz), 114.0 (d, J = 16.1 Hz), 61.9 (d, J = 5.3 Hz), 55.3, 16.3 (d, J = 6.6 Hz). ³¹P NMR (121 MHz, CDCl₃): δ 20.4. HRMS: calculated for C₁₁H₁₇O₄P [(M+H)⁺] 245.0937; found 245.0938.

Diethyl [4-(trifluoromethyl)phenyl]phosphonate (2e)^[26]

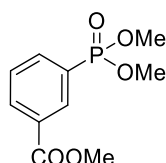
4-Bromobenzotrifluoride (25 mg, 0.11 mmol, 1 eq.), Rh.6G (5.34 mg, 0.0109 mmol, 0.1 eq.), triethyl phosphite (376 μ l, 2.2 mmol, 20 eq.) and DIPEA (44 μ l, 0.242 mmol, 2.2 eq.) were reacted in 1 mL of DMSO according to the general procedure. The reaction mixture was irradiated for 24 h. Four reactions were run in parallel. After completion, the combined reaction mixture was subjected to the workup protocol outlined in the general procedure and purified by flash chromatography (ethyl acetate/petroleum ether) to provide the title compound as a yellowish oil (34 mg, 27% yield). ¹H NMR (400 MHz, CDCl₃): δ 7.94 (dd, J = 13.0 Hz, 8.0 Hz, 1H), 7.73 (dd, J = 8.1 Hz, 3.5 Hz, 1H), 4.24 – 4.04 (m, 4H), 1.33 (t, J = 7.1 Hz, 3H). ¹³C NMR (151 MHz, CDCl₃): δ 134.0 (dd, J = 32.8 Hz, 3.3 Hz), 133.4, 132.2 (d, J = 10.2 Hz), 125.3 (dq, J = 15.5 Hz, 3.5 Hz), 123.5 (d, J = 272.8 Hz), 62.4 (d, J = 5.6 Hz), 16.3 (d, J = 6.4 Hz). ³¹P NMR (162 MHz, CDCl₃): δ 16.9 (s). ¹⁹F NMR (282 MHz, CDCl₃) δ -63.7 (s). HRMS: calculated for C₁₁H₁₄F₃O₃P [(M+H)⁺] 283.0711; found 283.0709.

Diethyl naphthalen-2-ylphosphonate (2f)^[26]

According to the general procedure, 2-bromonaphthalene (20.7 mg, 0.1 mmol, 1 eq.), Rh.6G (4.8 mg, 0.01 mmol, 0.1 eq.), triethyl phosphite (51.4 μ l, 0.3 mmol, 3 eq.) and DIPEA (37.4 μ l, 0.22 mmol, 2.2 eq.) were reacted in 1 mL of DMSO. After 24 h of irradiation additional Rh.6G (2.4 mg, 0.005 mmol, 0.05 eq.) dissolved in 80 μ l DMSO was added via a glass syringe and the reaction mixture was further irradiated for 22 h. Two reaction batches were run in parallel. After a total reaction time of 46 h the combined reaction mixture was subjected to the workup protocol outlined in the general procedure and purified by flash chromatography (ethyl acetate/petroleum ether) to provide the title compound as viscous oil (42.3 mg, 80%). (Note. 73.6 mg, 70% yield was observed with 20 eq. of triethyl phosphite. In this case Rh.6G (2.4 mg, 0.005 mmol, 0.05 eq.) dissolved in 80 μ l DMSO was added after 24 h of photoirradiation via a glass syringe and the mixture was further irradiated for 24 h. Four reactions were run in parallel with a total irradiation time of 48 h). ¹H NMR (300 MHz, CDCl₃): δ 8.56 – 8.33 (m, 1H), 7.98 – 7.83 (m, 3H), 7.81 – 7.71 (m, 1H), 7.66 – 7.51 (m, 2H), 4.32 – 3.97 (m, 4H), δ 1.33 (t, J = 7.1

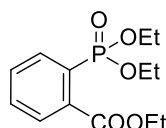
Hz, 6H). ^{13}C NMR (75 MHz, CDCl_3): δ 135 (d, $J = 2.6$ Hz), 134.1 (d, $J = 10.1$ Hz), 132.3 (d, $J = 16.7$ Hz), 128.9, 128.5, 128.3, 127.8, 126.9, 126.4 (d, $J = 9.8$ Hz), 125.3 (d, $J = 188.0$ Hz), 62.2 (d, $J = 5.3$ Hz), 16.4 (d, $J = 6.5$ Hz). ^{31}P NMR (121 MHz, CDCl_3): δ 19.7. HRMS: calculated for $\text{C}_{14}\text{H}_{17}\text{O}_3\text{P}$ [(M+H) $^+$] 265.0988; found 265.0989.

Methyl 3-(dimethoxyphosphoryl)benzoate (2g)^[29]



According to the general procedure, methyl 3-bromobenzoate (21.5 mg, 0.1 mmol, 1 eq.), Rh.6G (4.8 mg, 0.01 mmol, 0.1 eq.), trimethyl phosphite (236.3 μl , 2.0 mmol, 20 eq.) and DIPEA (37.4 μl , 0.22 mmol, 2.2 eq.) were reacted in 1 ml of DMSO. After 20 h of irradiation additional Rh.6G (2.4 mg, 0.005 mmol, 0.05 eq.) dissolved in 80 μl of DMSO was added via a glass syringe and the reaction mixture was further irradiated for 16 h. Four reactions were run in parallel. After a total reaction time of 36 h the combined reaction mixture was subjected to the workup protocol outlined in the general procedure and purified by flash chromatography (ethyl acetate/petroleum ether) to provide the title compound as viscous oil (73.8 mg, 76%). ^1H NMR (300 MHz, CDCl_3): δ 8.49 – 8.39 (m, 1H), 8.26 – 8.20 (m, 1H), 8.07 – 7.93 (m, 1H), 7.57 7.64 – 7.53 (m, 1H), 3.94 (s, 3H), 3.82 – 3.73 (m, 6H). ^{13}C NMR (75 MHz, CDCl_3): δ 166.1, 136.1 (d, $J = 10.0$ Hz), 133.6 (d, $J = 3.0$ Hz), 132.9 (d, $J = 10.8$ Hz), 130.6 (d, $J = 15.1$ Hz), 127.8 (d, $J = 190.6$ Hz), 128.8 (d, $J = 15.1$ Hz), 52.9 (d, $J = 5.6$ Hz), 52.4. ^{31}P NMR (121 MHz, CDCl_3): δ 20.6. LRMS: calculated for $\text{C}_{10}\text{H}_{13}\text{O}_5\text{P}$ [(M+H) $^+$] 245.0573; found 245.0582.

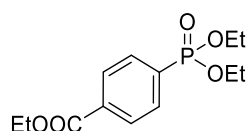
Ethyl 2-(diethoxyphosphoryl)benzoate (2h)^[30]



Ethyl 2-bromobenzoate (25 mg, 0.109 mmol, 1 eq.), Rh.6G (5.22 mg, 0.011 mmol, 0.1eq.), triethyl phosphite (55 μl , 0.327 mmol, 3 eq.) and DIPEA (44 μl , 0.242 mmol, 2.2 eq.) were reacted in 1 mL of DMSO following the general procedure. The reaction mixture was irradiated for 33h. For this reaction Rh.6G was added in two batches (10 mol% + 5 mol%), and the second batch on the Rh.6G (2.6 mg) was added after 20 h of irradiation. Four reactions were run in parallel. After 33 h, the combined reaction mixture was subjected to the workup protocol

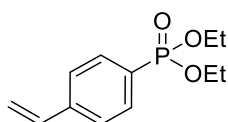
outlined in the general procedure and purified by flash chromatography (ethyl acetate/petroleum ether) to provide the title compound as a yellowish oil (81 mg, 65% yield). (Note. 78 mg, 63% yield was observed with 20 eq. of triethyl phosphite). ^1H NMR (400 MHz, CDCl_3): δ 8.04 – 7.94 (m, 1H), 7.74 – 7.69 (m, 1H), 7.62 – 7.51 (m, 2H), 4.40 (q, J = 7.2 Hz, 2H), 4.25 – 4.06 (m, 4H), 1.41 (t, J = 7.2 Hz, 3H), 1.34 (t, J = 7.1 Hz, 6H). ^{13}C NMR (151 MHz, CDCl_3): δ 168.0 (d, J = 4.8 Hz), 136.5 (d, J = 8.8 Hz), 133.9 (d, J = 8.4 Hz), 132.0 (d, J = 2.9 Hz), 130.4 (d, J = 14.0 Hz), 129.2 (d, J = 12.6 Hz), 127.3 (d, J = 186.8 Hz), 62.4 (d, J = 5.6 Hz), 61.8 (s), 16.3 (d, J = 6.6 Hz), 14.0 (s). ^{31}P NMR (162 MHz, CDCl_3): δ 16.9 (s). HRMS: calculated for $\text{C}_{13}\text{H}_{19}\text{O}_5\text{P}$ [(M+H) $^+$] 287.1048; found 287.1050.

Ethyl 4-(diethoxyphosphoryl)benzoate (2i)^[31]



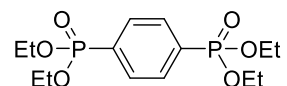
Following the general procedure, ethyl 4-bromobenzoate (25 mg, 0.109 mmol, 1 eq.), Rh.6G (5.22 mg, 0.011 mmol, 0.1 eq.), triethyl phosphite (55 μL , 0.327 mmol, 3 eq.) and DIPEA (44 μL , 0.242 mmol, 2.2 eq.) were reacted in 1 mL of DMSO. The reaction mixture was irradiated for 33 h. For this reaction Rh.6G was added in two batches (10 mol% + 5 mol%), and the second batch of Rh.6G (2.6 mg) was added after 20 h of irradiation. Four reactions were run in parallel. After 33 hours, the combined reaction mixture was subjected to the workup protocol outlined in the general procedure and purified by flash chromatography (ethyl acetate/petroleum ether) to provide the title compound as a yellowish liquid (79.3 mg, 64% yield). (Note. 94 mg, 76% yield was observed with 20 eq. of triethyl phosphite). ^1H NMR (400 MHz, CDCl_3): δ 8.14 – 8.09 (m, 2H), 7.88 (dd, J = 12.9 Hz, 8.4 Hz, 2H), 4.40 (q, J = 7.1 Hz, 2H), 4.22 – 4.03 (m, 4H), 1.40 (t, J = 7.1 Hz, 3H), 1.32 (t, J = 7.1 Hz, 6H). ^{13}C NMR (101 MHz, CDCl_3): δ 165.8 (s), 133.9 (d, J = 3.2 Hz), 133.5 (d, J = 94.8 Hz), 131.8 (d, J = 10.1 Hz), 129.4 (d, J = 15.0 Hz), 62.4 (d, J = 5.5 Hz), 61.5 (s), 16.3 (d, J = 6.4 Hz), 14.9 (s). ^{31}P NMR (162 MHz, CDCl_3): δ 17.8 (s). HRMS: calculated for $\text{C}_{13}\text{H}_{19}\text{O}_5\text{P}$ [(M+H) $^+$] 287.1048; found 287.1058.

Diethyl (4-vinylphenyl)phosphonate (2j)^[26]



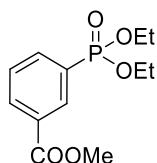
4-Bromostyrene (13.1 μ l, 0.1 mmol, 1 eq.), Rh.6G (4.8 mg, 0.01 mmol, 0.1 eq.), triethyl phosphite (51.4, 0.3 mmol, 3 eq.) and DIPEA (37.4 μ l, 0.22 mmol, 2.2 eq.) were reacted in 1 mL of DMSO following the general procedure. After 24 h of irradiation additional Rh.6G (2.4 mg, 0.005 mmol, 0.05 eq.) dissolved in 80 μ l of DMSO was added via a glass syringe and the reaction mixture was further irradiated for 22 h. Two reactions were run in parallel. After a total reaction time of 46 h the combined reaction mixture was subjected to the workup protocol outlined in the general procedure and purified by flash chromatography (ethyl acetate/petroleum ether) to provide the title compound as viscous oil (17.2 mg, 36%). (Note. 56.3 mg, 59% yield was observed with 20 eq. of triisopropyl phosphite. In this case Rh.6G (2.4 mg, 0.005 mmol, 0.05 eq.) dissolved in 80 μ l of DMSO was added after 20 h of irradiation via a glass syringe and the mixture was further irradiated for 22 h. Four reactions were run in parallel with a total irradiation time of 46 h). ^1H NMR (300 MHz, CDCl_3): δ 7.82 – 7.70 (m, 2H), 7.54 – 7.44 (m, 2H), 6.73 (dd, J = 17.6 Hz, 10.9 Hz, 1H), 5.93 – 5.78 (m, 1H) 5.38 (d, J = 10.9 Hz, 1H), 4.25 – 3.96 (m, 4H), 1.40 – 1.26 (m, 6H). ^{13}C NMR (75 MHz, CDCl_3): δ 141.4, 135.9, 132.1 (d, J = 10.2 Hz), 127.3 (d, J = 189.4 Hz), 126.2 (d, J = 15.4 Hz), 116.6, 62.1 (d, J = 5.5 Hz), 16.3 (d, J = 6.5 Hz). ^{31}P NMR (121 MHz, CDCl_3): δ 19.5. HRMS: calculated for $\text{C}_{12}\text{H}_{17}\text{O}_3\text{P}$ [(M+H) $^+$] 241.0988; found 241.0986.

Tetraethyl 1,4-phenylenebis(phosphonate) (2k)^[32]



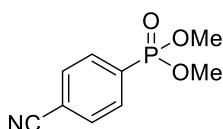
According to the general procedure, 1,4-dibromobenzene (23.6 mg, 0.1 mmol, 1 eq.), Rh.6G (4.8 mg, 0.01 mmol, 0.1 eq.), triethyl phosphite (51.4 μ l, 0.3 mmol, 3 eq.) and DIPEA (37.4 μ l, 0.22 mmol, 2.2 eq.) were reacted in 1 mL of DMSO. Two reactions were photoirradiated for 42 h in parallel. Afterwards the combined reaction mixture was subjected to the workup protocol outlined in the general procedure and purified by flash chromatography (ethyl acetate/petroleum ether) to provide the title compound as a colorless solid (22.3 mg, 32%). (Note. 65.3 mg, 47% yield was observed with 20 eq. of triethyl phosphite. In this case Rh.6G (2.4 mg, 0.005 mmol, 0.05 eq.) dissolved in 80 μ l DMSO was added after 20 h of photoirradiation via a glass syringe and the mixture further irradiated for 16 h. Four reactions were run in parallel with a total irradiation time of 36 h). ^1H NMR (300 MHz, CDCl_3): δ 7.97 – 7.84 (m, 4H), 4.24 – 4.01 (m, 8H), 1.39 – 1.28 (m, 12H). ^{13}C NMR (75 MHz, CDCl_3): δ 134.1 (d, J = 3.1 Hz), 131.8 – 131.4 (m), 63.3 – 62.3 (m), 16.5 – 16.2 (m). ^{31}P NMR (121 MHz, CDCl_3): δ 17.5. HRMS: calculated for $\text{C}_{14}\text{H}_{24}\text{O}_6\text{P}_2$ [(M+H) $^+$] 351.1121; found 351.1121.

Methyl 3-(diethoxyphosphoryl)benzoate (2l)^[33]



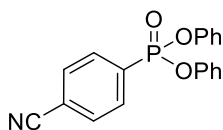
Following the general procedure, methyl 3-bromobenzoate (21.5 mg, 0.1 mmol, 1 eq.), Rh.6G (4.8 mg, 0.01 mmol, 0.1 eq.), triethyl phosphite (51.4 μ l, 0.3 mmol, 3 eq.) and DIPEA (37.4 μ l, 0.22 mmol, 2.2 eq.) were reacted in 1 mL of DMSO. Two reactions were irradiated for 36 h in parallel. Afterwards the combined reaction mixture was subjected to the workup protocol outlined in the general procedure and purified by flash chromatography (ethyl acetate/petroleum ether) to provide the title compound as viscous oil (37.1 mg, 68%). ¹H NMR (300 MHz, CDCl₃): δ 8.50 – 8.41 (m, 1H), 8.25 – 8.18 (m, 1H), 8.09 – 7.89 (m, 1H), 7.65 – 7.47 (m, 1H), 4.23 – 4.03 (m, 4H), 3.93 (s, 3H), 1.36 – 1.29 (m, 6H). ¹³C NMR (75 MHz, CDCl₃): δ 166.1, 136.0 (d, *J* = 10.1 Hz), 133.3 (d, *J* = 3.0 Hz), 132.8 (d, *J* = 11.0 Hz), 130.5 (d, *J* = 12.3 Hz), 129.2 (d, *J* = 187.2 Hz), 128.7 (d, *J* = 15.0 Hz), 62.4 (d, *J* = 5.6 Hz), 52.4, 16.3 (d, *J* = 6.5 Hz). ³¹P NMR (121 MHz, CDCl₃): δ 17.8. HRMS: calculated for C₁₂H₁₇O₅P [(M+H)⁺] 273.0886; found 273.0885.

Dimethyl (4-cyanophenyl)phosphonate (3a)^[34]



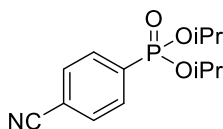
4-Bromobenzonitrile (18.2 mg, 0.1 mmol, 1 eq.), Rh.6G (4.8 mg, 0.01 mmol, 0.1 eq.), trimethyl phosphite (35.5 μ l 0.3 mmol, 3 eq.) and DIPEA (37.4 μ l, 0.22 mmol, 2.2 eq.) were reacted in 1 mL of DMSO according to the general procedure. Two reactions were irradiated in parallel for 18 h. Afterwards the combined reaction mixture was subjected to the workup protocol outlined in the general procedure and purified by flash chromatography (ethyl acetate/petroleum ether) to provide the title compound as viscous oil (33.2 mg, 79% yield). (Note. 67.8 mg, 80% yield was observed with 20 eq. of trimethyl phosphite). ¹H NMR (300 MHz, CDCl₃): δ 7.95 – 7.84 (m, 2H), 7.79 – 7.72 (m, 2H), 3.83 – 3.70 (m, 6H). ¹³C NMR (75 MHz, CDCl₃): δ 132.5, 132.4 (d, *J* = 188.5 Hz), 132.3, 132.2, 132, 117.8 (d, *J* = 1.6 Hz), 116.3 (d, *J* = 3.7 Hz), 53.1 (d, *J* = 5.7 Hz). ³¹P NMR (121 MHz, CDCl₃): δ 18.8. LRMS: calculated for C₉H₁₀NO₃P [(M+H)⁺] 212.0471; found 212.0474.

Diphenyl (4-cyanophenyl)phosphonate (4a)^[35]



4-Bromobenzonitrile (18.2 mg, 0.1 mmol, 1 eq.), Rh.6G (4.8 mg, 0.01 mmol, 0.1 eq.), triphenyl phosphite (521.5 μ l, 2.0 mmol, 20 eq.) and DIPEA (37.4 μ l, 0.22 mmol, 2.2 eq.) were reacted in 1 mL of DMSO following the general procedure. After 20 h of irradiation additional Rh.6G (2.4 mg, 0.005 mmol, 0.05 eq.) dissolved in 80 μ l of DMSO was added via a glass syringe and the reaction mixture was further irradiated for 18 h. Three reactions were run in parallel. After a total reaction time of 38 h the combined reaction mixture was subjected to the workup protocol outlined in the general procedure and purified by flash chromatography (ethyl acetate/petroleum ether) to provide the title compound as colorless oil (62.1 mg, 62%). ¹H NMR (300 MHz, CDCl₃): δ 8.14 – 8.03 (m, 2H), 7.83 – 7.76 (m, 2H), 7.36 – 7.27 (m, 4H), 7.22 – 7.14 (m, 6H). ¹³C NMR (75 MHz, CDCl₃): δ 149.9 (d, J = 7.7 Hz), 132.8 (d, J = 10.3 Hz), 132.2 (d, J = 15.8 Hz), 132.1 (d, J = 192.2 Hz), 129.9, 125.61 (d, J = 1.3 Hz), 120.5 (d, J = 4.6 Hz), 117.6 (d, J = 1.4 Hz), 116.9 (d, J = 3.7 Hz). ³¹P NMR (121 MHz, CDCl₃): δ 8.7. HRMS: calculated for C₁₉H₁₄NO₃P [(M+H)⁺] 336.0784; found 336.0782.

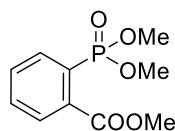
Diisopropyl (4-cyanophenyl)phosphonate (5a)^[35]



4-Bromobenzonitrile (18.2 mg, 0.1 mmol, 1 eq.), Rh.6G (4.8 mg, 0.01 mmol, 0.1 eq.), triisopropyl phosphite (68.4, 0.3 mmol, 3 eq.) and DIPEA (37.4 μ l, 0.22 mmol, 2.2 eq.) were reacted in 1 mL of MeCN following the general procedure. Two reactions were irradiated in parallel for 18 h. Afterwards the combined reaction mixture was subjected to the workup protocol outlined in the general procedure and purified by flash chromatography (ethyl acetate/petroleum ether) to provide the title compound as a yellowish liquid (42.3 mg, 80%). (Note. 78.9 mg, 74% yield was observed with 20 eq. of triisopropyl phosphite in DMF. In this case Rh.6G (2.4 mg, 0.005 mmol, 0.05 eq.) dissolved in 80 μ l of DMF was added after 20 h of irradiation via a glass syringe and the mixture was further irradiated for 3 h. Four reactions were run in parallel with a total irradiation time of 23 h). ¹H NMR (300 MHz, CDCl₃): δ 7.98 – 7.87 (m, 2H), 7.77 – 7.69 (m, 2H), 4.83 – 4.66 (m, 2H), 1.38 (d, J = 6.2 Hz, 6H), 1.23 (d, J = 6.2 Hz, 6H). ¹³C NMR (75 MHz, CDCl₃): δ 135.5 (d, J = 188.2 Hz), 132.2, 132.1, 132.0, 131.8, 117.9, 115.7 (d, J = 3.6 Hz), 71.6 (d, J = 5.8 Hz), 24.1 (d, J = 4.1 Hz), 23.8 (d, J = 4.8 Hz). ³¹P

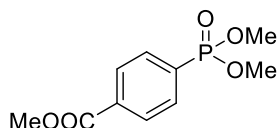
NMR (121 MHz, CDCl₃): δ 13.7. HRMS: calculated for C₁₃H₁₈NO₃P [(M+H)⁺] 268.1097; found 268.1096.

Methyl 2-(dimethoxyphosphoryl)benzoate (3h)



Methyl 2-bromobenzoate (21.5 mg, 14.0 μ l, 0.1 mmol, 1 eq.), Rh.6G (4.8 mg, 0.01 mmol, 0.1 eq.), trimethyl phosphite (236.3 μ l, 2.0 mmol, 20 eq.) and DIPEA (37.4 μ l, 0.22 mmol, 2.2 eq.) were reacted in 1 mL of DMSO according to the general procedure. After 20 h of irradiation additional Rh.6G (2.4 mg, 0.005 mmol, 0.05 eq.) dissolved in 80 μ l of DMSO was added via a glass syringe and the reaction mixture was further irradiated for 16 h. Four reactions were run in parallel. After a total reaction time of 36 h the combined reaction mixture was subjected to the workup protocol outlined in the general procedure and purified by flash chromatography (ethyl acetate/petroleum ether) to provide the title compound as viscous oil (71.7 mg, 73%). ¹H NMR (300 MHz, CDCl₃): δ 8.00 – 7.89 (m, 1H), 7.79 – 7.70 (m, 1H), 7.65 – 7.52 (m, 2H), 3.94 (d, *J* = 0.5 Hz, 3H), 3.82 – 3.78 (m, 6H). ¹³C NMR (75 MHz, CDCl₃): δ 168.1 (d, *J* = 4.8 Hz), 136.1 (d, *J* = 8.8 Hz), 133.9 (d, *J* = 8.2 Hz), 132.3 (d, *J* = 2.9 Hz), 130.8 (d, *J* = 14.0 Hz), 129.4 (d, *J* = 12.6 Hz), 126.4 (d, *J* = 188.6 Hz), 53.2 (d, *J* = 5.8 Hz), 52.8. ³¹P NMR (121 MHz, CDCl₃): δ 19.7. HRMS: calculated for C₁₀H₁₃O₅P [(M+H)⁺] 245.0573; found 245.0578.

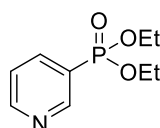
Methyl 4-(dimethoxyphosphoryl)benzoate (3i)^[36]



Methyl 4-bromobenzoate (21.5 mg, 0.1 mmol, 1 eq.), Rh.6G (4.8 mg, 0.01 mmol, 0.1 eq.), trimethyl phosphite (35.5 μ l 0.3 mmol, 3 eq.) and DIPEA (37.4 μ l, 0.22 mmol, 2.2 eq.) were reacted in 1 mL of DMSO following the general procedure. Two reactions were irradiated in parallel for 36 h. Afterwards the combined reaction mixture was subjected to the workup protocol outlined in the general procedure and purified by flash chromatography (ethyl acetate/petroleum ether) to provide the title compound as viscous oil (28.8 mg, 59% yield). (Note. 76.3 mg, 78% yield was observed with 20 eq. of trimethyl phosphite. In this case

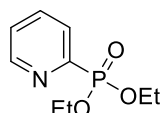
additional 5 mol% of Rh.6G were dissolved in 80 μ l of DMSO and added after 20 h of irradiation. Four reactions were run in parallel with a total irradiation time of 36 h). ^1H NMR (300 MHz, CDCl_3): δ 8.20 – 8.07 (m, 2H), 7.95 – 7.79 (m, 2H), 3.94 (s, 3H), 3.78 (d, J = 11.1 Hz, 6H). ^{13}C NMR (75 MHz, CDCl_3): δ 166.2, 133.7 (d, J = 3.3 Hz), 131.9 (d, J = 10.1 Hz), 131.7 (d, J = 187.3 Hz), 129.5 (d, J = 15.1 Hz), 52.9 (d, J = 5.6 Hz), 52.5. ^{31}P NMR (121 MHz, CDCl_3): δ 20.5. LRMS: calculated for $\text{C}_{10}\text{H}_{13}\text{O}_5\text{P}$ [(M+H) $^+$] 245.0573; found 245.0577.

Diethyl pyridin-3-ylphosphonate (7a)^[31]



According to the general procedure, 3-bromopyridine (20 mg, 0.126 mmol, 1 eq.), Rh.6G (6.06 mg, 0.012 mmol, 0.1 eq.), triethyl phosphite (65 μ l, 0.378 mmol, 3 eq.) and DIPEA (51 μ l, 0.277 mmol, 2.2 eq.) were reacted in 1 mL of DMSO. The reaction mixture was irradiated for 18 h. Four reactions were run in parallel. After completion of the reaction, the combined reaction mixture was subjected to the workup protocol outlined in the general procedure and purified by flash chromatography (DCM/MeOH) to provide the title compound as a yellowish oil (80 mg, 74% yield). (Note. 81 mg, 75% yield was observed with 20 eq. of triethyl phosphite). ^1H NMR (400 MHz, CDCl_3): δ 8.97 (d, J = 6.4 Hz, 1H), 8.80 – 8.75 (m, 1H), 8.17 – 8.08 (m, 1H), 7.46 – 7.39 (m, 1H), 4.25 – 4.07 (m, 4H), 1.34 (t, J = 7.1 Hz, 6H). ^{13}C NMR (151 MHz, CDCl_3): δ 152.5 (s), 151.8 (d, J = 12.3 Hz), 139.8 (d, J = 8.2 Hz), 125.2 (d, J = 189.3 Hz), 123.5 (d, J = 11.5 Hz), 62.6 (d, J = 5.6 Hz), 16.3 (d, J = 6.4 Hz). ^{31}P NMR (162 MHz, CDCl_3): δ 16.1 (s). HRMS: calculated for $\text{C}_9\text{H}_{14}\text{NO}_3\text{P}$ [(M+H) $^+$] 216.0790; found 216.0810.

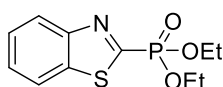
Diethyl pyridin-2-ylphosphonate (7b)^[37]



According to the general procedure, 2-bromopyridine (20 mg, 0.126 mmol, 1 eq.), Rh.6G (6.06 mg, 0.012 mmol, 0.1 eq.), triethyl phosphite (65 μ l, 0.378 mmol, 3 eq.) and DIPEA (51 μ l, 0.277 mmol, 2.2 eq.) were reacted in 1 mL of DMSO. The reaction mixture was irradiated for 18 h. Four reactions were run in parallel. After completion of the reaction, the combined reaction mixture was subjected to the workup protocol outlined in the general procedure and purified by flash chromatography (DCM/MeOH) to provide the title compound as a yellowish

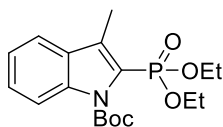
liquid (84 mg, 78% yield). (Note. 85 mg, 78% yield was observed with 20 eq. of triethyl phosphite). ^1H NMR (400 MHz, CDCl_3): δ 8.80 (d, J = 4.6 Hz, 1H), 7.97 (t, J = 7.2 Hz, 1H), 7.80 (m, 1H), 7.45 – 7.39 (m, 1H), 4.31 – 4.14 (m, 4H), 1.34 (t, J = 7.1 Hz, 6H). ^{13}C NMR (101 MHz, CDCl_3): δ 151.9 (d, J = 226.8 Hz), 150.5 (d, J = 22.8 Hz), 136.1 (d, J = 12.3 Hz), 128.2 (d, J = 25.2 Hz), 126.0 (d, J = 4.0 Hz), 63.0 (d, J = 6.0 Hz), 16.4 (d, J = 6.1 Hz). ^{31}P NMR (162 MHz, CDCl_3): δ 11.4 (s). HRMS: calculated for $\text{C}_9\text{H}_{14}\text{NO}_3\text{P}$ $[(\text{M}+\text{H})^+]$ 216.0790; found 216.0799.

Diethyl benzo[d]thiazol-2-ylphosphonate (7c)^[38]



According to the general procedure, 2-bromobenzothiazole (25 mg, 0.116 mmol, 1 eq.), Rh.6G (5.59 mg, 0.011 mmol, 0.1 eq.), triethyl phosphite (60 μL , 0.348 mmol, 3 eq.) and DIPEA (47 μL , 0.255 mmol, 2.2 eq.) were reacted in 1 mL of DMSO. The reaction mixture was irradiated for 18 h. Four reactions were run in parallel. After completion of the reaction, the combined reaction mixture was subjected to the workup protocol outlined in the general procedure and purified by flash chromatography (ethyl acetate/petroleum ether) to provide the title compound as a yellowish liquid (87 mg, 69% yield). (Note. 57 mg, 45% yield was observed with 20 eq. of triethyl phosphite). ^1H NMR (600 MHz, CDCl_3): δ 8.25 (d, J = 8.2 Hz, 1H), 8.01 (d, J = 7.9 Hz, 1H), 7.60 – 7.56 (m, 1H), 7.54 – 7.51 (m, 1H), 4.39 – 4.26 (m, 4H), 1.40 (t, J = 7.0 Hz, 6H). ^{13}C NMR (151 MHz, CDCl_3): δ 160.0 (d, J = 238.7 Hz), 154.6 (d, J = 28.4 Hz), 136.43 (s), 127.0 (s), 126.84 (s), 124.9 (s), 121.9 (d, J = 1.4 Hz), 64.1 (d, J = 5.8 Hz), 16.3 (d, J = 6.3 Hz). ^{31}P NMR (162 MHz, CDCl_3): δ 4.7 (s). HRMS: calculated for $\text{C}_{11}\text{H}_{14}\text{NO}_3\text{PS}$ $[(\text{M}+\text{H})^+]$ 272.0510; found 272.0519.

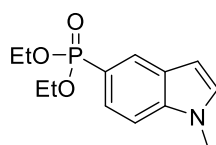
tert-Butyl 2-(diethoxyphosphoryl)-3-methyl-1*H*-indole-1-carboxylate (7d)



According to the general procedure, *N*-boc-2-bromo-3-methylindole (50 mg, 0.16 mmol, 1 eq.), Rh.6G (4.64 mg, 0.016 mmol, 0.1 eq.), triethyl phosphite (82 μL , 0.48 mmol, 3 eq.) and DIPEA (64 μL , 0.35 mmol, 2.2 eq.) were reacted in 1 mL of DMSO. The reaction mixture was irradiated for 33 h. Rh.6G was added in two batches (10 mol% + 5 mol%), and the second batch of

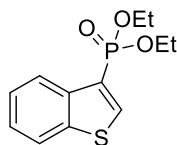
Rh.6G (3.8 mg) was added after 20 h of irradiation. After 33 h, the combined reaction mixture was subjected to the workup protocol outlined in the general procedure and purified by flash chromatography (ethyl acetate/petroleum ether) to provide the title compound as a yellowish oil (20 mg, 34% yield). (Note. 41 mg, 70% yield was observed with 20 eq. of triethyl phosphite). ^1H NMR (400 MHz, CDCl_3): δ 8.07 (d, J = 8.5 Hz, 1H), 7.60 (d, J = 7.9 Hz, 1H), 7.41 (t, J = 7.8 Hz, 1H), 7.30 – 7.24 (m, 1H), 4.27 – 4.08 (m, 4H), 2.59 (d, J = 2.2 Hz, 3H), 1.69 (s, 9H), 1.35 (t, J = 7.1 Hz, 6H). ^{13}C NMR (101 MHz, CDCl_3): δ 149.8 (s), 137.9 (d, J = 8.8 Hz), 131.9 (d, J = 16.9 Hz), 129.8 (d, J = 16.9 Hz), 127.2 (s), 122.6 (s), 122.3 (d, J = 214 Hz), 120.0 (s), 115.2 (d, J = 1.8 Hz), 84.8 (s), 62.3 (d, J = 5.5 Hz), 28.0 (s), 16.3 (d, J = 6.9 Hz), 10.9 (s). ^{31}P NMR (162 MHz, CDCl_3): δ 10.2 (s). HRMS: calculated for $\text{C}_{18}\text{H}_{26}\text{NO}_5\text{P}$ $[(\text{M}+\text{H})^+]$ 368.1627; found 368.1630.

Diethyl (1-methyl-1H-indol-5-yl)phosphonate (7e)



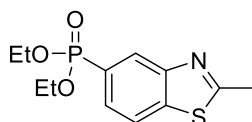
According to the general procedure, 5-bromo-1-methylindole (25 mg, 0.119 mmol, 1 eq.), Rh.6G (5.7 mg, 0.0119 mmol, 0.1 eq.), triethyl phosphite (61 μL , 0.357 mmol, 3 eq.) and DIPEA (48 μL , 0.26 mmol, 2.2 eq.) were reacted in 1 mL of DMSO. The reaction mixture was irradiated for 33 h. Rh.6G was added in two batches (10 mol% + 5 mol%), and the second batch of Rh.6G (2.8 mg) was added after 20 h of irradiation. Four reactions were run in parallel. After 33 h, the combined reaction mixture was subjected to the workup protocol outlined in the general procedure and purified by flash chromatography (ethyl acetate/petroleum ether) to provide the title compound as a yellowish oil (129 mg, 74% yield). (Note. 43 mg, 68% yield was observed with 20 eq. of triethyl phosphite). ^1H NMR (400 MHz, CDCl_3): δ 8.16 (d, J = 14.4 Hz, 1H), 7.63 (ddd, J = 12.0 Hz, 8.5 Hz, 1.3 Hz, 1H), 7.39 (dd, J = 8.5 Hz, 3.3 Hz, 1H), 7.13 (d, J = 3.1 Hz, 1H), 6.57 (dd, J = 3.1 Hz, 0.6 Hz, 1H), 4.20 – 3.98 (m, 4H), 3.82 (s, 3H), 1.31 (t, J = 7.1 Hz, 6H). ^{13}C NMR (101 MHz, CDCl_3): δ 138.6 (s), 130.2 (s), 128.1 (d, J = 17.9 Hz), 126.4 (d, J = 11.3 Hz), 124.4 (d, J = 12.1 Hz), 117.6 (d, J = 190.6 Hz), 109.4 (d, J = 16.7 Hz), 102.2 (d, J = 1.5 Hz), 61.8 (d, J = 5.1 Hz), 33.0 (s), 16.4 (d, J = 6.7 Hz). ^{31}P NMR (162 MHz, CDCl_3): δ 22.9 (s). HRMS: calculated for $\text{C}_{18}\text{H}_{26}\text{NO}_5\text{P}$ $[(\text{M}+\text{H})^+]$ 268.1103; found 268.1104.

Diethyl benzo[b]thiophen-3-ylphosphonate (7f)



According to the general procedure, 3-bromothiophene (35 mg, 0.164 mmol, 1 eq.), Rh.6G (7.87 mg, 0.016 mmol, 0.1 eq.), triethyl phosphite (84 μ l, 0.492 mmol, 3 eq.) and DIPEA (66 μ l, 0.36 mmol, 2.2 eq.) were reacted in 1 mL of DMSO. The reaction mixture was irradiated for 33 h. Rh.6G was added in two batches (10 mol% + 5 mol%), and the second batch of Rh.6G (3.9 mg) was added after 20 h of irradiation. After 33 hours, the reaction mixture was subjected to the workup protocol outlined in the general procedure and purified by flash chromatography (ethyl acetate/petroleum ether) to provide the title compound as a yellowish oil (25 mg, 57 % yield). (Note. 22 mg, 52% yield was observed with 20 eq. of triethyl phosphite). ^1H NMR (400 MHz, CDCl_3): δ 8.24 (d, J = 9.6 Hz, 1H), 8.14 (d, J = 7.7 Hz, 1H), 7.97 – 7.86 (m, 1H), 7.50 – 7.37 (m, 2H), 4.26 – 4.02 (m, 4H), 1.31 (t, J = 7.1 Hz, 6H). ^{13}C NMR (101 MHz, CDCl_3): δ 140.8 (d, J = 17.3 Hz), 139.3 (d, J = 17.4 Hz), 138.2 (d, J = 16.1 Hz), 125.2 (s), 125.1 (s), 124.7 (d, J = 202 Hz), 124.1 (s), 122.6 (s), 62.9 (d, J = 5.1 Hz), 16.4 (d, J = 6.7 Hz). ^{31}P NMR (162 MHz, CDCl_3): δ 12.9 (s). HRMS: calculated for $\text{C}_{12}\text{H}_{15}\text{O}_3\text{PS}$ [(M+H) $^+$] 271.0558; found 271.0565.

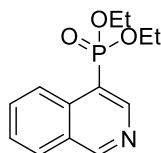
Diethyl (2-methylbenzo[d]thiazol-5-yl)phosphonate (7g)^[31]



According to the general procedure, 5-bromo-2-methylbenzothiazole (35 mg, 0.152 mmol, 1 eq.), Rh.6G (7.18 mg, 0.015 mmol, 0.1 eq.), triethyl phosphite (78 μ l, 0.460 mmol, 3 eq.) and DIPEA (61 μ l, 0.33 mmol, 2.2 eq.) were reacted in 1 mL of DMSO. The reaction mixture was irradiated for 33 h. Rh.6G was added in two batches (10 mol% + 5 mol%), and the second batch of Rh.6G (3.6 mg) was added after 20 h of irradiation. After 33 h, the reaction mixture was subjected to the workup protocol outlined in the general procedure and purified by flash chromatography (ethyl acetate/petroleum ether) to provide the title compound as a yellowish oil (41 mg, 95 % yield). (Note. 37 mg, 85% yield was observed with 20 eq. of triethyl phosphite). ^1H NMR (400 MHz, CDCl_3): δ 8.36 (d, J = 14.6, 1H), 7.88 – 7.94 (m, 1H), 7.81 – 7.72 (m, 1H), 4.24 – 4.00 (m, 4H), 2.85 (s, 3H), 1.31 (t, J = 7.0 Hz, 6H). ^{13}C NMR (101 MHz, CDCl_3): δ 168.4, 153.0 (d, J = 19.5 Hz), 140.1 (d, J = 3.4 Hz), 127.2 (d, J = 11.2 Hz), 126.1 (d, J = 191.9 Hz), 126.1 (d, J = 10.4 Hz), 121.8 (d, J = 17.0 Hz), 62.3 (d, J = 5.4 Hz), 20.2, 16.3 (d, J = 6.5 Hz).

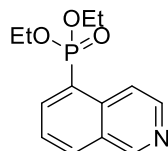
^{31}P NMR (162 MHz, CDCl_3): δ 19.1 (s). HRMS: calculated for $\text{C}_{12}\text{H}_{16}\text{NO}_3\text{PS}$ $[(\text{M}+\text{H})^+]$ 286.0667; found 286.0669.

Diethyl isoquinolin-4-ylphosphonate (7h)



According to the general procedure, 4-bromoisoquinoline (20 mg, 0.094 mmol, 1 eq.), Rh.6G (4.4 mg, 0.009, 0.1 eq.), triethyl phosphite (319 μL , 1.92 mmol, 20 eq.) and DIPEA (39 μL , 0.21 mmol, 2.2 eq.) were reacted in 1 mL of DMSO. The reaction mixture was irradiated for 33 h. Rh.6G was added in two batches (10 mol% + 5 mol%), and the second batch of Rh.6G (2.3 mg) was added after 20 h of irradiation. After 33 h, the reaction mixture was subjected to the workup protocol outlined in the general procedure and purified by flash chromatography (DCM/MeOH) to provide the title compound as a yellowish oil (24 mg, 94 % yield). ^1H NMR (300 MHz, CDCl_3): δ 9.39 (s, 1H), 9.06 (d, J = 9.4 Hz, 1H), 8.48 (d, J = 8.5 Hz, 1H), 8.08 – 8.00 (m, 1H), 7.88 – 7.78 (m, 1H), 7.73 – 7.64 (m, 1H), 4.31 – 4.06 (m, 4H), 1.33 (t, J = 7.1 Hz, 6H). ^{13}C NMR (101 MHz, CDCl_3): δ 157.2 (d, J = 2.4 Hz), 149.0 (d, J = 12.2 Hz), 135.2 (d, J = 9.3 Hz), 132.0, 128.6 (d, J = 1.7 Hz), 128.2 (d, J = 9.9 Hz), 128.0, 125.8 (d, J = 4.1 Hz), 118.8 (d, J = 184.2 Hz), 62.6 (d, J = 5.5 Hz), 16.3 (d, J = 6.4 Hz). ^{31}P NMR (121 MHz, CDCl_3): δ 17.3 (s). HRMS: calculated for $\text{C}_{13}\text{H}_{16}\text{NO}_3\text{P}$ $[(\text{M}+\text{H})^+]$ 266.0946; found 266.0946.

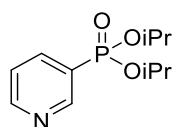
Diethyl isoquinolin-5-ylphosphonate (7i)



According to the general procedure, 5-bromoisoquinoline (20 mg, 0.096 mmol, 1 eq.), Rh.6G (4.4 mg, 0.009 mmol, 0.1 eq.), triethyl phosphite (319 μL , 1.92 mmol, 20 eq.) and DIPEA (39 μL , 0.21 mmol, 2.2 eq.) were reacted in 1 mL of DMSO. The reaction mixture was irradiated for 33 h. Rh.6G was added in two batches (10 mol% + 5 mol%), and the second batch of Rh.6G (2.3 mg) was added after 20 h of irradiation. After 33 h, the reaction mixture was subjected to the workup protocol outlined in the general procedure and purified by flash chromatography (DCM/MeOH) to provide the title compound as a yellowish oil (23 mg, 92% yield). ^1H NMR

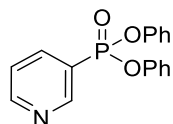
(400 MHz, CDCl₃): δ 9.34 (s, 1H), 8.64 (d, J = 6.1 Hz, 1H), 8.45 (ddd, J = 15.9 Hz, 7.1 Hz, 1.3 Hz, 1H), 8.34 (d, J = 6.1 Hz, 1H), 8.20 (d, J = 8.2 Hz, 1H), 7.71 (ddd, J = 8.3 Hz, 7.1 Hz, 3.2 Hz, 1H), 4.31 – 4.03 (m, 4H), 1.32 (t, J = 7.1 Hz, 6H). ¹³C NMR (101 MHz, CDCl₃): δ 152.6 (s), 143.6 (s), 138.7 (d, J = 9.1 Hz), 135.8 (d, J = 10.8 Hz), 133.1 (d, J = 3.4 Hz), 126.4 (d, J = 15.9 Hz), 125.6 (s), 123.8 (d, J = 185.8 Hz), 119.7 (s), 62.5 (d, J = 5.5 Hz), 16.4 (d, J = 6.4 Hz). ³¹P NMR (162 MHz, CDCl₃): δ 17.5 (s). HRMS: calculated for C₁₃H₁₆NO₃P [(M+H)⁺] 266.0946; found 266.0948.

Diisopropyl pyridin-3-ylphosphonate (8a)^[35]



3-Bromopyridine (9.8 μ l, 0.1 mmol, 1 eq.), Rh.6G (4.8 mg, 0.01 mmol, 0.1 eq.), triisopropyl phosphite (455.7 μ l, 2.0 mmol, 20 eq.) and DIPEA (37.4 μ l, 0.22 mmol, 2.2 eq.) were reacted in 1 mL of MeCN following the general procedure. Three reactions were irradiated in parallel for 18 h. The combined reaction mixture was subjected to the workup protocol outlined in the general procedure and purified by flash chromatography (ethyl acetate/petroleum ether) to provide the title compound as viscous oil (49.0 mg, 50% yield). ¹H NMR (400 MHz, CDCl₃): δ 9.02 – 8.91 (m, 1H), 8.77 – 8.69 (m, 1H), 8.16 – 8.02 (m, 1H), 7.43 – 7.33 (m, 1H), 4.84 – 4.64 (m, 2H), 1.37 (d, J = 6.2 Hz, 6H), 1.24 (d, J = 6.2 Hz, 6H). ¹³C NMR (75 MHz, CDCl₃): δ 152.6 (d, J = 1.8 Hz), 152.2 (d, J = 12.1 Hz), 139.4 (d, J = 8.2 Hz), 126.4 (d, J = 189.8 Hz), 123.3 (d, J = 11.6 Hz), 71.4 (d, J = 5.8 Hz), 24.1 (d, J = 4.1 Hz), 23.9 (d, J = 4.8 Hz). ³¹P NMR (121 MHz, CDCl₃): δ 14.1. HRMS: calculated for C₁₁H₁₈NO₃P [(M+H)⁺] 244.1097; found 244.1098.

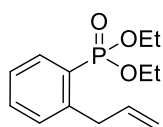
Diphenyl pyridin-3-ylphosphonate (9a)



3-Bromopyridine (9.8 μ l, 0.1 mmol, 1 eq.), Rh.6G (4.8 mg, 0.01 mmol, 0.1 eq.), triphenyl phosphite (521.5 μ l, 2.0 mmol, 20 eq.) and DIPEA (37.4 μ l, 0.22 mmol, 2.2 eq.) were reacted in 1 mL of DMSO according to the general procedure. After 22 h of irradiation additional Rh.6G (2.4 mg, 0.005 mmol, 0.05 eq.) dissolved in 80 μ l of DMSO was added via a glass syringe and the reaction mixture was further irradiated for 18 h. Four reactions were run in parallel. After a

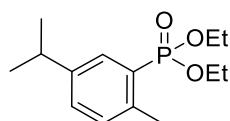
total reaction time of 38 h the combined reaction mixture was subjected to the workup protocol outlined in the general procedure and purified by flash chromatography (ethyl acetate/petroleum ether) to provide the title compound as pale white solid (39.1 mg, 31%). ^1H NMR (300 MHz, CDCl_3): δ 9.19 – 9.10 (m, 1H), 8.87 – 8.79 (m, 1H), 8.33 – 8.17 (m, 1H), 7.52 – 7.39 (m, 1H), 7.38 – 7.26 (m, 4H), 7.25 – 7.12 (m, 6H). ^{13}C NMR (75 MHz, CDCl_3): δ 153.7 (d, J = 1.7 Hz), 152.6 (d, J = 12.6 Hz), 149.9 (dd, J = 7.7, 5.0 Hz), 140.0 (d, J = 8.7 Hz), 132.8 (d, J = 10.3 Hz), 132.2 (d, J = 15.8 Hz), 129.9 (d, J = 2.0 Hz), 125.6 (dd, J = 6.0, 1.3 Hz), 123.5 (d, J = 12.0 Hz), 120.5 (t, J = 5.1 Hz). ^{31}P NMR (121 MHz, CDCl_3): δ 9.1. HRMS: calculated for $\text{C}_{17}\text{H}_{14}\text{NO}_3\text{P}$ [(M+H) $^+$] 312.0784; found 312.0780.

Diethyl (2-allylphenyl)phosphonate (12b)



According to the general procedure, 2-allylphenyl trifluoromethanesulfonate (25.4 mg, 0.1 mmol, 1 eq.), Rh.6G (4.8 mg, 0.01 mmol, 0.1 eq.), triethyl phosphite (51.4 μL , 0.3 mmol, 3 eq.) and DIPEA (37.4 μL , 0.22 mmol, 2.2 eq.) were reacted in 1 mL of DMSO. Two reactions were irradiated for 48 h in parallel. Afterwards the combined reaction mixture was subjected to the workup protocol outlined in the general procedure and purified by flash chromatography (ethyl acetate/petroleum ether) to provide the title compound as a yellowish viscous oil (18.6 mg, 37%). ^1H NMR (300 MHz, CDCl_3): δ 7.98 – 7.88 (m, 1H), 7.52 – 7.44 (m, 1H), 7.37 – 7.27 (m, 2H), 6.08 – 5.91 (m, 1H), 5.15 – 5.02 (m, 2H), 4.23 – 4.00 (m, 4H), 3.74 (dd, J = 6.6, 1.5 Hz, 2H), 1.33 (t, J = 7.1 Hz, 6H). ^{13}C NMR (75 MHz, CDCl_3): δ 143.8 (d, J = 10.7 Hz), 137.0, 134.0 (d, J = 10.3 Hz), 132.5 (d, J = 2.9 Hz), 130.4 (d, J = 14.7 Hz), 126.6 (d, J = 183.9 Hz), 125.8 (d, J = 14.6 Hz), 116.2, 62.0 (d, J = 5.5 Hz), 38.2, 16.3. ^{31}P NMR (121 MHz, CDCl_3): δ 19.2. HRMS: calculated for $\text{C}_{13}\text{H}_{19}\text{O}_3\text{P}$ [(M+H) $^+$] 255.1145; found 255.1144.

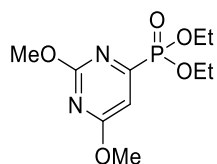
Diethyl (5-isopropyl-2-methylphenyl)phosphonate (12c)



According to the general procedure, 5-isopropyl-2-methylphenyl trifluoromethanesulfonate (28.2 mg, 0.1 mmol, 1 eq.), Rh.6G (4.8 mg, 0.01 mmol, 0.1 eq.), triethyl phosphite (51.4 μL , 0.3 mmol, 3 eq.) and DIPEA (37.4 μL , 0.22 mmol, 2.2 eq.) were reacted in 1 mL of DMSO. Two

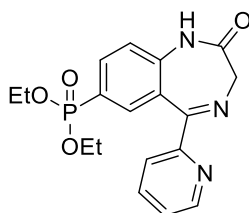
reactions were irradiated for 48 h in parallel. Afterwards the combined reaction mixture was subjected to the workup protocol outlined in the general procedure and purified by flash chromatography (ethyl acetate/petroleum ether) to provide the title compound as colorless viscous oil (13.7 mg, 25%). ^1H NMR (400 MHz, CDCl_3): δ 7.81 – 7.74 (m, 1H), 7.32 – 7.27 (m, 1H), 7.20 – 7.15 (m, 1H), 4.21 – 4.02 (m, 4H), 2.97 – 2.85 (m, 1H), 2.54 – 2.50 (m, 3H), 1.33 (t, J = 7.1 Hz, 6H), 1.24 (d, J = 6.9 Hz, 6H). ^{13}C NMR (101 MHz, CDCl_3): δ 146 (d, J = 14.1 Hz), 139 (d, J = 10.0 Hz), 132.2 (d, J = 10.7 Hz), 131.2 (d, J = 15.7 Hz), 130.5 (d, J = 3.1 Hz), 126.5 (d, J = 182.6 Hz), 61.8 (d, J = 5.4 Hz), 33.6, 23.9, 20.7 (d, J = 3.5 Hz), 16.3 (d, J = 6.7 Hz). ^{31}P NMR (162 MHz, CDCl_3): δ 20.9. HRMS: calculated for $\text{C}_{14}\text{H}_{23}\text{O}_3\text{P}$ 271.1458; found 271.1463.

Diethyl (2,6-dimethoxypyrimidin-4-yl)phosphonate (12f)



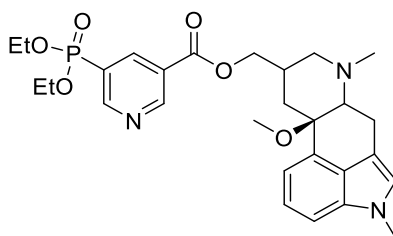
According to the general procedure, 4-chloro-2,6-dimethoxypyrimidine (20 mg, 0.114 mmol, 1 eq.), Rh.6G (5.46 mg, 0.011 mmol, 0.1 eq.), triethyl phosphite (389 μL , 2.29 mmol, 20 eq.) and DIPEA (46 μL , 0.25 mmol, 2.2 eq.) were reacted in 1 mL of DMSO. The reaction mixture was irradiated for 33 h. Rh.6G was added in two batches (10 mol% + 5 mol%), and the second batch of Rh.6G (2.7 mg) was added after 20 h of irradiation. Five reactions were run in parallel. After 33 h, the reaction mixture was subjected to the workup protocol outlined in the general procedure and purified by flash chromatography (ethyl acetate/petroleum ether) to provide the title compound as a yellowish oil (136 mg, 86% yield). ^1H NMR (400 MHz, CDCl_3): δ 6.90 (d, J = 8.6 Hz, 1H), 4.29 – 4.14 (m, 4H), 3.97 (s, 3H), 3.94 (s, 3H), 1.31 (t, J = 7.0 Hz, 6H). NMR (101 MHz, CDCl_3): δ 171.8 (d, J = 18.2 Hz), 165.6 (d, J = 27.4 Hz), 161.2 (d, J = 222.7 Hz), 106.9 (d, J = 23.9 Hz), 63.5 (d, J = 6.1 Hz), 55.1 (s), 54.2 (s), 16.4 (d, J = 6.1 Hz). ^{31}P NMR (162 MHz, CDCl_3): δ 8.8 (s). HRMS: calculated for $\text{C}_{10}\text{H}_{17}\text{N}_2\text{O}_5\text{P}$ [(M+H) $^+$] 277.0953; found 277.0975.

Diethyl [2-oxo-5-(pyridin-2-yl)-2,3-dihydro-1*H*-benzo[e][1,4]diazepin-7-yl]phosphonate (14)



According to the general procedure, 7-bromo-5-(pyridin-2-yl)-1,3-dihydro-2*H*-benzo[e][1,4]diazepin-2-one (30 mg, 0.095 mmol, 1 eq.), Rh.6G (4.3 mg, 0.0095 mmol, 0.1 eq.), triethyl phosphite (315 μ l, 1.89 mmol, 20 eq.) and DIPEA (38 μ l, 0.21 mmol, 2.2 eq.) were reacted in 1 mL of DMSO. The reaction mixture was irradiated for 38 h. Rh.6G was added in two batches (10 mol% + 5 mol%), and the second batch of Rh.6G (2.27 mg) was added after 20 h of irradiation. After 38 h, the reaction mixture was subjected to the workup protocol outlined in the general procedure and purified by flash chromatography (DCM/MeOH) to provide the title compound as a yellowish oil (13 mg, 37% yield). ^1H NMR (600 MHz, CDCl_3): δ 8.85 (s, 1H, NH), 8.59 – 8.56 (m, 1H), 8.05 (d, J = 7.8 Hz, 1H), 7.92 – 7.80 (m, 3H), 7.41–7.37 (m, 1H), 7.20 (dd, J = 8.4, 3.4 Hz, 1H), 4.39 (s, 2H), 4.17 – 4.04 (m, 4H), 1.30 (t, J = 7.1 Hz, 6H). NMR (151 MHz, CDCl_3): δ 170.5 (s), 169.2 (s), 148.7 (s), 141.8 (s), 137.1 (s), 136.37 (d, J = 11.7 Hz), 134.79 (d, J = 9.9 Hz), 125.5 (s), 125.1 (s), 124.3 (s), 123.26 (d, J = 192.6 Hz), 121.3 (s), 121.2 (s), 62.41 (d, J = 5.4 Hz), 56.5 (s), 16.29 (d, J = 6.6 Hz). ^{31}P NMR (162 MHz, CDCl_3): δ 17.6 (s). HPLC-MS: calculated for $\text{C}_{18}\text{H}_{20}\text{N}_3\text{O}_4\text{P}$ [(M+H) $^+$] 374.1270; found 374.1269.

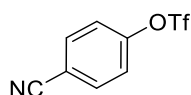
[(10a*R*)-10a-methoxy-4,7-dimethyl-4,6,6a,7,8,9,10,10a-octahydroindolo[4,3-*fg*]quinolin-9-yl]methyl 5-(diethoxyphosphoryl)nicotinate (16)



According to general procedure, ((10a*R*)-10a-methoxy-4,7-dimethyl-4,6,6a,7,8,9,10,10a-octahydroindolo[4,3-*fg*]quinolin-9-yl)methyl 5-bromonicotinate (30 mg, 0.064 mmol, 1 eq.), Rh.6G (3 mg, 0.0064 mmol, 0.1 eq.), triethyl phosphite (106 μ l, 0.64 mmol, 10 eq.) and DIPEA (26 μ l, 0.14 mmol, 2.2 eq.) were reacted in 1 mL of DMSO. The reaction mixture was irradiated for 38 h. Rh.6G was added in two batches (10 mol% + 5 mol%), and the second batch of

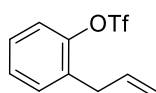
Rh.6G (1.5 mg) was added after 20 h of irradiation. After 38 h, the reaction mixture was subjected to the workup protocol outlined in the general procedure and purified by flash chromatography (DCM/MeOH) to provide the title compound as a yellowish oil (22 mg, 66% yield). ¹H NMR (600 MHz, CDCl₃): δ 9.36 (t, *J* = 2.1 Hz, 1H), 9.15 (dd, *J* = 6.3 Hz, 1.9 Hz, 1H), 8.67 (dt, *J* = 13.6 Hz, 2.1 Hz, 1H), 7.25 – 7.15 (m, 2H), 7.05 (dd, *J* = 6.8 Hz, 1.2 Hz, 1H), 6.80 (d, *J* = 1.5 Hz, 1H), 4.45 (dd, *J* = 10.9 Hz, 4.6 Hz, 1H), 4.34 (dd, *J* = 10.7 Hz, 7.4 Hz, 1H), 4.28 – 4.10 (m, 5H), 3.78 (s, 3H), 3.22 (dd, *J* = 15.2 Hz, 6.0 Hz, 3H), 3.11– 3.01 (m, 1H), 3.00 (s, 3H), 2.75 – 2.57 (m, 2H), 2.50 (s, 3H), 1.84 (m, 1H), 1.36 (t, *J* = 7.1 Hz, 6H). NMR (151 MHz, CDCl₃): 164.3 (s), 155.71 (d, *J* = 12.4 Hz), 153.66 (d, *J* = 1.7 Hz), 150.8 (s), 140.35 (d, *J* = 8.8 Hz), 137.1 (s), 135.1 (s), 126.2 (s), 125.4 (d, *J* = 190.5 Hz), 123.5 (s), 123.4 (s), 121.5 (s), 114.9 (s), 109.2 (s), 73.5 (s), 69.9 (s), 68.0 (s), 62.85 (d, *J* = 5.8 Hz), 60.9 (s), 49.6 (s), 32.8 (s), 30.1 (s), 22.1 (s), 16.34 (d, *J* = 6.2 Hz). ³¹P NMR (162 MHz, CDCl₃): δ 14.7 (s). HPLC-MS: calculated for C₂₈H₃₆N₃O₆P [(M+H)⁺] 542.2420; found 542.2419.

4-Cyanophenyl trifluoromethanesulfonate (11a)^[39]



2,6-Lutidine (834 µl, 7.2 mmol, 2.4 eq.) was added to a stirred solution of 4-nitrophenol (357 mg, 3.0 mmol, 1 eq.) in dry DCM (25 mL) at -30 °C under nitrogen atmosphere. After 15 min triflic anhydride (400 µl, 2.4 mmol, 0.8 eq.) was added dropwise. The reaction mixture was stirred for 18 h at room temperature before it was quenched with water (20 mL). The aqueous phase was extracted 3 times with DCM (3 × 15 mL) and the combined organic layers were washed with 1 M NaOH, 1 M HCl and brine. Afterwards the organic phase was dried over Na₂SO₄. The solvent was removed at reduced pressure and the product was purified by silica gel column chromatography (ethyl acetate/petroleum ether) to provide colorless hygroscopic crystals (609 mg, 81%). ¹H NMR (300 MHz, CDCl₃): δ 7.89 – 7.75 (m, 2H), 7.48 – 7.38 (m, 2H). ¹³C NMR (75 MHz, CDCl₃): δ 151.9, 134.5, 122.6, 117.1, 116.5, 112.9. ¹⁹F NMR (282 MHz, CDCl₃): δ -73.1. HRMS: calculated for C₈H₄F₃NO₃S [(M+H)⁺] 251.9937; found 251.9935.

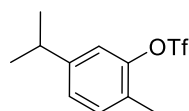
2-Allylphenyl trifluoromethanesulfonate (11b)^[40]



2,6-Lutidine (559 µl, 4.8 mmol, 2.4 eq.) was added to a stirred solution of 2-allylphenol (261 µl, 2.0 mmol, 1 eq.) in dry DCM (20 ml) at 0 °C under nitrogen atmosphere. After 10 min triflic

anhydride (336 μ l, 2.1 mmol, 1.05 eq.) was added dropwise. The reaction mixture was stirred for 18 h at room temperature before it was quenched with water (20 mL). The aqueous phase was extracted 3 times with DCM (3×15 mL) and the combined organic layers were washed with 1 M NaOH, 1 M HCl and brine. Afterwards the organic phase was dried over Na₂SO₄. The solvent was removed at reduced pressure and the product was purified by silica gel column chromatography (ethyl acetate/petroleum ether) to provide a yellowish oil (204.8 mg, 38%). ¹H NMR (300 MHz, CDCl₃): δ 7.56 – 7.15 (m, 4H), 6.10 – 5.49 (m, 1H), 5.31 – 4.92 (m, 1H), 3.50 (dt, J = 6.6, 1.5 Hz, 2H). ¹³C NMR (75 MHz, CDCl₃): δ 147.91, 134.58, 132.83, 131.41, 128.41, 128.15, 121.3, 118.59 (d, J = 320.0 Hz), 117.4, 34.01. ¹⁹F NMR (282 MHz, CDCl₃): δ -74.38. HRMS: calculated for C₁₀H₉F₃O₃S [M⁺] 266.0224; found 266.0216.

5-Isopropyl-2-methylphenyl trifluoromethanesulfonate (11c)^[41]



2,6-Lutidine (559 μ l, 4.8 mmol, 2.4 eq.) was added to a stirred solution of carvacrol (308 μ l, 2.0 mmol, 1 eq.) in dry DCM (20 mL) at 0°C under nitrogen atmosphere. After 10 min, triflic anhydride (336 μ l, 2.1 mmol, 1.05 eq.) was added dropwise. The reaction mixture was stirred for 18 h at room temperature before it was quenched with water (20 mL). The aqueous phase was extracted 3 times with DCM (3×15 mL) and the combined organic layers were washed with 1 M NaOH, 1 M HCl and brine. Afterwards the organic phase was dried over Na₂SO₄. The solvent was removed at reduced pressure and the product was purified by silica gel column chromatography (ethyl acetate/petroleum ether) to provide a colorless oil (310 mg, 55%). ¹H NMR (300 MHz, CDCl₃): δ 7.24 – 7.03 (m, 3H), 3.01 – 2.81 (m, 1H), 2.37 – 2.31 (m, 3H), 1.24 (d, J = 6.9 Hz, 6H). ¹³C NMR (75 MHz, CDCl₃): δ 149.1, 148.5, 131.9, 127.8, 126.3, 119.2, 118.6 (d, J = 320.2 Hz), 33.6, 23.8, 15.9. ¹⁹F NMR (282 MHz, CDCl₃): δ -74.3.

5.5 References

- [1] C. S. Dammer, N. K. Larsen, L. Bunch *Chem. Rev.* **2011**, *111*, 7981-8006.
- [2] a) K. Luo, Y. Z. Chen, W. C. Yang, J. Zhu, L. Wu, *Org. Lett.* **2016**, *18*, 452-455; b) K. Moonen, I. laureyn, C. V. Stevens, *Chem. Rev.* **2004**, *104*, 6177-6216; c) P. Guga, *Curr. Top. Med. Chem.* **2007**, *7*, 695-713.
- [3] a) J. L. Montchamp, Y. R. Dumond, *J. Am. Chem. Soc.* **2001**, *123*, 510-511; b) A. L. Schwan, *Chem. Soc. Rev.* **2004**, *33*, 218-224; c) T. Chen, J. S. Zhang, B. L. Han, *Dalton Trans.* **2016**, *45*, 1843-1849; d) Y. H. Budnikova, O. G. Sinyashin, *Russ. Chem. Rev.* **2015**, *84*, 917-951.
- [4] a) A. J. Bloomfield, S. B. Herzon, *Org. Lett.* **2012**, *14*, 4370-4373; b) E. L. Deal, C. Petit, J. L. Montchamp, *Org. Lett.* **2011**, *13*, 3270- 3273; c) K. Xu, H. Hu, F. Yang, Y. Wu, *Eur. J. Org. Chem.* **2013**, *2013*, 319-325; d) M. Kalek, M. Jerowska, J. Stawinski, *Adv. Synth. Catal.* **2009**, *351*, 3207-3216.
- [5] M. Kalek, A. Ziadi, J. Stawnski, *Org. Lett.* **2008**, *10*, 4637-4640.
- [6] a) T. Fu, H. Qiao, Z. Peng, G. Hu, X. Wu, Y. X. Gao, Y. Zhao, *Org. Biomol. Chem.* **2014**, *12*, 2895-2902; b) M. Andaloussi, J. Lindh, J. Sävmarker, P. J. Sjöberg, M. Larhed, *Chem. Eur. J.* **2009**, *15*, 13069-13074.
- [7] W. C. Fu, C. M. So, F. Y. Kwong, *Org. Lett.* **2015**, *17*, 5906-5909.
- [8] T. Wang, S. Sang, L. Liu, H. Qiao, Y. Gao, Y. Zhao, *J. Org. Chem.* **2014**, *79*, 608-614.
- [9] a) J. Ke, Y. Tang, H. Yi, Y. Li, Y. Cheng, C. Liu, A. Li, *Angew. Chem. Int. Ed.* **2015**, *54*, 6604-6607; b) R. Zhuang, J. Xu, Z. Cai, G. Tang, M. Fang, Y. Zhao, *Org. Lett.* **2011**, *13*, 2010-2014; c) G. Hu, W. Chen, T. Fu, Z. Peng, H. Qiao, Y. Gao, Y. Zhao, *Org. Lett.* **2013**, *15*, 5362-5365; d) J. Yang, T. Chen, L. B. Han, *J. Am. Chem. Soc.* **2015**, *137*, 1782-1785; e) Y. L. Zhao, G. J. Wu, Y. Li, L. X. Gao, F. S. Han, *Chem. Eur. J.* **2012**, *18*, 9622-9627; f) H. Zhang, X. Y. Zhang, D. Q. Dong, Z. L. Wang, *RSC Adv.* **2015**, *5*, 52824-52831; g) E. Jablonkai, G. Keglevich, *Curr. Org. Syn.* **2014**, *11*, 429-453; h) Y. M. Li, S. D. Yang, *Synlett* **2013**, *24*, 1739-1744; i) C. Shen, G. Yang, W. Zhang, *Org. Biomol. Chem.* **2012**, *10*, 3500-3505; j) Q. Yao, S. Levchik, *Tetrahedron Lett.* **2006**, *47*, 277-281.
- [10] a) W. J. Yoo, S. Kobayashi, *Green Chem.* **2014**, *16*, 2438-2442; b) Y. He, H. Wu, F. D. Toste, *Chem. Sci.*, **2015**, *6*, 1194-1198; c) J. Xuan, T. T. Zhen, J. R. Chen, L. Q. Lu, W. J. Xiao, *Chem. Eur. J.* **2015**, *21*, 4962-4965.
- [11] a) C. K Prier, D. A. Rankic, D. W. C. MacMillan, *Chem. Rev.* **2013**, *113*, 5322-5363; b) D. M. Schultz, T. P. Yoon, *Science* **2014**, *343*, 1239176-1 - 1239176-8.
- [12] a) T. Hering, B. Mühldorf, R. Wolf, B. König, *Angew. Chem. Int. Ed.* **2016**, *55*, 5342-5345; b) A. U. Meyer, K. Strakova, T. Slanina, B. König, *Chem. Eur. J.* **2016**, *22*,

- 8694-8699; c) M. A. Ischay, M. E. Anzovino, J. Du, T. P. Yoon, *J. Am. Chem. Soc.* **2008**, *130*, 12886-12887; d) L. J. Rono, H. G. Yayla, D. Y. Wang, M. F. Armstrong, R. R. Knowles, *J. Am. Chem. Soc.* **2013**, *135*, 17735-17738.
- [13] a) D. Ravelli, S. Protti, M. Fagnoni, *Chem. Rev.* **2016**, *116*, 9850–9913; b) N. A. Romero, D. A. Nicewicz, *Chem. Rev.* **2016**, *116*, 10075–10166; c) K. L. Skubi, T. R. Blum, T. P. Yoon, *Chem. Rev.* **2016**, *116*, 10035–10074.
- [14] a) D. P. Hari, P. Schroll, B. König, *J. Am. Chem. Soc.* **2012**, *134*, 2958–2961; b) D. P. Hari, T. Hering, B. König, *Angew. Chem. Int. Ed.* **2014**, *53*, 725–728.
- [15] A. U. Meyer, T. Slanina, C. J. Yao, B. König, *ACS Catal.* **2016**, *6*, 369–375.
- [16] I. Ghosh, T. Ghosh, J. I. Bardagi, B. König, *Science*, **2014**, *346*, 725-728.
- [17] L. Pause, M. Robert, J. M. Saveant, *J. Am. Chem. Soc.* **1999**, *121*, 7158-7159.
- [18] M. Beija, C. A. M. Afonso, J. M. G. Martinho, *Chem. Soc. Rev.* **2009**, *38*, 2410-2433.
- [19] I. Ghosh, B. König, *Angew. Chem. Int. Ed.* **2016**, *55*, 7676-7679.
- [20] S. Van de Linde, A. Löscheberger, T. Klein, M. Heidbreder, S. Walter, M. Sauer, *Nat. Protoc.* **2011**, *6*, 991-1009.
- [21] S. van de Linde, I. Krstic, T. Prisner, S. Doose, M. Heilemann, M. Sauer, *Photochem. Photobiol. Sci.* **2011**, *10*, 499-506.
- [22] M. Costentin, M. Robert, J. M. Saveant, *J. Am. Chem. Soc.* **2004**, *126*, 16051-16057.
- [23] a) J. B. Plumb, R. Obrycki, C. E. Griffin, *J. Org. Chem.* **1966**, *31*, 2455-2458; b) R. Obrycki, C. E. Griffin, *J. Org. Chem.* **1968**, *33*, 632-636.
- [24] a) K. Pomeisl, A. Holy, R. Pohl, K. Horska, *Tetrahedron*, **2009**, *65*, 8486-8492; b) N. M. Goudgaon, F. N. M. Naguib, M. H. Kouni, R. F. Schinazi, *J. Med. Chem.* **1993**, *36*, 4250-4254.
- [25] J. J. L. Fu, W. G. Bentrude, C. E. Griffin, *J. Am. Chem. Soc.* **1972**, *94*, 7717-7722.
- [26] R. Zhuang, J. Xu, Z. Cai, G. Tang, M. Fang, Y. Zhao, *Org. Lett.* **2011**, *13*, 2110-2113.
- [27] L. J. Gu, C. Jin, R. Wang, H. Y. Ding, *ChemCatChem* **2014**, *6*, 1225-1228.
- [28] G. Keglevich, E. Jablonkai, L. B. Balazs, *RSC Adv.* **2014**, *4*, 22808-22816.
- [29] E. N. Tsvetkov, D. I. Lobanov, L. A. Izosenkova, M. I. Kabachnik, *Zh. Obshch. Khim.* **1969**, *39*, 2177-2184.
- [30] H. Takenaka, Y. Hayase, *Heterocycles*, **1989**, *29*, 1185-1189.
- [31] W. C. Fu, C. M. So, F. Y. Kwong, *Org. Lett.* **2015**, *17*, 5906-5909.
- [32] S. S. Iremonger, J. Liang, R. Vaidhyanathan, G. K. H. Shimizu, *Chem. Commun.* **2011**, *47*, 4430-4432.
- [33] K. S. Petrakis, T. L. Nagabhushan, *J. Am. Chem. Soc.* **1987**, *109*, 2831-2833.
- [34] Y.-L. Zhao, G.-J. Wu, Y. Li, L.-X. Gao, F.-S. Han, *Chem. Eur. J.* **2012**, *18*, 9622-9627.
- [35] J. Yang, J. Xiao, T. Chen, L.-B. Han, *J. Org. Chem.* **2016**, *81*, 3911-3916.
- [36] S. Y. Chen, R. S. Zeng, J. P. Zou, O. T. Asekun, *J. Org. Chem.* **2014**, *79*, 1449-1453.

- [37] C. B. Xiang, Y. J. Bian, X. R. Mao, Z. Z. Huang, *J. Org. Chem.* **2012**, 77, 7707-7710.
- [38] X. L. Chen, X. Li, L. B. Qu, Y. C. Tang, W. P. Mai, D. H. Wei, W. Z. Bi, L. K. Duan, K. Sun, J. Y. Chen, D. D. Ke, Y. F. Zhao, *J. Org. Chem.* **2014**, 79, 8407-8416.
- [39] M. Uchiyama, Y. Kobayashi, T. Furuyama, S. Nakamura, Y. Kajihara, T. Miyoshi, T. Sakamoto, Y. Kondo, K. Morokuma, *J. Am. Chem. Soc.* **2008**, 130, 472-480.
- [40] D. R. White, J. T. Hutt, J. P. Wolfe, *J. Am. Chem. Soc.* **2015**, 137, 11246-11249.
- [41] J. E. McMurry, S. Mohanraj, *Tetrahedron Lett.* **1983**, 24, 2723-2726.

6. Summary

This thesis presents various approaches for the photocatalytic functionalization of organic compounds with sp^2 -hybridized carbon atoms. Visible-light mediated oxidative nitration and chlorination reactions (Chapters 2-3) as well as reductive alkenylation and phosphonylation reactions (Chapters 4-5) were developed in this context.

Chapter 1 gives an overview of the application and benefits of photocatalysis in organic synthesis. Selected examples of photoredox-catalyzed reactions are compared with their thermal counterparts.

In **Chapter 2**, a visible-light mediated method for the nitration of protected anilines is presented. *Ortho*- and *para*-nitrated compounds are obtained in an acid- and transition metal-free process. Aerial oxygen serves as terminal electron acceptor and riboflavin tetraacetate as organic photocatalyst. Persistent NO_2 -radicals that are generated upon oxidation of sodium sulfate are postulated to be key intermediates of this nitration reaction.

A new system for the photochlorination of electron rich arenes is described in **Chapter 3**. The starting material is activated by *in situ* bromination within a first photoredox-catalyzed oxidation step, followed by a photocatalyzed *ipso*-chlorination. Both oxidative steps are enabled by the use of 4CzIPN as organic photoredox catalyst, dioxygen and visible-light.

Two strategies for the photoredox-catalyzed alkenylation of unactivated alkyl bromides are presented in **Chapter 4**. *In situ* generated silyl radicals are postulated to abstract bromine atoms from alkyl bromides to form C-centered alkyl radicals. These radicals can add to vinyl sulfones and the final product is obtained by subsequent elimination of a phenyl sulfonyl radical. Alternatively, the alkyl radicals can be included into the catalytic cycle of a nickel co-catalyst, for the coupling with vinyl bromides.

In **Chapter 5**, a photoredox-catalyzed Arbuzov-type reaction is presented. Aryl bromides are reduced via a consecutive photoinduced electron transfer process from an excited rhodamine 6G radical anion species. The generated aryl radicals react with aryl or alkyl phosphites yielding phosphonylated products.

7. Zusammenfassung

In dieser Arbeit werden photokatalytische Methoden zur Funktionalisierung von organischen Verbindungen an sp^2 -hybridisierten Kohlenstoffatomen vorgestellt. In diesem Kontext wurden durch sichtbares Licht vermittelte, oxidative Nitrierungs- und Chlorierungsreaktionen (Kapitel 2-3) und reduktive Alkenylierungs- und Phosphonylierungsreaktionen (Kapitel 4-5) entwickelt.

Kapitel 1 gibt einen Überblick über die Verwendung und Vorteile der Photokatalyse in der organischen Synthese. Ausgewählte Beispiele von photokatalysierten Reaktionen werden mit ihren entsprechenden thermischen Varianten verglichen.

In **Kapitel 2** wird eine durch sichtbares Licht vermittelte Nitrierung von geschützten Anilinen vorgestellt. *Ortho*- und *para*-nitrierte Verbindungen werden durch einen Säure- und Übergangsmetall-freien Prozess erhalten. Luftsauerstoff dient als terminales Oxidationsmittel und Riboflavintetraacetat als organischer Photokatalysator. Persistente NO_2 -Radikale, die durch die Oxidation von Natriumnitrit entstehen, werden als Schlüsselintermediate dieser Nitrierungsreaktion postuliert.

In **Kapitel 3** wird ein neues System für die Photochlorierung von elektronenreichen Aromaten beschrieben. Die Edukte werden in einem ersten, photokatalysierten Oxidationsschritt *in situ* bromiert. Anschließend findet eine *ipso*-Chlorierung statt. Beide oxidativen Reaktionsschritte werden durch die Anwesenheit von 4CzIPN als organischem Photokatalysator, Sauerstoff und sichtbarem Licht ermöglicht.

In **Kapitel 4** werden zwei Strategien für die photokatalytische Alkenylierung von inaktivierten Alkylbromiden vorgestellt. Es wird postuliert, dass *in situ* generierte Silylradikale Bromatome von Alkylbromiden abstrahieren und somit C-zentrierte Alkylradikale entstehen. Diese Radikale können an Vinylsulfone addieren. Das Endprodukt wird durch die Abspaltung eines Phenylsulfonradikals erhalten. Alternativ können die Alkylradikale auch in den katalytischen Zyklus eines Nickel-Cokatalysators eingebunden werden, um so die Kupplung mit Vinylbromiden zu ermöglichen.

In **Kapitel 5** wird eine photokatalysierte Variante der Arbuzov-Reaktion vorgestellt. Arylbromide werden durch einen konsekutiven photoinduzierten Elektronentransfer-Prozess, ausgehend vom angeregten Rhodamin 6G Radikalanion, reduziert. Die generierten Arylradikale reagieren mit Aryl- oder Alkylphosfiten zu phosphonylierten Produkten.

8. Abbreviations

A	A	ampere
	Ac	acyl
	AIBN	azobisisobutyronitrile
	Ar	aryl
	ATR	attenuated total reflection
	ATRA	atom transfer radical addition
	aq	aqueous
B	BINAP	2,2'-bis(diphenylphosphino)-1,1'-binaphthyl
	Bn	benzyl
	Boc	<i>tert</i> -butoxycarbonyl
	BPO	benzoyl peroxide
	bpy	2,2'-bipyridine
	Bu	butyl
	Bz	benzoyl
C	c	concentration
	°C	degree Celsius
	calc.	calculated
	Cbz	benzyloxycarbonyl
	cm	centimeter
	COD	1,5-cyclooctadiene
	conPET	consecutive photoinduced electron transfer
	CPS	counts per second
	CV	cyclic voltammetry
	4CzIPN	2,4,5,6-Tetra(9H-carbazol-9-yl)isophthalonitrile
D	DABCO	1,4-diazabicyclo[2.2.2]octane
	DCE	1,2-dichloroethane
	DCM	dichloromethane
	DDQ	2,3-dichloro-5,6-dicyano-1,4-benzoquinone
	DEPT	distortionless enhancement by polarization transfer
	DIPEA	<i>N,N</i> -diisopropylethylamine
	DMA	<i>N,N</i> -dimethylacetamide
	DME	dimethoxyethane
	DMF	<i>N,N</i> -dimethylformamide
	DMPU	<i>N,N</i> -Dimethylpropyleneurea

	DMSO	dimethyl sulfoxide
	dpe	1,2-bis(diphenylphosphino)ethane
	dtbbpy	4,4'-di- <i>tert</i> -butyl-2,2'-dipyridyl
	DTPB	di- <i>tert</i> -butylperoxid
E	ϵ	molar extinction coefficient
	eq.; equiv.	equivalent
	E _{ox}	oxidation potential
	E _{red}	reduction potential
	ESI	electrospray ionization
	Et	ethyl
	EE	ethyl acetate
	ESI	electrospray ionization
F	Fc	ferrocene
	Fc ⁺	ferrocenium
	FID	flame ionization detector
	Fmoc	fluorenylmethyloxycarbonyl
	FTIR	Fourier-transform infrared spectroscopy
G	GC	gas chromatography
H	h	hour
	HAT	hydrogen atom transfer
	HPLC	high-performance liquid chromatography
	HRMS	high resolution mass spectrometry
I	I	signal intensity
	ⁱ Pr	isopropyl
J	J	coupling constant
L	λ	wavelength
	LDA	lithium diisopropylamide
	LED	light emitting diode
M	M	molarity [mol·L ⁻¹]
	Me	methyl
	MeCN	acetonitrile
	MHz	mega hertz
	min	minute
	mL	milliliter
	μ L	microliter
	mmole	millimole
	mol%	mole percent

	Mp	melting point
	MS	mass spectrometry
	Ms	mesyl
	MSD	mass spectrometric detector
	MTBD	7-methyl-1,5,7-triazabicyclo[4.4.0]dec-5-ene
N	NCS	<i>N</i> -chlorosuccinimide
	nm	nanometer
	NMR	nuclear magnetic resonance
	Nu	nucleophile
P	p.a.	per analysis
	PC	photocatalyst
	PE	petrol ether
	PET	photoinduced electron transfer
	PG	protecting group
	ppm	parts per million
	ppy	2-phenylpyridine
	Pr	propyl
	PTFE	polytetrafluoroethylene
Q	Q-TOF	quadrupole time-of-flight
R	R	alkyl, aryl or functional group
	RFTA	riboflavin tetraacetate
	Rh.6G	rhodamine 6G
	rt; r.t.	room temperature
S	s	second
	SAMP	(<i>S</i>)-1-amino-2-(methoxymethyl)pyrrolidine
	SCE	saturated calomel electrode
	SET	single electron transfer
T	TBHP	<i>tert</i> -butyl hydroperoxide
	TEMPO	(2,2,6,6-tetramethylpiperidin-1-yl)oxyl
	Tf	trifluoromethanesulfonyl
	THF	tetrahydrofuran
	TLC	thin-layer chromatography
	Tos; Ts	toluenesulfonyl
	TPT	triphenylpyrylium tetrafluoroborate
	TTMSS	tris(trimethylsilyl)silane
U	UV	ultraviolet
V	V	volt

	Vis	visible
	vs	versus
W	W	watt

9. Curriculum Vitae

Personal Data

Name	Simon Josef Siegfried Düsel
Date of birth	15.01.1991
Place of birth	Haßfurt
Nationality	German



Education

11/2015 – 04/2019	PhD in Chemistry (Dr. rer. nat.) University of Regensburg, Institute of organic chemistry <i>“Functionalization of sp^2-hybridized carbon atoms via visible-light photoredox catalysis”</i> Supervisor: Prof. Dr. Burkhard König
10/2013 – 09/2015	Master of Science in Chemistry University of Regensburg (Grade: “very good“, 1.1) Master thesis: <i>“The use of deep eutectic solvents in catalyst design and as special reaction media”</i> Supervisor: Prof. Dr. Burkhard König
04/2011 – 09/2013	Bachelor of Science in Chemistry University of Regensburg (Grade: “good“, 1.6) Bachelor thesis: <i>“Studien zur Synthese eines Dehydro-Xanthatin-Derivats”</i> Supervisor: Prof. Dr. Oliver Reiser
09/2001 – 07/2010	Allgemeine Hochschulreife (A-Levels) Graf-Münster Gymnasium Bayreuth (Grade: “very good“, 1.5)

Further professional activities

01/2011 – 03/2011	Technical Development Assistant Grundig Business Systems Bayreuth
07/2010 – 12/2010	Military Service Joint Medical service of the Bundeswehr

Scientific publications

12/2016	<i>“Visible-Light Photo-Arbuzov Reaction of Aryl Bromides and Trialkyl Phosphites Yielding Aryl Phosphonates”</i> Rizwan S. Shaikh, Simon J. S. Düsel und Burkhard König <i>ACS Catal.</i> , 2016 , 6, 8410–8414
03/2018	<i>“Visible-Light-Mediated Nitration of Protected Anilines”</i> Simon J. S. Düsel and Burkhard König <i>J. Org. Chem.</i> , 2018 , 83, 2802–2807
01/2019	<i>“Alkenylation of unactivated alkyl bromides through visible light photocatalysis”</i> Quan-Quan Zhou [‡] , Simon J. S. Düsel [‡] , Liang-Qiu Lu, Burkhard König and Wen-Jing Xiao <i>Chem. Commun.</i> , 2019 , 55, 107-110
2019	<i>“Photocatalytic Oxidative Iodination of Electron-Rich Arenes”</i> Rok Narobe, Simon J. S. Düsel and Burkhard König (Manuscript submitted)
2019	<i>“Oxidative photochlorination of electron rich arenes via in situ bromination”</i> Simon J. S. Düsel and Burkhard König (Manuscript submitted)
2019	<i>“Impact of visible-light photoredox catalysis on traditional synthetic protocols”</i> Simon J. S. Düsel and Burkhard König (Manuscript submitted)

Scientific presentations

08/2016	6 th Chemistry Congress EuCheMS – Sevilla, Spain (poster)
07/2017	28 th International Conference on Photochemistry – Strasbourg, France (poster)
09/2018	26 th Lecture Conference on Photocatalysis – Garching, Germany (poster)
10/2015 – 03/2019	23 rd -35 th Seminar Days of the GRK 1626 – Bavaria, Germany (oral and poster contributions)

10. Danksagung

Allen voran gilt mein besonderer Dank Herrn Prof. Dr. Burkhard König für die Möglichkeit meine Master- und Doktorarbeit in seinem Arbeitskreis anfertigen zu dürfen. Ich bedanke mich für seine Unterstützung während der gesamten Zeit, die angenehme Arbeitsatmosphäre, seine wissenschaftlichen Impulse und hilfreichen Diskussionen sowie seine guten Hinweise beim Schreiben der Publikationen. Zudem bedanke ich mich für die Ermöglichung meines Auslandsaufenthalts in China und der Gelegenheiten meine Forschungsergebnisse auf Konferenzen im In- und Ausland präsentieren zu können.

Für die Übernahme des Zweitgutachtens möchte ich Frau Prof. Dr. Julia Rehbein danken. Weiterhin danke ich Prof. Dr. Arno Pfitzner und Prof. Dr. Frank-Michael Matysik für ihre Bereitschaft im Promotionsprüfungsausschuss mitzuwirken.

Ich bedanke mich bei Herrn Prof. Dr. Wen-Jing Xiao und Herrn Prof. Dr. Liang-Qui Lu sowie ganz besonders bei Quan-Quan Zhou für die Projektzusammenarbeit und die gute Zeit am Chemical College der Central China Normal University in Wuhan.

Dr. Rizwan Shaikh danke ich für die gute Zusammenarbeit bei der Entwicklung der photokatalysierten Arbuzov Reaktion und Rok Narobe für die gemeinsame Arbeit im Bereich der photokatalysierten Iodierung.

Ich möchte mich bei Katharina Nickl, Britta Badziura, Viola Rappenecker, Simone Strauss, Julia Zach und Ernst Lautenschlager bedanken. Für ihre Hilfe bei allen möglichen auftretenden Problemen, organisatorischer, bürokratischer oder technischer Natur. Mein besonderer Dank gilt Regina Hoheisel für die CV-Messungen und Dr. Rudolf Vasold für die GC/MS Messungen.

Ich danke den Mitgliedern der Zentralen Analytik der Universität Regensburg sowie der Elektronik- und Feinmechanikwerkstatt für die schnelle Bearbeitung sämtlicher Aufträge.

Für die Finanzierung von Teilen meiner Promotion und der Auslandsreisen danke ich dem Graduiertenkolleg „GRK 1626 Chemische Photokatalyse“.

Großer Dank für die schöne Zeit gilt auch allen ehemaligen und aktuellen Kollegen des Arbeitskreises. Für die Unterstützung und Diskussionen bei fachlichen Themen sowie bei Unternehmungen und Gesprächen fachfremder Natur. Vor allem bedanke ich mich bei meinen Laborkollegen Daniel Lachmann und Daniel Petzold für die tolle Zeit im Labor 32.1.24.

Abschließen möchte ich mich noch bei meiner Familie bedanken. Den Personen die mich schon mein ganzes Leben bei allen Belangen unterstützt haben und ohne die ich nicht so weit gekommen wäre. Danke an meine Eltern Christian und Christine und danke an meinen Bruder Andreas mit seiner Frau Kerstin. Und vielen Dank an dich Anna-Lena. Danke für deine Unterstützung und Liebe, sowie die wundervollen gemeinsamen Jahre die wir hatten und haben werden.